

STUDY OF HYDROCARBON MISCIBLE SOLVENT SLUG INJECTION
PROCESS FOR IMPROVED RECOVERY OF HEAVY OIL FROM
SCHRADER BLUFF POOL, MILNE POINT UNIT, ALASKA

FINAL REPORT

NOVEMBER 1995

Work Performed Under Contract No. DE-FG22-93BC14864

Prepared for
U.S. Department of Energy
Assistant Secretary for Fossil Energy

Thomas B. Reid, Project Manager
Bartlesville Project Office
P.O. Box 1393
Bartlesville, OK 74005

Prepared by
University of Alaska Fairbanks
Petroleum Development Laboratory
Fairbanks, AK 99775-5380

MASTER

DISTRIBUTION OF THIS DOCUMENT IS UNLIMITED *OK*

NOV 17 1995
NOV 17 1995
NOV 17 1995

ABSTRACT

The National Energy Strategy Plan (NES) has called for 900,000 barrels/day production of heavy oil in the mid-1990s to meet our national needs. To achieve this goal, it is important that the Alaskan heavy oil fields be brought to production. Alaska has more than 25 billion barrels of heavy oil deposits. Conoco, and now BP Exploration have been producing from Schrader Bluff Pool, which is part of the super heavy oil field known as West Sak Field.

Schrader Bluff reservoir, located in the Milne Point Unit, North Slope of Alaska, is estimated to contain up to 1.5 billion barrels of (14 to 21° API) oil in place. The field is currently under production by primary depletion; however, the primary recovery will be much smaller than expected. Hence, waterflooding will be implemented earlier than anticipated. The eventual use of enhanced oil recovery (EOR) techniques, such as hydrocarbon miscible solvent slug injection process, is vital for recovery of additional oil from this reservoir.

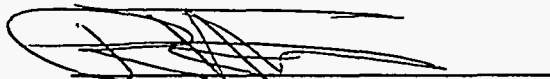
The purpose of this research project was to determine the nature of miscible solvent slug which would be commercially feasible, to evaluate the performance of the hydrocarbon miscible solvent slug process, and to assess the feasibility of this process for improved recovery of heavy oil from Schrader Bluff reservoir. The laboratory experimental work includes: slim tube displacement experiments and coreflood experiments. The components of solvent slug includes only those which are available on the North Slope of Alaska.

DISCLAIMER

This report was prepared as an account of work sponsored by an agency of the United States Government. Neither the United States Government nor any agency thereof, nor any of their employees, makes any warranty, express or implied, or assumes any legal liability or responsibility for the accuracy, completeness, or usefulness of any information, apparatus, product, or process disclosed, or represents that its use would not infringe privately owned rights. Reference herein to any specific commercial product, process, or service by trade name, trademark, manufacturer, or otherwise does not necessarily constitute or imply its endorsement, recommendation, or favoring by the United States Government or any agency thereof. The views and opinions of authors expressed herein do not necessarily state or reflect those of the United States Government or any agency thereof.

ACKNOWLEDGEMENT

This report was prepared for the U.S. Department of Energy under the Cooperative Agreement No. DE-FG22-93BC14864. The financial support of the U.S. Department of Energy, Bartlesville Project Office is gratefully acknowledged. The matching support was provided by the Petroleum Development Laboratory, University of Alaska Fairbanks, and Conoco, Inc. The research work described herein was made possible by the cooperation and assistance of North Slope Operators, who provided oil and gas samples. This report is a result of the work performed by Dr. G.D. Sharma, Principal Investigator, and the following co-investigators: Dr. V.A. Kamath, Dr. Santanu Khataniar, and Mr. Shirish L. Patil; and the following graduate students: Ansar Ali, Maruti Inaganti, and Santosh Chandra.



Dr. Robert H. Trent, Director
Petroleum Development Laboratory

TABLE OF CONTENTS

ABSTRACT	ii
ACKNOWLEDGEMENT	iii
LIST OF FIGURES.....	v
LIST OF TABLES	xi
CHAPTER 1: INTRODUCTION	1.1
CHAPTER 2: SCHRADER BLUFF RESERVOIR DESCRIPTION	2.1
A. Characterization of Tract 14 Wells	2.2
B. Log Derived Petrophysical Properties	2.3
C. Spatial Distribution of Petrophysical Properties.....	2.4
D. Sand Quality Distribution.....	2.5
E. Characterization of Schrader Bluff Pool (Outside Tract 14).....	2.6
CHAPTER 3: SLIM TUBE DISPLACEMENT STUDIES.....	3.1
A. Introduction.....	3.1
B. Reservoir Fluid Characteristics.....	3.3
C. Multiple Contact Test Runs.....	3.4
D. Slim Tube Simulation	3.5
E. Experimental Apparatus	3.6
F. Experimental Procedure.....	3.10
G. Results and Discussions	3.12
H. Conclusions	3.17
I. References	3.18
J. APPENDIX	3.48
CHAPTER 4: COREFLOOD EXPERIMENTS.....	4.1
A. Introduction.....	4.1
B. Experimental Apparatus	4.2
C. Experimental Procedure.....	4.5
D. Results and Discussions	4.8
E. Conclusions	4.16
F. APPENDIX	4.80

LIST OF FIGURES (CON'T.)

3.9	P-X Diagram for CO ₂ /NGL Mixture.....	3.28
3.10	P-X Diagram for PBG/NGL Mixture.....	3.29
3.11	Slim Tube Displacement Experiment and Simulation Results (Solvent: 100% Kuparuk-Schrader Bluff Gas)	3.30
3.12	Slim Tube Displacement Experiment and Simulation Results (Solvent: 100% CO ₂)	3.31
3.13	Slim Tube Displacement Experiment and Simulation Results (Solvent: 90% CO ₂ and 10% NGL)	3.32
3.14	Slim Tube Displacement Experiment and Simulation Results (Solvent: 85% CO ₂ and 15% NGL)	3.33
3.15	Slim Tube Displacement Experiment and Simulation Results (Solvent: 100% Prudhoe Bay Gas)	3.34
3.16	Slim Tube Displacement Experiment and Simulation Results (Solvent: 70% PBG and 30% NGL)	3.35
3.17	Slim Tube Displacement Experiment and Simulation Results (Solvent: 60% PBG and 40% NGL)	3.36
3.18	Slim Tube Displacement Experiment and Simulation Results (Solvent: 50% PBG and 50% NGL)	3.37
3.19	Density vs. Number of Contacts (Solvent: 40% PBG/60% NGL).....	3.38
3.20	K-values vs. Number of Contacts (Solvent: 40% PBG/60% NGL).....	3.39
3.21	X _i vs. Number of Contacts (Solvent: 40% PBG/60% NGL)	3.40
3.22	Y _i vs. Number of Contacts (Solvent: 40% PBG/60% NGL)	3.41
3.23	Density vs. Number of Contacts (Solvent: 36% PBG/64% NGL).....	3.42
3.24	K-values vs. Number of Contacts (Solvent: 36% PBG/64% NGL).....	3.43
3.25	X _i vs. Number of Contacts (Solvent: 36% PBG/64% NGL)	3.44
3.26	Y _i vs. Number of Contacts (Solvent: 36% PBG/64% NGL)	3.45

CHAPTER 4

4.1	Schematic Diagram of Experimental Setup.....	4.17
4.2	Oil-Water Relative Permeability Curves for the Sandpack.....	4.18
4.3	Oil Recovery vs. PV Injected (Unsteady State Waterflood)	4.19
4.4	WOR vs. PV Injected (Unsteady State Waterflood).....	4.20
4.5	GOR vs. PV Injected (Unsteady State Waterflood).....	4.21

LIST OF FIGURES (CONT.)

4.23	Oil Recovery vs. PV Injected, Multiple WAG, WAG Ratio: 11.....	4.39
	(MCM Solvent: 50% PBG/50% NGL)	
4.24	WOR vs. PV Injected, Multiple WAG, WAG Ratio: 11	4.40
	(MCM Solvent: 50% PBG/50% NGL)	
4.25	GOR vs. PV Injected, Multiple WAG, WAG Ratio: 11	4.41
	(MCM Solvent: 50% PBG/50% NGL)	
4.26	Pressure Drop vs. PV Injected, Multiple WAG, WAG Ratio: 11	4.42
	(MCM Solvent: 50% PBG/50% NGL)	
4.27	Oil Recovery vs. PV Injected, Multiple WAG, WAG Ratio: 5.....	4.43
	(MCM Solvent: 50% PBG/50% NGL)	
4.28	WOR vs. PV Injected, Multiple WAG, WAG Ratio: 5	4.44
	(MCM Solvent: 50% PBG/50% NGL)	
4.29	GOR vs. PV Injected, Multiple WAG, WAG Ratio: 5	4.45
	(MCM Solvent: 50% PBG/50% NGL)	
4.30	Pressure Drop vs. PV Injected, Multiple WAG, WAG Ratio: 5	4.46
	(MCM Solvent: 50% PBG/50% NGL)	
4.31	Oil Recovery vs. PV Injected, Multiple WAG, WAG Ratio: 3.....	4.47
	(MCM Solvent: 50% PBG/50% NGL)	
4.32	WOR vs. PV Injected, Multiple WAG, WAG Ratio: 3	4.48
	(MCM Solvent: 50% PBG/50% NGL)	
4.33	GOR vs. PV Injected, Multiple WAG, WAG Ratio: 3	4.49
	(MCM Solvent: 50% PBG/50% NGL)	
4.34	Pressure Drop vs. PV Injected, Multiple WAG, WAG Ratio: 3	4.50
	(MCM Solvent: 50% PBG/50% NGL)	
4.35	Oil Recovery vs. PV Injected, FCM Solvent Slug Size: 0.05 PV	4.51
	(Solvent: Propane)	
4.36	WOR vs. PV Injected, FCM Solvent Slug Size: 0.05 PV	4.52
	(Solvent: Propane)	
4.37	GOR vs. PV Injected, FCM Solvent Slug Size: 0.05 PV	4.53
	(Solvent: Propane)	
4.38	Pressure Drop vs. PV Injected, FCM Solvent Slug Size: 0.05 PV	4.54
	(Solvent: Propane)	
4.39	Oil Recovery vs. PV Injected, FCM Solvent Slug Size: 0.10 PV	4.55
	(Solvent: Propane)	

LIST OF FIGURES (CON'T.)

4.61	Effect of Slug Size on Incremental Oil Recovery.....	4.77
	(FCM Solvent: Propane)	
4.62	Effect of Solvent Type, Recovery vs. PV Injected Comparison.....	4.78

CHAPTER 1

INTRODUCTION

During the past years, oil production in the U.S. has been steadily declining while the demand for foreign imported oil has been steadily increasing. To abate the over-reliance on foreign oil imports, and in order to maintain our economic and military security, the U.S. has formulated a National Energy Strategy Plan. The plan has been developed by the U.S. Department of Energy and is based on the current and future resources in the U.S. which could be economically developed. This plan specifically calls for a production of 900,000 barrels of heavy oil per day. Currently, most of the heavy oil production in the U.S. comes from California. However, although the production of heavy oil from California can be further increased, it could not meet the NES projections by the mid-1990s.

Alaska currently produces about 24% of the nation's output of oil. However, the production from the Prudhoe Bay field providing about 1.5 million barrels a day has begun to decline and must be supplemented by developing other nearby fields for oil flow through the Trans-Alaskan Pipeline to Lower 48 states. Fortunately, Alaska also has the second largest heavy oil resources in the U.S. It is estimated that the super giant West Sak field, which includes Kuparuk River and Milne Point units, contains over 25 billion barrels of oil. The field is so large and widespread that the gravity of the oil varies from 10.0 to 22.5° API. Small production from some regions of this giant field is underway, while others await improved production technology. The past field tests and laboratory studies clearly demonstrated that entirely new and innovative technologies for oil displacement and production will be required for large-scale production from this reservoir.

The shallow Cretaceous sands of the Schrader Bluff reservoir occur between depths of 4,000 and 4,800 feet below surface and are estimated to contain up to 1.5 billion barrels of oil in place. The gravity of oil therein varies between 14 to 21° API. The gravity of the oil in these sands changes rather abruptly from well to well and is of great concern for development of enhanced oil recovery techniques. The average oil gravity is 17 to 18° API. The field is currently under production by primary depletion. Initial production indicated that primary recovery will fall short of earlier estimates and waterflooding will have to be employed much earlier than expected. A

CHAPTER 2

SCHRADER BLUFF RESERVOIR DESCRIPTION

Schrader Bluff Pool lies in the Milne Point Unit and is a part of the West Sak reservoir. Conoco Inc. has drilled 22 wells in Tract 14 (now owned by B.P. Exploration, AK) of Schrader Bluff Pool. The reservoir is complexly faulted with numerous producing horizons separated by shales. Therefore, accurate characterization is necessary to predict fluid flow and production behavior of this reservoir under enhanced oil recovery methods. The following sections provide a brief reservoir description of Schrader Bluff Pool.

B. LOG DERIVED PETROPHYSICAL PROPERTIES

By using geological markers supplied by CONOCO, six unconsolidated N sand members and seven consolidated O sand members were identified in the Schrader Bluff interval. Going from top to bottom these sands can be named as follows:

(a) N Sands

1. Sand NA1
2. Sand NB1
3. Sand NC1
4. Sand NE1
5. Sand NE2
6. Sand NF

(b) O Sands

1. Sand OA1
2. Sand OA2
3. Sand OA3
4. Sand OB4
5. Sand OB1
6. Sand OC1
7. Sand OE

The NB1 and OB1 were identified to be sands of high quality. The NE1, NF, OE, and OC1 sands were identified to be mudstone intervals. The other sands form a spectrum that spans from muddy sands to sandy muds.

Petrophysical properties such as net pay thickness, effective porosity, water saturation, and sand quality were computed for NB1 and OB1 sands by analyzing the well logs using the WORK-BENCH software on an IBM RISC 6000 workstation. The cutoffs used in the well log analysis were as follows: $S_w < 60\%$, $\phi_e > 24\%$, and $V_{sh} = 0$. Archie's water saturation model was used. Contour maps showing the spatial distribution of these petrophysical properties were then prepared and are discussed below.

D. SAND QUALITY DISTRIBUTION

The hydrocarbon pore volume was the parameter used to evaluate the sand quality distribution of the studied sands. Using the previously mentioned cutoffs, illustrative contour maps were generated to show the distribution of sand quality of sand NB1 and sand OB1 across the Schrader Bluff formation.

Figure 2.9 shows the contour map of the distribution of NB1 sand quality over the studied area. It is evident from the map that the best productive NB1 sands occur in the middle of the studied area. The sand quality shows gradual deterioration moving away from the center. The sands on the fringes of the productive sands are also of marginal quality and become poorer further North-East and South-West away from the center. This poor quality can be attributed to the small net pays in the northern and southern portions of the studied area.

Figure 2.10 is the contour map of sand quality generated for the OB1. The sand quality is high in the G-pad wells with the exception of MPU G-2, MPU G-1, and MPU G-5, which exhibited low sand quality. The quality in the southern part of the J-pad and the northern part of the I-pad are of intermediate quality. Wells in the H-pad exhibit low quality.

In general, the NB1 sands exhibit better petrophysical properties than the OB1 sands due partly to the overburden pressure that leads to a decrease in effective porosities of the OB1 sands. The G-pad has the best petrophysical properties, while the H-pad has the poorest. The I and J. pads have petrophysical properties that lie between the two extremes.

however, there is a steep dip between the wells A2 and A1 indicating possible faulting. Following the generation of cross sections, open hole well log analysis was performed. For this purpose, the log traces were first corrected for borehole environment. Then, the bulk density traces were normalized to account for miscellaneous errors by using the same methodology as that used in normalizing the bulk density traces of Tract 14. Table 2.2 lists the wells whose density traces were normalized and the corresponding shift amounts.

After environmental correction and normalization, open hole analysis was run to determine petrophysical properties of the individual zones from top MA1 to base OE1. The following cutoff values were used:

porosity = 25%
water saturation = 60%
shale volume = 0%

Net pay thickness, effective porosity, water saturation, and sand quality (net hydrocarbon pore volume) of each zone in each well were obtained from this open hole analysis. Thus a spatial distribution of the petrophysical properties was obtained.

Based on the results of open hole log analysis, contour maps of net pay thickness, porosity, water saturation, and sand quality for the NA1, NB1, NE1, OA1, and OB1 sands were generated. The remaining sands were determined to be extremely poor quality and hence were not mapped. Sample contour maps of the petrophysical properties for the NB1 and OB1 sands are shown in Figures 2.14 through 2.21. It is evident that NB1 is the best quality sand. Good quality NB1 sand is seen in the northern and eastern sections of the field. OB1 and OA1 show good quality in the southeastern section of the field. The western part of the field generally does not show good sands, NE1 and NA1 are of marginal quality throughout the field.

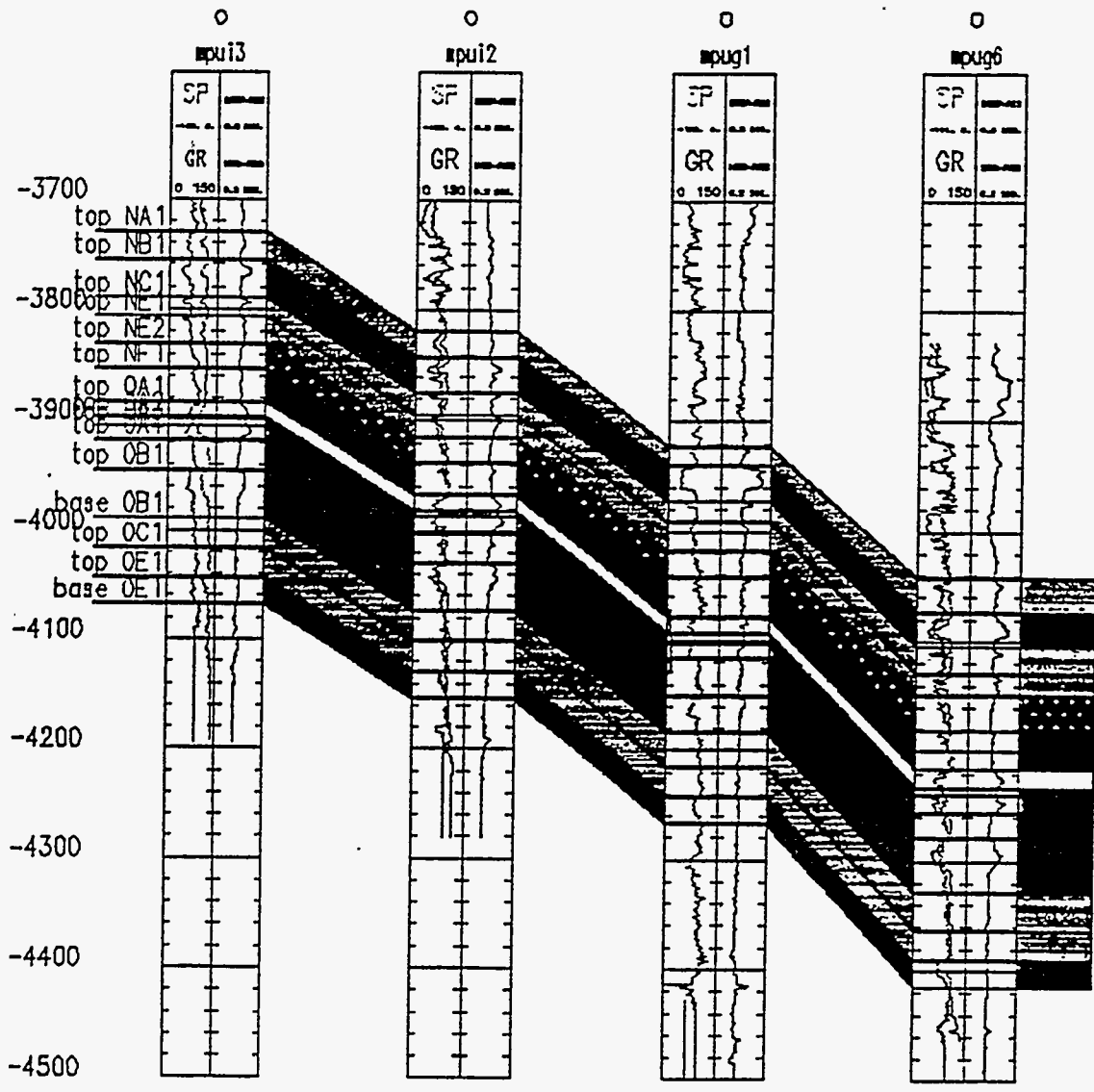


Figure 2.2 SW-NE Cross Section of Schrader Bluff in Tract 14

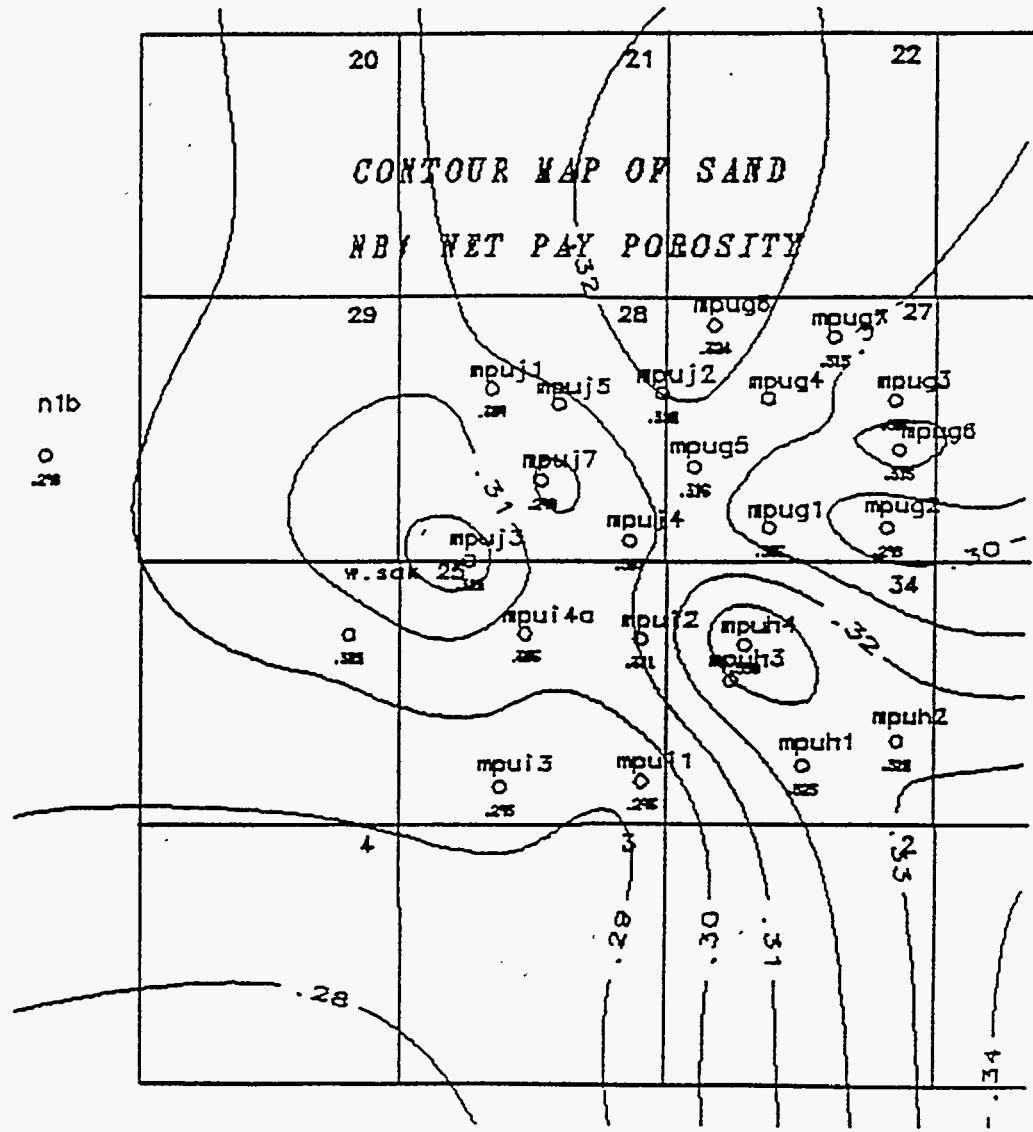


Figure 2.4 Effective Porosity Distribution in Sand NB1

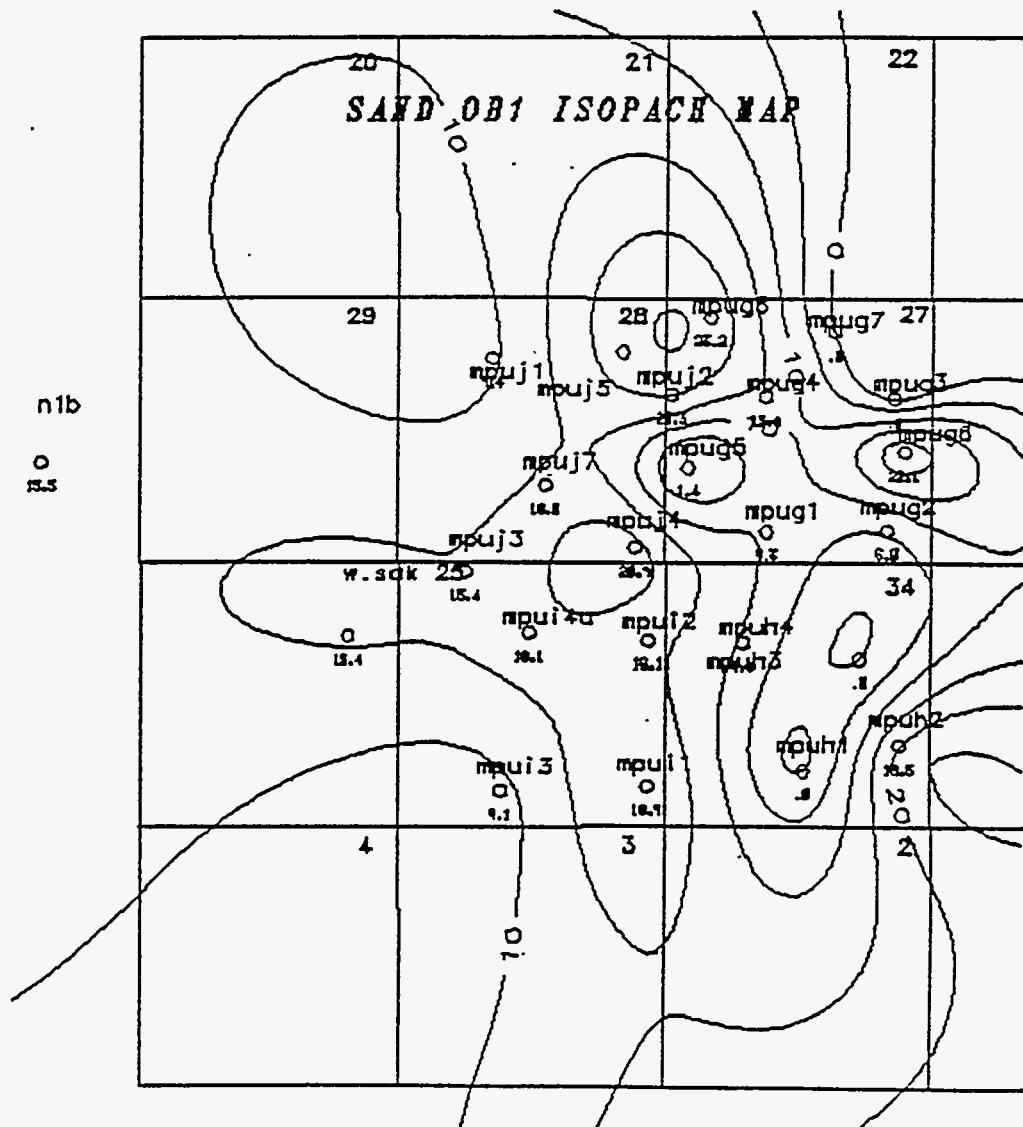


Figure 2.6 Isopach Map of Sand OB1

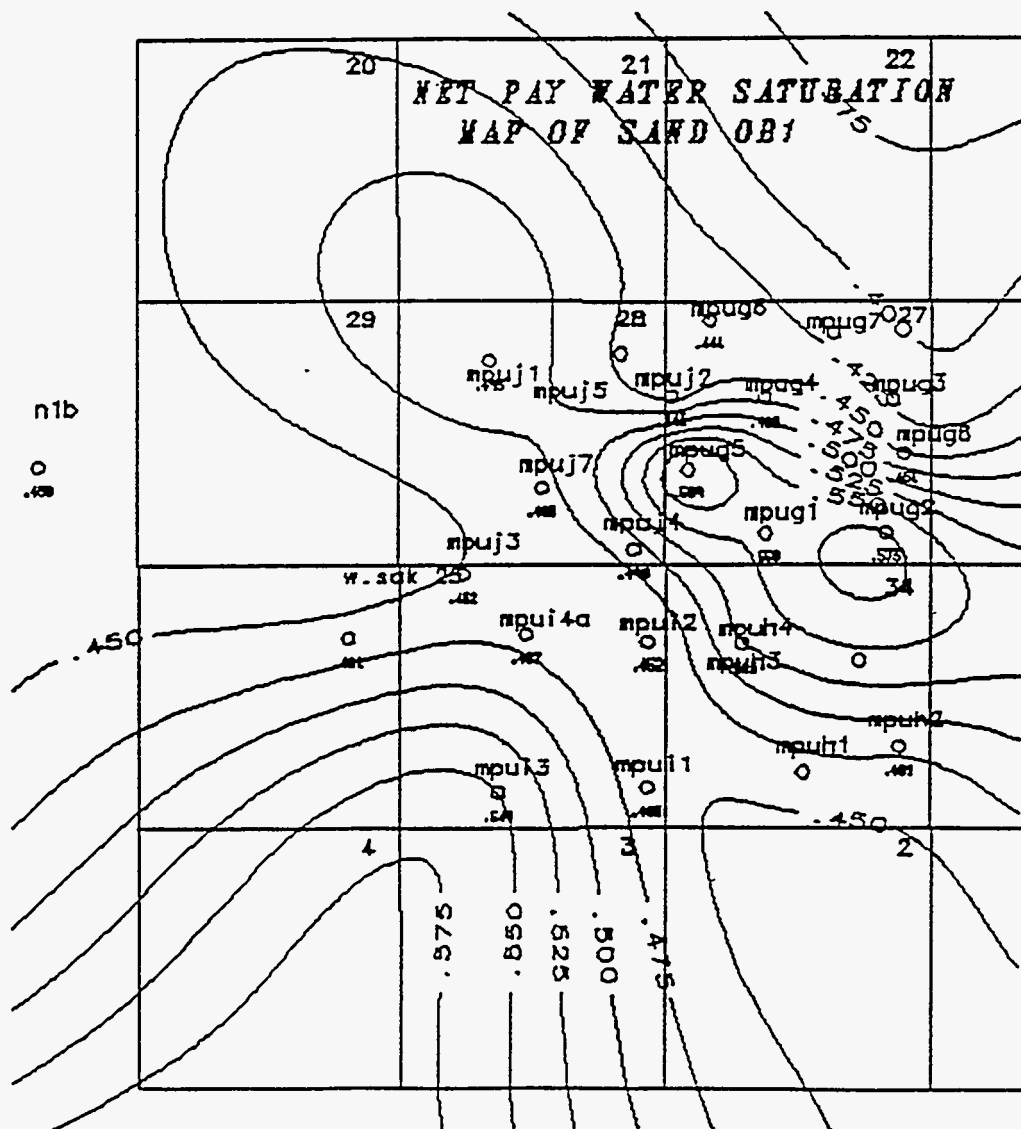


Figure 2.8 Water Saturation Distribution in Sand OB1

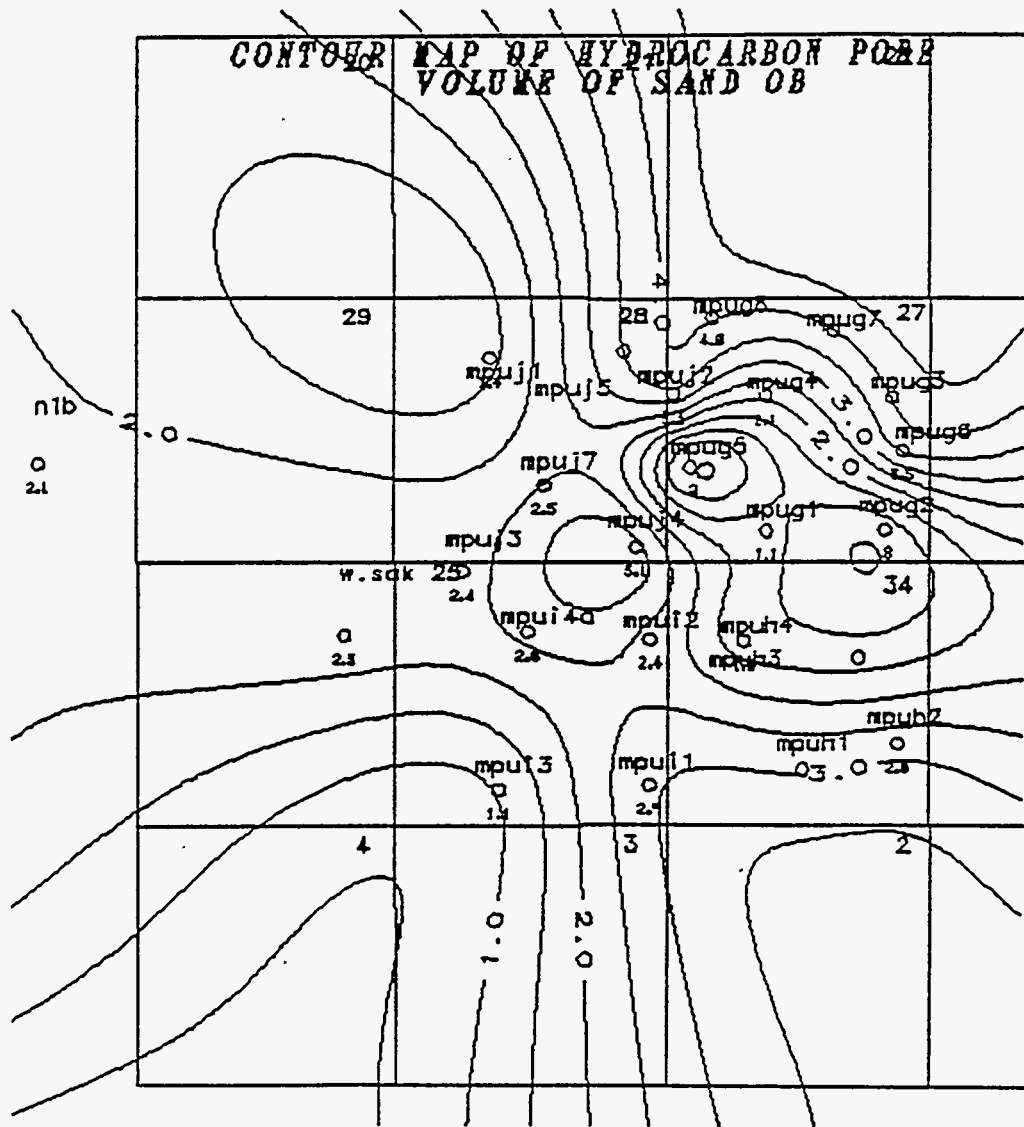


Figure 2.10 Sand Quality Contour Map for OB1

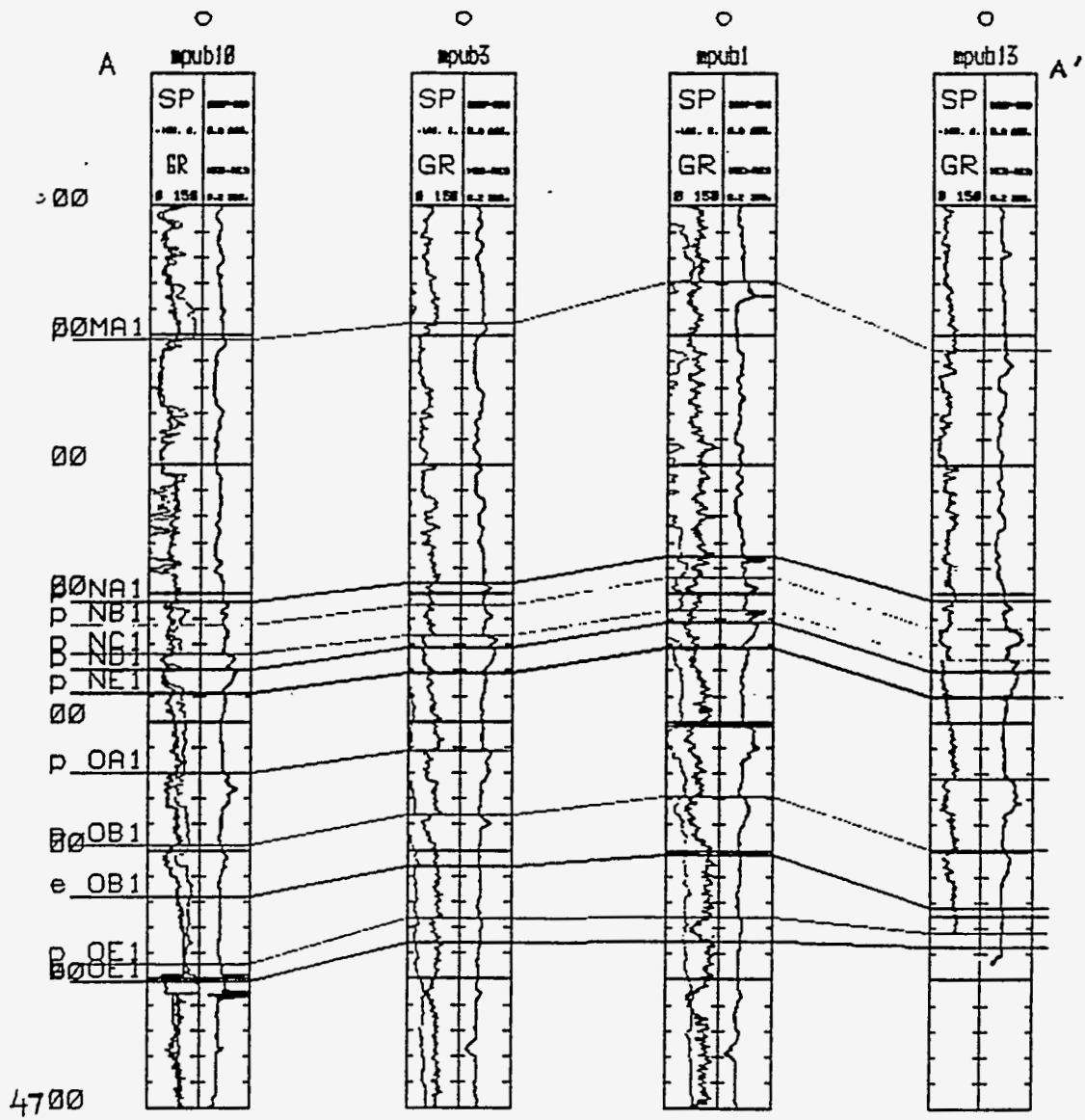


Figure 2.12 NW-SE Stratigraphic Cross Section Along A-A'

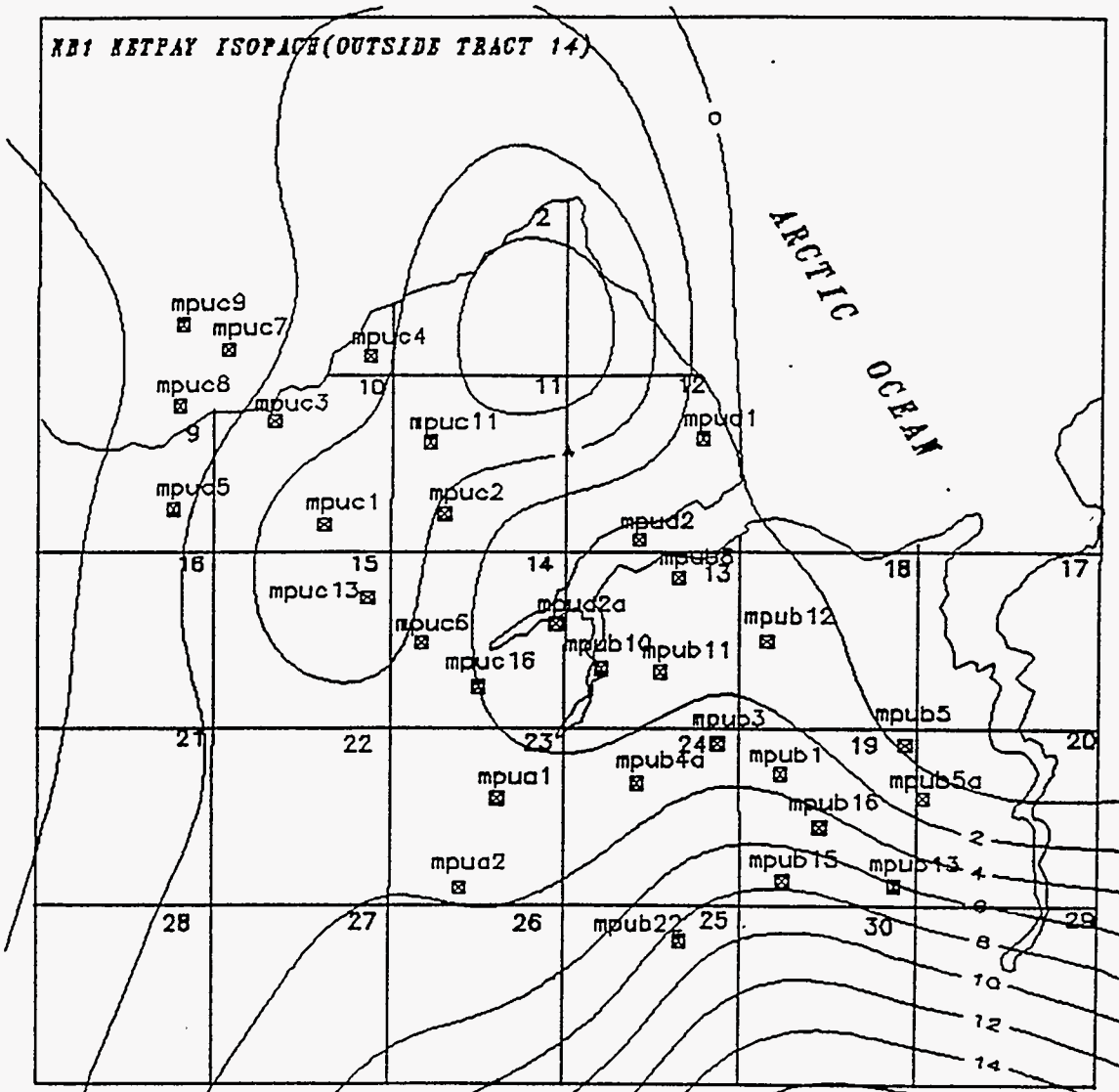


Figure 2.14 Net Pay Isopach for NB1 Sand

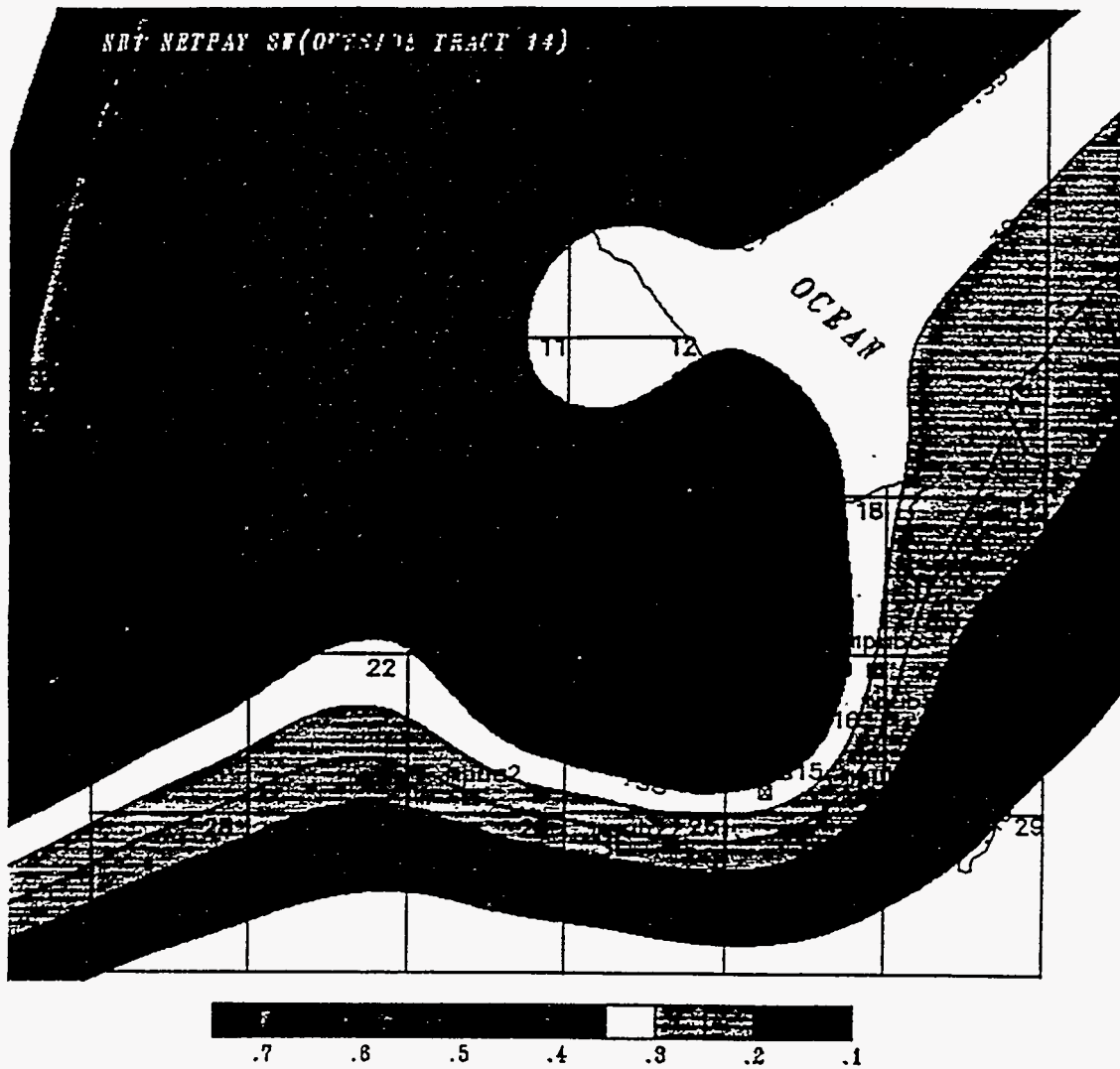


Figure 2.16 Water Saturation Contour Map for NB1 Sand

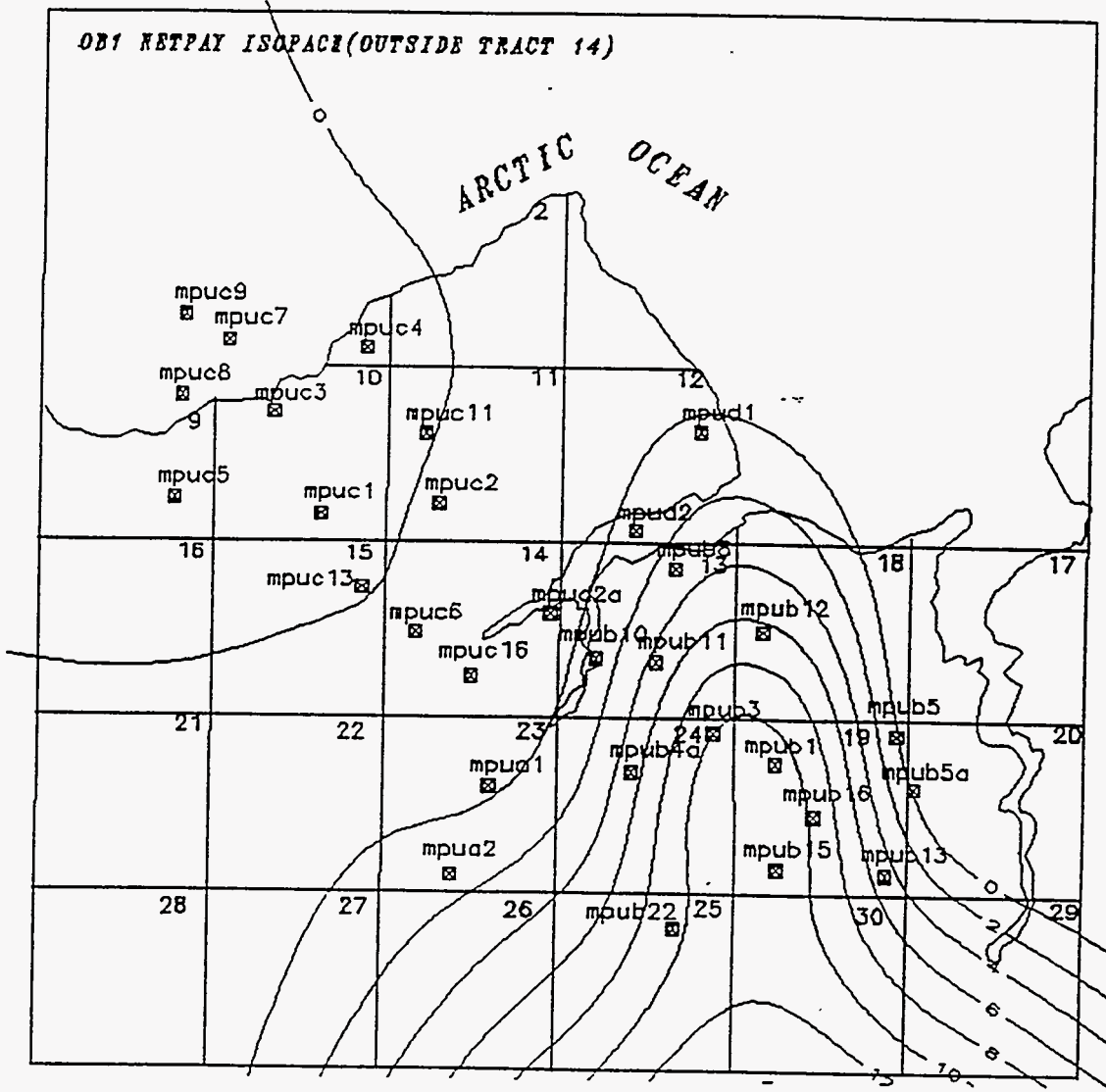


Figure 2.18 Net Pay Isopach for OB1 Sand

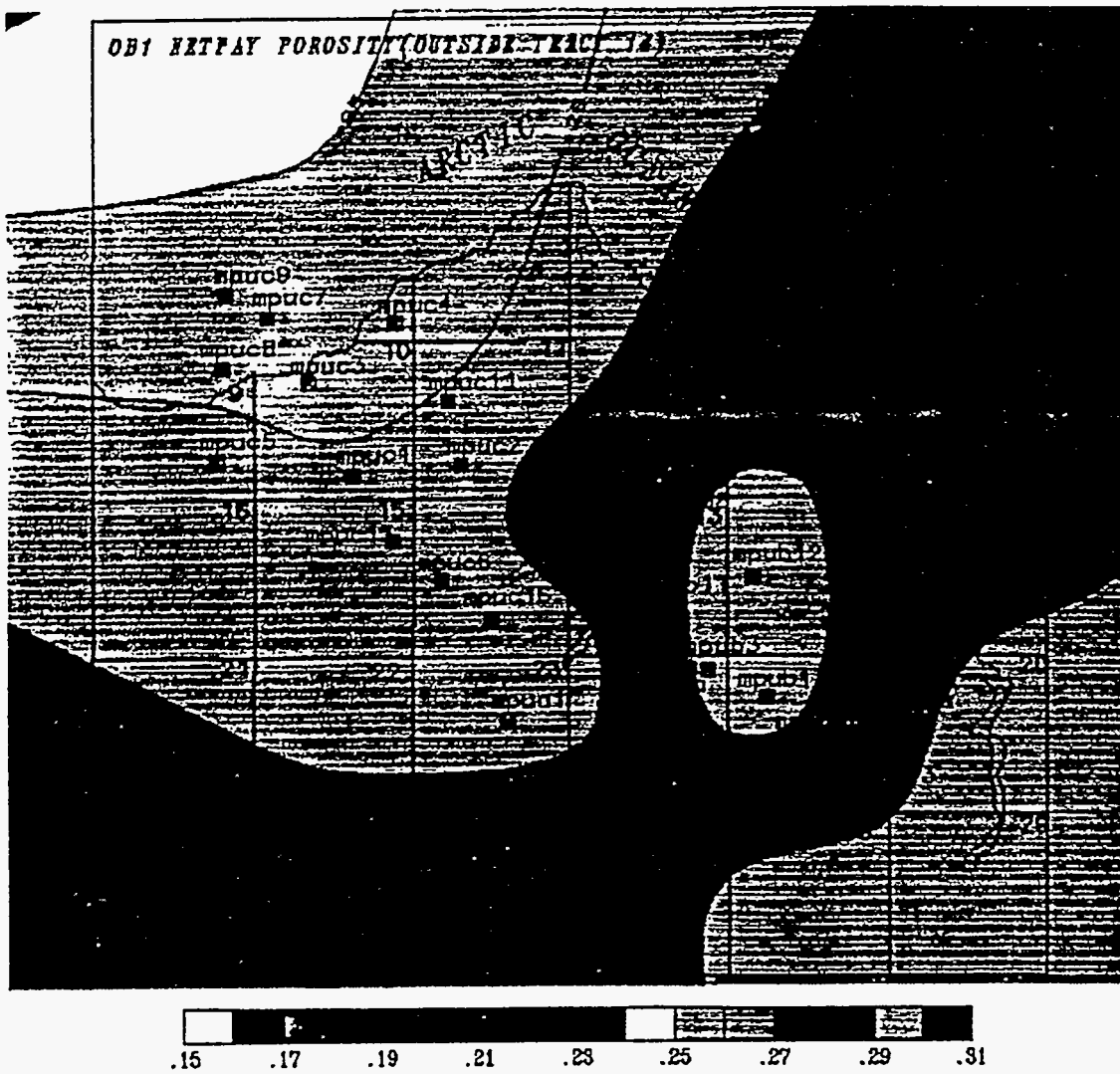


Figure 2.19 Effective Porosity Contour Map for OB1 Sand

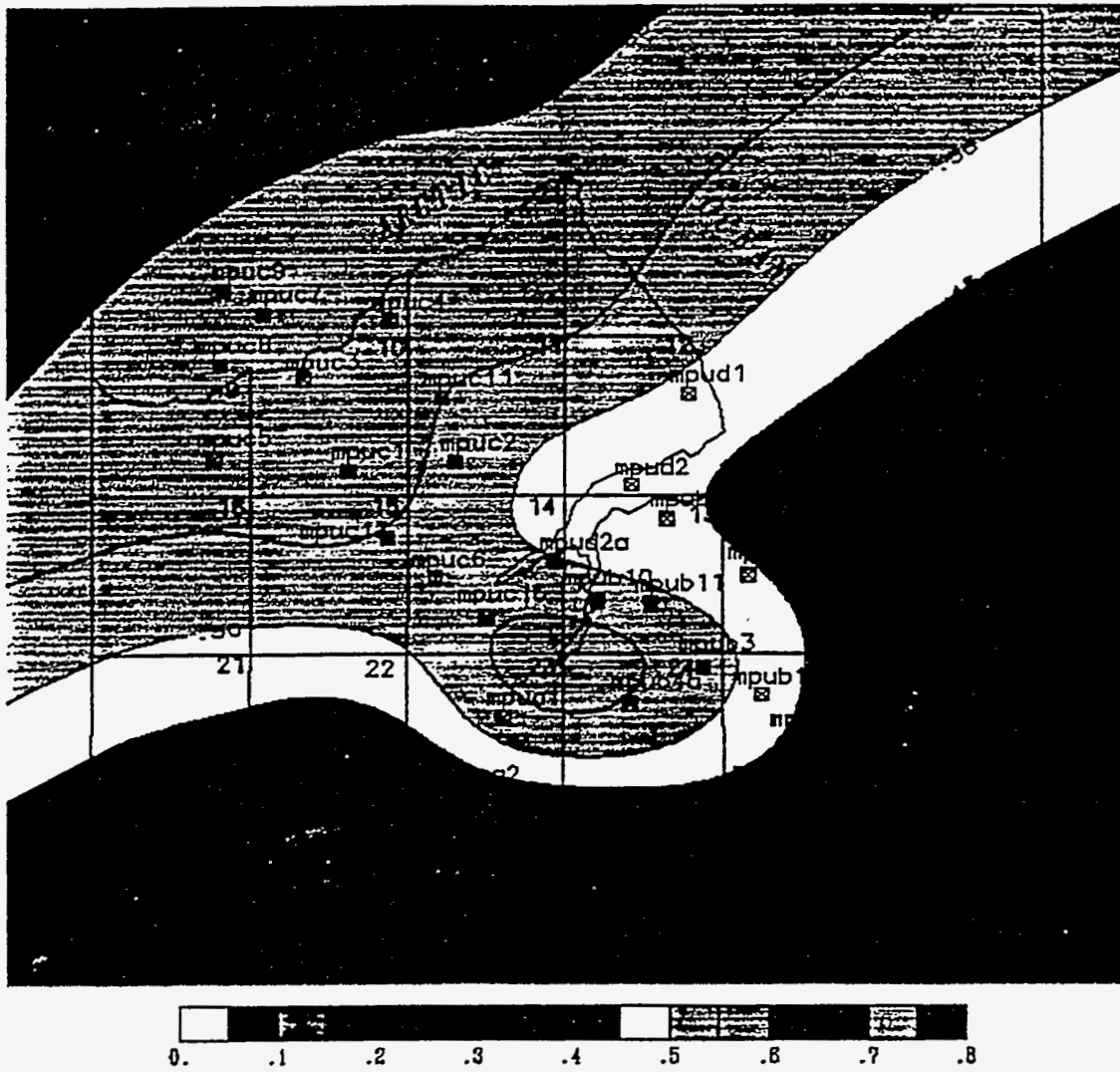


Figure 2.20 Water Saturation Contour Map for OB1 Sand

Table 2.1 List of Milne Point Wells for Second Phase Reservoir Characterization

No	Well Proposed by Conoco	Well Analyzed	Well Status*
1	A-1	A-1	Suspended
2	A-2	A-2	Suspended
3	A-3	A-3	Suspended
4	B-1	B-1	Suspended
5	B-2	B-2	Suspended
6	B-3	B-3	Oil Producer
7	B-4	B-4	Plugged and Abandoned
8	B-4A	B-4A	Oil Producer
9	B-5	B-5	Suspended
10	B-8	B-8	Drilled as a Gas Injector
11	B-10	B-10	Oil Producer
12	B-13	B-13	Oil Producer
13	B-18	No Log Data	Drilled as a Water Injector
14	B-22	No Log Data	Oil Producer
15	C-1	C-1	Suspended Oil Producer
16	C-2	C-2	Oil Producer
17	C-3	C-3	Oil Producer
18	C-4	C-4	Oil Producer
19	C-5	C-5	Plugged and Abandoned
20	C-8	C-8	Converted to Water Injector
21	C-11	C-11	Drilled as a Water Injector
22	C-16	C-16	Converted to Water Injector
23	C-19	C-19	Suspended
24	D-1	D-1	Suspended
25	D-2	D-2	Plugged and Abandoned
26	D-2A	D-2A	Oil Producer
27	E-2	E-2	Suspended
28	E-6	E-6	Oil Producer
29	L-1	L-1	Suspended
30	L-3	No Log Data	Oil Producer
31	L-10	L-10	Drilled as a Gas Injector
32	M-1	M-1	Plugged and Abandoned
33	M-1A	M-1A	Suspended
34	N-1	No Log Data	Plugged and Abandoned
35	N-1A	No Log Data	Plugged and Abandoned
36	N-1B	Analysed in 1st Phase	Suspended

* Well Status are taken from a AOGCC Map of Jan. , 1992

Table 2.2 List of Normalized Wells

Normalized Well	Shift Amount
A-1	+0.10549
A-3	+0.03672
B-13	-0.02538
CFP2	-0.0267
D-1	+0.03556
D-2A	-0.03013
E-2	-0.03135
M-1A	+0.0467
3012	+0.0927
3k6	+0.070

CHAPTER 3

SLIM TUBE DISPLACEMENT STUDIES

A. INTRODUCTION

The API gravity and viscosity of oil in the Schrader Bluff sands varies considerably from horizon to horizon. Thus, a single enhanced oil recovery method may not be sufficient to produce this reservoir. Miscible processes may be more suitable to lighter crude in the deeper sections of Schrader Bluff reservoir. The available natural gas on the North Slope which currently is not marketed, can be enriched to provide injection gas for miscible flooding in Schrader Bluff reservoir. Currently, miscible flood is underway in Prudhoe Bay Unit and Kuparuk River Pool of the Kuparuk River Unit.

Slim tube displacement (STD) tests are usually performed to determine minimum enrichment (ME) requirements at reservoir conditions to achieve multi-contact miscibility (MCM) between enriched solvents and light crudes. In this study, STD tests are being conducted to evaluate characteristics and applicability of this method when applied to heavy crudes. The emphasis of this study is placed on evaluating various solvents such as CO₂, various mixtures of Prudhoe Bay Natural Gas (PBG), Kuparuk-Schrader Bluff Natural Gas (KUPSCH), and natural gas liquids (NGL) for the ability to achieve dynamic miscibility with Schrader Bluff crude. Equation-of-state (EOS) predictions are performed to compare the results of STD tests and to gain further insight into the mechanism of displacement.

Phase behavior of solvent-crude mixtures are the most important tools in understanding the mechanism of miscibility development in either CO₂ drives, or enriched hydrocarbon solvent drives. Pseudo-ternary diagrams have been often used to explain the mechanisms of oil displacement by vaporizing gas drive or condensing gas drives (1). For the past three decades, it has been considered that enriched hydrocarbon miscible displacement occurs via condensing mechanism (2), and high pressure lean miscible hydrocarbon gas (3) displacement occurs via vaporizing mechanism. In condensing gas drives, the in-situ generation of miscibility occurs due to gradual enrichment of reservoir fluids in intermediate components of solvent to a point where it becomes fully miscible with the injected solvent. In the vaporizing drive

on the other hand, the in-situ generation of miscibility occurs due to extraction of intermediate components of the reservoir fluid by the solvent and its gradual enrichment with these intermediates as it flows in the reservoir. The displacement by any mechanism is further characterized with the help of pseudo-ternary diagram as immiscible (IMM), multi-contact miscible (MCM), and first contact miscible (FCM) (4). In 1960, Benham et al. (5), proposed a method of predicting minimum miscibility pressure (MMP) or minimum enrichment (ME) required to achieve multi-contact miscibility by constructing pseudo-ternary diagrams and determining limiting tie-line intersections with the light-intermediate component axis. This method has been used ever since, although it has been updated slightly in recent years (6, 7).

However, the work of Stalkup (8) and Zick (9) challenged this traditional concept for some rich gas displacements. Zick (9) provided evidence indicating that the mechanism of enriched gas drives is not condensing type, but it is simultaneously both vaporizing and condensing types.

Recently, Novasad and Costain (10) using STD tests and EOS calculations showed that in Canadian reservoir rich gas projects the principal mechanism is liquid extraction drive, and provided further interpretation of this process.

A more rigorous procedure for determining minimum enrichment (ME) or minimum miscibility pressure (MMP) in case of a dual drive mechanism calls for proper characterization of reservoir fluid and solvent, determination of compositional path followed by solvent-reservoir fluid mixtures in multi-contact test calculations, and use of solvent-reservoir fluid, pressure-composition isothermal diagrams. This procedure was used to determine solvent enrichments.

B. RESERVOIR FLUID CHARACTERIZATION

Reservoir fluid characterization is one of the most important considerations in simulation of slim tube experiments and simulation of miscible flood performance in a reservoir. PVT simulator, developed by Scientific Software Intercomp, is used in developing reservoir fluid characterization for Schrader Bluff crude. The PVT simulator is useful in simulating and/or matching laboratory PVT tests. Its regression capabilities allow determination of EOS parameter values, which results in the best agreement between calculated data and laboratory data. These EOS parameters determined from this simulator can be used as an input data for multidimensional compositional reservoir simulation models.

The PVT simulator is capable of simulating saturation pressure calculations, density, viscosity calculations, flash expansion calculations, flash calculations, and multiple contact calculations experiments. This simulator splits any plus fraction in hydrocarbon systems into an automatically determined or specified number of extended fractions. This simulator uses Redlich-Kwong, Zudkevitch-Joffe-Redlich-Kwong, Soave-Redlich-Kwong, and Peng-Robinson equation-of-state equations. Peng-Robinson equation-of-state is used in the fluid characterization of Schrader Bluff reservoir oil.

From the laboratory PVT report of Schrader Bluff reservoir oil, the fluid system consists of thirteen components, from C1 to C11+, N₂, and CO₂. These thirteen components are regrouped into ten components using two pseudo-components. C6 to C8 is grouped into one pseudo-component (PC1) and C9 to C10 group is grouped into another pseudo-component (PC2). The grouping of these pseudo-components is done on weight basis. Regression is reported on the pseudoized system for optimal match with laboratory data.

C. MULTIPLE CONTACT TEST RUNS

The EOS parameters obtained from the regression on the pseudoized fluid system are used in conducting multiple contact tests using PVT simulator. Multiple contact tests were performed up to fifteen contacts. In Schrader Bluff reservoir, the produced gas from the reservoir is reinjected back into the Schrader Bluff formation. 90% of the gas is produced from Kuparuk formation and 10% is from Schrader Bluff formation. From the PVT analysis report of these two gases, their compositions are mixed in the ratio 9:1 to obtain the injected gas (KUPSCH GAS) composition. The injection gas is enriched with different amounts of NGL in each multiple contact test run. The enrichment of NGL varied from 0 to 45%. The multiple contact test runs were conducted for 0, 5, 15, 25, and 35% of NGL enrichment with the lean gas.

Figures 3.1 through 3.3 show the results obtained from the multiple contact test runs. These figures are plotted for density vs. number of contacts. For a miscible test run, the liquid and gas density vs. number of contacts should converge, showing that the two fluids form one phase. From these figures, it is clear that these runs did not result in miscibility since the gas and liquid density lines do not converge. The liquid density decreases gradually due to the in-situ mass transfer of intermediates from liquid phase to gas phase.

Figures 3.4 through 3.6 are plotted for equilibrium constants, K-values for different fractions (C1, C2, C3, C4, C5, PC1, PC2, and C11+) vs. number of contacts. For a miscible test run all lines representing each fraction in the K-value plots should converge to an equilibrium constant value of one. These K-plots also do not show achievement of miscibility since the lines do not converge to a value of one.

D. SLIM TUBE SIMULATION

The EOS parameters obtained from the PVT simulator are used to simulate slim tube displacement runs on GEM simulator, developed by Computer Modelling Group. The EOS parameters are included in Table 3.1. GEM is a multidimensional EOS compositional simulator which can simulate all the important mechanisms of a miscible gas injection process, i.e., vaporization and swelling of oil, condensation of gas, viscosity and IFT reduction, and the formation of a miscible solvent bank through multiple contacting. GEM can be run in explicit, fully implicit, and adaptive implicit modes. GEM uses dual porosity and dual permeability models. GEM simulator can also perform flash calculations. The quasi-Newton successive substitution method is used to solve the nonlinear equations associated with flash calculations. GEM utilizes either the Peng-Robinson or Soave-Redlich-Kwong equation-of-state equations. Peng-Robinson EOS is used in the simulation of slim tube experiments.

In the experimental setup, the slim tube is 40 feet in length and is coiled in one foot diameter. The slim tube has an outer diameter of 0.236 inches, and it is filled with Ottawa sand of 0.352 porosity and 5 darcy permeability. The pore volume of the slim tube is determined by injecting toluene.

For simulation purposes, slim tube is represented by one dimensional model of $40 \times 1 \times 1$ grid blocks. Each grid block is one foot in length, and in j and k directions lengths are adjusted to represent exact slim tube volume. One injector and one producer are included in this model at the first and last block respectively. The grid diagram is shown in Figure 3.7. The slim tube porosity and permeability values are input into the simulator. The solvent injection rate was maintained at 3 cc/hr and a total of 1.2 PV of solvent is injected in each simulation run.

GEM simulator has two models, large memory model and small memory model. Small memory model handles greater numbers of components than large memory model. Small memory model uses ten components. All the EOS parameters for the regular components are stored in the simulator. For user defined components, all the EOS parameters have to be input into the simulator. The EOS parameters listed in Table 3.1 for pseudo-components and plus fractions are input into the GEM simulator. Slim tube simulation results are compared with the experimental results in the later sections.

E. EXPERIMENTAL APPARATUS

To obtain accurate data in laboratory experiments, it is essential that certain requirements are met. Extremely accurate flow control must be maintained at all pressures. Reliable pressure readings should be monitored frequently throughout the experimental run. Accurate and constant back pressure must be kept throughout the run. A reliable method for measuring volumes of fluids under high pressures and at atmospheric conditions must be available. In order to meet these requirements and assure the reproducibility of the resulting data, the high pressure high temperature miscibility apparatus designed by D.B. Robinson and Assoc. was modified, assembled, and used in the laboratory to determine MMP relations. This assembly is schematically shown in Figure 3.8. The major components of this assembly consist of the following:

1. One motorized positive displacement pump.
2. One slim tube.
3. Two forced air temperature controlled ovens.
4. One high pressure capillary sight glass.
5. Three digital pressure gauges.
6. One differential pressure transducer.
7. One calibrated glass receiver and optical liquid measuring device.
8. One precision 40 liter gasometer.
9. Six transfer cells.
10. One recombination cell and shaking device.
11. One dome type back pressure regulator.
12. One high volume vacuum pump.
13. One Constametric pump.

The equipment was designed for operation at pressures up to 10,000 psi and temperatures to 200°C. The driving force behind the slim tube miscibility apparatus was the motorized JEFRI positive displacement pump which was used throughout the experiment to accurately meter, feed and proportionately displace liquids and gases under high pressure. More specifically, it effectively had four functions.

1. Provide constant pressure while recombining West Sak Crude samples.
2. Compress and transfer gases and NGLs during the solvent mixing process.

3. Drive recombined oil to saturate the slim tube before each run and drive solvents to clean the slim tube after each run.
4. Inject the gas solvent mixture during each run.

The pump was equipped with a DC servo motor and chain drive which in turn was controlled by a microprocessor indexer. This allowed the pump to either displace fluids at constant flow rates from 1 to 1,000 cc/hr, or to maintain a constant pressure, regardless of the direction of flow, at variable speeds. Pump operation could be monitored throughout the run with the use of high and low pressure limit alarms.

The slim tube itself was composed of a 12 meter section of 6.4 mm O.D. high pressure stainless steel tubing which was packed with Ottawa sand and coiled to a diameter of approximately one foot. The final porous medium had an average porosity of roughly 35.2% which could provide an average frontal advance rate of about 120 cm/hr. Average slim tube permeability was calculated to be 5.0 darcies, using pure toluene as the test fluid of known viscosity.

The slim tube and recombination cell were enclosed in a windowed, forced air, temperature controlled oven. Oven temperature was controlled through the simultaneous heating of a main bulk heating coil and a smaller microprocessor controlled heating coil. The main bulk heater was set with a simple rheostat and was the main source for the oven, while smaller coils were used to control the oven's temperature within 0.2°C of the desired set point. During operation, the main bulk heater was set to a few degrees below the desired temperature according to an individual calibration curve. Additional heat, provided by the small coils, raised the temperature to the desired setting and was constantly monitored by a thermocouple and microprocessor. In the event that the main bulk temperature increased above the desired point, due to an increase in ambient temperature or decrease in volumetric flow rate through the slim tube due to reduced flashing, an alarm set point had the ability to shut down the main heat source until temperature control was once again achieved.

At the effluent end of the slim tube, a JEFRI high pressure capillary sight glass was used to visually observe displaced fluids during the dynamic miscible process. The sight glass consisted of a Pyrex capillary tube, 4.390 inches in length with a 7.7 mm I.D. and 1.5 mm O.D., mounted within a windowed overburden cell. In the overburden cell, distilled water was compressed by a hand operated pressure generator

to a pressure approximately 300 psi. greater than that within the capillary tube. While maintaining this pressure differential, it was possible to observe the transient phase behavior of fluids at operating conditions of up to 200°C and 10,000 psi. Visibility was excellent due to the fact that the overburden fluid had similar refractive characteristics to that of glass, decreasing refractive distortion between the windowed cells.

The overall operating pressure of the slim tube system was controlled by a gas driven, dome type back pressure regulator. Operating on the principle of balanced pressure, a stainless steel diaphragm separated the effluent pressure from the pressure exerted by the operator's set point. A pressure reaction chamber allowed for precise pressure imbalance control thus maintaining predetermined run pressures.

Once the effluent is flashed to atmospheric conditions, through the back pressure regulator, the resulting gas and liquid components were collected and measured volumetrically. The gas was measured by a JEFRI precision gasometer using a calibrated stainless steel cylinder and piston fixed to a threaded rod which was linked to an electric motor. As gas entered the cylinder, atmospheric pressure was maintained in the gasometer by a system which moved the piston to expand the cylinder's volume. Such volume control was achieved using an oil filled manometer equipped with a pair of optical interrupter switches. An increase in pressure within the cylinder was indicated by a change in manometer fluid meniscus level. Any such change in meniscus level was noted by the optical sensors, and a signal was sent to the motor drive which increased the volume of the cylinder to accommodate the additional gas. Piston location was measured and displayed by an optical linear encoder, and converted through a calibrated constant to standard cubic centimeters.

A specially designed glass cylinder collected the condensed liquid after it passed through a condenser. An optical sensor, similar to that used in the gasometer, was mounted on a motor driven lead-screw. As the opaque oil meniscus rose up the glass cylinder it interrupted the path of the laser sighted optical sensor, which in turn signaled the motor to raise it according to the level of the air liquid interface. Once again, a linear encoder measured the calibrated sensor level which was converted into cubic centimeters of oil.

During the run, the upstream pressure was monitored by a precision pressure transducer linked to the motorized pump's microprocessor, while the downstream

pressure was monitored by a digital Heise pressure gauge. An external Heise gauge was also linked into the system to monitor gas pressures during solvent mixing. A Validine differential pressure transducer was used to monitor the differential pressure across the slim tube during the displacement process. The external Heise gauge was calibrated using a dead weight tester and was then used to calibrate the other gauges.

Six cells, five of them with pistons and one without a piston, were used to recombine oil, mix solvents, and transfer fluids during each experiment. Two of the pistoned cylinders, manufactured by Temco of Tulsa, OK., were used to compress gas for solvent mixtures and the back pressure regulator, as well as drive cleaning solvents through the slim tube. The remaining JEFRI cylinders were used to recombine oil, transfer NGLs, and drive final solvent mixtures during each experimental run. Whether pistoned, or unpistoned cylinders used with mercury, each cell was rated to 10,000 psi and designed to be used with single phase fluids. For this reason, it was imperative that the gas solvent mixture used in each experiment existed in a single phase to insure consistent composition throughout the run.

Each piece of equipment was connected with 1/8 and 1/16 inch high pressure 316 stainless steel tubing and HIP fittings. Generally, lines containing liquid were of the larger 1/8 inch O.D. to accommodate the fluid's higher viscosity, while gas lines were constructed of 1/16 inch tubing. Whenever possible, it was important to reduce line size and length to minimize dead volume in the apparatus. The HIP fittings used were easily broken and refitted without reducing their high pressure sealing capabilities.

When transferring fluids from one cell to another through stainless steel tubing, it was necessary to thoroughly evacuate the system to maintain compositional purity and avoid contamination. This was accomplished with the use of a Welsh high volume vacuum pump capable of inducing effective vacuums down to 50 microns. Generally, less than 200 microns were achieved before transferring oil, solvents, or gases.

F. EXPERIMENTAL PROCEDURE

It was very important to accurately measure the pore volume of the slim tube to determine oil recovery. Toluene was used to find the pore volume of the slim tube. The slim tube is evacuated first and then isolated from inlet valve to the inlet valve of the BPR. A piston cylinder filled with toluene was pressurized using positive displacement pump, to pressure of 2,000 psi, which is above the vapor pressure of toluene at room temperature. The initial pump reading was noted and then the inlet valve of the slim tube was opened slowly and pumping of toluene was started under the displacement pump's constant pressure mode. Once the slim tube pressure was equilibrated at 2,000 psi, a final pump reading was recorded. The amount of toluene injected was obtained from subtracting initial and final readings. To this value 0.22 cc was added to account for the dead volume of the back pressure regulator (BPR). Thus the pore volume of the slim tube was determined to be 76.82 cc.

Before each experimental run, injected solvent is prepared in the solvent chamber. When pure carbon dioxide was used as solvent it was simply compressed in one of the transfer cells and injected into the solvent chamber. The same process was followed when Kuparuk-Schrader Bluff and Prudhoe Bay Gas (PBG) were used as solvents. However, for the preparation of mixtures of CO₂ and NGL, or PBG and NGL, a series of calculations were done to obtain the volume of each component required to obtain the desired solvent mixture. The calculated volumes were injected into the solvent chamber which was then rocked to give a uniform, single phase mixture.

The next step was to prepare a "live" oil sample from the "dead" oil sample. The calculated amount of "dead" oil was taken into the recombination cell and then by injecting solution gas the cell was pressurized to bubble point pressure. The cell was rocked for over twelve hours for thorough mixing of gas and oil. As the gas started dissolving in solution, the pressure in the cell dropped. Pressure reduction was monitored by the pump. This process was repeated until the oil was saturated at the bubble point pressure.

The recombined oil was then used to saturate the slim tube. While saturating the slim tube, it was very important to maintain the slim tube pressure above the bubble point pressure at experimental temperature, to make sure that oil was never allowed to flash. This was done by raising the pressure of the BPR to above the bubble

STUDY OF HYDROCARBON MISCIBLE SOLVENT SLUG INJECTION
PROCESS FOR IMPROVED RECOVERY OF HEAVY OIL FROM
SCHRADER BLUFF POOL, MILNE POINT UNIT, ALASKA

FINAL REPORT

NOVEMBER 1995

Work Performed Under Contract No. DE-FG22-93BC14864

Prepared for
U.S. Department of Energy
Assistant Secretary for Fossil Energy

Thomas B. Reid, Project Manager
Bartlesville Project Office
P.O. Box 1393
Bartlesville, OK 74005

Prepared by
University of Alaska Fairbanks
Petroleum Development Laboratory
Fairbanks, AK 99775-5389

MASTER

DEC 7 1995
LIBRARY
U.S. DEPARTMENT OF ENERGY

ABSTRACT

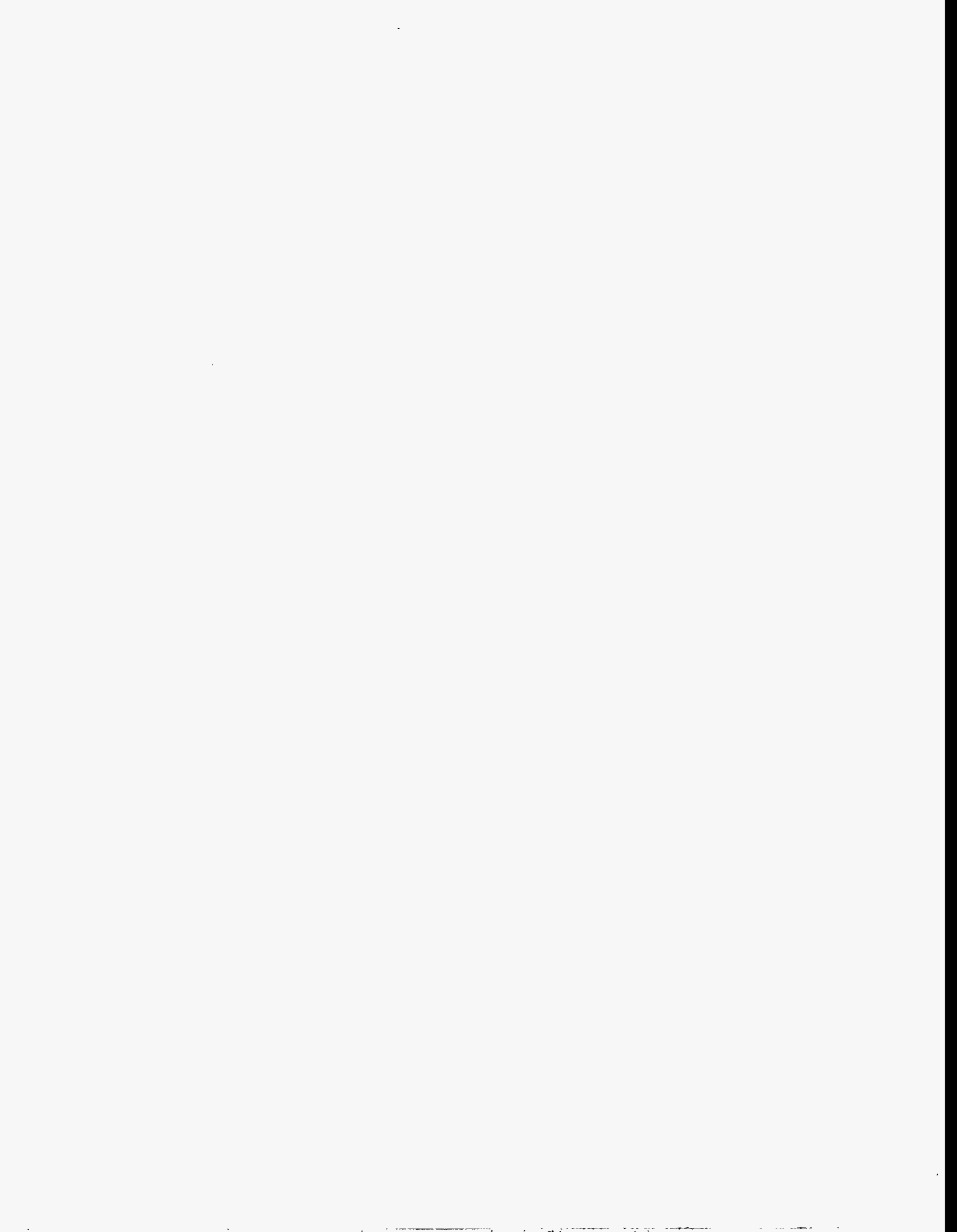
The National Energy Strategy Plan (NES) has called for 900,000 barrels/day production of heavy oil in the mid-1990s to meet our national needs. To achieve this goal, it is important that the Alaskan heavy oil fields be brought to production. Alaska has more than 25 billion barrels of heavy oil deposits. Conoco, and now BP Exploration have been producing from Schrader Bluff Pool, which is part of the super heavy oil field known as West Sak Field.

Schrader Bluff reservoir, located in the Milne Point Unit, North Slope of Alaska, is estimated to contain up to 1.5 billion barrels of (14 to 21° API) oil in place. The field is currently under production by primary depletion; however, the primary recovery will be much smaller than expected. Hence, waterflooding will be implemented earlier than anticipated. The eventual use of enhanced oil recovery (EOR) techniques, such as hydrocarbon miscible solvent slug injection process, is vital for recovery of additional oil from this reservoir.

The purpose of this research project was to determine the nature of miscible solvent slug which would be commercially feasible, to evaluate the performance of the hydrocarbon miscible solvent slug process, and to assess the feasibility of this process for improved recovery of heavy oil from Schrader Bluff reservoir. The laboratory experimental work includes: slim tube displacement experiments and coreflood experiments. The components of solvent slug includes only those which are available on the North Slope of Alaska.

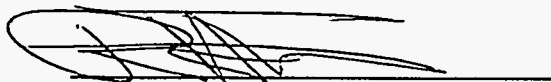
DISCLAIMER

This report was prepared as an account of work sponsored by an agency of the United States Government. Neither the United States Government nor any agency thereof, nor any of their employees, makes any warranty, express or implied, or assumes any legal liability or responsibility for the accuracy, completeness, or usefulness of any information, apparatus, product, or process disclosed, or represents that its use would not infringe privately owned rights. Reference herein to any specific commercial product, process, or service by trade name, trademark, manufacturer, or otherwise does not necessarily constitute or imply its endorsement, recommendation, or favoring by the United States Government or any agency thereof. The views and opinions of authors expressed herein do not necessarily state or reflect those of the United States Government or any agency thereof.



ACKNOWLEDGEMENT

This report was prepared for the U.S. Department of Energy under the Cooperative Agreement No. DE-FG22-93BC14864. The financial support of the U.S. Department of Energy, Bartlesville Project Office is gratefully acknowledged. The matching support was provided by the Petroleum Development Laboratory, University of Alaska Fairbanks, and Conoco, Inc. The research work described herein was made possible by the cooperation and assistance of North Slope Operators, who provided oil and gas samples. This report is a result of the work performed by Dr. G.D. Sharma, Principal Investigator, and the following co-investigators: Dr. V.A. Kamath, Dr. Santanu Khataniar, and Mr. Shirish L. Patil; and the following graduate students: Ansar Ali, Maruti Inaganti, and Santosh Chandra.



Dr. Robert H. Trent, Director
Petroleum Development Laboratory

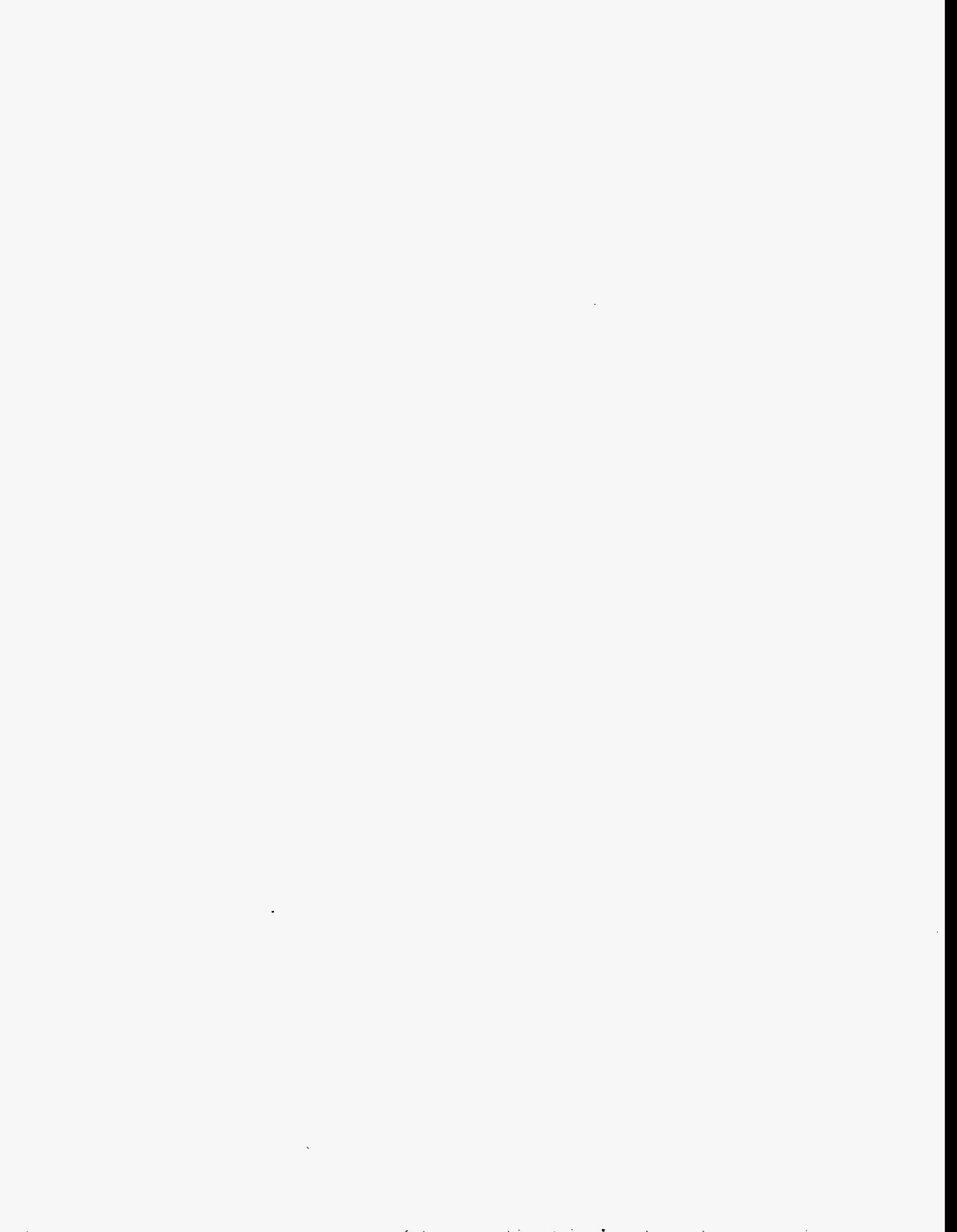


TABLE OF CONTENTS

ABSTRACT.....	ii
ACKNOWLEDGEMENT	iii
LIST OF FIGURES.....	v
LIST OF TABLES	xi
CHAPTER 1: INTRODUCTION	1.1
CHAPTER 2: SCHRADER BLUFF RESERVOIR DESCRIPTION	2.1
A. Characterization of Tract 14 Wells	2.2
B. Log Derived Petrophysical Properties.....	2.3
C. Spatial Distribution of Petrophysical Properties.....	2.4
D. Sand Quality Distribution.....	2.5
E. Characterization of Schrader Bluff Pool (Outside Tract 14).....	2.6
CHAPTER 3: SLIM TUBE DISPLACEMENT STUDIES	3.1
A. Introduction.....	3.1
B. Reservoir Fluid Characteristics.....	3.3
C. Multiple Contact Test Runs.....	3.4
D. Slim Tube Simulation	3.5
E. Experimental Apparatus	3.6
F. Experimental Procedure.....	3.10
G. Results and Discussions	3.12
H. Conclusions	3.17
I. References	3.18
J. APPENDIX	3.48
CHAPTER 4: COREFLOOD EXPERIMENTS	4.1
A. Introduction.....	4.1
B. Experimental Apparatus	4.2
C. Experimental Procedure.....	4.5
D. Results and Discussions	4.8
E. Conclusions	4.16
F. APPENDIX	4.80

LIST OF FIGURES

<u>Figure No.</u>	<u>CHAPTER 2</u>	<u>Page</u>
2.1	NW-SE Cross Section of Schrader Bluff in Tract 14.....	2.8
2.2	SW-NE Cross Section of Schrader Bluff in Tract 14.....	2.9
2.3	Isopach Map of Sand NB1.....	2.10
2.4	Effective Porosity Distribution in Sand NB1.....	2.11
2.5	Water Saturation Distribution in Sand NB1.....	2.12
2.6	Isopach Map of Sand OB1.....	2.13
2.7	Effective Porosity Distribution in Sand OB1.....	2.14
2.8	Water Saturation Distribution in Sand OB1.....	2.15
2.9	Sand Quality Contour Map for NB1.....	2.16
2.10	Sand Quality Contour Map for OB1.....	2.17
2.11	Base Map With Locations of Milne Point Wells Outside Tract 14.....	2.18
2.12	NW-SE Stratigraphic Cross Section Along A-A'.....	2.19
2.13	NE-SW Stratigraphic Cross Section Along C-C'.....	2.20
2.14	Net Pay Isopach for NB1 Sand.....	2.21
2.15	Effective Porosity Contour Map for NB1 Sand.....	2.22
2.16	Water Saturation Contour Map for NB1 Sand.....	2.23
2.17	Sand Quality Distribution for NB1 Sand.....	2.24
2.18	Net Pay Isopach for OB1 Sand.....	2.25
2.19	Effective Porosity Contour Map for OB1 Sand.....	2.26
2.20	Water Saturation Contour Map for OB1 Sand.....	2.27
2.21	Sand Quality Distribution for OB1 Sand.....	2.28

CHAPTER 3

3.1	Density vs. Contact Number (100% KUPSCH Gas).....	3.20
3.2	Density vs. Contact Number (85% KUPSCH/15% NGL).....	3.21
3.3	Density vs. Contact Number (65% KUPSCH/35% NGL).....	3.22
3.4	K-value vs. Contact Number (100% KUPSCH Gas).....	3.23
3.5	K-value vs. Contact Number (85% KUPSCH/15% NGL).....	3.24
3.6	K-value vs. Contact Number (65% KUPSCH/35% NGL).....	3.25
3.7	Grid Blocks for Simulating Slim Tube Experiments.....	3.26
3.8	Schematic Diagram of Slim Tube Experimental Setup.....	3.27

LIST OF FIGURES (CON'T.)

3.9	P-X Diagram for CO ₂ /NGL Mixture.....	3.28
3.10	P-X Diagram for PBG/NGL Mixture.....	3.29
3.11	Slim Tube Displacement Experiment and Simulation Results (Solvent: 100% Kuparuk-Schrader Bluff Gas)	3.30
3.12	Slim Tube Displacement Experiment and Simulation Results (Solvent: 100% CO ₂)	3.31
3.13	Slim Tube Displacement Experiment and Simulation Results (Solvent: 90% CO ₂ and 10% NGL)	3.32
3.14	Slim Tube Displacement Experiment and Simulation Results (Solvent: 85% CO ₂ and 15% NGL)	3.33
3.15	Slim Tube Displacement Experiment and Simulation Results (Solvent: 100% Prudhoe Bay Gas)	3.34
3.16	Slim Tube Displacement Experiment and Simulation Results (Solvent: 70% PBG and 30% NGL)	3.35
3.17	Slim Tube Displacement Experiment and Simulation Results (Solvent: 60% PBG and 40% NGL)	3.36
3.18	Slim Tube Displacement Experiment and Simulation Results (Solvent: 50% PBG and 50% NGL)	3.37
3.19	Density vs. Number of Contacts (Solvent: 40% PBG/60% NGL).....	3.38
3.20	K-values vs. Number of Contacts (Solvent: 40% PBG/60% NGL).....	3.39
3.21	X _i vs. Number of Contacts (Solvent: 40% PBG/60% NGL)	3.40
3.22	Y _i vs. Number of Contacts (Solvent: 40% PBG/60% NGL)	3.41
3.23	Density vs. Number of Contacts (Solvent: 36% PBG/64% NGL).....	3.42
3.24	K-values vs. Number of Contacts (Solvent: 36% PBG/64% NGL).....	3.43
3.25	X _i vs. Number of Contacts (Solvent: 36% PBG/64% NGL)	3.44
3.26	Y _i vs. Number of Contacts (Solvent: 36% PBG/64% NGL)	3.45

CHAPTER 4

4.1	Schematic Diagram of Experimental Setup.....	4.17
4.2	Oil-Water Relative Permeability Curves for the Sandpack.....	4.18
4.3	Oil Recovery vs. PV Injected (Unsteady State Waterflood).....	4.19
4.4	WOR vs. PV Injected (Unsteady State Waterflood).....	4.20
4.5	GOR vs. PV Injected (Unsteady State Waterflood).....	4.21

LIST OF FIGURES (CON'T.)

4.6	Pressure Drop vs. PV Injected (Unsteady State Waterflood).....	4.22
4.7	Oil Recovery vs. PV Injected, MCM Solvent Slug Size: 0.05 PV..... (Solvent: 50% PBG/50% NGL)	4.23
4.8	WOR vs. PV Injected, MCM Solvent Slug Size: 0.05 PV..... (Solvent: 50% PBG/50% NGL)	4.24
4.9	GOR vs. PV Injected, MCM Solvent Slug Size: 0.05 PV	4.25
	(Solvent: 50% PBG/50% NGL)	
4.10	Pressure Drop vs. PV Injected, MCM Solvent Slug Size: 0.05 PV	4.26
	(Solvent: 50% PBG/50% NGL)	
4.11	Oil Recovery vs. PV Injected, MCM Solvent Slug Size: 0.10 PV.....	4.27
	(Solvent: 50% PBG/50% NGL)	
4.12	WOR vs. PV Injected, MCM Solvent Slug Size: 0.10 PV.....	4.28
	(Solvent: 50% PBG/50% NGL)	
4.13	GOR vs. PV Injected, MCM Solvent Slug Size: 0.10 PV	4.29
	(Solvent: 50% PBG/50% NGL)	
4.14	Pressure Drop vs. PV Injected, MCM Solvent Slug Size: 0.10 PV	4.30
	(Solvent: 50% PBG/50% NGL)	
4.15	Oil Recovery vs. PV Injected, MCM Solvent Slug Size: 0.20 PV.....	4.31
	(Solvent: 50% PBG/50% NGL)	
4.16	WOR vs. PV Injected, MCM Solvent Slug Size: 0.20 PV.....	4.32
	(Solvent: 50% PBG/50% NGL)	
4.17	GOR vs. PV Injected, MCM Solvent Slug Size: 0.20 PV	4.33
	(Solvent: 50% PBG/50% NGL)	
4.18	Pressure Drop vs. PV Injected, MCM Solvent Slug Size: 0.20 PV	4.34
	(Solvent: 50% PBG/50% NGL)	
4.19	Oil Recovery vs. PV Injected, MCM Solvent Slug Size: 0.40 PV.....	4.35
	(Solvent: 50% PBG/50% NGL)	
4.20	WOR vs. PV Injected, MCM Solvent Slug Size: 0.40 PV.....	4.36
	(Solvent: 50% PBG/50% NGL)	
4.21	GOR vs. PV Injected, MCM Solvent Slug Size: 0.40 PV	4.37
	(Solvent: 50% PBG/50% NGL)	
4.22	Pressure Drop vs. PV Injected, MCM Solvent Slug Size: 0.40 PV	4.38
	(Solvent: 50% PBG/50% NGL)	

LIST OF FIGURES (CON'T.)

4.23	Oil Recovery vs. PV Injected, Multiple WAG, WAG Ratio: 11.....	4.39
	(MCM Solvent: 50% PBG/50% NGL)	
4.24	WOR vs. PV Injected, Multiple WAG, WAG Ratio: 11	4.40
	(MCM Solvent: 50% PBG/50% NGL)	
4.25	GOR vs. PV Injected, Multiple WAG, WAG Ratio: 11	4.41
	(MCM Solvent: 50% PBG/50% NGL)	
4.26	Pressure Drop vs. PV Injected, Multiple WAG, WAG Ratio: 11	4.42
	(MCM Solvent: 50% PBG/50% NGL)	
4.27	Oil Recovery vs. PV Injected, Multiple WAG, WAG Ratio: 5.....	4.43
	(MCM Solvent: 50% PBG/50% NGL)	
4.28	WOR vs. PV Injected, Multiple WAG, WAG Ratio: 5	4.44
	(MCM Solvent: 50% PBG/50% NGL)	
4.29	GOR vs. PV Injected, Multiple WAG, WAG Ratio: 5	4.45
	(MCM Solvent: 50% PBG/50% NGL)	
4.30	Pressure Drop vs. PV Injected, Multiple WAG, WAG Ratio: 5	4.46
	(MCM Solvent: 50% PBG/50% NGL)	
4.31	Oil Recovery vs. PV Injected, Multiple WAG, WAG Ratio: 3.....	4.47
	(MCM Solvent: 50% PBG/50% NGL)	
4.32	WOR vs. PV Injected, Multiple WAG, WAG Ratio: 3	4.48
	(MCM Solvent: 50% PBG/50% NGL)	
4.33	GOR vs. PV Injected, Multiple WAG, WAG Ratio: 3	4.49
	(MCM Solvent: 50% PBG/50% NGL)	
4.34	Pressure Drop vs. PV Injected, Multiple WAG, WAG Ratio: 3	4.50
	(MCM Solvent: 50% PBG/50% NGL)	
4.35	Oil Recovery vs. PV Injected, FCM Solvent Slug Size: 0.05 PV	4.51
	(Solvent: Propane)	
4.36	WOR vs. PV Injected, FCM Solvent Slug Size: 0.05 PV	4.52
	(Solvent: Propane)	
4.37	GOR vs. PV Injected, FCM Solvent Slug Size: 0.05 PV	4.53
	(Solvent: Propane)	
4.38	Pressure Drop vs. PV Injected, FCM Solvent Slug Size: 0.05 PV	4.54
	(Solvent: Propane)	
4.39	Oil Recovery vs. PV Injected, FCM Solvent Slug Size: 0.10 PV	4.55
	(Solvent: Propane)	

LIST OF FIGURES (CON'T.)

4.40	WOR vs. PV Injected, FCM Solvent Slug Size: 0.10 PV 4.56 (Solvent: Propane)
4.41	GOR vs. PV Injected, FCM Solvent Slug Size: 0.10 PV 4.57 (Solvent: Propane)
4.42	Pressure Drop vs. PV Injected, FCM Solvent Slug Size: 0.10 PV 4.58 (Solvent: Propane)
4.43	Oil Recovery vs. PV Injected, FCM Solvent Slug Size: 0.20 PV 4.59 (Solvent: Propane)
4.44	WOR vs. PV Injected, FCM Solvent Slug Size: 0.20 PV 4.60 (Solvent: Propane)
4.45	GOR vs. PV Injected, FCM Solvent Slug Size: 0.20 PV 4.61 (Solvent: Propane)
4.46	Pressure Drop vs. PV Injected, FCM Solvent Slug Size: 0.20 PV 4.62 (Solvent: Propane)
4.47	Oil Recovery vs. PV Injected (Solvent: Prudhoe Bay Gas)..... 4.63
4.48	WOR vs. PV Injected (Solvent: Prudhoe Bay Gas)..... 4.64
4.49	GOR vs. PV Injected (Solvent: Prudhoe Bay Gas)..... 4.65
4.50	Pressure Drop vs. PV Injected (Solvent: Prudhoe Bay Gas) 4.66
4.51	Oil Recovery vs. PV Injected (Solvent: Carbon Dioxide) 4.67
4.52	WOR vs. PV Injected (Solvent: Carbon Dioxide)..... 4.68
4.53	GOR vs. PV Injected (Solvent: Carbon Dioxide)..... 4.69
4.54	Pressure Drop vs. PV Injected (Solvent: Carbon Dioxide)..... 4.70
4.55	Effect of Slug Size, Oil Recovery vs. PV Injected Comparison..... 4.71 (MCM Solvent: 50% PBG/50% NGL)
4.56	Effect of Slug Size on Incremental Oil Recovery..... 4.72 (MCM Solvent: 50% PBG/50% NGL)
4.57	Effect of WAG Ratio, Comparison of Recovery vs. PV Injected..... 4.73 (MCM Solvent: 50% PBG/50% NGL)
4.58	Effect of WAG Ratio on Incremental Oil Recovery..... 4.74 (MCM Solvent: 50% PBG/50% NGL)
4.59	Effect of WAG Ratio on Incremental Oil Recovery, Single-slug 4.75 vs. Multi-slug WAG (MCM Solvent: 50% PBG/50% NGL)
4.60	Effect of Slug Size, Recovery vs. PV Injected Comparison 4.76 (FCM Solvent: Propane)

LIST OF FIGURES (CON'T.)

4.61	Effect of Slug Size on Incremental Oil Recovery.....	4.77
	(FCM Solvent: Propane)	
4.62	Effect of Solvent Type, Recovery vs. PV Injected Comparison.....	4.78

LIST OF TABLES

<u>Table No.</u>	<u>CHAPTER 2</u>	<u>Page</u>
2.1	List of Milne Point Wells for Second Phase..... Reservoir Characterization	2.29
2.2	List of Normalized Wells	2.30
<u>CHAPTER 3</u>		
3.1	EOS Parameters for Schrader Bluff Reservoir Fluid.....	3.46
3.2	Recoveries From Slim Tube Experiments and Simulation.....	3.47
<u>CHAPTER 4</u>		
4.1	Summary of Experimental Results.....	4.79

CHAPTER 1

INTRODUCTION

During the past years, oil production in the U.S. has been steadily declining while the demand for foreign imported oil has been steadily increasing. To abate the over-reliance on foreign oil imports, and in order to maintain our economic and military security, the U.S. has formulated a National Energy Strategy Plan. The plan has been developed by the U.S. Department of Energy and is based on the current and future resources in the U.S. which could be economically developed. This plan specifically calls for a production of 900,000 barrels of heavy oil per day. Currently, most of the heavy oil production in the U.S. comes from California. However, although the production of heavy oil from California can be further increased, it could not meet the NES projections by the mid-1990s.

Alaska currently produces about 24% of the nation's output of oil. However, the production from the Prudhoe Bay field providing about 1.5 million barrels a day has begun to decline and must be supplemented by developing other nearby fields for oil flow through the Trans-Alaskan Pipeline to Lower 48 states. Fortunately, Alaska also has the second largest heavy oil resources in the U.S. It is estimated that the super giant West Sak field, which includes Kuparuk River and Milne Point units, contains over 25 billion barrels of oil. The field is so large and widespread that the gravity of the oil varies from 10.0 to 22.5° API. Small production from some regions of this giant field is underway, while others await improved production technology. The past field tests and laboratory studies clearly demonstrated that entirely new and innovative technologies for oil displacement and production will be required for large-scale production from this reservoir.

The shallow Cretaceous sands of the Schrader Bluff reservoir occur between depths of 4,000 and 4,800 feet below surface and are estimated to contain up to 1.5 billion barrels of oil in place. The gravity of oil therein varies between 14 to 21° API. The gravity of the oil in these sands changes rather abruptly from well to well and is of great concern for development of enhanced oil recovery techniques. The average oil gravity is 17 to 18° API. The field is currently under production by primary depletion. Initial production indicated that primary recovery will fall short of earlier estimates and waterflooding will have to be employed much earlier than expected. A

large portion of the oil in place thus would still be left behind in this reservoir after primary and secondary recovery methods have been applied. Enhanced oil recovery (EOR) techniques are needed to recover the additional portion of the remaining oil in this huge reservoir, and to add significant additional reserves.

The availability of natural gas and natural gas liquids to generate hydrocarbon solvents on the Alaskan North Slope make the hydrocarbon miscible flooding process an important viable consideration for the EOR project in the Milne Point Unit. To reduce requirements of costly hydrocarbon solvents and to make this process commercially feasible, optimum composition of relatively small size slugs of miscible hydrocarbon solvent must be determined in the laboratory.

The enhanced oil recovery technique such as hydrocarbon miscible process is vital for recovery of additional oil from Schrader Bluff reservoir. In the first part of this study, various solvents were tested in slim tube experiments to determine the enrichment required to achieve miscibility with the Schrader Bluff crude at reservoir conditions. The solvents include, carbon-dioxide (CO₂) and Prudhoe Bay natural gas (PBG) enriched by natural gas liquids (NGL). An equation-of-state (EOS) simulator was used to develop fluid characterization of Schrader Bluff oil, and this was then used in a compositional simulator to match the slim tube experimental data, and to conduct multiple contact tests to determine the minimum enrichment requirement.

To evaluate the feasibility of a miscible WAG process for Schrader Bluff reservoir, an experimental coreflood study was undertaken. The effect of solvent type, solvent slug size, and WAG ratio on the incremental oil recovery (IOR), and the displacement behavior were identified.

CHAPTER 2

SCHRADER BLUFF RESERVOIR DESCRIPTION

Schrader Bluff Pool lies in the Milne Point Unit and is a part of the West Sak reservoir. Conoco Inc. has drilled 22 wells in Tract 14 (now owned by B.P. Exploration, AK) of Schrader Bluff Pool. The reservoir is complexly faulted with numerous producing horizons separated by shales. Therefore, accurate characterization is necessary to predict fluid flow and production behavior of this reservoir under enhanced oil recovery methods. The following sections provide a brief reservoir description of Schrader Bluff Pool.

A. CHARACTERIZATION OF TRACT 14 WELLS

ZONAL CORRELATION

The SP, GR, Deep, and Medium resistivity traces were plotted on the true vertical depth. These trace plots were then used for zonal correlation. The individual N and O sands were correlated horizontally. Cross sections were generated across NW-SE and SW-NE directions. These plots show the magnitude of dip of the various sands across the taken cross sections. The NW-SE cross section (Figure 2.1), shows a very steep dip between well MPU J-1 and MPU J-7 and a very gentle dip between wells MPU J-7 through MPU H-4. The thickness of sands and shales are consistent laterally across with virtually no missing zones. The SW-NE cross section (Figure 2.2), however, exhibits steep dips between MPU I-3 and MPU I-2, MPU I-2 and MPU G-1, and MPU G-1 and MPU G-6. Laterally across, zone thickness consistency is well displayed. The areas where steep dips occur are likely to be prone to faults. Due to the absence of pertinent information on faults and throws, the exact locations of these faults are difficult to ascertain.

Reservoir sand quality can be expressed in terms of formation storage capacity and transmissibility. In this work, sand quality was evaluated using the hydrocarbon pore volume. The value of hydrocarbon pore volume in bbl/acre is expressed mathematically in the equation below.

$$\text{HCF} = 7758 h (1 - S_w) \phi_e$$

where:

HCF = hydrocarbon pore volume (bbl/acre)

h = average net pay thickness (ft)

S_w = average water saturation (fraction)

ϕ_e = average effective porosity (fraction)

B. LOG DERIVED PETROPHYSICAL PROPERTIES

By using geological markers supplied by CONOCO, six unconsolidated N sand members and seven consolidated O sand members were identified in the Schrader Bluff interval. Going from top to bottom these sands can be named as follows:

(a) N Sands

1. Sand NA1
2. Sand NB1
3. Sand NC1
4. Sand NE1
5. Sand NE2
6. Sand NF

(b) O Sands

1. Sand OA1
2. Sand OA2
3. Sand OA3
4. Sand OB4
5. Sand OB1
6. Sand OC1
7. Sand OE

The NB1 and OB1 were identified to be sands of high quality. The NE1, NF, OE, and OC1 sands were identified to be mudstone intervals. The other sands form a spectrum that spans from muddy sands to sandy muds.

Petrophysical properties such as net pay thickness, effective porosity, water saturation, and sand quality were computed for NB1 and OB1 sands by analyzing the well logs using the WORK-BENCH software on an IBM RISC 6000 workstation. The cutoffs used in the well log analysis were as follows: $S_w < 60\%$, $\phi_e > 24\%$, and $V_{sh} = 0$. Archie's water saturation model was used. Contour maps showing the spatial distribution of these petrophysical properties were then prepared and are discussed below.

C. SPATIAL DISTRIBUTION OF PETROPHYSICAL PROPERTIES

The petrophysical properties derived from the well log analysis were used to generate isopach and contour maps for NB1 and OB1 sands. The isopach of sand NB1 is shown in Figure 2.3. The net pay thickness ranges from a low of 0 feet in MPU G-4 to a high of 27 feet in West Sak 25. Typical net pay thicknesses range between 10 to 20 feet. Figure 2.4 shows the average effective porosity contour map of sand NB1. Even though porosities seem evenly distributed, there are discernible high porosities around the G-pad. Typical porosities lie between 29% to 33%. Figure 2.5 is the plot of average water saturation for the sand NB1. A typically low value of 23% is observed around MPU G-1 and a high of 50% around MPU I-1. Values in between these extremes are evenly distributed around the other wells. Figure 2.6 shows the isopach map of sand OB1. Concentration of high net pay thickness is observed in the northern portion of the G-pad (except MPU G-7) and very low ones in the H-pad. The I and J pads exhibit average net pay thickness which spans from about 9 feet to 20 feet. The highest net pay thickness, 23.2 feet is observed at MPU G-8, and the lowest, 0 feet, is found at MPU G-4 and MPU H-1. As in the previous NB1 sand, an even distribution of net pay thicknesses is fairly well replicated.

Figure 2.7 shows the contour map of the average porosity of sand OB1. The average values lie between the range 25% to 32%. These values are lower than those observed in the NB1 sand previously. The reasons for the observed trend can be attributed primarily to the fact that the deeper OB1 sand is more likely to be subjected to overburden pressure which ultimately leads to reduction in porosity. Higher porosities are observed in the upper G and J pads with a gradual decrease downwards toward the I and J pads.

Figure 2.8 is the contour map of the net pay water saturation distribution of the sand OB1. High saturations are observed in the southern portion of the G-pad. Typical water saturation values lie within the range of 40% - 50% with 55% considered to be the highest value. There are seldom observations of peaks and valleys in the water saturation distribution of sand OB1.

D. SAND QUALITY DISTRIBUTION

The hydrocarbon pore volume was the parameter used to evaluate the sand quality distribution of the studied sands. Using the previously mentioned cutoffs, illustrative contour maps were generated to show the distribution of sand quality of sand NB1 and sand OB1 across the Schrader Bluff formation.

Figure 2.9 shows the contour map of the distribution of NB1 sand quality over the studied area. It is evident from the map that the best productive NB1 sands occur in the middle of the studied area. The sand quality shows gradual deterioration moving away from the center. The sands on the fringes of the productive sands are also of marginal quality and become poorer further North-East and South-West away from the center. This poor quality can be attributed to the small net pays in the northern and southern portions of the studied area.

Figure 2.10 is the contour map of sand quality generated for the OB1. The sand quality is high in the G-pad wells with the exception of MPU G-2, MPU G-1, and MPU G-5, which exhibited low sand quality. The quality in the southern part of the J-pad and the northern part of the I-pad are of intermediate quality. Wells in the H-pad exhibit low quality.

In general, the NB1 sands exhibit better petrophysical properties than the OB1 sands due partly to the overburden pressure that leads to a decrease in effective porosities of the OB1 sands. The G-pad has the best petrophysical properties, while the H-pad has the poorest. The I and J pads have petrophysical properties that lie between the two extremes.

E. CHARACTERIZATION OF SCHRADER BLUFF POOL (OUTSIDE TRACT 14)

In the first phase of reservoir characterization of Milne Point Unit, the tract 14 wells from G-, H-, I- and J-pads, W.Sak 25, and N1B were included. For the second phase of reservoir characterization, a total of 36 wells were proposed by Conoco Inc. Out of these 36 wells, 29 wells were included in the study. The rest of the wells could not be analyzed due to lack of well log and other pertinent information. The proposed wells and their present status (i.e. whether producer, injector, abandoned, or suspended) are listed in Table 2.1.

As in the previous phase, the second phase reservoir characterization was also based on computerized well log analysis. The well log analysis package (WORK-BENCH) developed by Scientific Software Inc. (SSI) was used for this study as well. All the log data and other well information were obtained either from Conoco Inc., or from the Alaska Oil and Gas Conservation Commission (AOGCC). The raw log data were obtained either on diskette in ASCII format, or on a magnetic tape spool. The ASCII well log data were directly loaded to WORK-BENCH from diskettes. Well log data in magnetic tape spool were first loaded into the VAX mainframe and converted to ASCII format using the LOGCALC software, and then transferred to the RISC workstation.

For this phase of reservoir characterization a base map with well locations was generated by digitizing the well locations from a Milne Point Unit map. Figure 2.11 shows this base map with locations of Milne Point wells outside of Tract 14.

The geologic sand top information for the zones of interest were supplied by Conoco Inc. Using this information, selected curves were plotted and sand tops were picked for each well. The locations of some of the sand tops were then fine tuned upon consultation with Conoco Inc. As suggested by Conoco Inc., two new sands zones were introduced which were not present in the Tract 14 analysis. These sands are MA1 sand overlying the NA1 sand, and the ND1 sand between the NC1 and NE1 sands. Once the sand tops were finalized, a series of stratigraphic cross sections were generated by correlating these sand tops from well to well. In the base map of Figure 2.11, the orientations of the cross sections are shown. Two sample cross sections are shown in Figure 2.12 and 2.13. Figure 2.12 shows the A-A' (Northwest-Southeast) cross section and Figure 2.13 shows the C-C' (Northeast-Southwest) cross section. The sands exhibit gentle dips between wells in the NW-SE cross section. In the NE-SW cross section,

however, there is a steep dip between the wells A2 and A1 indicating possible faulting. Following the generation of cross sections, open hole well log analysis was performed. For this purpose, the log traces were first corrected for borehole environment. Then, the bulk density traces were normalized to account for miscellaneous errors by using the same methodology as that used in normalizing the bulk density traces of Tract 14. Table 2.2 lists the wells whose density traces were normalized and the corresponding shift amounts.

After environmental correction and normalization, open hole analysis was run to determine petrophysical properties of the individual zones from top MA1 to base OE1. The following cutoff values were used:

porosity = 25%
water saturation = 60%
shale volume = 0%

Net pay thickness, effective porosity, water saturation, and sand quality (net hydrocarbon pore volume) of each zone in each well were obtained from this open hole analysis. Thus a spatial distribution of the petrophysical properties was obtained.

Based on the results of open hole log analysis, contour maps of net pay thickness, porosity, water saturation, and sand quality for the NA1, NB1, NE1, OA1, and OB1 sands were generated. The remaining sands were determined to be extremely poor quality and hence were not mapped. Sample contour maps of the petrophysical properties for the NB1 and OB1 sands are shown in Figures 2.14 through 2.21. It is evident that NB1 is the best quality sand. Good quality NB1 sand is seen in the northern and eastern sections of the field. OB1 and OA1 show good quality in the southeastern section of the field. The western part of the field generally does not show good sands, NE1 and NA1 are of marginal quality throughout the field.

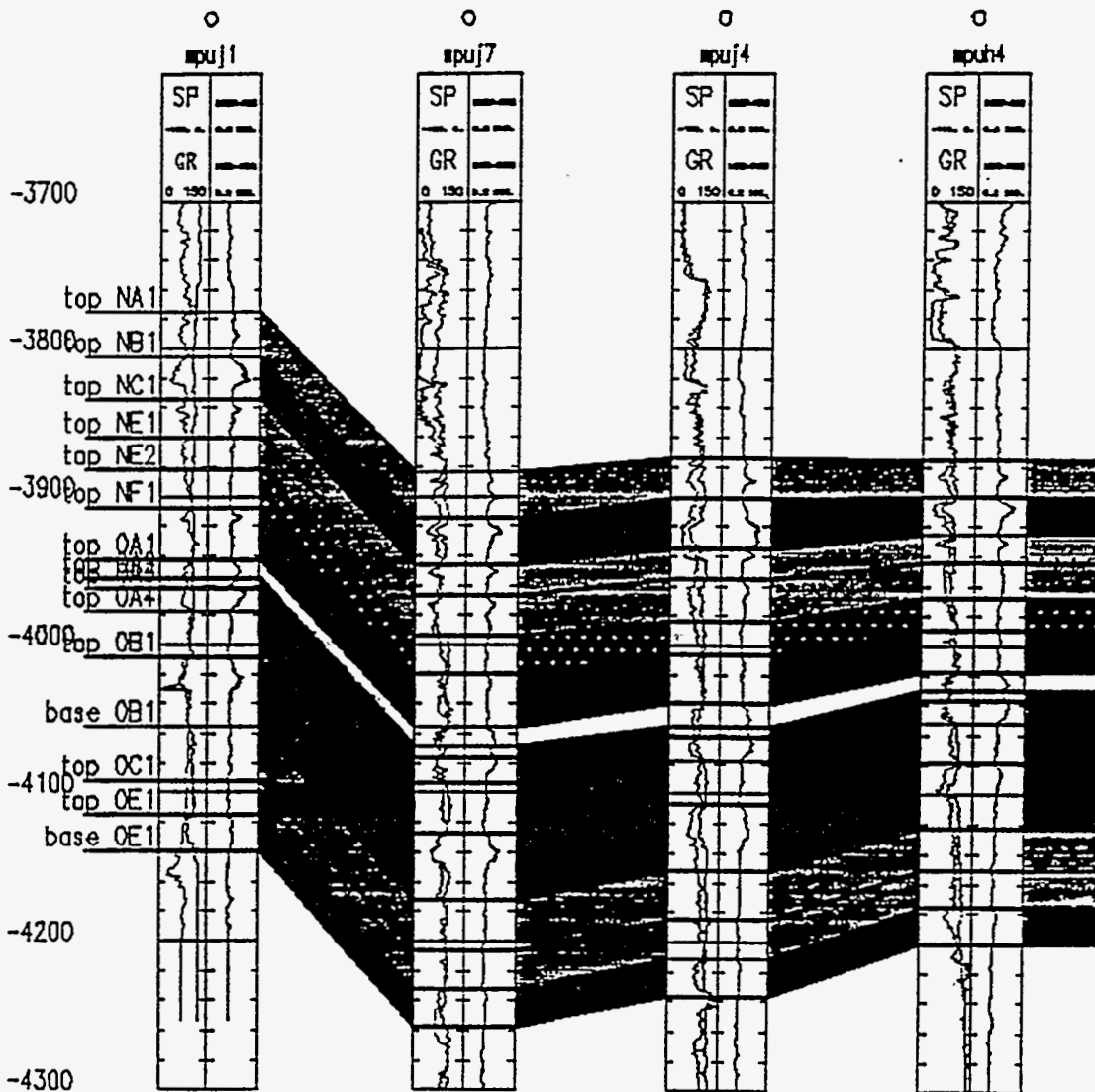


Figure 2.1 NW-SE Cross Section of Schrader Bluff in Tract 14

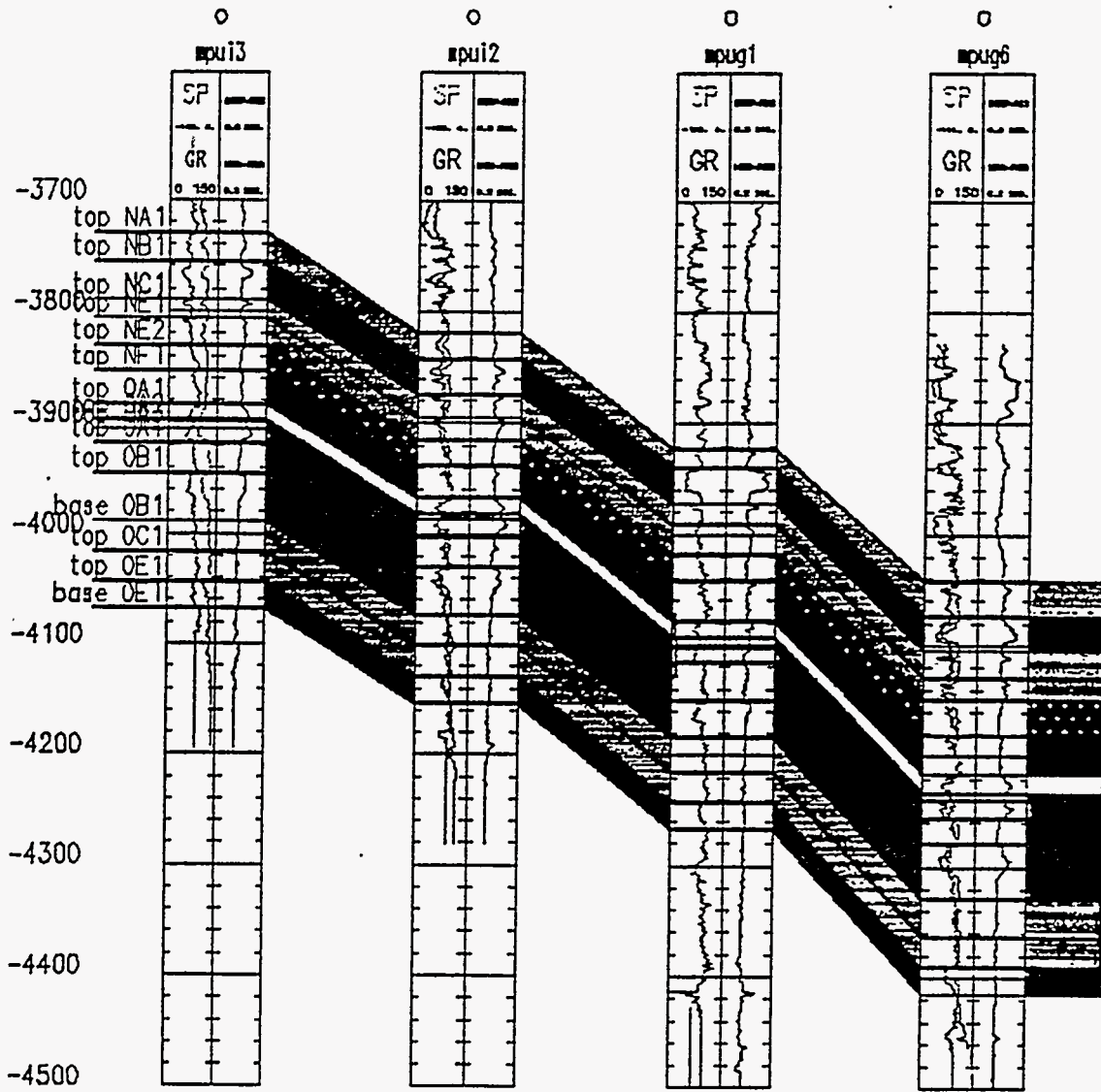


Figure 2.2 SW-NE Cross Section of Schrader Bluff in Tract 14

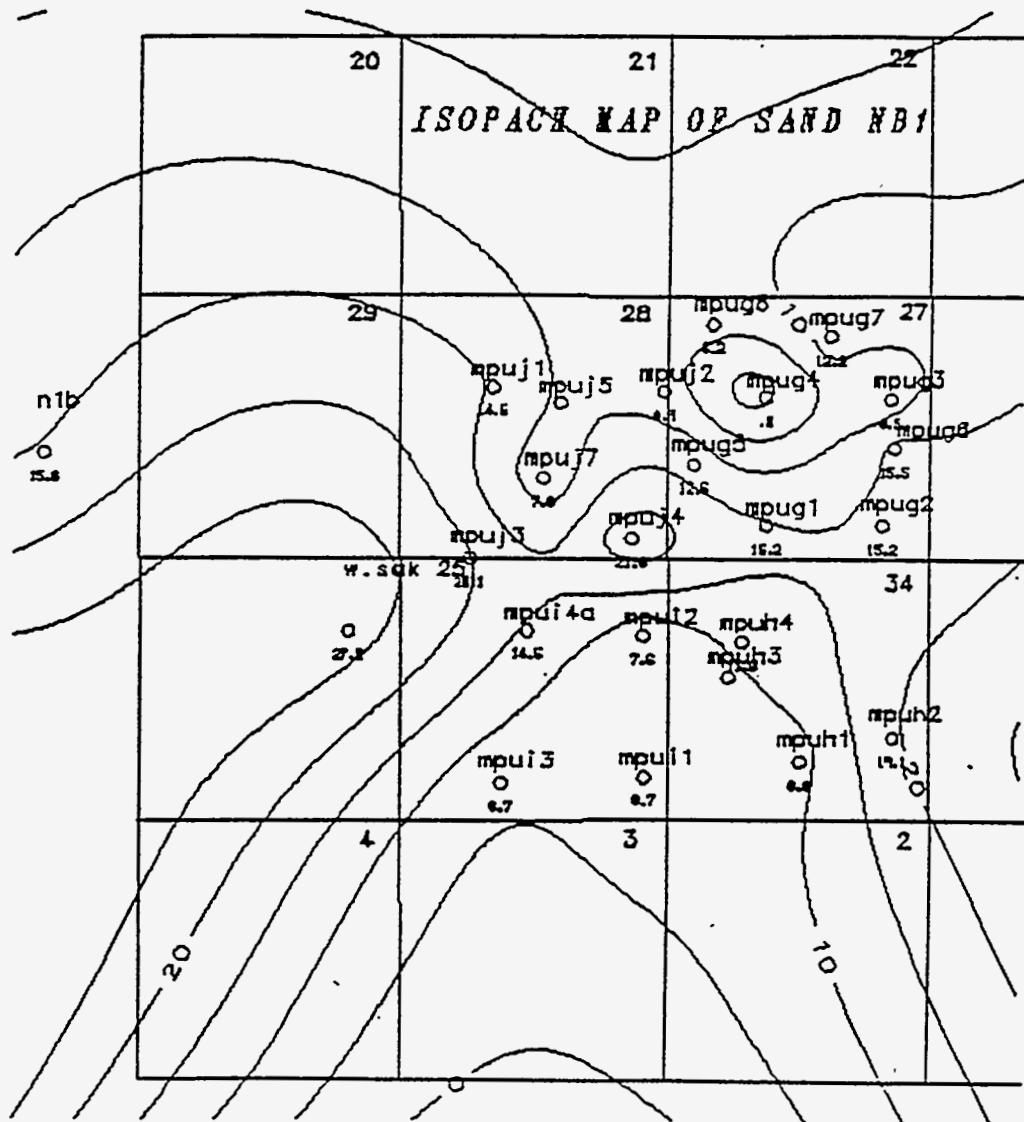


Figure 2.3 Isopach Map of Sand NB1

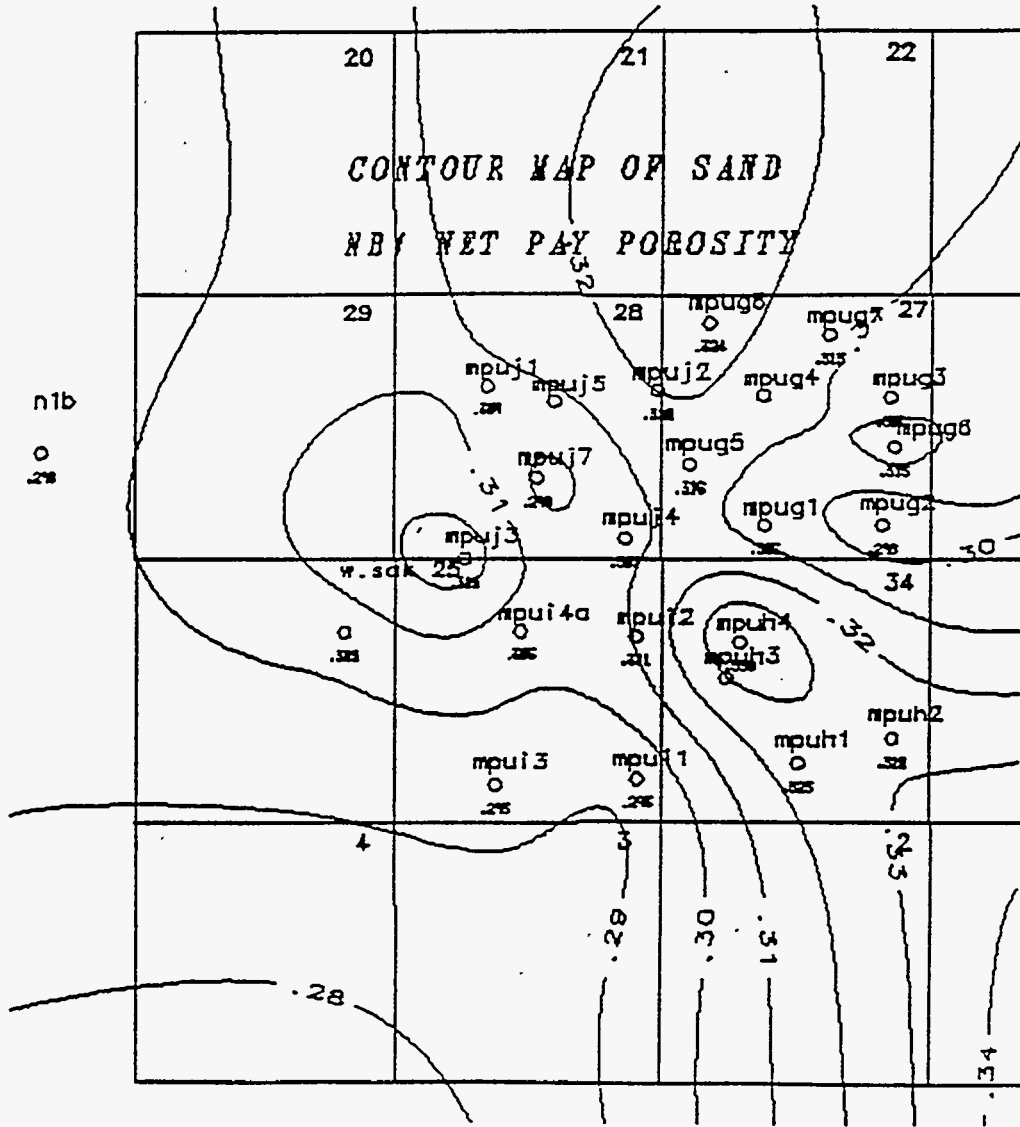


Figure 2.4 Effective Porosity Distribution in Sand NB1

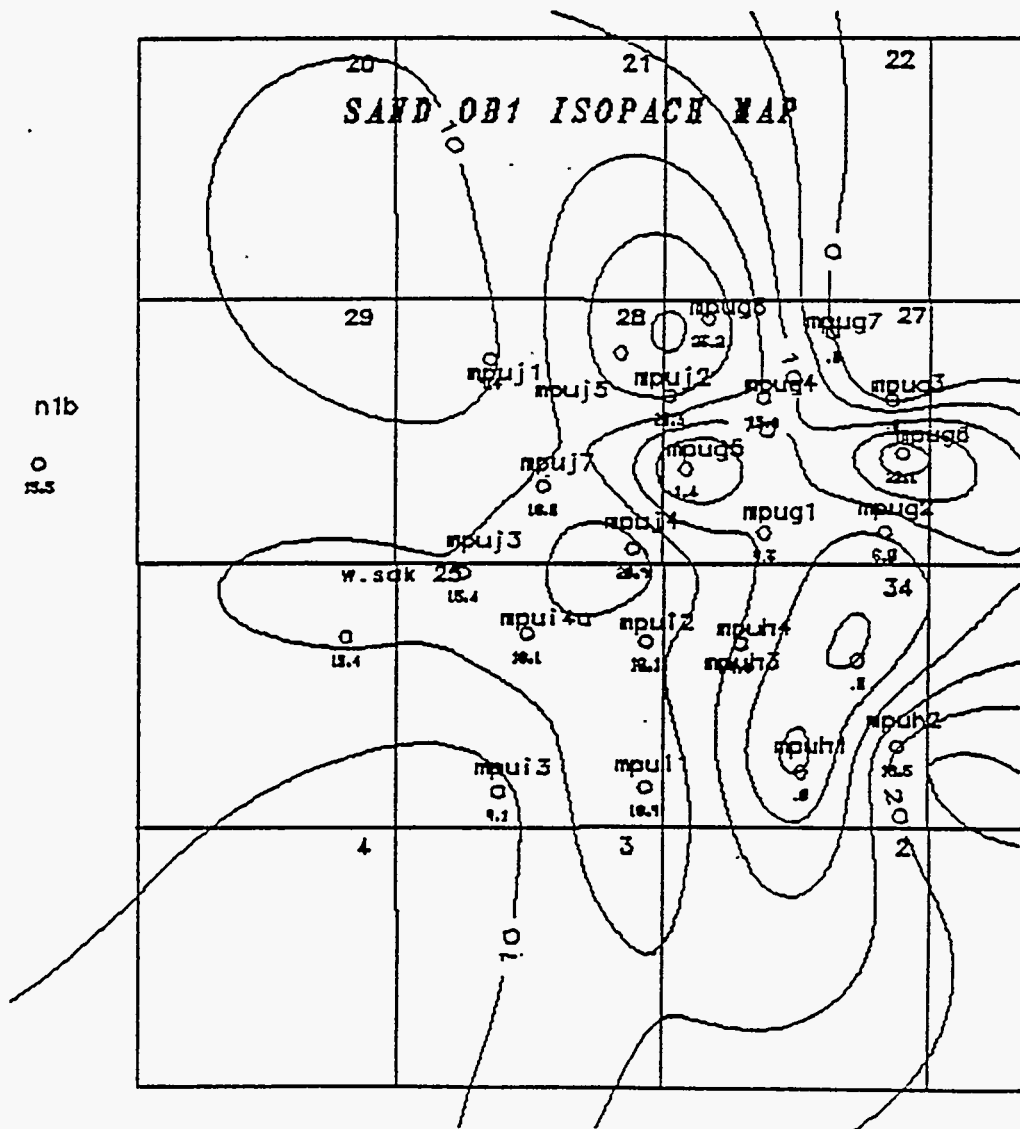


Figure 2.6 Isopach Map of Sand OB1

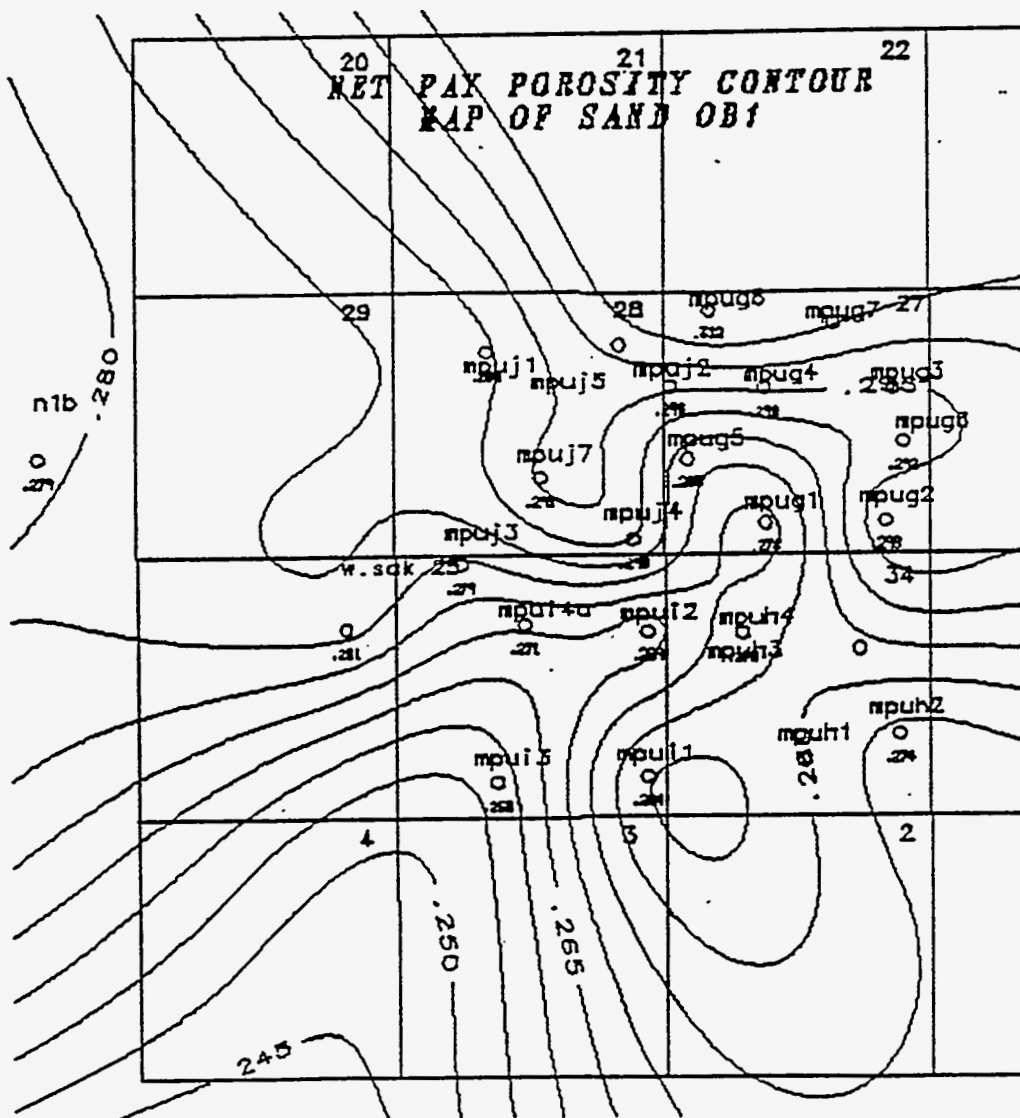


Figure 2.7 Effective Porosity Distribution in Sand OB1

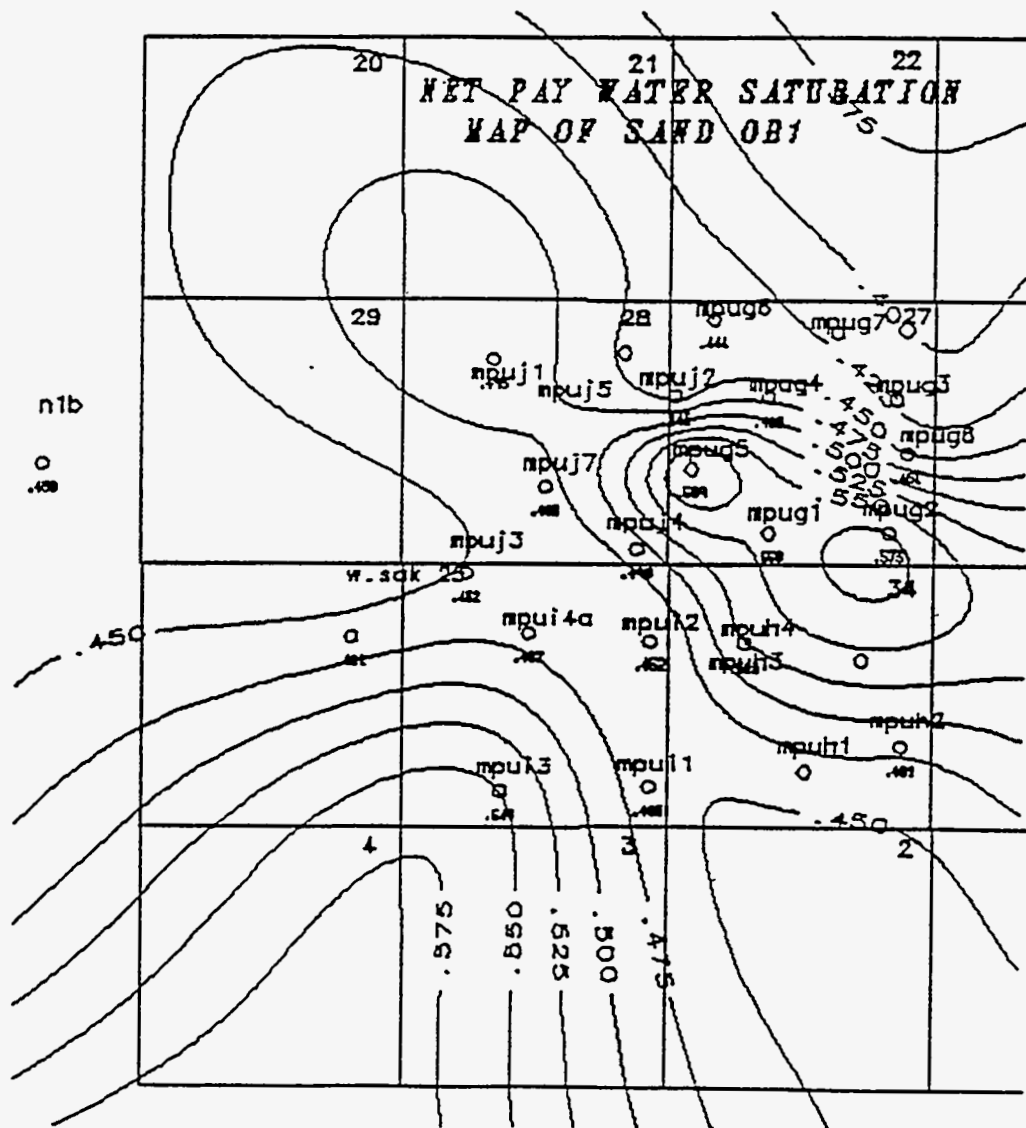


Figure 2.8 Water Saturation Distribution in Sand OB1

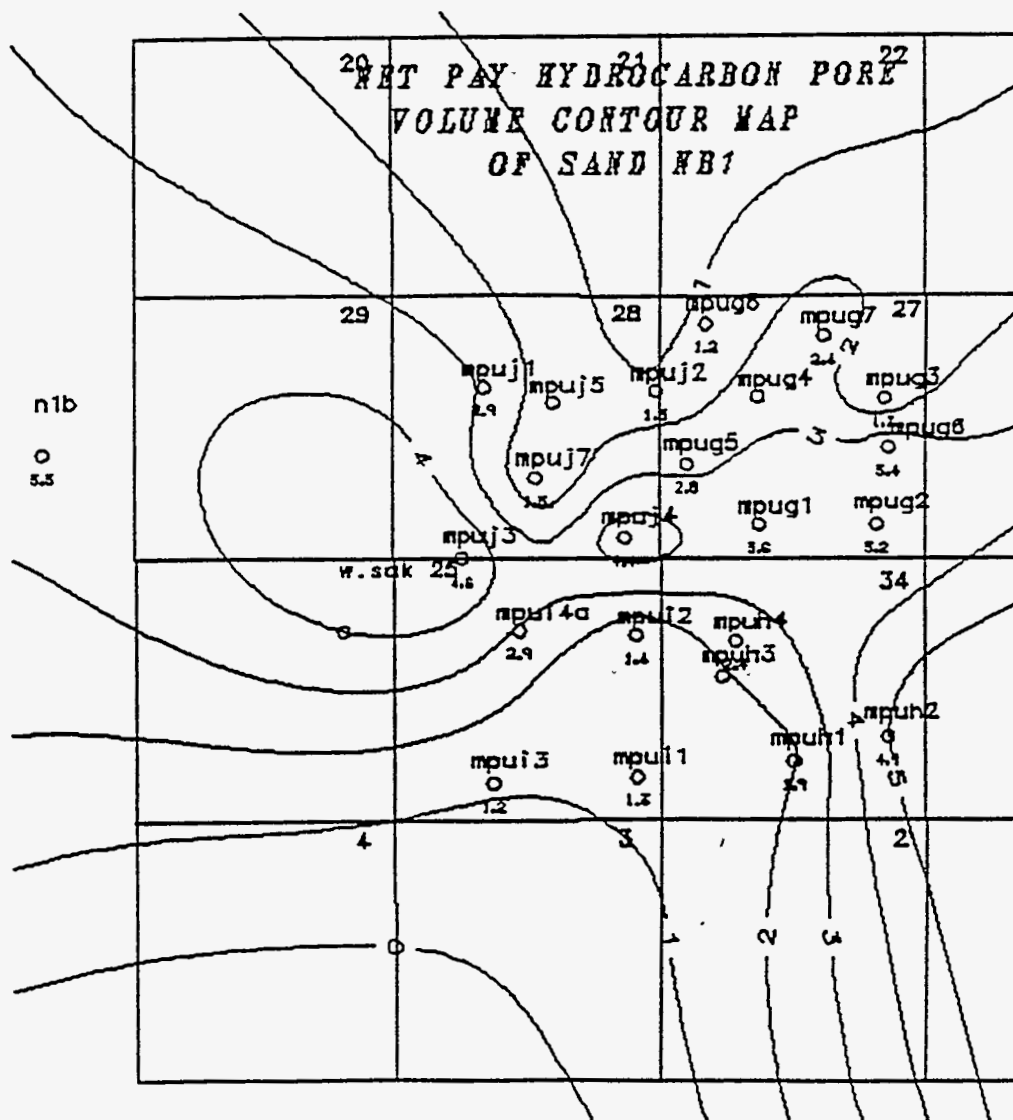


Figure 2.9 Sand Quality Contour Map for NB1

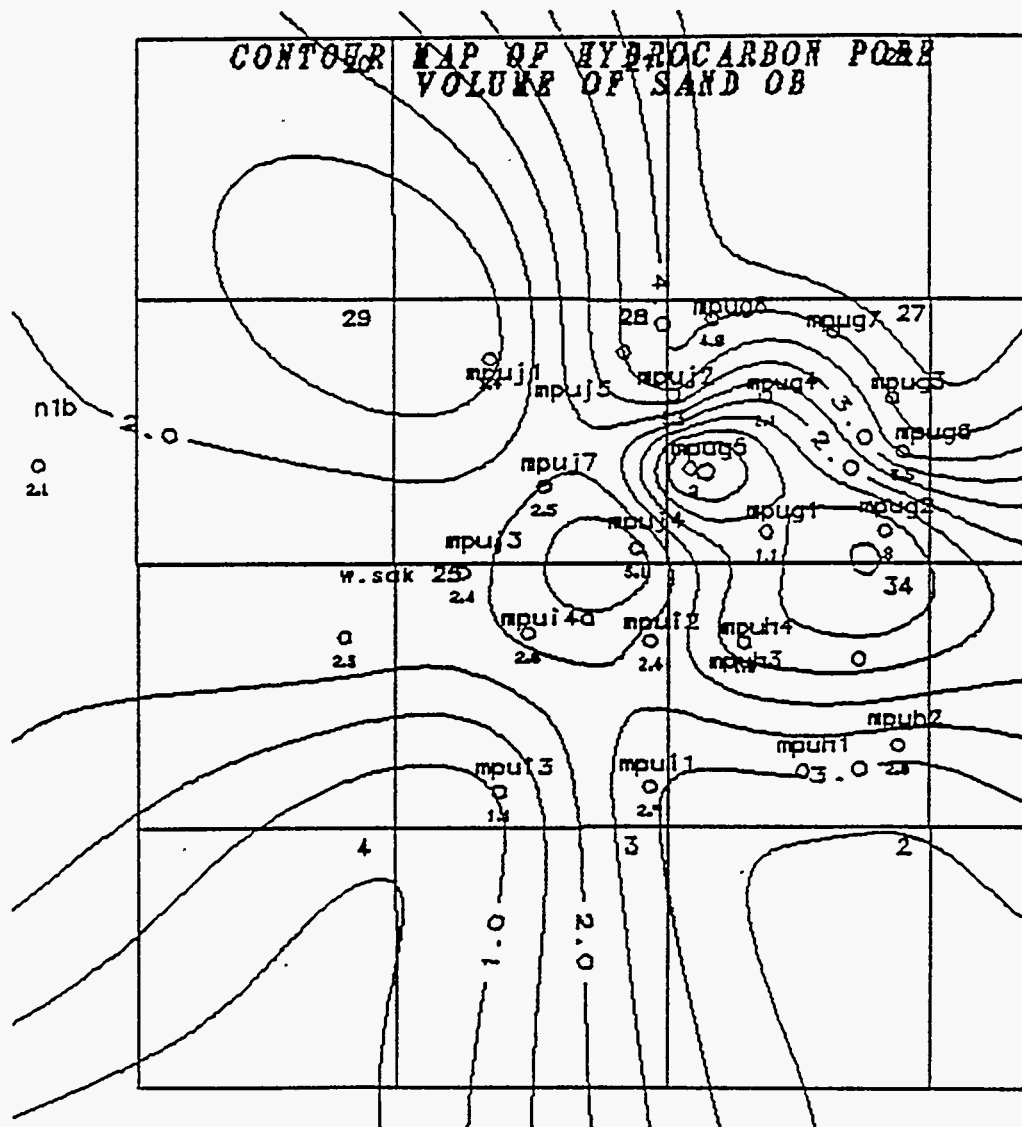


Figure 2.10 Sand Quality Contour Map for OB1

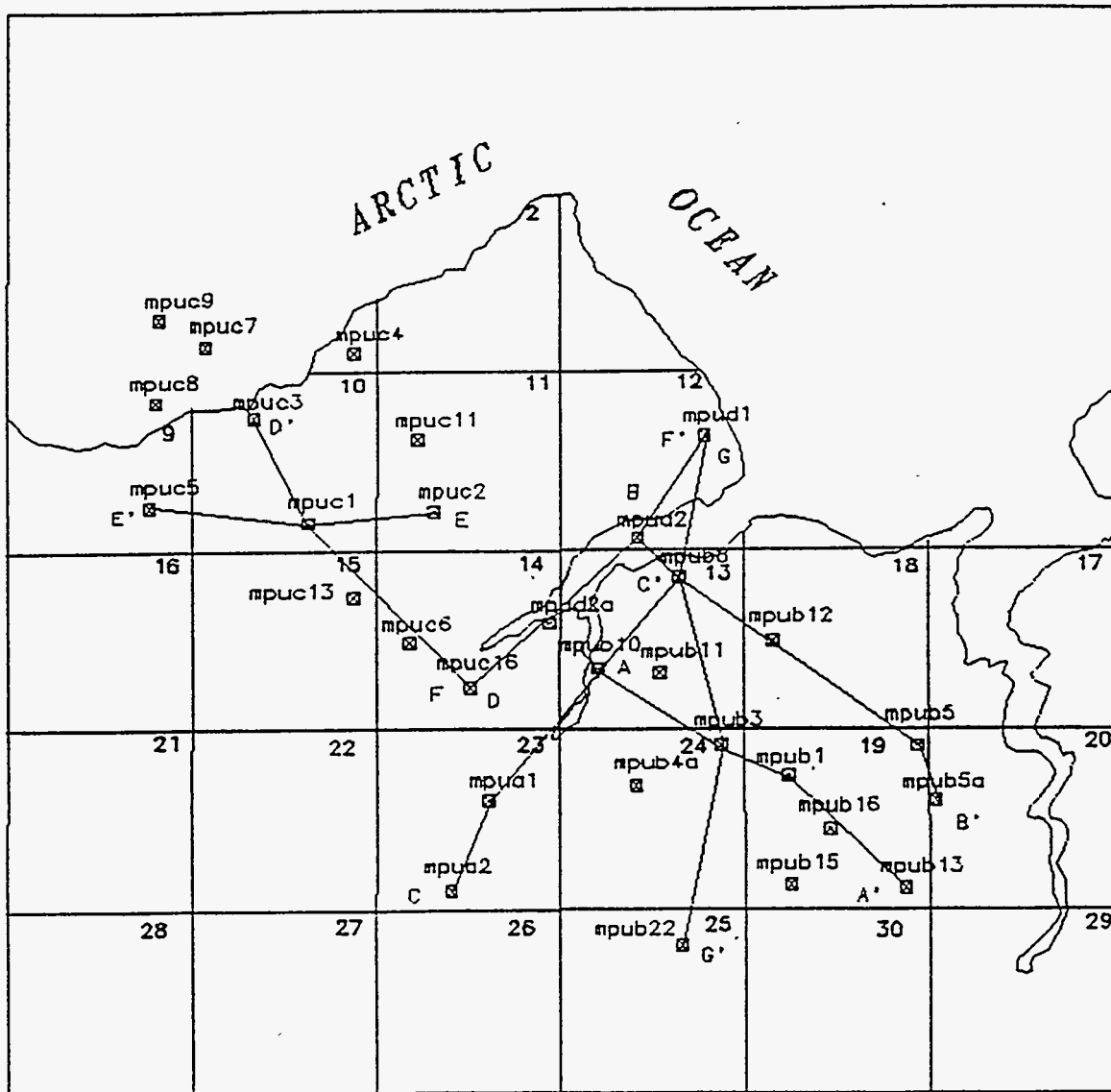


Figure 2.11 Base Map With Locations of Milne Point Wells Outside Tract 14

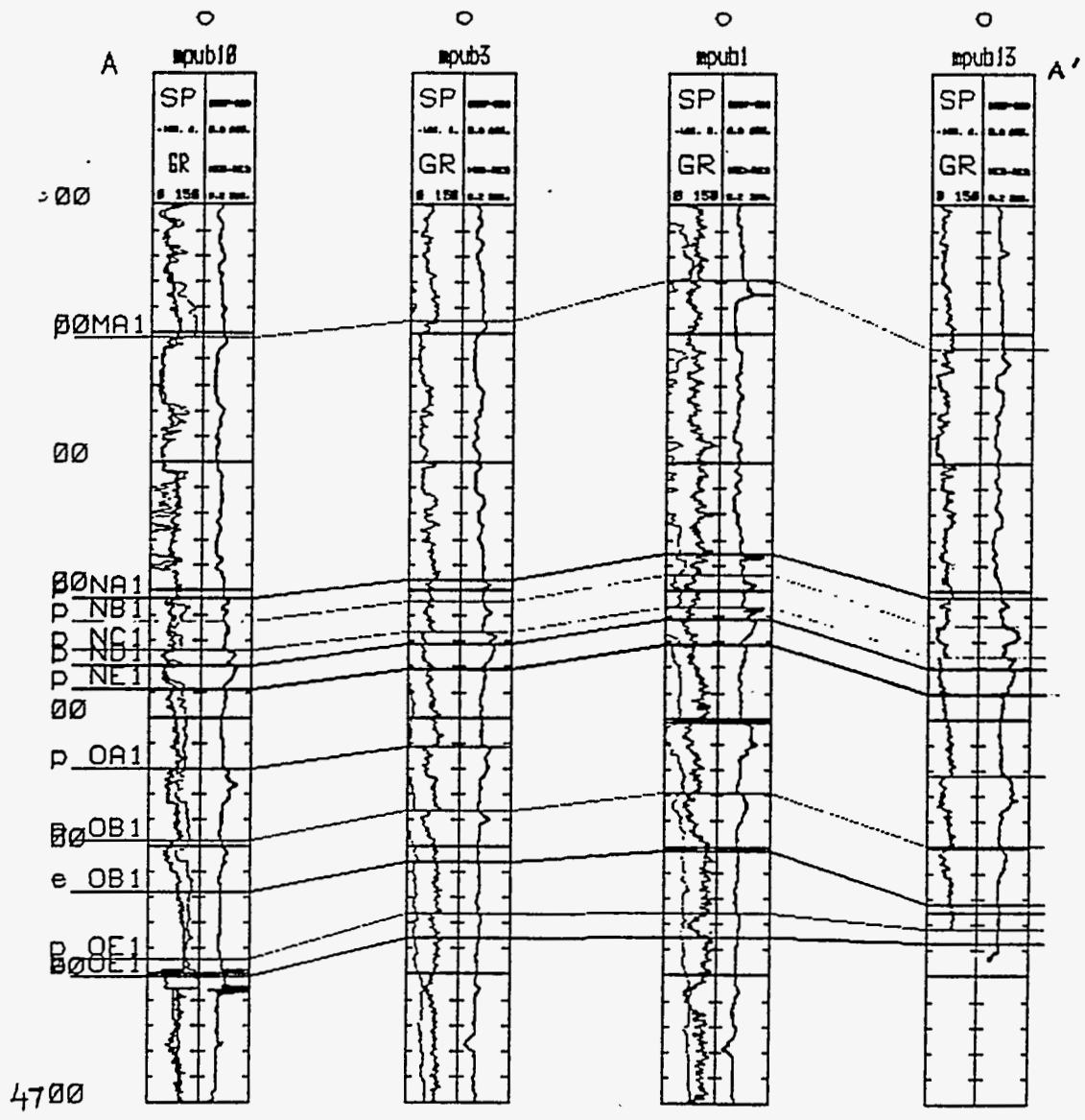


Figure 2.12 NW-SE Stratigraphic Cross Section Along A-A'

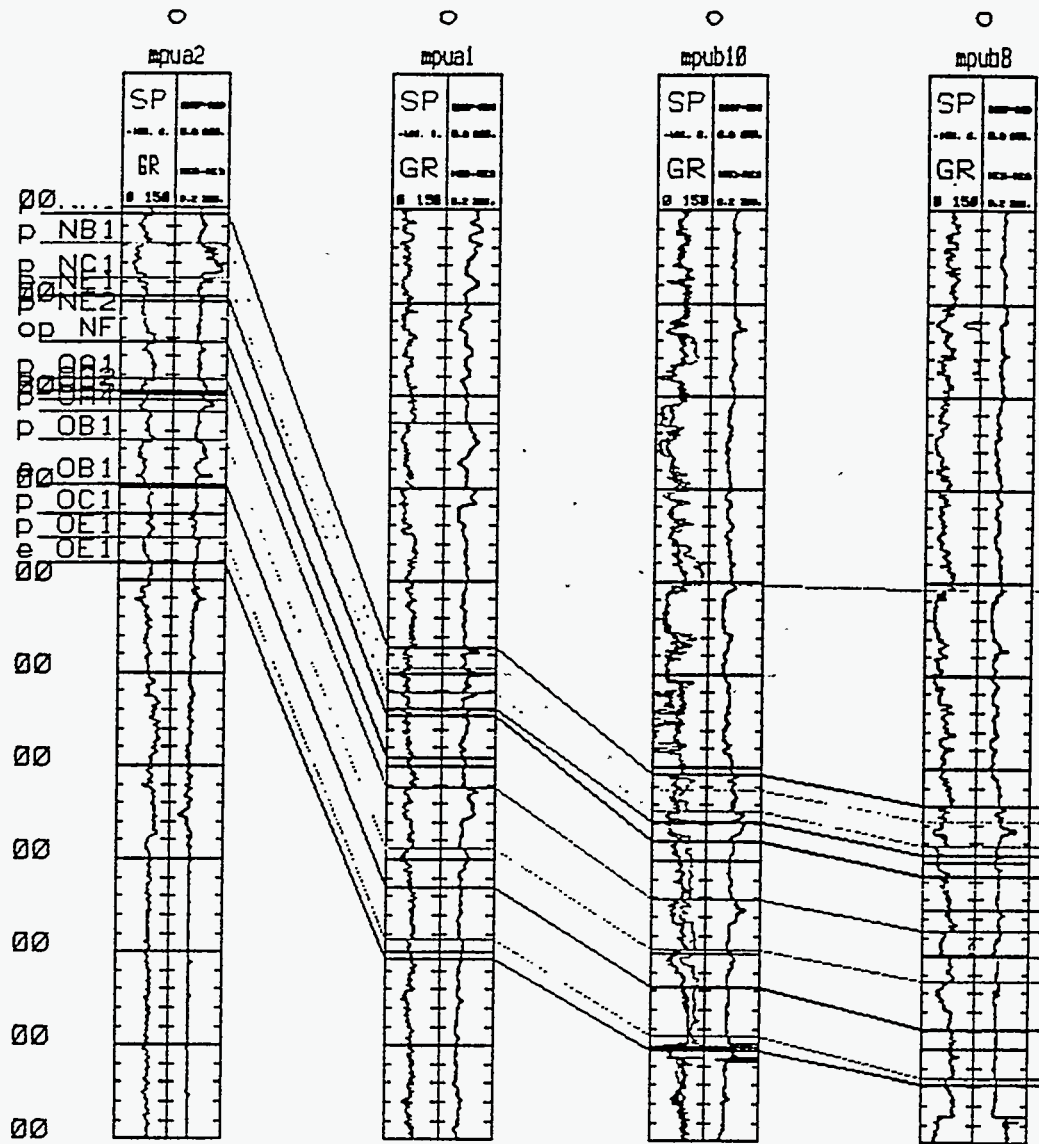


Figure 2.13 NE-SW Stratigraphic Cross Section Along C-C'

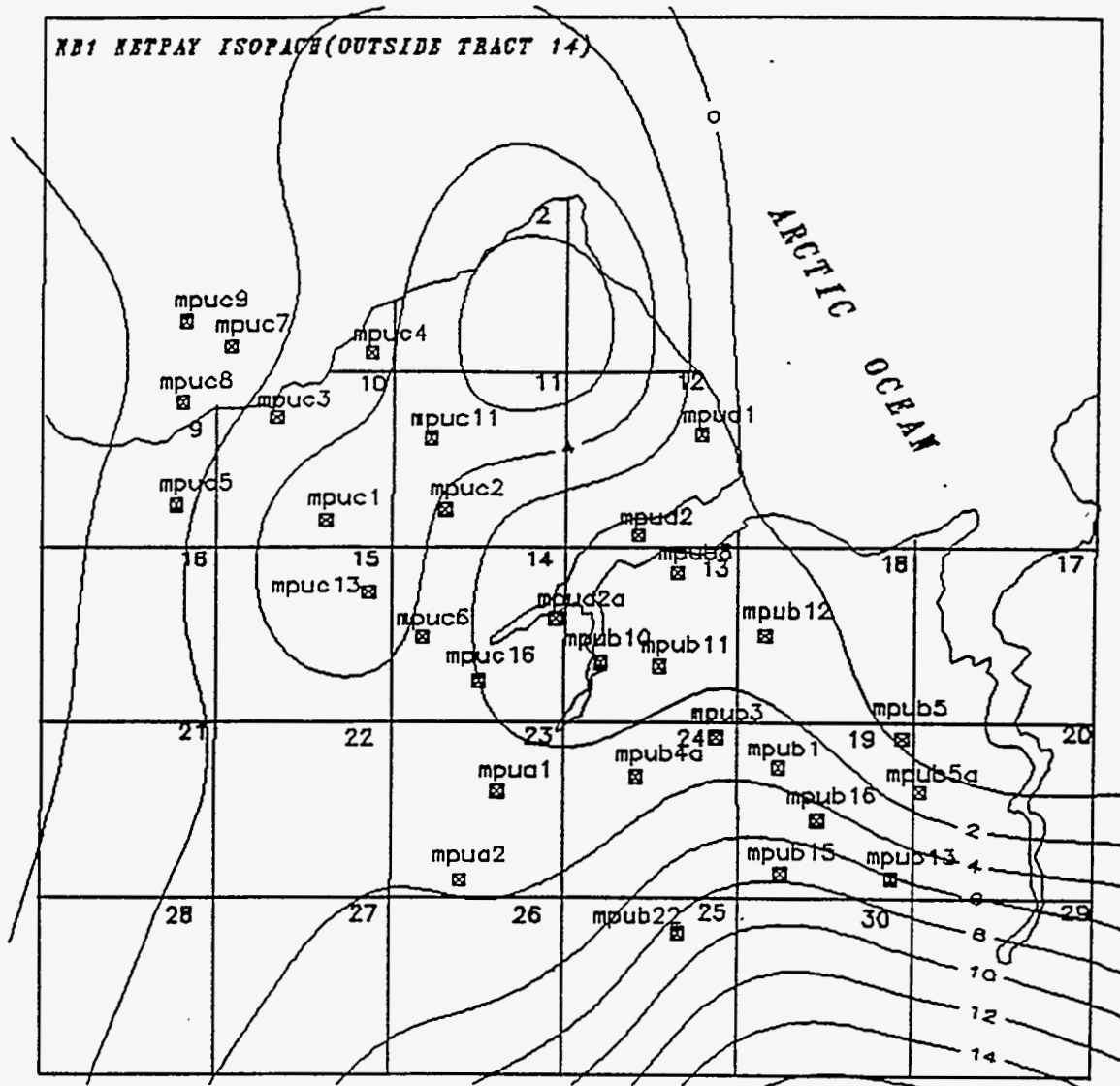


Figure 2.14 Net Pay Isopach for NB1 Sand

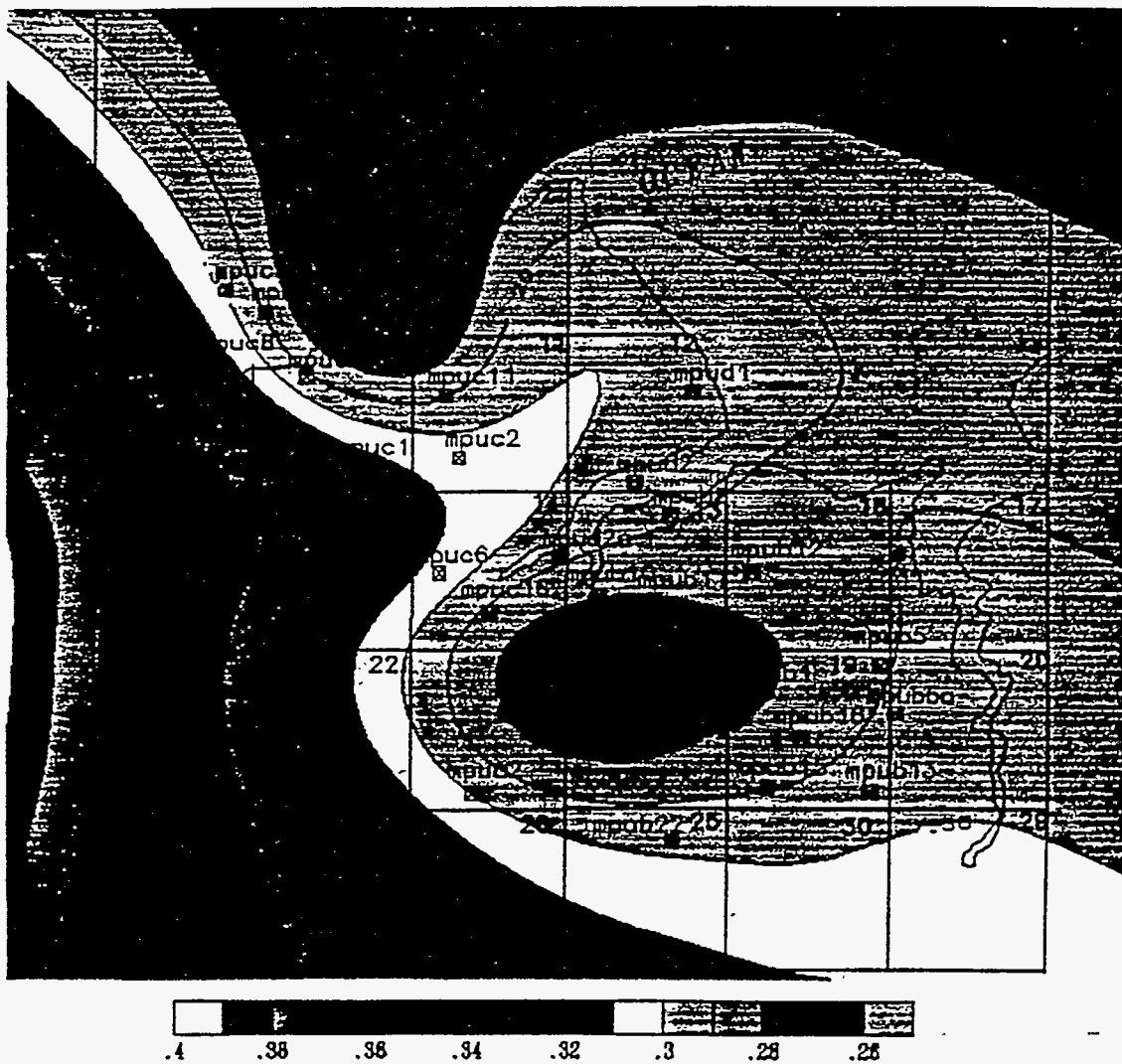


Figure 2.15 Effective Porosity Contour Map for NB1 Sand

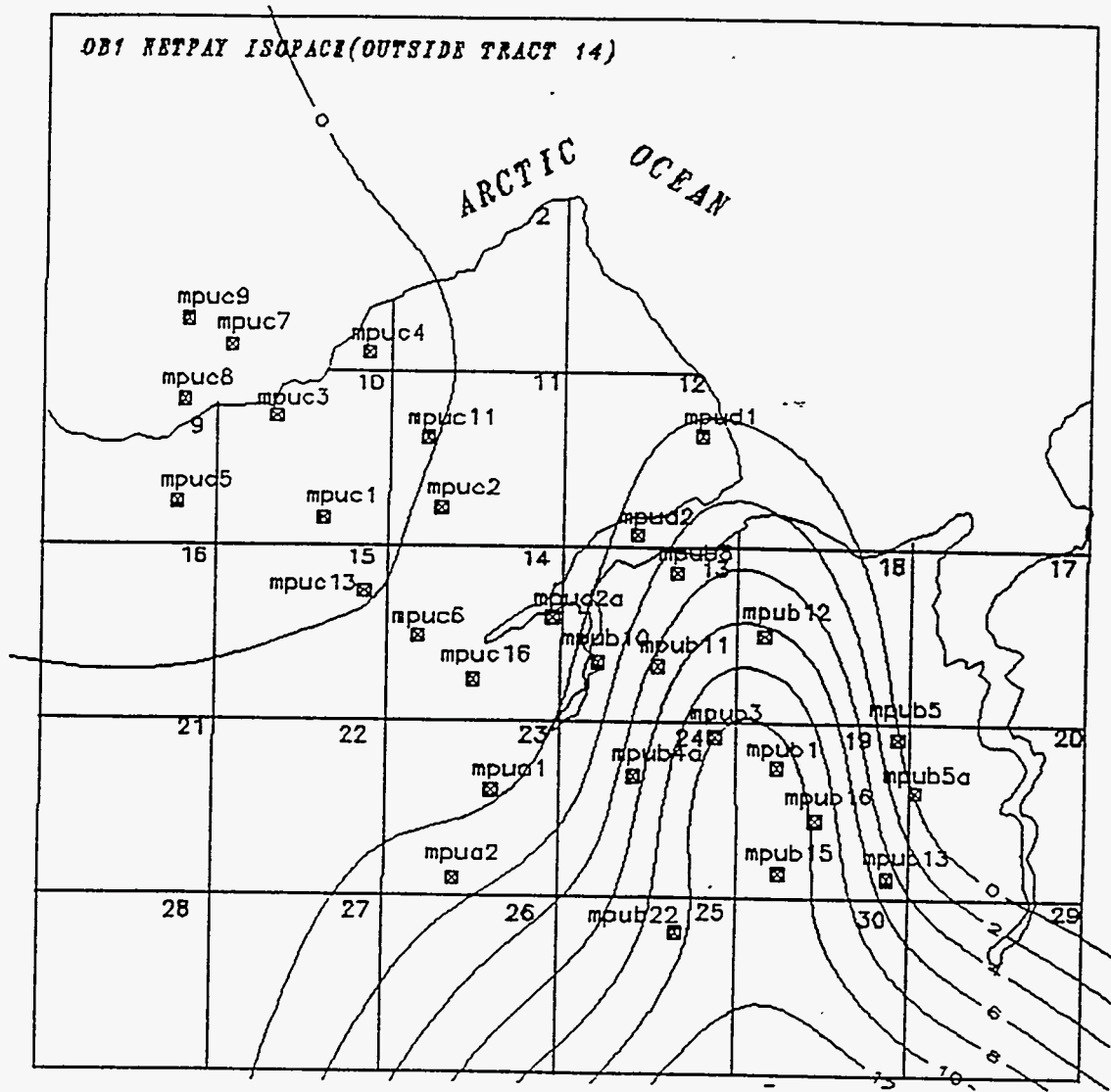


Figure 2.18 Net Pay Isopach for OB1 Sand

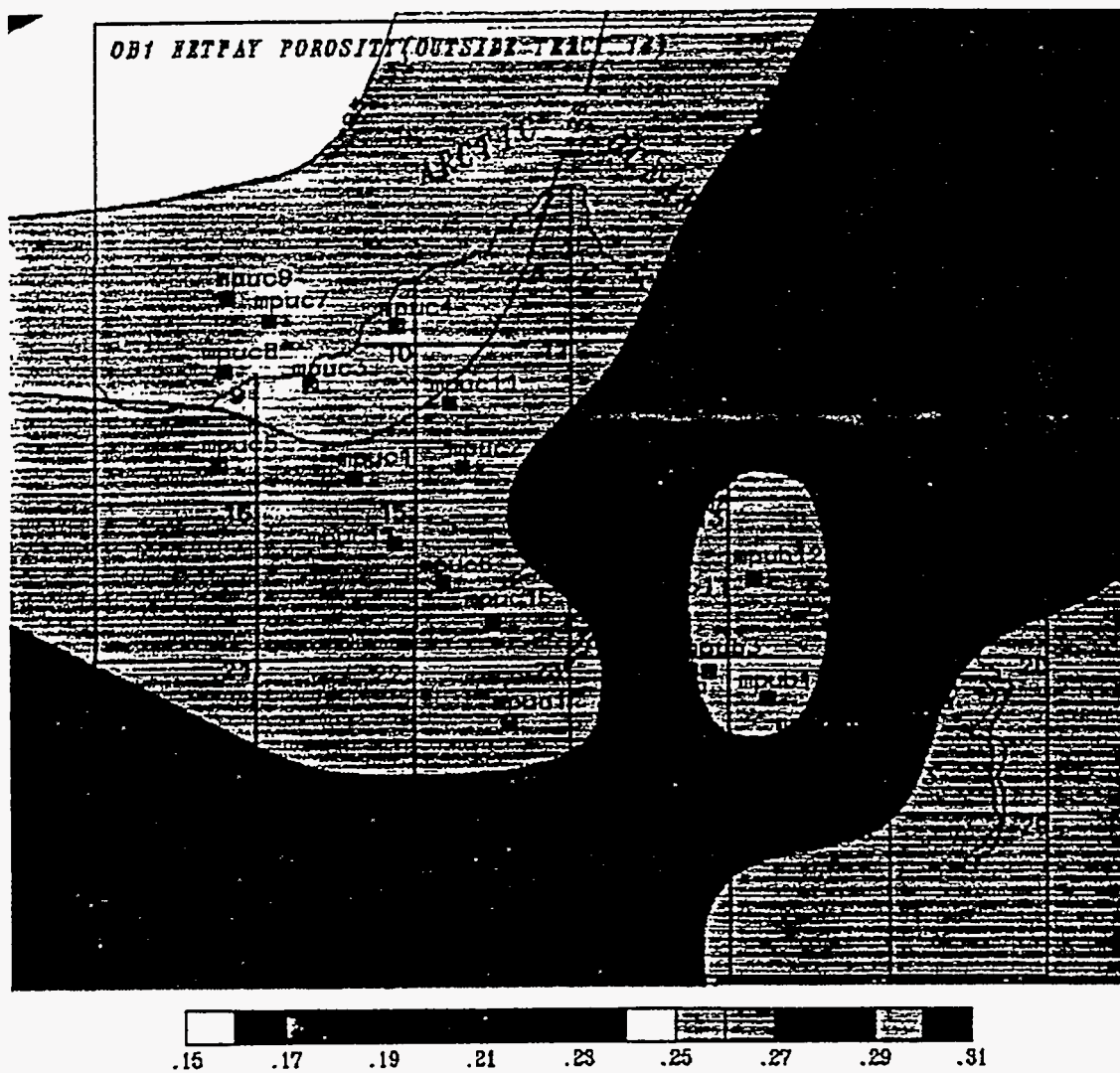


Figure 2.19 Effective Porosity Contour Map for OB1 Sand

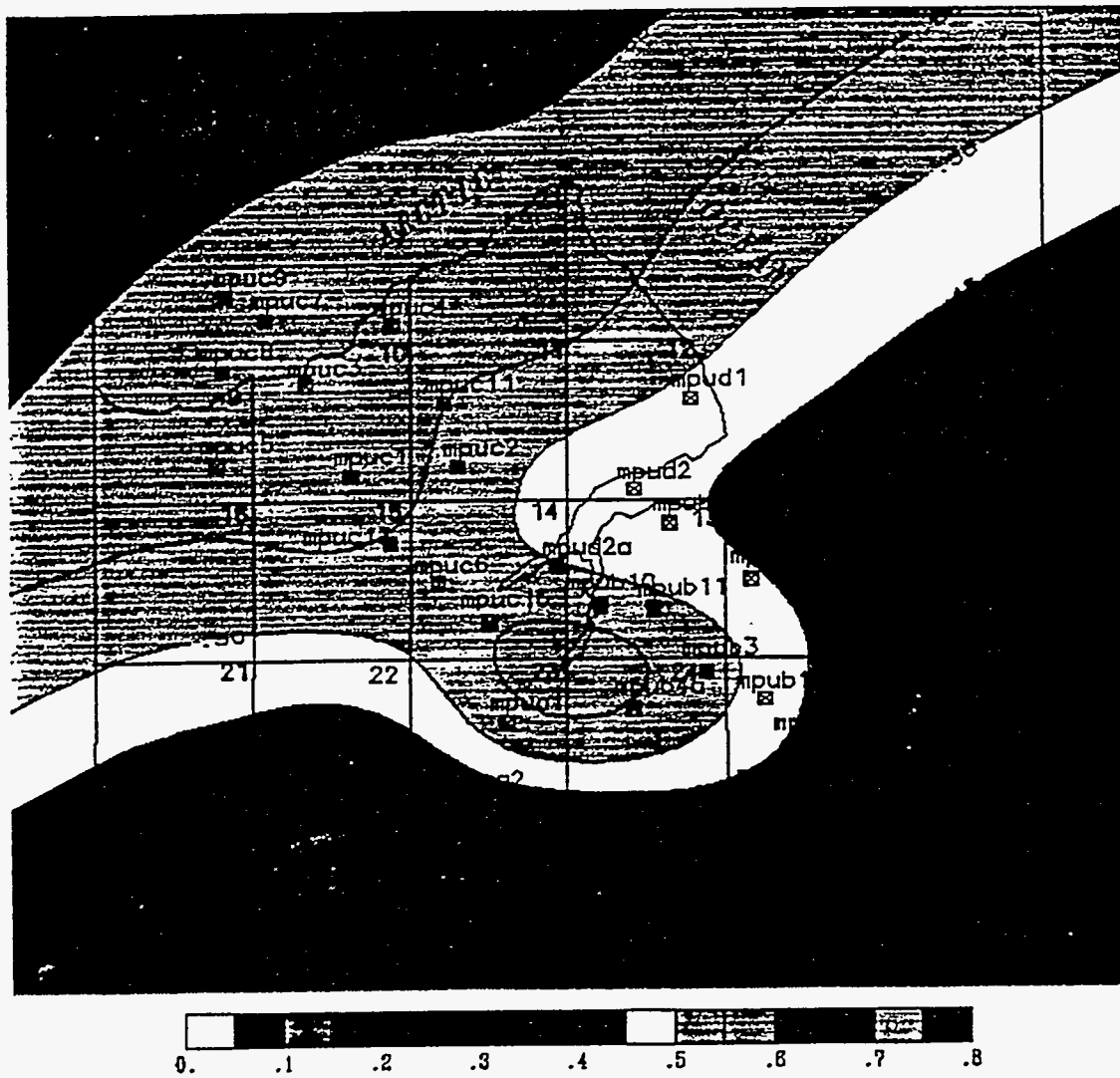


Figure 2.20 Water Saturation Contour Map for OB1 Sand

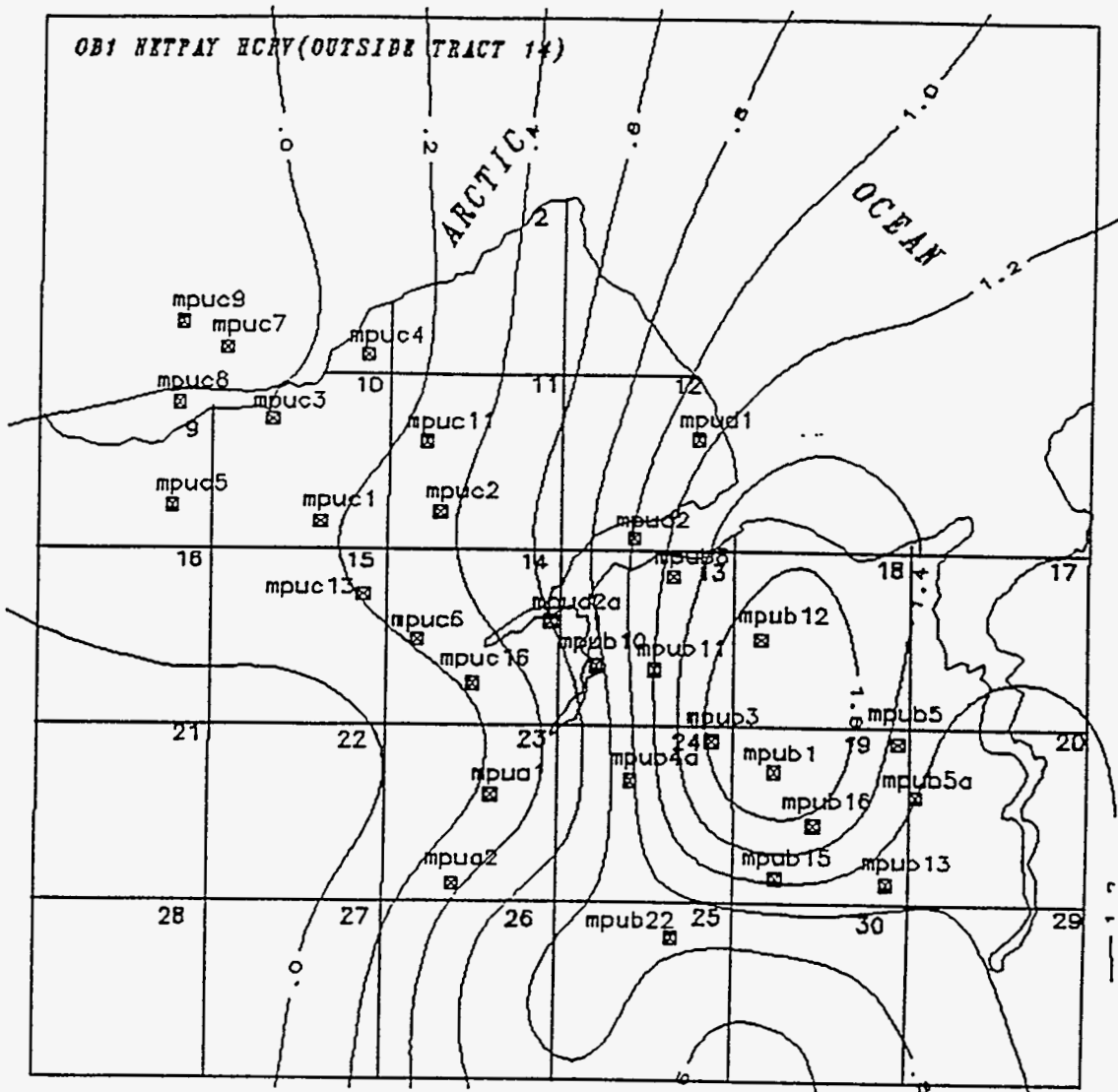


Figure 2.21 Sand Quality Distribution for OB1 Sand

Table 2.1 List of Milne Point Wells for Second Phase Reservoir Characterization

No	Well Proposed by Conoco	Well Analyzed	Well Status*
1	A-1	A-1	Suspended
2	A-2	A-2	Suspended
3	A-3	A-3	Suspended
4	B-1	B-1	Suspended
5	B-2	B-2	Suspended
6	B-3	B-3	Oil Producer
7	B-4	B-4	Plugged and Abandoned
8	B-4A	B-4A	Oil Producer
9	B-5	B-5	Suspended
10	B-8	B-8	Drilled as a Gas Injector
11	B-10	B-10	Oil Producer
12	B-13	B-13	Oil Producer
13	B-18	No Log Data	Drilled as a Water Injector
14	B-22	No Log Data	Oil Producer
15	C-1	C-1	Suspended Oil Producer
16	C-2	C-2	Oil Producer
17	C-3	C-3	Oil Producer
18	C-4	C-4	Oil Producer
19	C-5	C-5	Plugged and Abandoned
20	C-8	C-8	Converted to Water Injector
21	C-11	C-11	Drilled as a Water Injector
22	C-16	C-16	Converted to Water Injector
23	C-19	C-19	Suspended
24	D-1	D-1	Suspended
25	D-2	D-2	Plugged and Abandoned
26	D-2A	D-2A	Oil Producer
27	E-2	E-2	Suspended
28	E-6	E-6	Oil Producer
29	L-1	L-1	Suspended
30	L-3	No Log Data	Oil Producer
31	L-10	L-10	Drilled as a Gas Injector
32	M-1	M-1	Plugged and Abandoned
33	M-1A	M-1A	Suspended
34	N-1	No Log Data	Plugged and Abandoned
35	N-1A	No Log Data	Plugged and Abandoned
36	N-1B	Analysed in 1st Phase	Suspended

* Well Status are taken from a AOGCC Map of Jan. , 1992

Table 2.2 List of Normalized Wells

Normalized Well	Shift Amount
A-1	+0.10549
A-3	+0.03672
B-13	-0.02538
CFP2	-0.0267
D-1	+0.03556
D-2A	-0.03013
E-2	-0.03135
M-1A	+0.0467
3012	+0.0927
3k6	+0.070

CHAPTER 3

SLIM TUBE DISPLACEMENT STUDIES

A. INTRODUCTION

The API gravity and viscosity of oil in the Schrader Bluff sands varies considerably from horizon to horizon. Thus, a single enhanced oil recovery method may not be sufficient to produce this reservoir. Miscible processes may be more suitable to lighter crude in the deeper sections of Schrader Bluff reservoir. The available natural gas on the North Slope which currently is not marketed, can be enriched to provide injection gas for miscible flooding in Schrader Bluff reservoir. Currently, miscible flood is underway in Prudhoe Bay Unit and Kuparuk River Pool of the Kuparuk River Unit.

Slim tube displacement (STD) tests are usually performed to determine minimum enrichment (ME) requirements at reservoir conditions to achieve multi-contact miscibility (MCM) between enriched solvents and light crudes. In this study, STD tests are being conducted to evaluate characteristics and applicability of this method when applied to heavy crudes. The emphasis of this study is placed on evaluating various solvents such as CO₂, various mixtures of Prudhoe Bay Natural Gas (PBG), Kuparuk-Schrader Bluff Natural Gas (KUPSCH), and natural gas liquids (NGL) for the ability to achieve dynamic miscibility with Schrader Bluff crude. Equation-of-state (EOS) predictions are performed to compare the results of STD tests and to gain further insight into the mechanism of displacement.

Phase behavior of solvent-crude mixtures are the most important tools in understanding the mechanism of miscibility development in either CO₂ drives, or enriched hydrocarbon solvent drives. Pseudo-ternary diagrams have been often used to explain the mechanisms of oil displacement by vaporizing gas drive or condensing gas drives (1). For the past three decades, it has been considered that enriched hydrocarbon miscible displacement occurs via condensing mechanism (2), and high pressure lean miscible hydrocarbon gas (3) displacement occurs via vaporizing mechanism. In condensing gas drives, the in-situ generation of miscibility occurs due to gradual enrichment of reservoir fluids in intermediate components of solvent to a point where it becomes fully miscible with the injected solvent. In the vaporizing drive

on the other hand, the in-situ generation of miscibility occurs due to extraction of intermediate components of the reservoir fluid by the solvent and its gradual enrichment with these intermediates as it flows in the reservoir. The displacement by any mechanism is further characterized with the help of pseudo-ternary diagram as immiscible (IMM), multi-contact miscible (MCM), and first contact miscible (FCM) (4). In 1960, Benham et al. (5), proposed a method of predicting minimum miscibility pressure (MMP) or minimum enrichment (ME) required to achieve multi-contact miscibility by constructing pseudo-ternary diagrams and determining limiting tie-line intersections with the light-intermediate component axis. This method has been used ever since, although it has been updated slightly in recent years (6, 7).

However, the work of Stalkup (8) and Zick (9) challenged this traditional concept for some rich gas displacements. Zick (9) provided evidence indicating that the mechanism of enriched gas drives is not condensing type, but it is simultaneously both vaporizing and condensing types.

Recently, Novasad and Costain (10) using STD tests and EOS calculations showed that in Canadian reservoir rich gas projects the principal mechanism is liquid extraction drive, and provided further interpretation of this process.

A more rigorous procedure for determining minimum enrichment (ME) or minimum miscibility pressure (MMP) in case of a dual drive mechanism calls for proper characterization of reservoir fluid and solvent, determination of compositional path followed by solvent-reservoir fluid mixtures in multi-contact test calculations, and use of solvent-reservoir fluid, pressure-composition isothermal diagrams. This procedure was used to determine solvent enrichments.

B. RESERVOIR FLUID CHARACTERIZATION

Reservoir fluid characterization is one of the most important considerations in simulation of slim tube experiments and simulation of miscible flood performance in a reservoir. PVT simulator, developed by Scientific Software Intercomp, is used in developing reservoir fluid characterization for Schrader Bluff crude. The PVT simulator is useful in simulating and/or matching laboratory PVT tests. Its regression capabilities allow determination of EOS parameter values, which results in the best agreement between calculated data and laboratory data. These EOS parameters determined from this simulator can be used as an input data for multidimensional compositional reservoir simulation models.

The PVT simulator is capable of simulating saturation pressure calculations, density, viscosity calculations, flash expansion calculations, flash calculations, and multiple contact calculations experiments. This simulator splits any plus fraction in hydrocarbon systems into an automatically determined or specified number of extended fractions. This simulator uses Redlich-Kwong, Zudkevitch-Joffe-Redlich-Kwong, Soave-Redlich-Kwong, and Peng-Robinson equation-of-state equations. Peng-Robinson equation-of-state is used in the fluid characterization of Schrader Bluff reservoir oil.

From the laboratory PVT report of Schrader Bluff reservoir oil, the fluid system consists of thirteen components, from C1 to C11+, N₂, and CO₂. These thirteen components are regrouped into ten components using two pseudo-components. C6 to C8 is grouped into one pseudo-component (PC1) and C9 to C10 group is grouped into another pseudo-component (PC2). The grouping of these pseudo-components is done on weight basis. Regression is reported on the pseudoized system for optimal match with laboratory data.

C. MULTIPLE CONTACT TEST RUNS

The EOS parameters obtained from the regression on the pseudoized fluid system are used in conducting multiple contact tests using PVT simulator. Multiple contact tests were performed up to fifteen contacts. In Schrader Bluff reservoir, the produced gas from the reservoir is reinjected back into the Schrader Bluff formation. 90% of the gas is produced from Kuparuk formation and 10% is from Schrader Bluff formation. From the PVT analysis report of these two gases, their compositions are mixed in the ratio 9:1 to obtain the injected gas (KUPSCH GAS) composition. The injection gas is enriched with different amounts of NGL in each multiple contact test run. The enrichment of NGL varied from 0 to 45%. The multiple contact test runs were conducted for 0, 5, 15, 25, and 35% of NGL enrichment with the lean gas.

Figures 3.1 through 3.3 show the results obtained from the multiple contact test runs. These figures are plotted for density vs. number of contacts. For a miscible test run, the liquid and gas density vs. number of contacts should converge, showing that the two fluids form one phase. From these figures, it is clear that these runs did not result in miscibility since the gas and liquid density lines do not converge. The liquid density decreases gradually due to the in-situ mass transfer of intermediates from liquid phase to gas phase.

Figures 3.4 through 3.6 are plotted for equilibrium constants, K-values for different fractions (C1, C2, C3, C4, C5, PC1, PC2, and C11+) vs. number of contacts. For a miscible test run all lines representing each fraction in the K-value plots should converge to an equilibrium constant value of one. These K-plots also do not show achievement of miscibility since the lines do not converge to a value of one.

D. SLIM TUBE SIMULATION

The EOS parameters obtained from the PVT simulator are used to simulate slim tube displacement runs on GEM simulator, developed by Computer Modelling Group. The EOS parameters are included in Table 3.1. GEM is a multidimensional EOS compositional simulator which can simulate all the important mechanisms of a miscible gas injection process, i.e., vaporization and swelling of oil, condensation of gas, viscosity and IFT reduction, and the formation of a miscible solvent bank through multiple contacting. GEM can be run in explicit, fully implicit, and adaptive implicit modes. GEM uses dual porosity and dual permeability models. GEM simulator can also perform flash calculations. The quasi-Newton successive substitution method is used to solve the nonlinear equations associated with flash calculations. GEM utilizes either the Peng-Robinson or Soave-Redlich-Kwong equation-of-state equations. Peng-Robinson EOS is used in the simulation of slim tube experiments.

In the experimental setup, the slim tube is 40 feet in length and is coiled in one foot diameter. The slim tube has an outer diameter of 0.236 inches, and it is filled with Ottawa sand of 0.352 porosity and 5 darcy permeability. The pore volume of the slim tube is determined by injecting toluene.

For simulation purposes, slim tube is represented by one dimensional model of $40 \times 1 \times 1$ grid blocks. Each grid block is one foot in length, and in j and k directions lengths are adjusted to represent exact slim tube volume. One injector and one producer are included in this model at the first and last block respectively. The grid diagram is shown in Figure 3.7. The slim tube porosity and permeability values are input into the simulator. The solvent injection rate was maintained at 3 cc/hr and a total of 1.2 PV of solvent is injected in each simulation run.

GEM simulator has two models, large memory model and small memory model. Small memory model handles greater numbers of components than large memory model. Small memory model uses ten components. All the EOS parameters for the regular components are stored in the simulator. For user defined components, all the EOS parameters have to be input into the simulator. The EOS parameters listed in Table 3.1 for pseudo-components and plus fractions are input into the GEM simulator. Slim tube simulation results are compared with the experimental results in the later sections.

E. EXPERIMENTAL APPARATUS

To obtain accurate data in laboratory experiments, it is essential that certain requirements are met. Extremely accurate flow control must be maintained at all pressures. Reliable pressure readings should be monitored frequently throughout the experimental run. Accurate and constant back pressure must be kept throughout the run. A reliable method for measuring volumes of fluids under high pressures and at atmospheric conditions must be available. In order to meet these requirements and assure the reproducibility of the resulting data, the high pressure high temperature miscibility apparatus designed by D.B. Robinson and Assoc. was modified, assembled, and used in the laboratory to determine MMP relations. This assembly is schematically shown in Figure 3.8. The major components of this assembly consist of the following:

1. One motorized positive displacement pump.
2. One slim tube.
3. Two forced air temperature controlled ovens.
4. One high pressure capillary sight glass.
5. Three digital pressure gauges.
6. One differential pressure transducer.
7. One calibrated glass receiver and optical liquid measuring device.
8. One precision 40 liter gasometer.
9. Six transfer cells.
10. One recombination cell and shaking device.
11. One dome type back pressure regulator.
12. One high volume vacuum pump.
13. One Constametric pump.

The equipment was designed for operation at pressures up to 10,000 psi and temperatures to 200°C. The driving force behind the slim tube miscibility apparatus was the motorized JEFRI positive displacement pump which was used throughout the experiment to accurately meter, feed and proportionately displace liquids and gases under high pressure. More specifically, it effectively had four functions.

1. Provide constant pressure while recombining West Sak Crude samples.
2. Compress and transfer gases and NGLs during the solvent mixing process.

3. Drive recombined oil to saturate the slim tube before each run and drive solvents to clean the slim tube after each run.
4. Inject the gas solvent mixture during each run.

The pump was equipped with a DC servo motor and chain drive which in turn was controlled by a microprocessor indexer. This allowed the pump to either displace fluids at constant flow rates from 1 to 1,000 cc/hr, or to maintain a constant pressure, regardless of the direction of flow, at variable speeds. Pump operation could be monitored throughout the run with the use of high and low pressure limit alarms.

The slim tube itself was composed of a 12 meter section of 6.4 mm O.D. high pressure stainless steel tubing which was packed with Ottawa sand and coiled to a diameter of approximately one foot. The final porous medium had an average porosity of roughly 35.2% which could provide an average frontal advance rate of about 120 cm/hr. Average slim tube permeability was calculated to be 5.0 darcies, using pure toluene as the test fluid of known viscosity.

The slim tube and recombination cell were enclosed in a windowed, forced air, temperature controlled oven. Oven temperature was controlled through the simultaneous heating of a main bulk heating coil and a smaller microprocessor controlled heating coil. The main bulk heater was set with a simple rheostat and was the main source for the oven, while smaller coils were used to control the oven's temperature within 0.2°C of the desired set point. During operation, the main bulk heater was set to a few degrees below the desired temperature according to an individual calibration curve. Additional heat, provided by the small coils, raised the temperature to the desired setting and was constantly monitored by a thermocouple and microprocessor. In the event that the main bulk temperature increased above the desired point, due to an increase in ambient temperature or decrease in volumetric flow rate through the slim tube due to reduced flashing, an alarm set point had the ability to shut down the main heat source until temperature control was once again achieved.

At the effluent end of the slim tube, a JEFRI high pressure capillary sight glass was used to visually observe displaced fluids during the dynamic miscible process. The sight glass consisted of a Pyrex capillary tube, 4.390 inches in length with a 7.7 mm I.D. and 1.5 mm O.D., mounted within a windowed overburden cell. In the overburden cell, distilled water was compressed by a hand operated pressure generator

to a pressure approximately 300 psi. greater than that within the capillary tube. While maintaining this pressure differential, it was possible to observe the transient phase behavior of fluids at operating conditions of up to 200°C and 10,000 psi. Visibility was excellent due to the fact that the overburden fluid had similar refractive characteristics to that of glass, decreasing refractive distortion between the windowed cells.

The overall operating pressure of the slim tube system was controlled by a gas driven, dome type back pressure regulator. Operating on the principle of balanced pressure, a stainless steel diaphragm separated the effluent pressure from the pressure exerted by the operator's set point. A pressure reaction chamber allowed for precise pressure imbalance control thus maintaining predetermined run pressures.

Once the effluent is flashed to atmospheric conditions, through the back pressure regulator, the resulting gas and liquid components were collected and measured volumetrically. The gas was measured by a JEFRI precision gasometer using a calibrated stainless steel cylinder and piston fixed to a threaded rod which was linked to an electric motor. As gas entered the cylinder, atmospheric pressure was maintained in the gasometer by a system which moved the piston to expand the cylinder's volume. Such volume control was achieved using an oil filled manometer equipped with a pair of optical interrupter switches. An increase in pressure within the cylinder was indicated by a change in manometer fluid meniscus level. Any such change in meniscus level was noted by the optical sensors, and a signal was sent to the motor drive which increased the volume of the cylinder to accommodate the additional gas. Piston location was measured and displayed by an optical linear encoder, and converted through a calibrated constant to standard cubic centimeters.

A specially designed glass cylinder collected the condensed liquid after it passed through a condenser. An optical sensor, similar to that used in the gasometer, was mounted on a motor driven lead-screw. As the opaque oil meniscus rose up the glass cylinder it interrupted the path of the laser sighted optical sensor, which in turn signaled the motor to raise it according to the level of the air liquid interface. Once again, a linear encoder measured the calibrated sensor level which was converted into cubic centimeters of oil.

During the run, the upstream pressure was monitored by a precision pressure transducer linked to the motorized pump's microprocessor, while the downstream

pressure was monitored by a digital Heise pressure gauge. An external Heise gauge was also linked into the system to monitor gas pressures during solvent mixing. A Validine differential pressure transducer was used to monitor the differential pressure across the slim tube during the displacement process. The external Heise gauge was calibrated using a dead weight tester and was then used to calibrate the other gauges.

Six cells, five of them with pistons and one without a piston, were used to recombine oil, mix solvents, and transfer fluids during each experiment. Two of the pistoned cylinders, manufactured by Temco of Tulsa, OK., were used to compress gas for solvent mixtures and the back pressure regulator, as well as drive cleaning solvents through the slim tube. The remaining JEFRI cylinders were used to recombine oil, transfer NGLs, and drive final solvent mixtures during each experimental run. Whether pistoned, or unpistoned cylinders used with mercury, each cell was rated to 10,000 psi and designed to be used with single phase fluids. For this reason, it was imperative that the gas solvent mixture used in each experiment existed in a single phase to insure consistent composition throughout the run.

Each piece of equipment was connected with 1/8 and 1/16 inch high pressure 316 stainless steel tubing and HIP fittings. Generally, lines containing liquid were of the larger 1/8 inch O.D. to accommodate the fluid's higher viscosity, while gas lines were constructed of 1/16 inch tubing. Whenever possible, it was important to reduce line size and length to minimize dead volume in the apparatus. The HIP fittings used were easily broken and refitted without reducing their high pressure sealing capabilities.

When transferring fluids from one cell to another through stainless steel tubing, it was necessary to thoroughly evacuate the system to maintain compositional purity and avoid contamination. This was accomplished with the use of a Welsh high volume vacuum pump capable of inducing effective vacuums down to 50 microns. Generally, less than 200 microns were achieved before transferring oil, solvents, or gases.

F. EXPERIMENTAL PROCEDURE

It was very important to accurately measure the pore volume of the slim tube to determine oil recovery. Toluene was used to find the pore volume of the slim tube. The slim tube is evacuated first and then isolated from inlet valve to the inlet valve of the BPR. A piston cylinder filled with toluene was pressurized using positive displacement pump, to pressure of 2,000 psi, which is above the vapor pressure of toluene at room temperature. The initial pump reading was noted and then the inlet valve of the slim tube was opened slowly and pumping of toluene was started under the displacement pump's constant pressure mode. Once the slim tube pressure was equilibrated at 2,000 psi, a final pump reading was recorded. The amount of toluene injected was obtained from subtracting initial and final readings. To this value 0.22 cc was added to account for the dead volume of the back pressure regulator (BPR). Thus the pore volume of the slim tube was determined to be 76.82 cc.

Before each experimental run, injected solvent is prepared in the solvent chamber. When pure carbon dioxide was used as solvent it was simply compressed in one of the transfer cells and injected into the solvent chamber. The same process was followed when Kuparuk-Schrader Bluff and Prudhoe Bay Gas (PBG) were used as solvents. However, for the preparation of mixtures of CO₂ and NGL, or PBG and NGL, a series of calculations were done to obtain the volume of each component required to obtain the desired solvent mixture. The calculated volumes were injected into the solvent chamber which was then rocked to give a uniform, single phase mixture.

The next step was to prepare a "live" oil sample from the "dead" oil sample. The calculated amount of "dead" oil was taken into the recombination cell and then by injecting solution gas the cell was pressurized to bubble point pressure. The cell was rocked for over twelve hours for thorough mixing of gas and oil. As the gas started dissolving in solution, the pressure in the cell dropped. Pressure reduction was monitored by the pump. This process was repeated until the oil was saturated at the bubble point pressure.

The recombined oil was then used to saturate the slim tube. While saturating the slim tube, it was very important to maintain the slim tube pressure above the bubble point pressure at experimental temperature, to make sure that oil was never allowed to flash. This was done by raising the pressure of the BPR to above the bubble

point pressure. Then the "live" oil was pumped at 3 cc/hr into the slim tube. Two pore volumes of oil were injected to make sure that all traces of toluene were displaced from the slim tube. At this point, the apparatus was ready for conducting an experiment.

After saturating the slim tube, the pump was stopped and sufficient time was allowed for the slim tube inlet and outlet pressures to equilibrate. The pressure in the solvent chamber was raised by 50 psi above the downstream pressure to assure positive displacement and solvent was injected into the slim tube at 3 cc/hr. The experiment was monitored by recording various variables required to evaluate a slim tube experiment. Initial readings of the experiment were taken at one to two hour intervals. As the miscible front passed through the sight glass, and large volumes of gas were produced, the time intervals between the readings was reduced. Production of large volumes of gas were the indication of the breakthrough of the injected solvent. Generally, the run was terminated after 1.2 PV of the solvent injected, and when three consecutive recovery readings taken at one hour intervals were the same.

Following each experimental run, it was necessary to clean the slim tube for further experiments. This was done by injecting two to three pore volumes of toluene at 3 cc/hr until pure colorless toluene was produced at the effluent end. After this, fresh solvent was prepared, and the slim tube was saturated with oil for the next experimental run.

G. RESULTS AND DISCUSSIONS

Experimental And Simulation Results:

Various experimental runs were conducted in the slim tube apparatus to test for the miscibility between Schrader Bluff crude and the solvent mixtures. The compositions of the solvent mixtures with various levels of CO₂ and PBG by NGL are given in Appendix A. Experimental oil recovery of 95% or more was set as the criterion for miscibility achievement. Then for each tested solvent in the slim tube, using the same solvent composition, slim tube simulation was conducted on GEM compositional simulator (CMG, Canada). Initially, pressure-composition (P-X) diagrams (Figure 3.9 and Figure 3.10) were plotted from the data obtained from PVT Coats simulator (SSI) for CO₂/NGL mixture and PBG/NGL mixture, in order to ensure that the solvents injected would be in a single phase. The following sections describe and discuss each experimental and simulation run with various solvents. Raw data for all the experimental runs is provided in Appendix B.

EXPERIMENTAL RESULTS

100% Kuparuk-Schrader Bluff gas at 1300 psi and 82°F

The first experimental run was conducted using the lean gas from Kuparuk and Schrader Bluff formation. This run was conducted at a pressure of 1300 psi and at a temperature of 82°F. This run resulted in an ultimate recovery of 37.92% at 1.2 PV injection of the solvent (Figure 3.11). Figure 3.11 shows the breakthrough in experimental run has occurred at approximately 0.48 PV injection. The capillary sight glass showed the presence of two phases which suggests the lack of miscibility development. Slim tube simulation run resulted in an ultimate recovery of 41.85%. The breakthrough in slim tube simulation is earlier than the one in experiment. The relative deviation between the experimental and slim tube simulation was 9.39%.

100% CO₂ at 1300 psi and 82°F

In this run, pure CO₂ was injected as the solvent. This experimental run resulted in a recovery of 71.63% (Figure 3.12). The capillary sight glass showed the presence of two phases which definitely suggests the lack of miscibility. The

breakthrough occurred after 67% of pore volume injection (Figure 3.12). The slim tube simulation predicted a recovery of 76.45% (Figure 3.12). In this case also, the slim tube breakthrough occurred slightly earlier than in experiment. The density plot (Figure 3.12) and K-values plot (Figure 3.12) were plotted from the data obtained from the multi-contact test (MCT) runs conducted on PVT Coats simulator. From Figure 3.12, it is clear that there is great increase in gas density. This is due to the transfer of intermediates and heavies from the oil to the solvent. It can also be seen from this graph that there is a slight increase in liquid density. This is due to the partial dilution of high density CO₂ into the liquid phase. From this plot it is clear that miscibility did not occur, because the two curves did not converge. But the density and K-values plots (Figure 3.12) suggest that there is a high degree of mass transfer.

90% CO₂ and 10% NGL at 1300 psi and 82°F

This run resulted in a recovery of 88.48% and the breakthrough occurred after 89% of pore volume injection (Figure 3.13). The slim tube simulation run resulted in a recovery of 95.25% and breakthrough occurred after 89% of pore volume injection. The increase in recovery in slim tube experiments is due to the presence of intermediates in the solvent. Both slim tube simulation and the MCT results (Figure 3.13) verify that this run resulted in miscibility but the recovery from experiment and sight glass observation indicates that there is occasional presence of a two phase zone. Thus, it is inferred that complete miscibility did not occur. From Figure 3.13, it can be inferred that there is a high degree of mass transfer.

85% CO₂ and 15% NGL at 1300 psi and 82°F

This experimental run resulted in a 98.01% oil recovery after 1.2 pore volume of solvent injection (Figure 3.14). The breakthrough occurred after 1.08 PV injection (Figure 3.14). In slim tube simulation, the breakthrough occurred slightly before the experimental run. The simulation recover is 100%. The sight glass observations did not indicate any presence of a two phase region. MCT run results (Figure 3.14) on PVT Coats simulator indicated achievement of direct contact miscibility.

The following runs were conducted using mixtures of Prudhoe Bay Gas and NGL at the bubble point pressure of 1300 psi and at the reservoir temperature of 82°F.

100% Prudhoe Bay Gas at 1300 psi and 82°F

The first run in this set of runs was conducted using PBG obtained from Prudhoe Bay reservoir. This experiment resulted in a recovery of 45.01% (Figure 3.15) and solvent breakthrough occurred after approximately 0.46 PV injection (Figure 3.15). The slim tube simulation resulted in a recovery of 48.46% and solvent breakthrough occurred at 0.35 PV injection. From sight glass observation, it is clear that there is presence of a two phase region. This clearly shows there is no miscibility development. Also, from density and K-values plots (Figure 3.15), it is apparent that there is no miscibility development.

70% Prudhoe Bay Gas and 30% NGL at 1300 psi and 82°F

In this run, PBG was enriched with 30% NGL and used as a solvent. This resulted in a recovery of 86.63% after 1.2 PV of solvent injection (Figure 3.16). The solvent breakthrough occurred after 0.92 PV of solvent injection. From Figure 3.16, the ultimate recovery from slim tube simulation is 85.56%. Sight glass observations clearly indicate the presence of two phases. Thus, miscibility is not achieved in this case. The density and K-values plots (Figure 3.16) clearly show that there is no development of miscibility.

60% Prudhoe Bay Gas and 40% NGL at 1300 psi and 82°F

Further enrichment of PBG by increasing the NGL content to 40% resulted in a recovery of 92.57% (Figure 3.17). From Figure 3.17, the solvent breakthrough occurred after 0.97 PV injection of solvent. The slim tube simulation recovery after 1.2 PV injection was 94.55%. The sight glass observations did not indicate any clear two phase region. Based on recovery it is concluded that miscibility has not developed completely. The density and K-value plots (Figure 3.17) obtained from MCT runs do not indicate any presence of miscibility.

50% Prudhoe Bay Gas and 50% NGL at 1300 psi and 82°F

50% NGL in the solvent resulted in the recovery of 99% oil in the slim tube experimental run (Figure 3.18). The solvent breakthrough occurred after nearly 1 PV of solvent injection. The slim tube simulation resulted in a recovery of 100% after 1.2 PV

of solvent injection. Sight glass observation did not show any presence of two phases. Even though the density and K-value plots (Figure 3.18) did not indicate miscibility development, based on slim tube recovery it is concluded that this run resulted in miscibility.

40% Prudhoe Bay Gas and 60% NGL at 1300 psi and 82°F

Using PVT Coats simulator, MCT run was conducted by using 40% PBG/60% NGL mixture as solvent. The density and K-values plots (Figure 3.19 and Figure 3.20) obtained for this run did not indicate the achievement of miscibility. Figure 3.21 and Figure 3.22 are plotted from the liquid and gas fractions of various components obtained at various contacts during MCT run. It is possible that a second liquid hydrocarbon phase may have formed at these solvent compositions, but since the simulator is a two-phase simulator, it was unable to handle such a situation.

36% Prudhoe Bay Gas and 64% NGL at 1300 psi and 82°F

MCT run was conducted on PVT simulator using 36% PBG/64% NGL as solvent. This run indicated that this resulted in a direct contact miscibility. Figure 3.23 and Figure 3.24 are the density and K-value plots, plotted for the data obtained from the MCT run. In Figure 3.23 the gas density is zero because this run resulted in a direct contact miscibility. Figure 3.25 and Figure 3.26 give the liquid and gas fraction at each contact during MCT run.

DISCUSSION OF RESULTS

The first slim tube run was conducted using 100% lean gas from Kuparuk-Schrader Bluff formation. This run resulted in an immiscible displacement with very low recovery. After this, slim tube runs were conducted using the mixtures of CO₂ and NGL, and PBG and NGL. 85% CO₂/15% NGL mixture showed miscibility experimentally at 1300 psi and 82°F, but slim tube simulation and PVT Coats MCM tests showed multiple contact miscibility at 90% CO₂/10% NGL, but for this composition experimental run, sight glass observations showed the presence of a two phase zone. PVT Coats simulator for 85% CO₂/15% NGL solvent mixture predicted direct contact miscibility. The runs using CO₂ as solvent showed that primarily vaporizing drive mechanism is responsible for the development of miscibility.

In case of PBG/NGL mixtures, 50% PBG/50% NGL mixture developed miscibility during experimental run. Slim tube simulation also predicted miscibility for the solvent. But PVT Coats and MCM tests did not indicate the presence of miscibility. This may be due to the fact that a second hydrocarbon phase may be formed at these solvent compositions and the simulator is not capable of handling three phases. PVT Coats has predicted direct contact miscibility for 36% PBG/64% NGL mixture. For PBG/NGL also, vaporizing mechanism is responsible for development of miscibility. Table 3.2 compares the recoveries obtained from experiment and slim tube simulation.

H. CONCLUSIONS

From the results discussed in this chapter, the following conclusions were drawn.

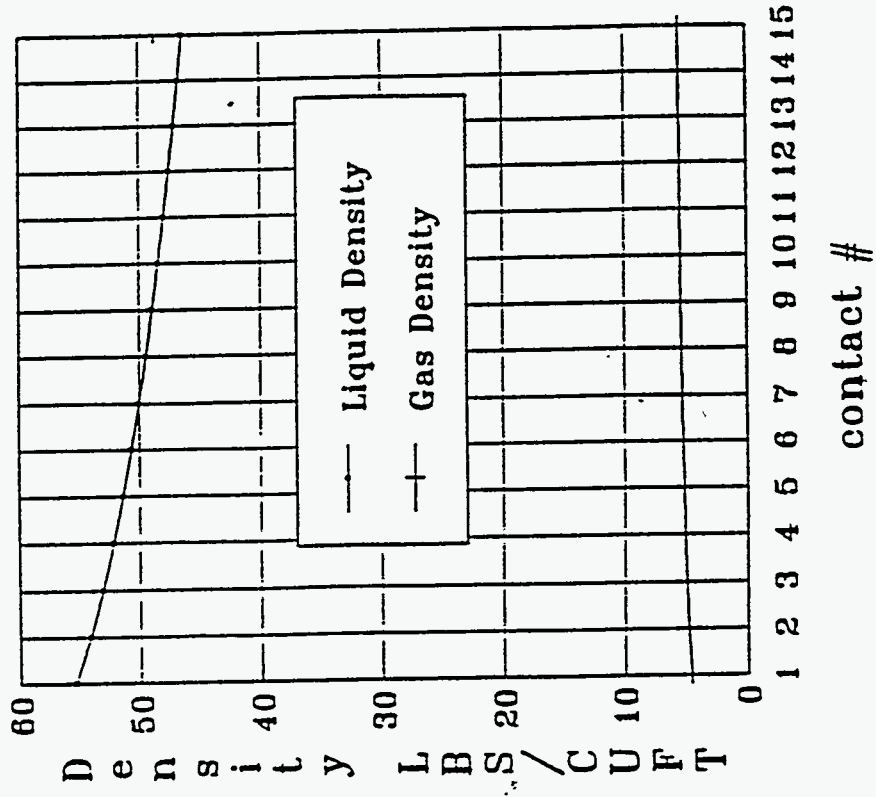
1. The pure lean gas from Kuparuk-Schrader Bluff formation is immiscible at reservoir pressure of 1300 psi and temperature of 82°F, yielding very low recovery in slim tube experiment. Thus, if this gas is to be used in field applications, it will be immiscible WAG type process.
2. Pure CO₂ and PBG are also immiscible with Schrader Bluff crude at reservoir conditions. Very high recovery is obtained during pure CO₂ slim tube experimental run. This indicates that use of CO₂ may be promising in the field application.
3. The enrichment of CO₂ by NGL at 15 mol% NGL resulted in dynamic miscibility at reservoir conditions. This run resulted in 98% oil recovery after injection of 1.2 PV. The compositional slim tube simulation and the EOS predictions also confirmed generation of miscibility. The miscibility was developed by primarily vaporizing drive mechanism.
4. PBG achieved miscibility after enriching it at 50 mol% of NGL. This slim tube experimental run resulted in 99% recovery after injection of 1.2 PV of solvent. The compositional simulation predicted 100% recovery after injection of 1.2 PV of solvent. But the MCT runs conducted on 2-phase EOS simulator did not predict miscibility development for this mixture.
5. The lumping of pseudo-components and determination of EOS parameters appeared to be very critical in matching laboratory slim tube data.

I. REFERENCES

1. Hutchinson, C.A. Jr. and Braun, P.H.: "Phase Relations of Miscible Displacement in Oil Recovery," AIChE J. (1961), vol. 7, 64-72.
2. Clark, N.J., Schultz, W.P., and Shearin, H.M.: "Condensing Gas Drive, Critical Displacement Process - New Injection Method Affords Total Oil Recovery," Pet. Eng. (Oct. 1956), vol. 28, B-45.
3. Slobod, R.L. and Koch, H.A. Jr.: "High Pressure Gas Injection - Mechanism of Recovery Increase," Drill and Proc. Prac. API (1953), 82.
4. Stalkup, F.I. Jr.: "Miscible Displacement," Henry L. Doherty Series Monograph, vol. 8, SPE-AIME, New York (1983).
5. Benham, A.L., Dowden, W.E., and Kunzman, W.J.: "Miscible Fluid Displacement - Prediction of Miscibility," Trans. AIME (1960), vol. 219, 229-237.
6. Williams, C.A., Zana, E.N., and Humphreys, G.E.: "Use of The Peng-Robinson Equation-of-State to Predict Hydrocarbon Phase Behavior and Miscibility for Fluid Displacement," SPE 8817, A paper presented at the SPE/DOE Symposium on Enhanced Oil Recovery at Tulsa, OK (April 20-23, 1980).
7. Wu, R.S., Batycky, J.P., Harker, B., and Rancier, D.: "Enriched Gas Displacement: Design of Solvent Compositions," J. of Can. Pet. Tech. (May-June, 1986), vol. 25, 55-59.
8. Stalkup, F.I.: "Using Phase Surfaces to Describe Condensing - Gas - Drive Experiments," SPE J (Sept. 1965), 186-188.

9. Zick, A.A.: "A Combined Condensing/Vaporizing Mechanism in the Displacement of Oil by Enriched Gases," SPE 15493, A paper presented at the 61st Annual Technical Conference and Exhibition SPE, New Orleans, Louisiana (Oct. 5-8, 1986).
10. Novasod, Z., and Costain, T.: "New Interpretation of Recovery Mechanisms in Enriched Gas Drives," J. of Can. Pet. Tech. (March-April, 1988), vol. 27, No. 2, 54-60.

95%KUPSCH GAS & 5%NGL



100% KUPSCH GAS

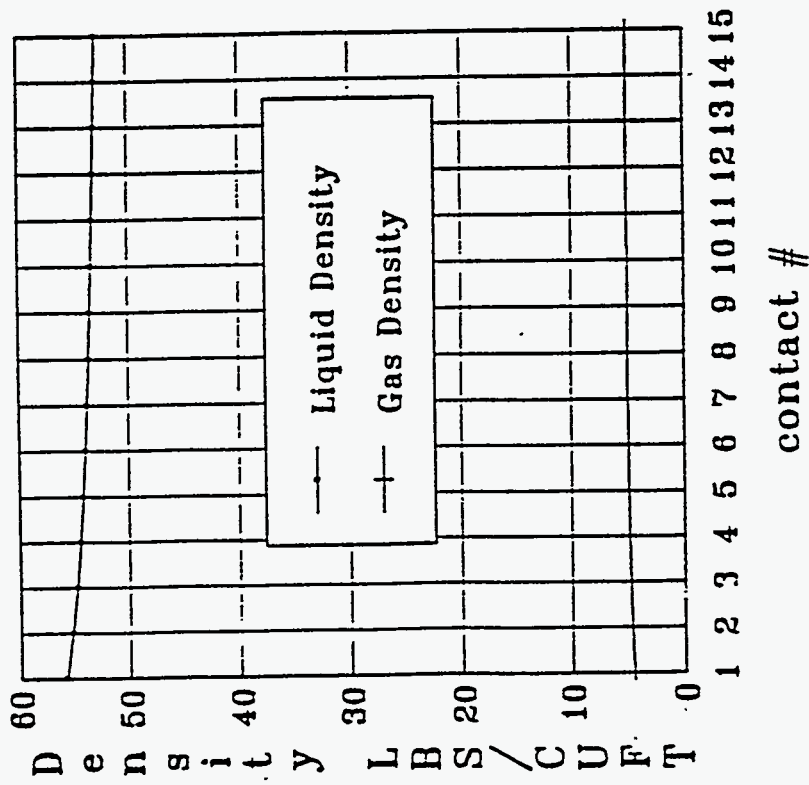
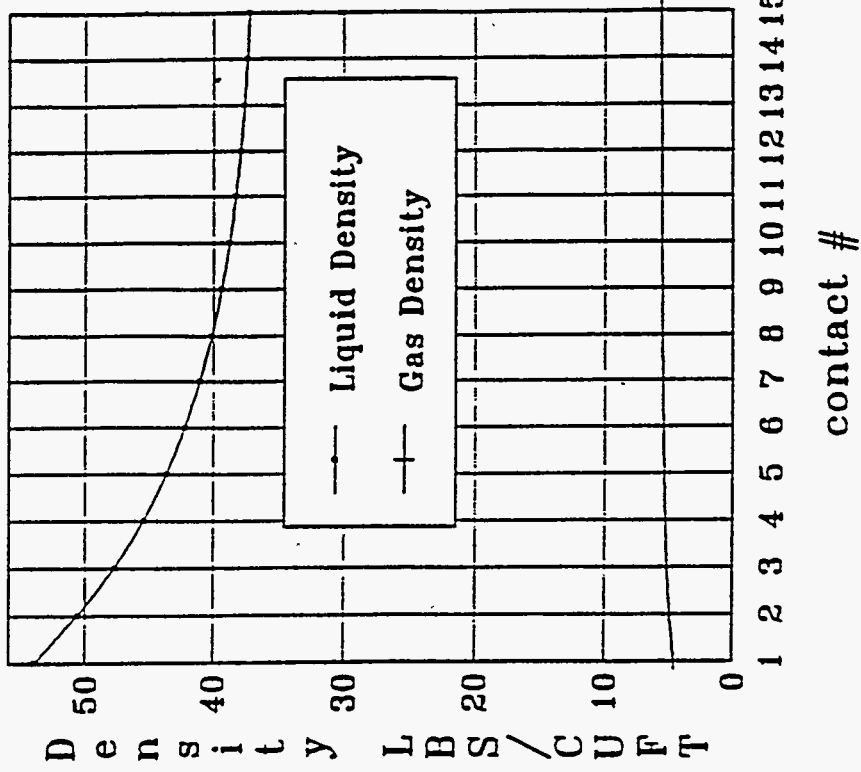


Figure 3.1 Density vs. Contact Number (100% KUPSCH Gas)

75%KUPSCH GAS 25%NGL



85%KUPSCH GAS & 15%NGL

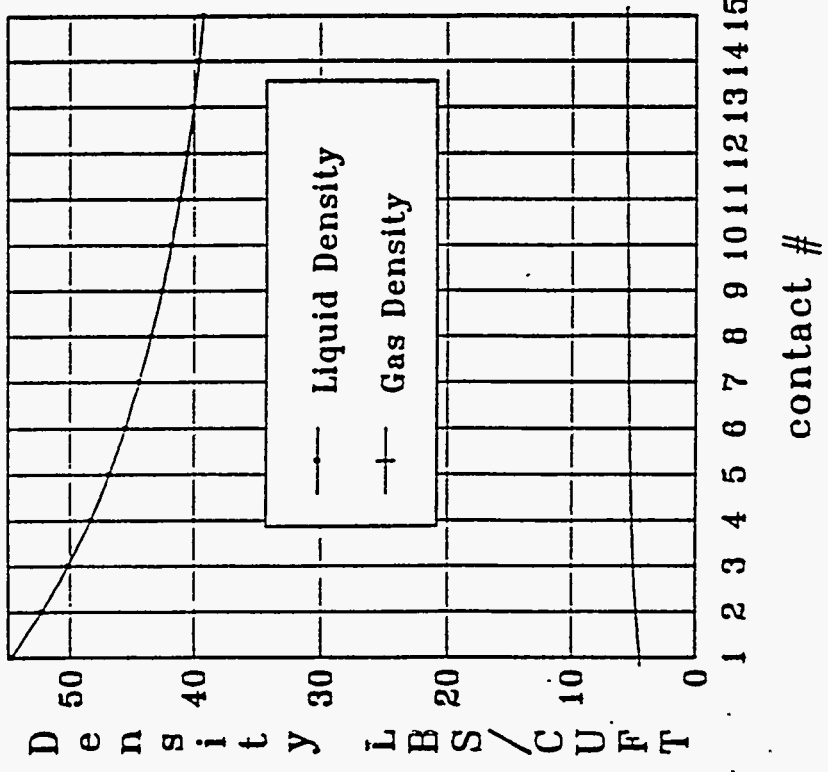
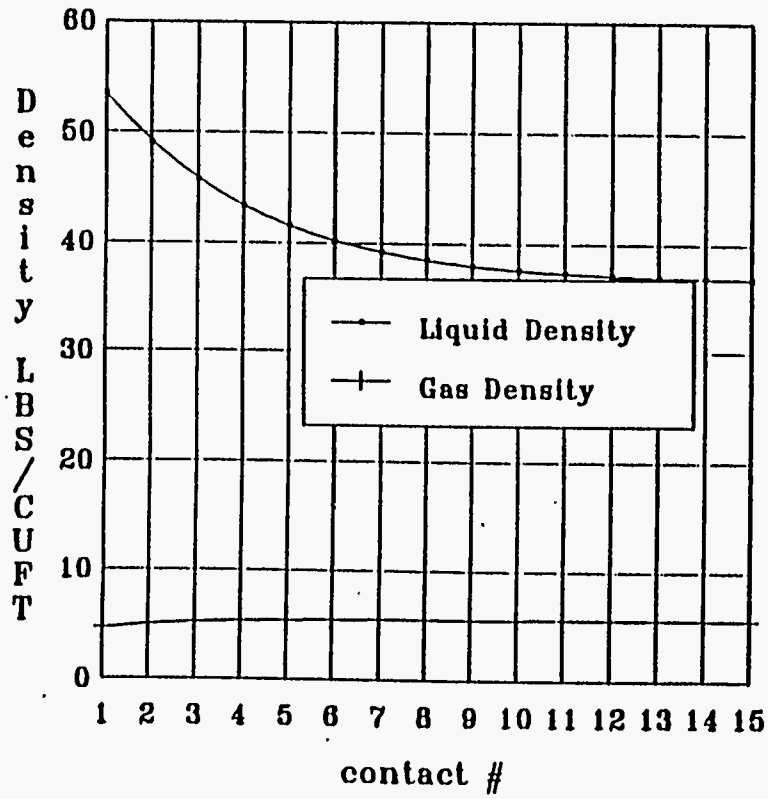


Figure 3.2 Density vs. Contact Number (85% KUPSCH/15% NGL)

65%KUPSCH GAS & 35%NGL



55%KUPSCH GAS & 45%NGL

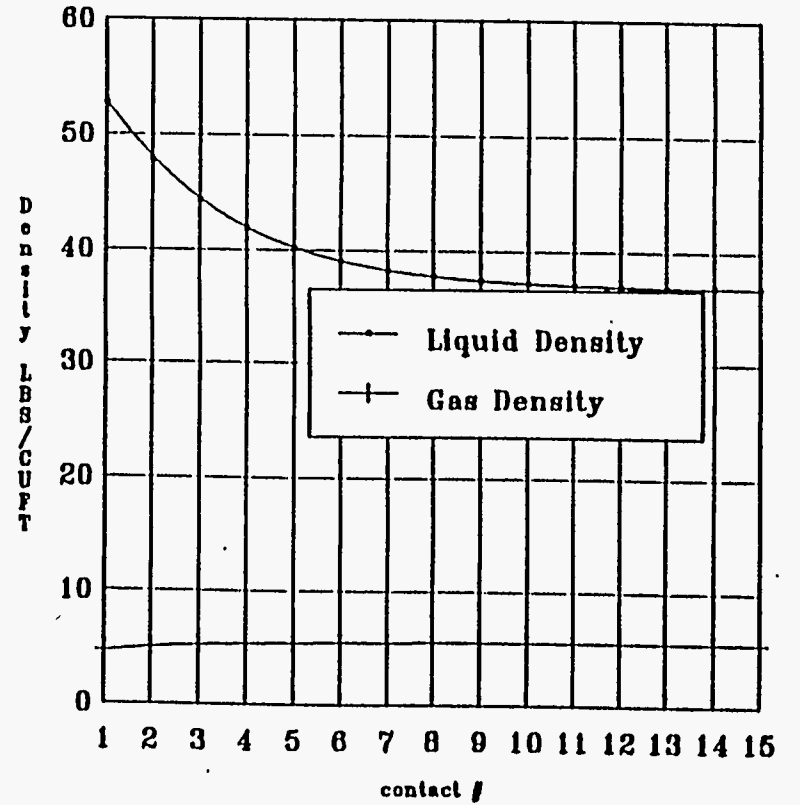
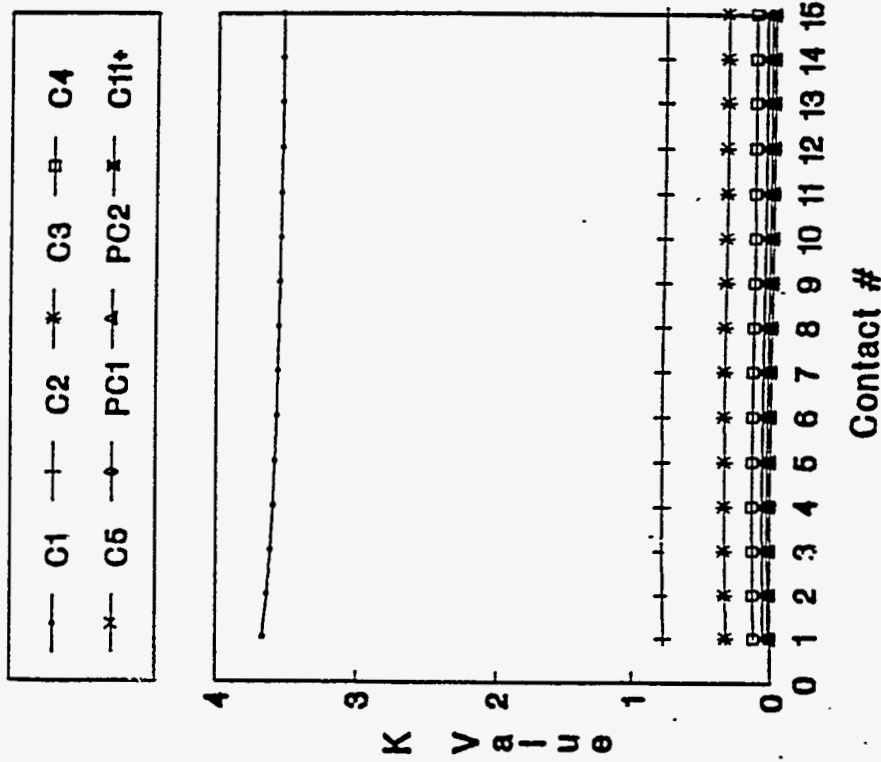


Figure 3.3 Density vs. Contact Number (65% KUPSCH/35% NGL)

100% KUPSCH GAS



95% KUPSCH GAS & 5%NGL

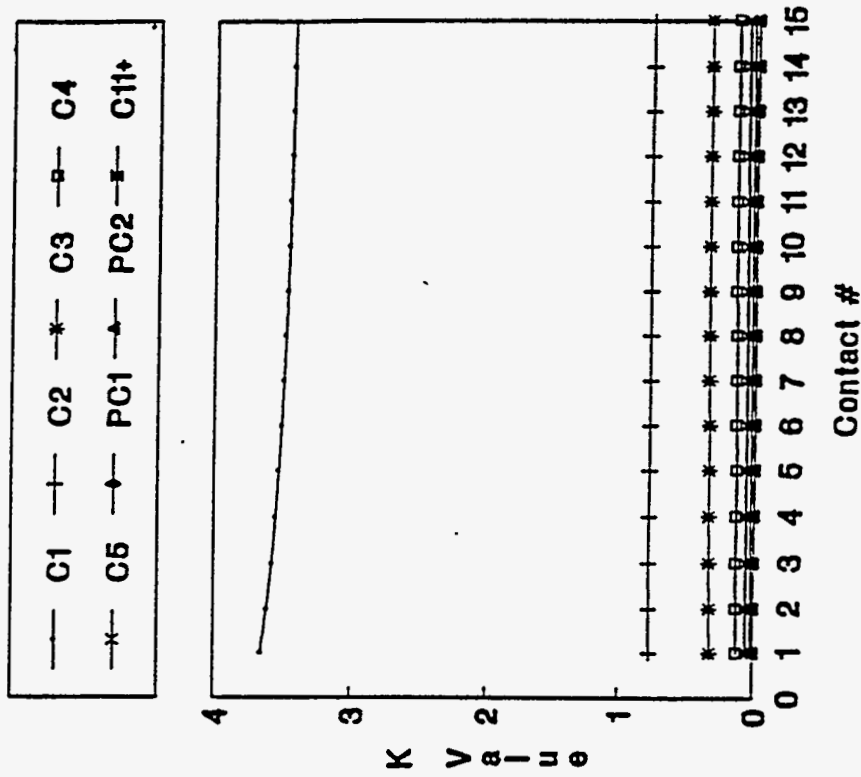
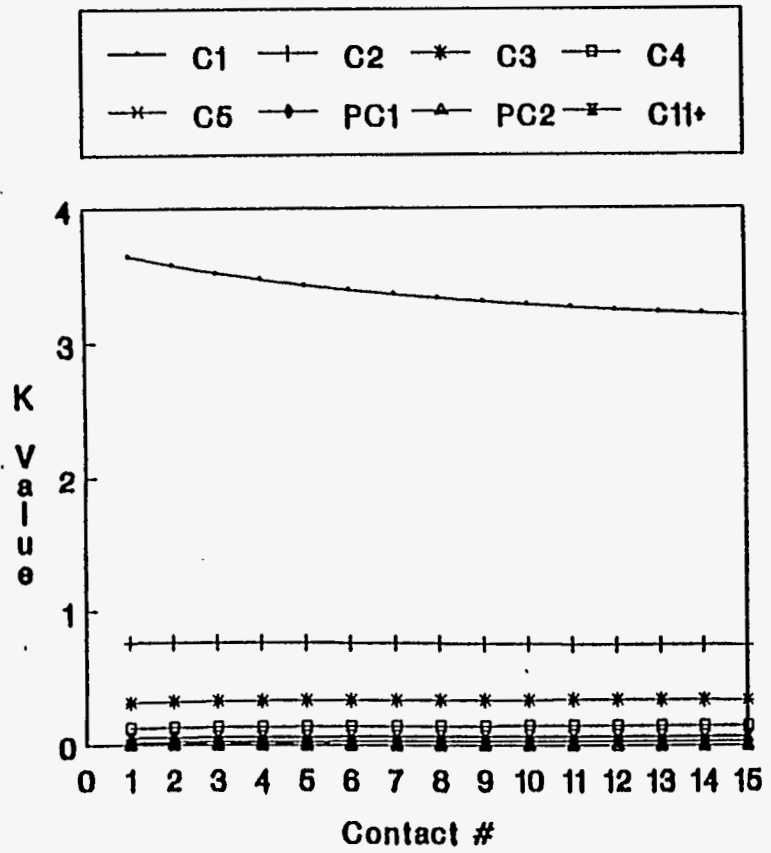


Figure 3.4 K-value vs. Contact Number (100% KUPSCH Gas)

85% KUPSCH GAS & 15%NGL



75%KUPSCH GAS & 25% NGL

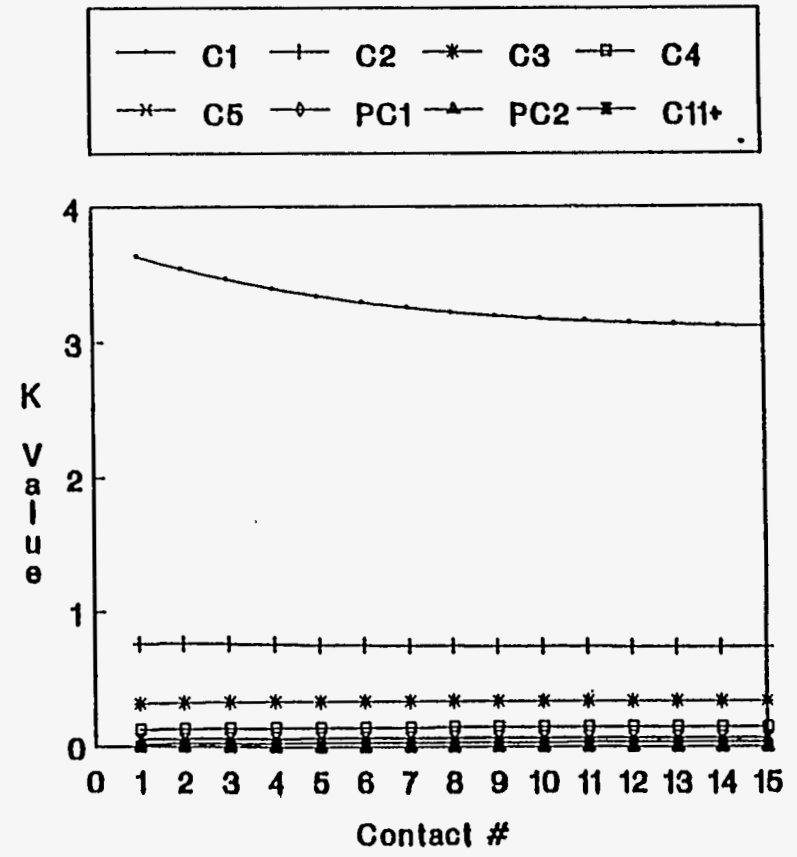


Figure 3.5 K-value vs. Contact Number (85% KUPSCH/15% NGL)

65% KUPSCH GAS & 35%NGL

55% KUPSCH GAS & 45%NGL

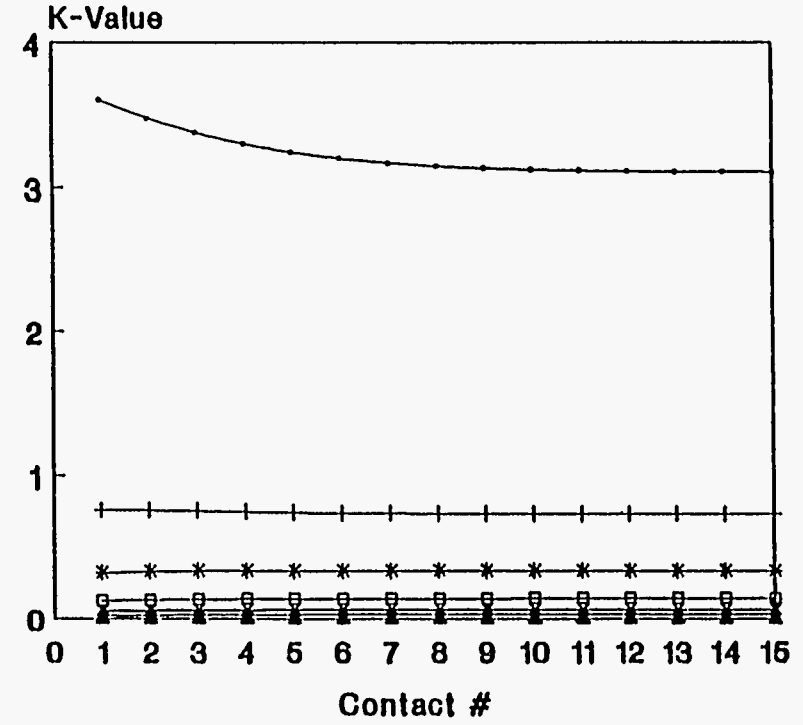
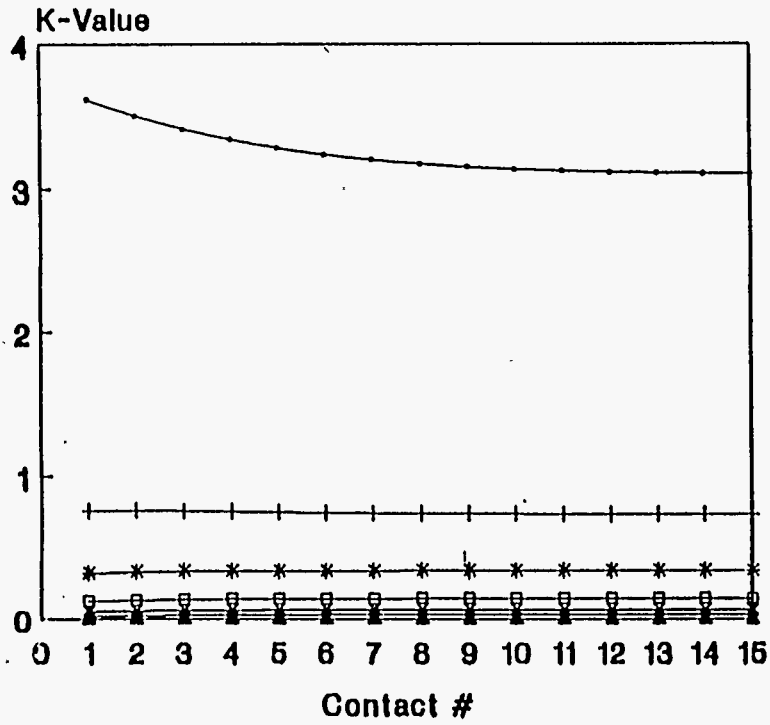
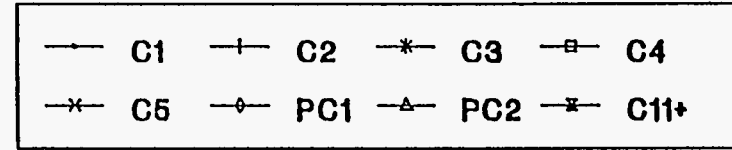
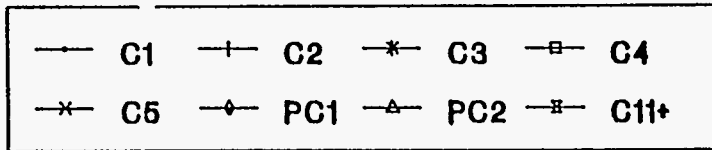


Figure 3.6 K-value vs. Contact Number (65% KUPSCH/35% NGL)

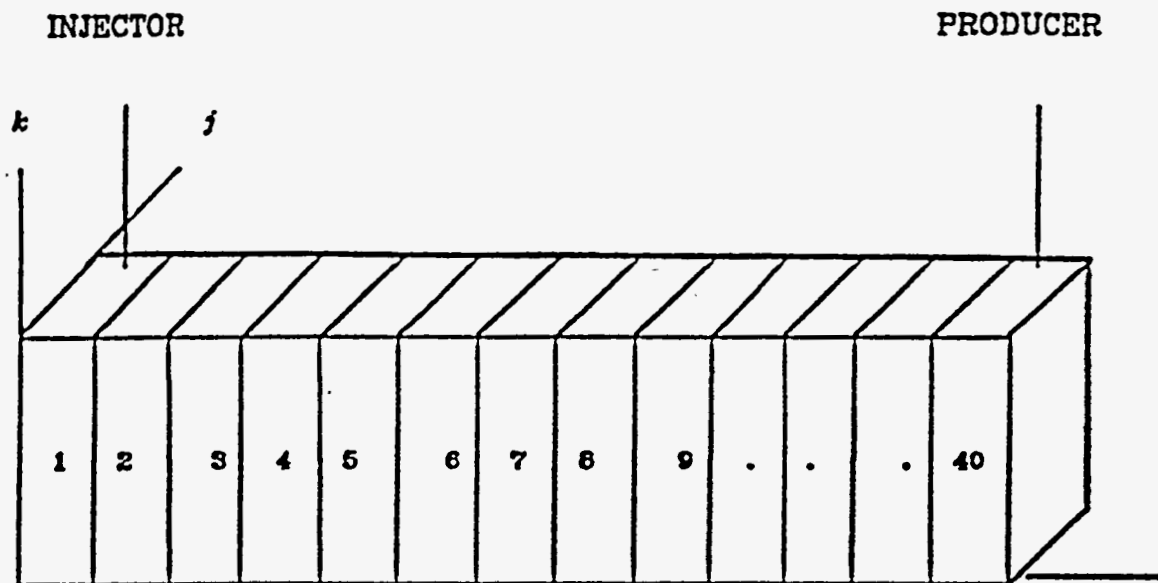


Figure 3.7 Grid Blocks for Simulating Slim Tube Experiments

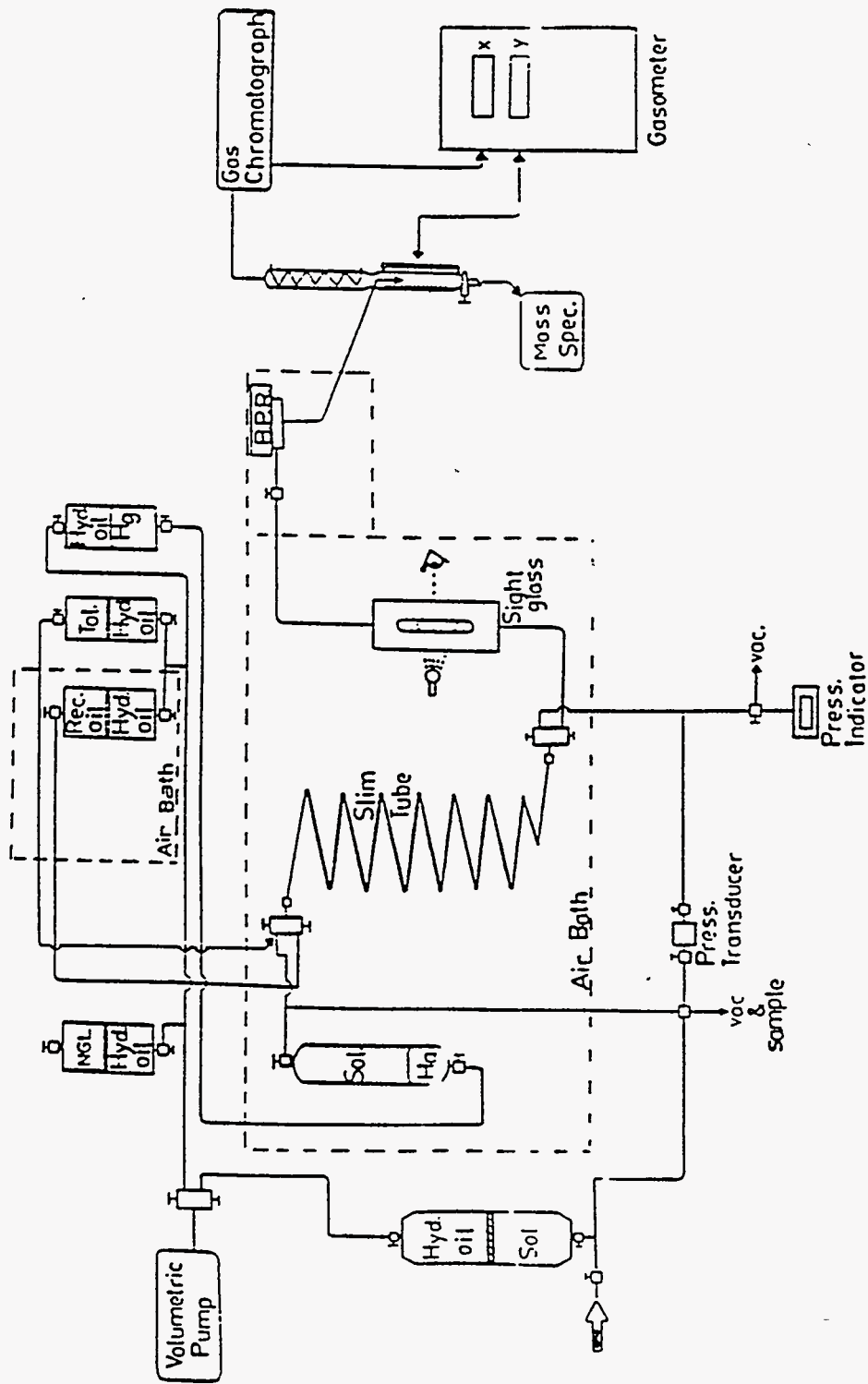


Figure 3.8 Schematic Diagram of Slim Tube Experimental Setup

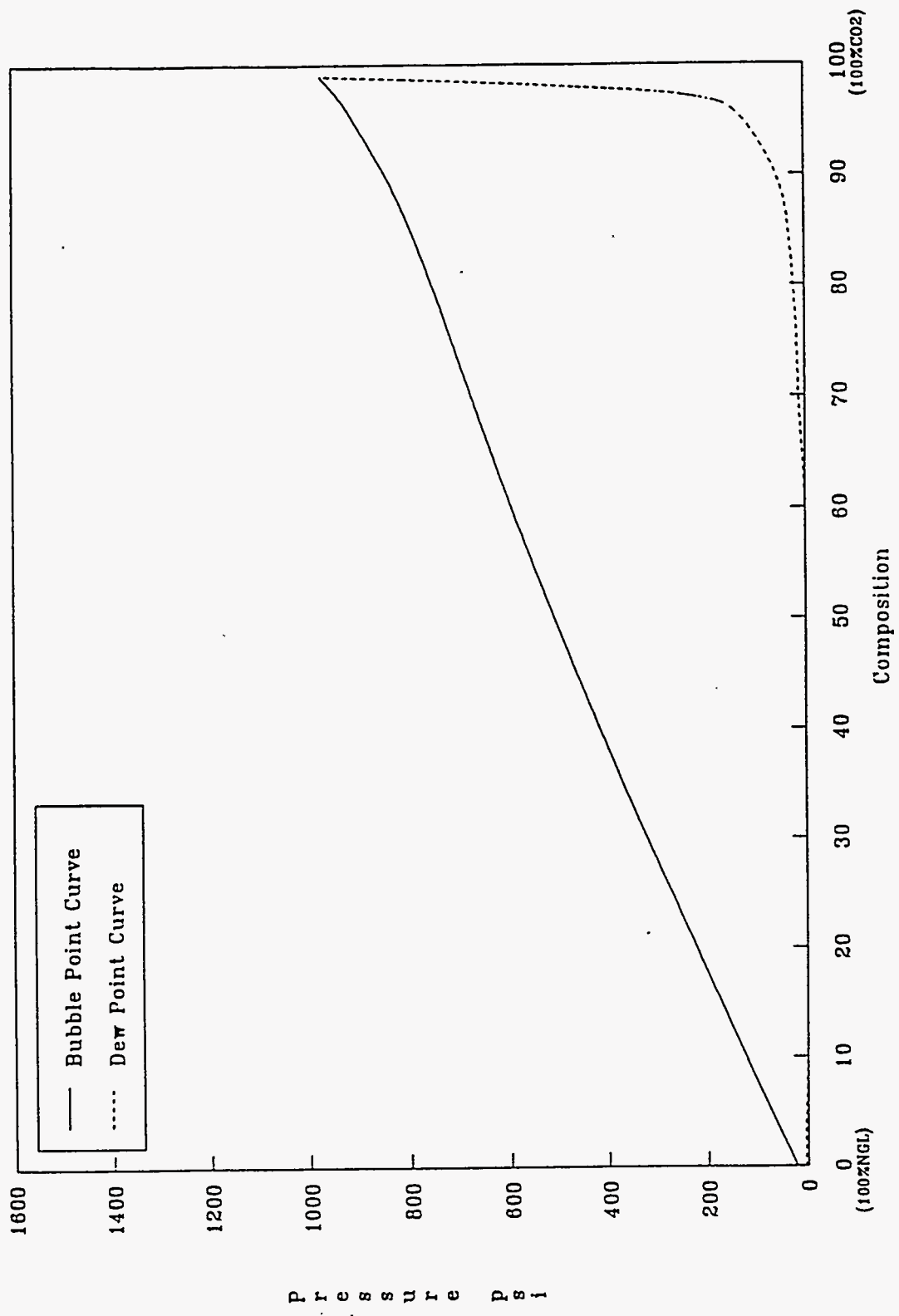


Figure 3.9 P-X Diagram for CO₂/NGL Mixture

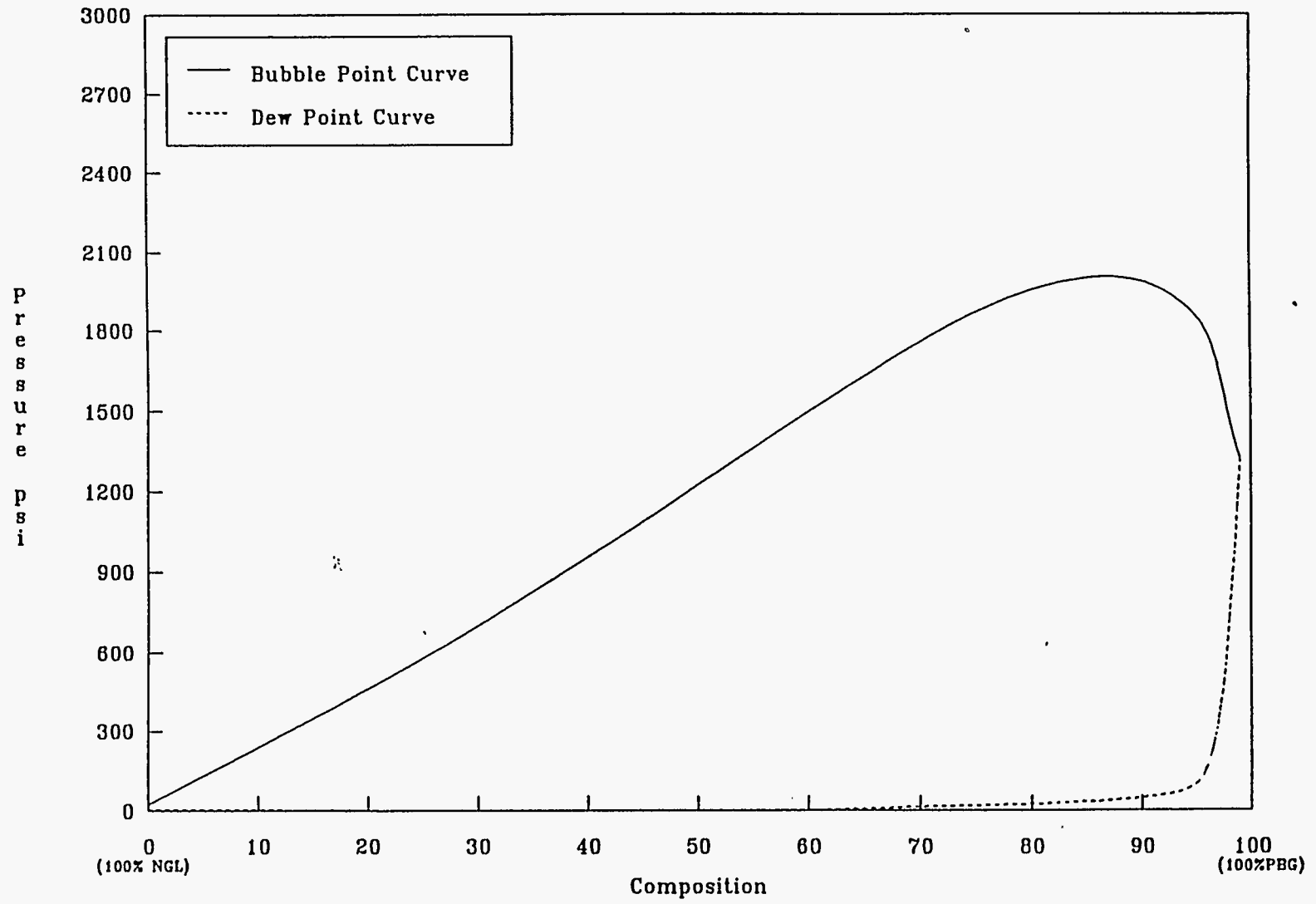
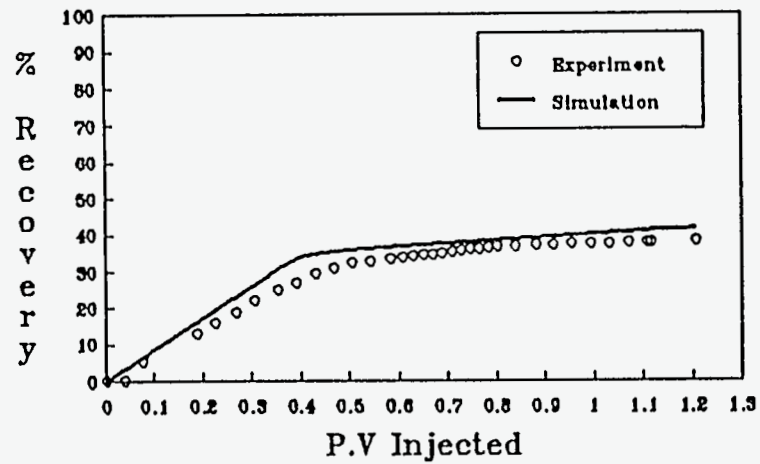


Figure 3.10 P-X Diagram for PBG/NGL Mixture

Recovery vs Pore Volume Injected
Solvent: 100% Kuparuk-Schrader Bluff Gas



GOR vs Pore Volume Injected
Solvent: 100% Kuparuk-Schrader Bluff Gas

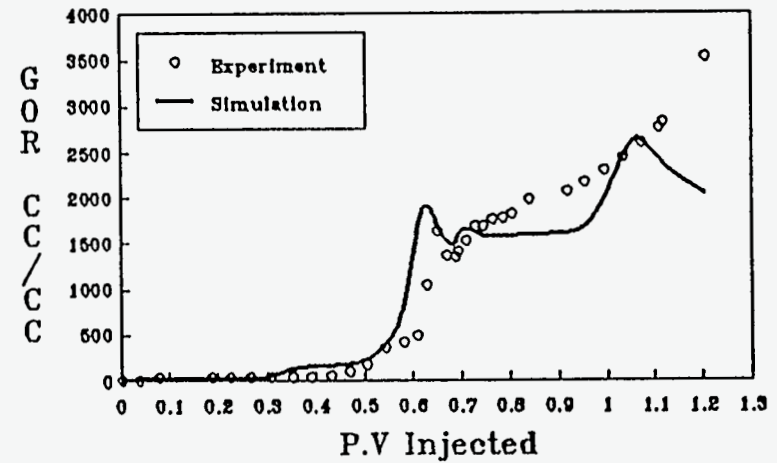
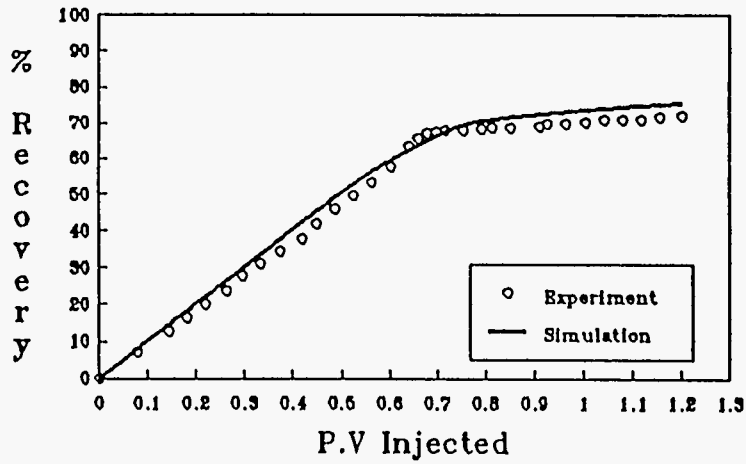


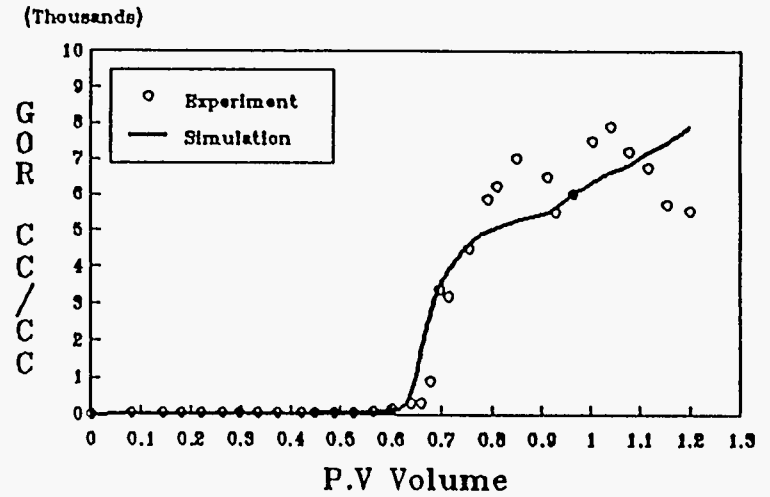
Figure 3.11 Slim Tube Displacement Experiment and Simulation Results

(Solvent: 100% Kuparuk-Schrader Bluff Gas)

Recovery vs. Pore Volume Injected
Solvent: 100% CO₂

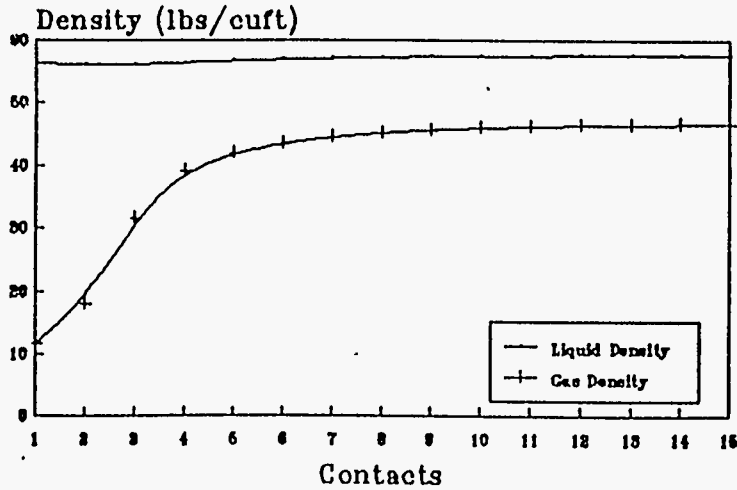


GOR vs Pore Volume Injected
Solvent: 100% CO₂



3.31

Density vs No of Contacts
Solvent 100% CO₂



K-Values vs No. of Contacts
Solvent: 100 CO₂

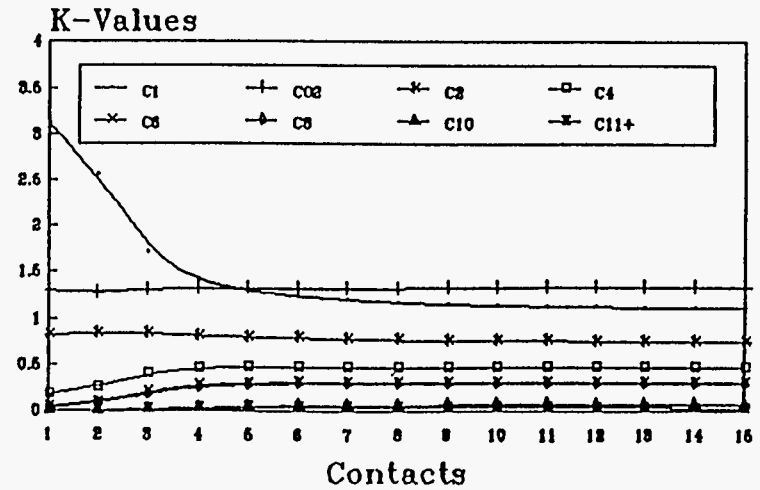
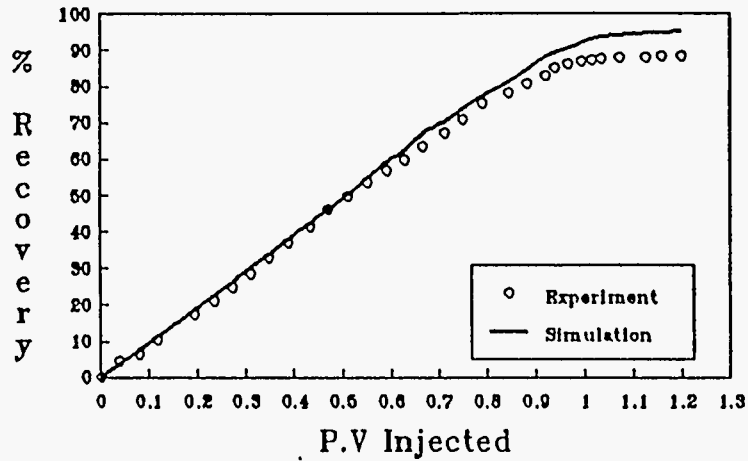


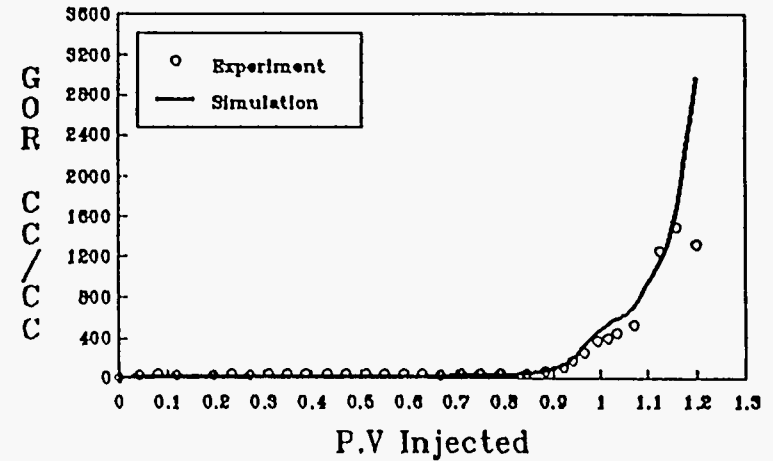
Figure 3.12 Slim Tube Displacement Experiment and Simulation Results

(Solvent: 100% CO₂)

Recovery vs. Pore Volume Injected
Solvent: 90% CO₂/10% NGL

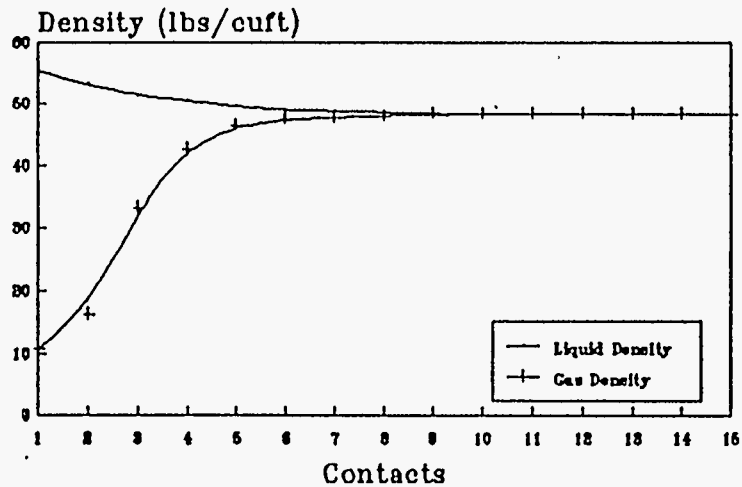


GOR vs Pore Volume Injected
Solvent: 90% CO₂/10% NGL



3.32

Density vs No. of Contacts
Solvent: 90% CO₂/10% NGL



K-Values vs No. of Contacts
Solvent: 90% CO₂/10% CO₂

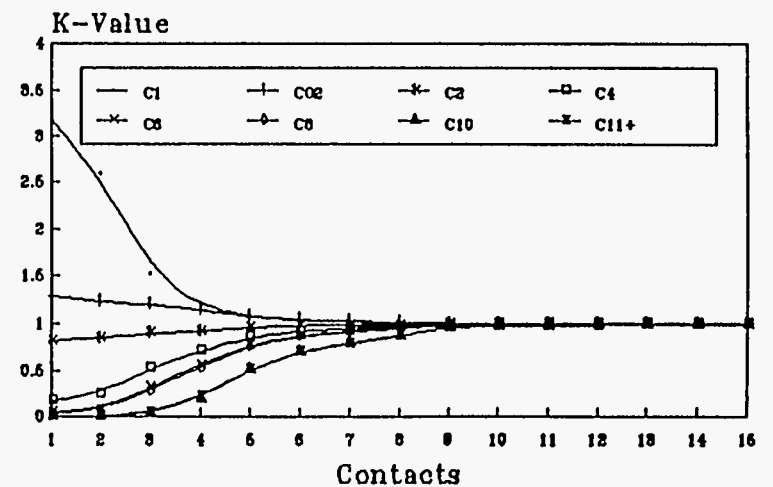
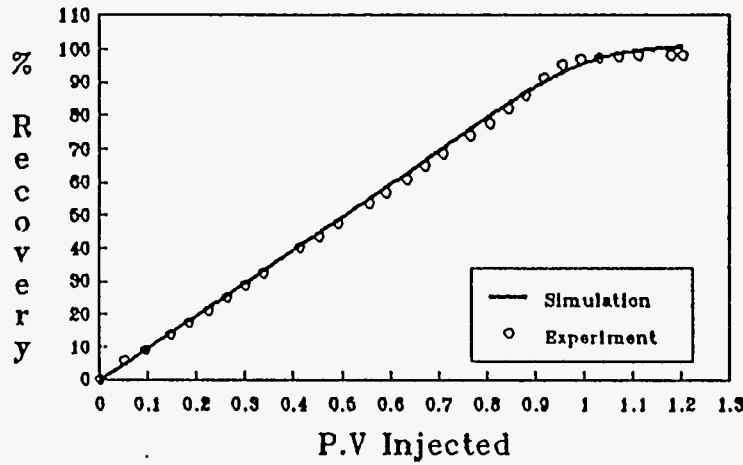
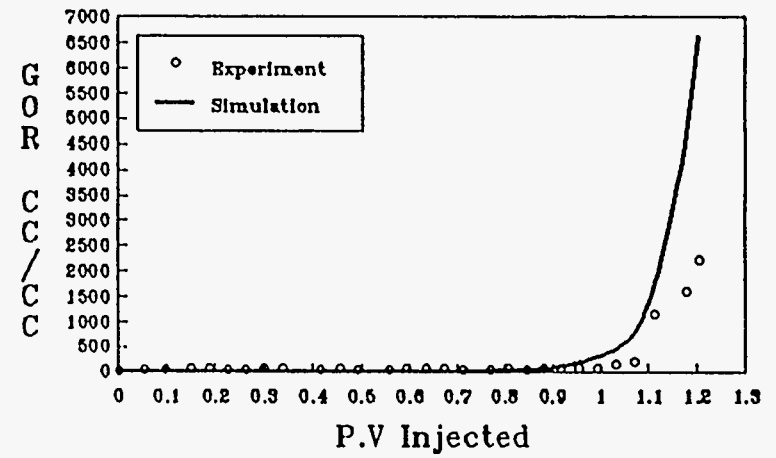


Figure 3.13 Slim Tube Displacement Experiment and Simulation Results
(Solvent: 90% CO₂ and 10% NGL)

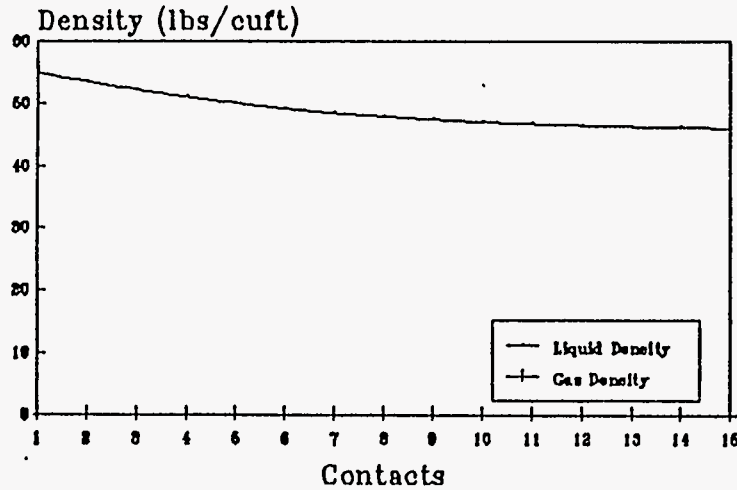
Recovery vs Pore Volume Injected
solvent: 85% CO₂/15% NGL



GOR vs Pore Volume Injected
Solvent: 85% CO₂/15% NGL



Density vs No. of Contacts
Solvent: 85% CO₂/15% NGL



K-Values vs No of Contacts
Solvent: 85% CO₂/15% NGL

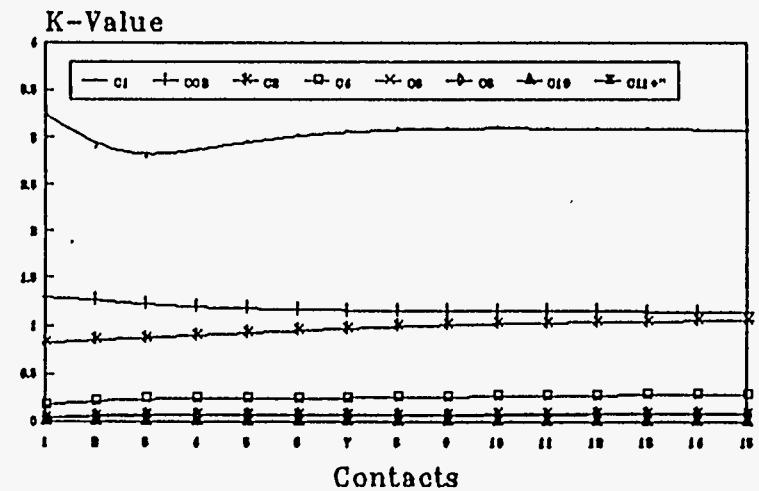
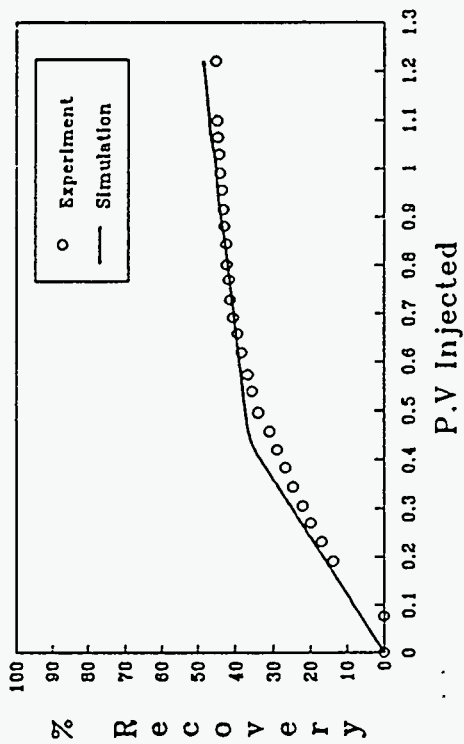
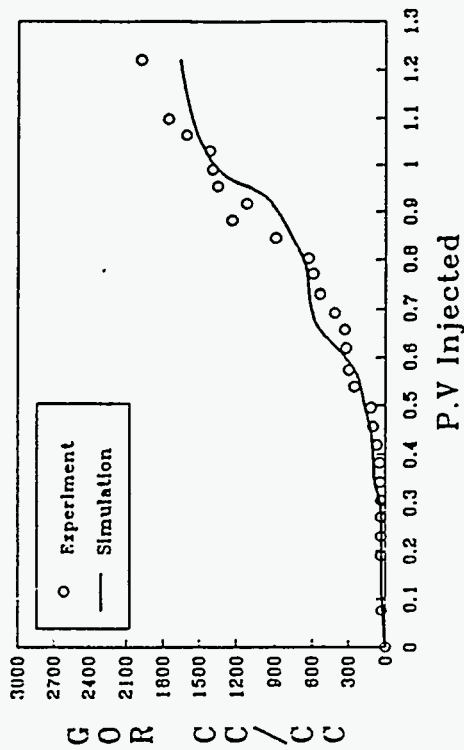


Figure 3.14 Slim Tube Displacement Experiment and Simulation Results
(Solvent: 85% CO₂ and 15% NGL)

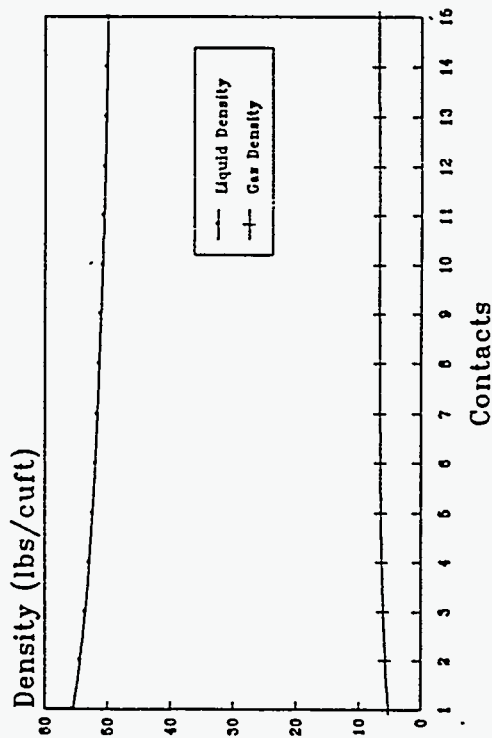
Recovery vs Pre Volume Injected
Solvent: 100% PBG



GOR vs Pore Volume Injected
Solvent: 100% PBG



Density vs No. of Contacts
Solvent: 100% PBG



K-Values vs No of Contacts
Solvent: 100% PBG

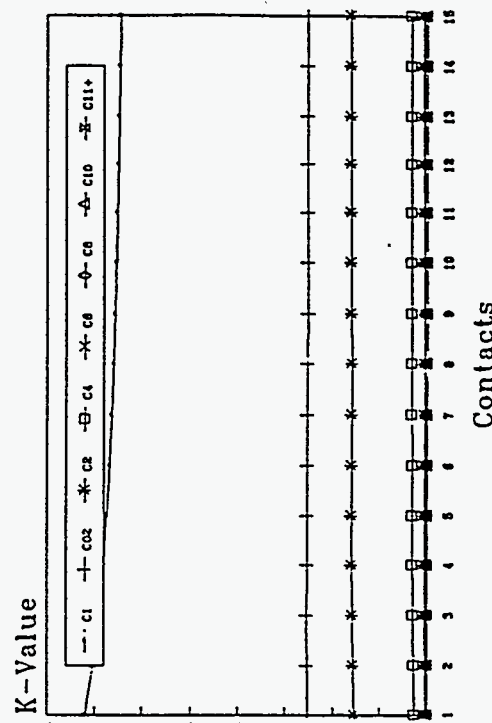
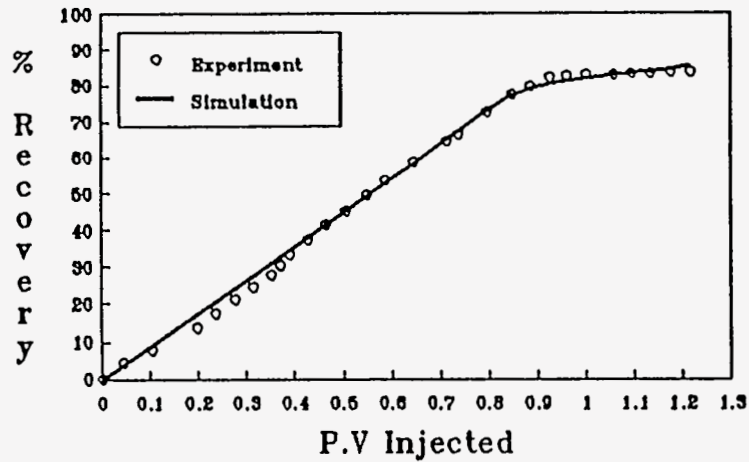
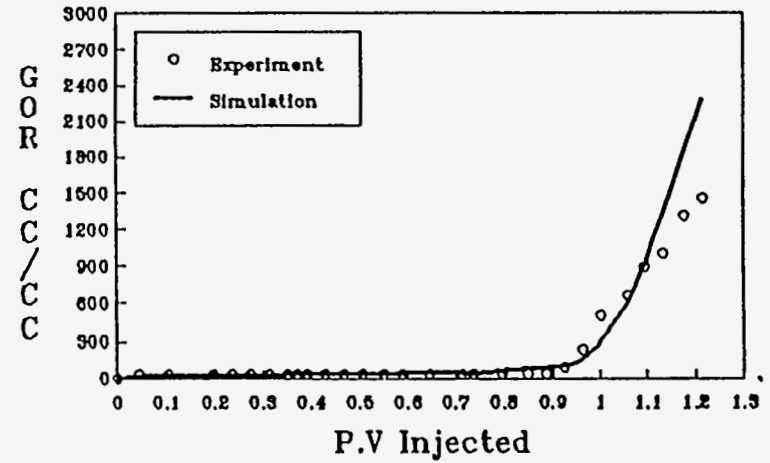


Figure 3.15 Slim Tube Displacement Experiment and Simulation Results
(Solvent: 100% Prudhoe Bay Gas)

Recovery vs Pore Volume Injected
Solvent: 70% PBG/30% NGL

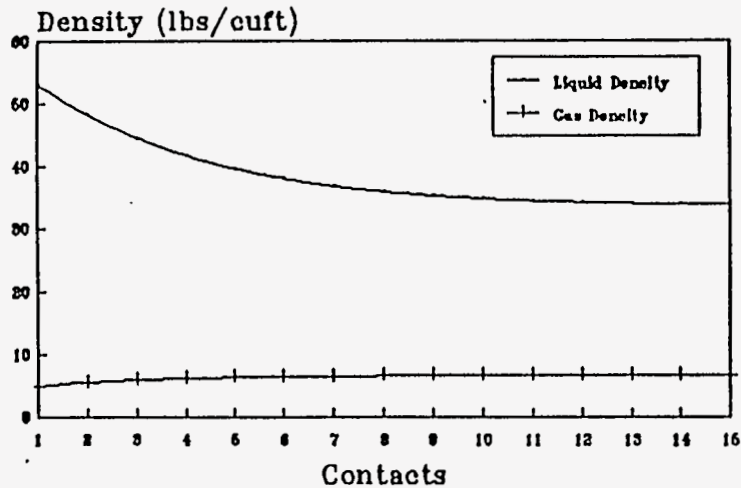


GOR vs Pore Volume Injected
Solvent: 70% PBG/30% NGL



3.35

Density vs. No. of Contacts
Solvent: 70% PBG/30% NGL



K-Values vs No of Contacts
Solvent: 70% PBG/30% NGL

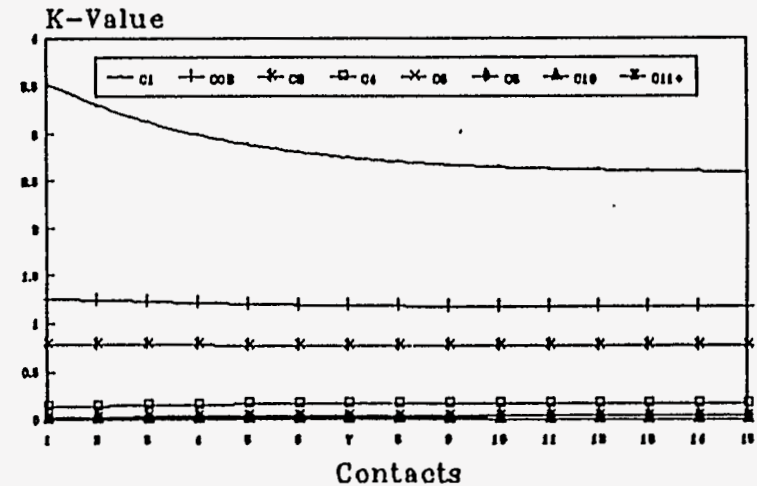
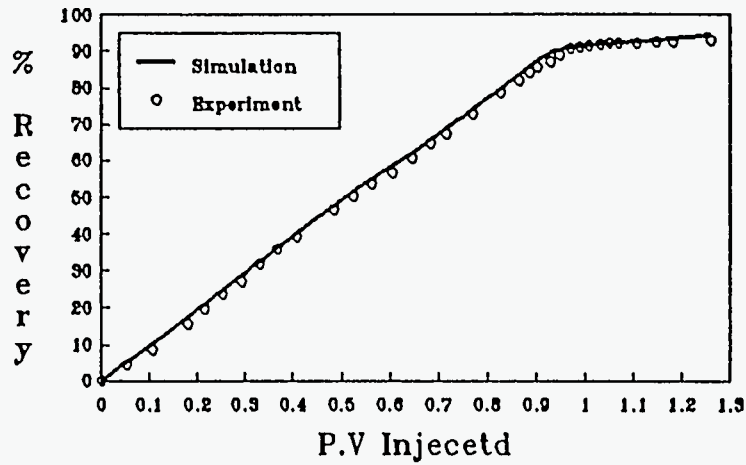
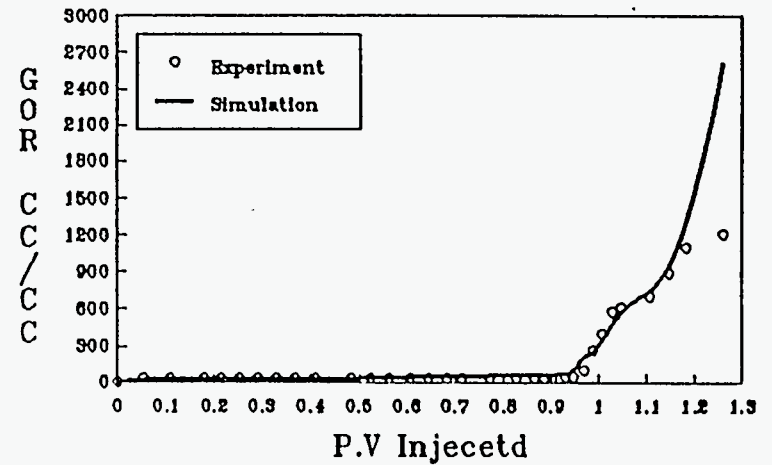


Figure 3.16 Slim Tube Displacement Experiment and Simulation Results
(Solvent: 70% PBG and 30% NGL)

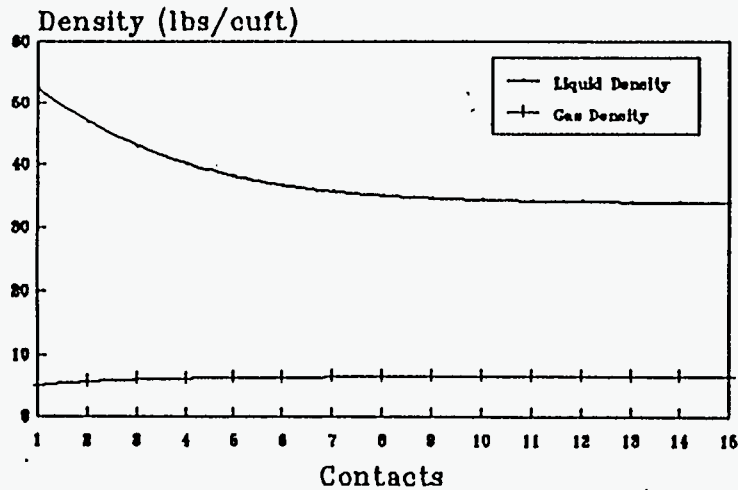
Recovery vs Pore Volume Injected
Solvent: 60% PBG/40% NGL



GOR vs Pore Volume Injected
Solvent: 60% PBG/40% NGL



Density vs No. of Contacts
Solvent: 60% PBG/40% NGL



K-Values vs No of Contacts
Solvent: 60% PBG/40% NGL

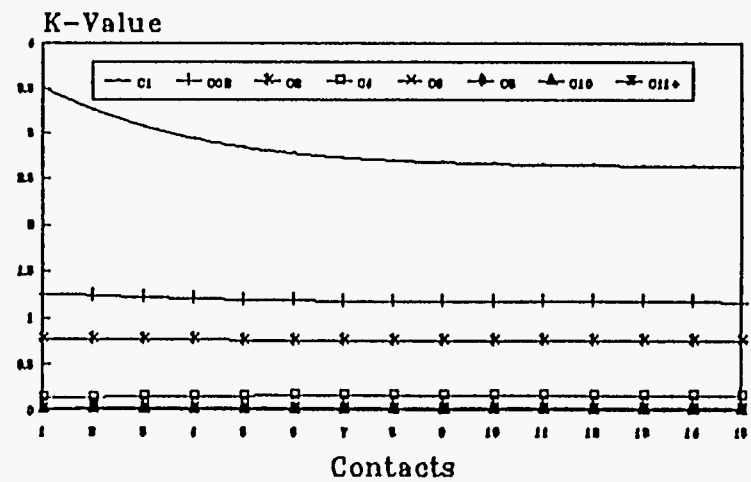
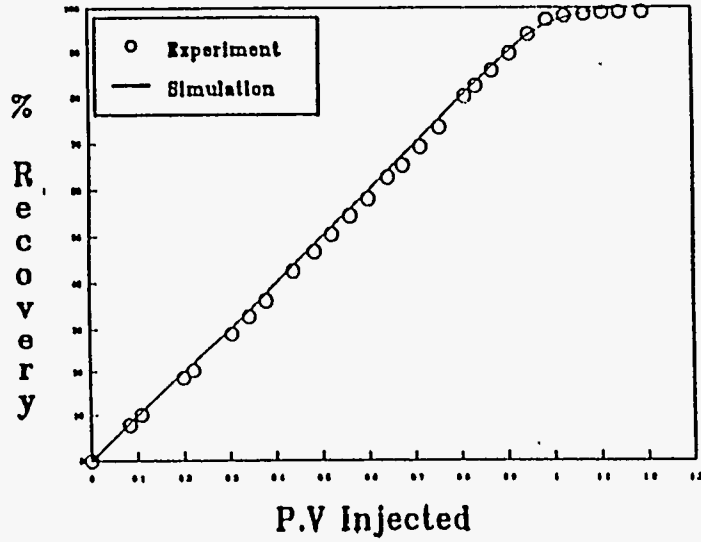


Figure 3.17 Slim Tube Displacement Experiment and Simulation Results
(Solvent: 60% PBG and 40% NGL)

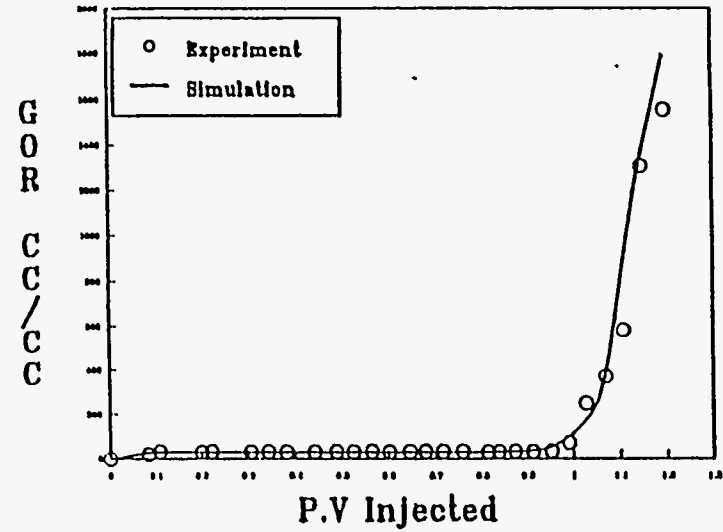
Recovery vs Pre Volume Injected

Solvent: 50% PBG/50% NGL



GOR vs Pore Volume Injected

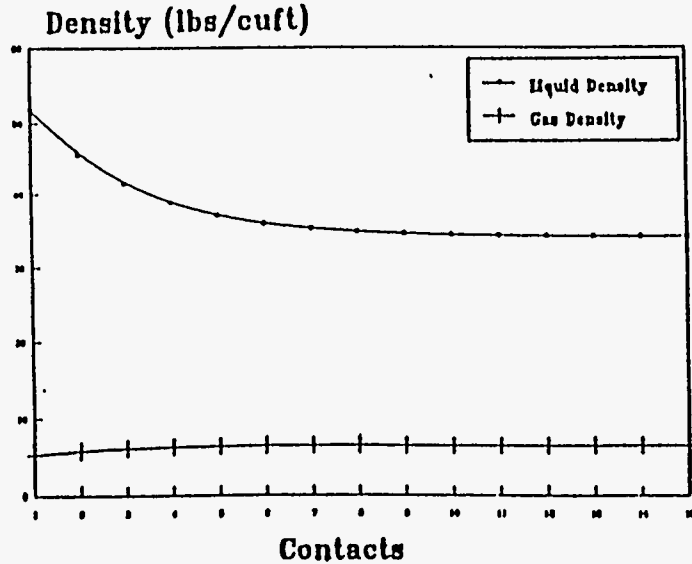
Solvent: 50% PBG/50% NGL



3.37

Density vs No. of Contacts

Solvent: 50% PBG/50% NGL



K-Values vs No of Contacts

Solvent: 50% PBG/50% NGL

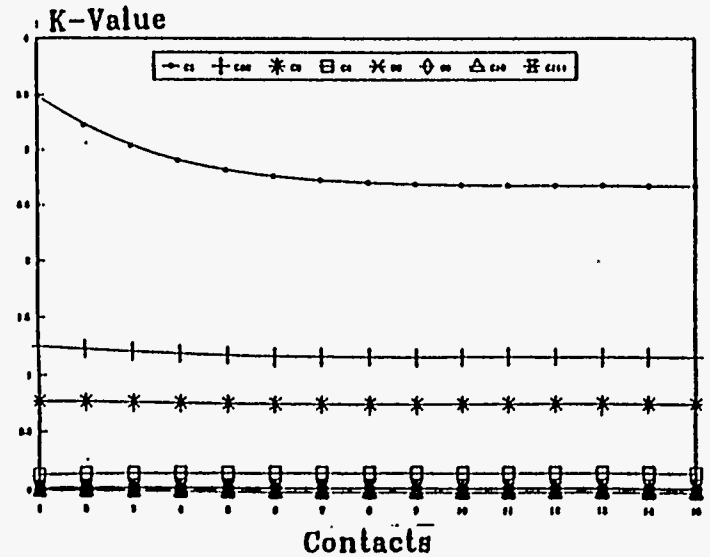


Figure 3.18 Slim Tube Displacement Experiment and Simulation Results

(Solvent: 50% PBG and 50% NGL)

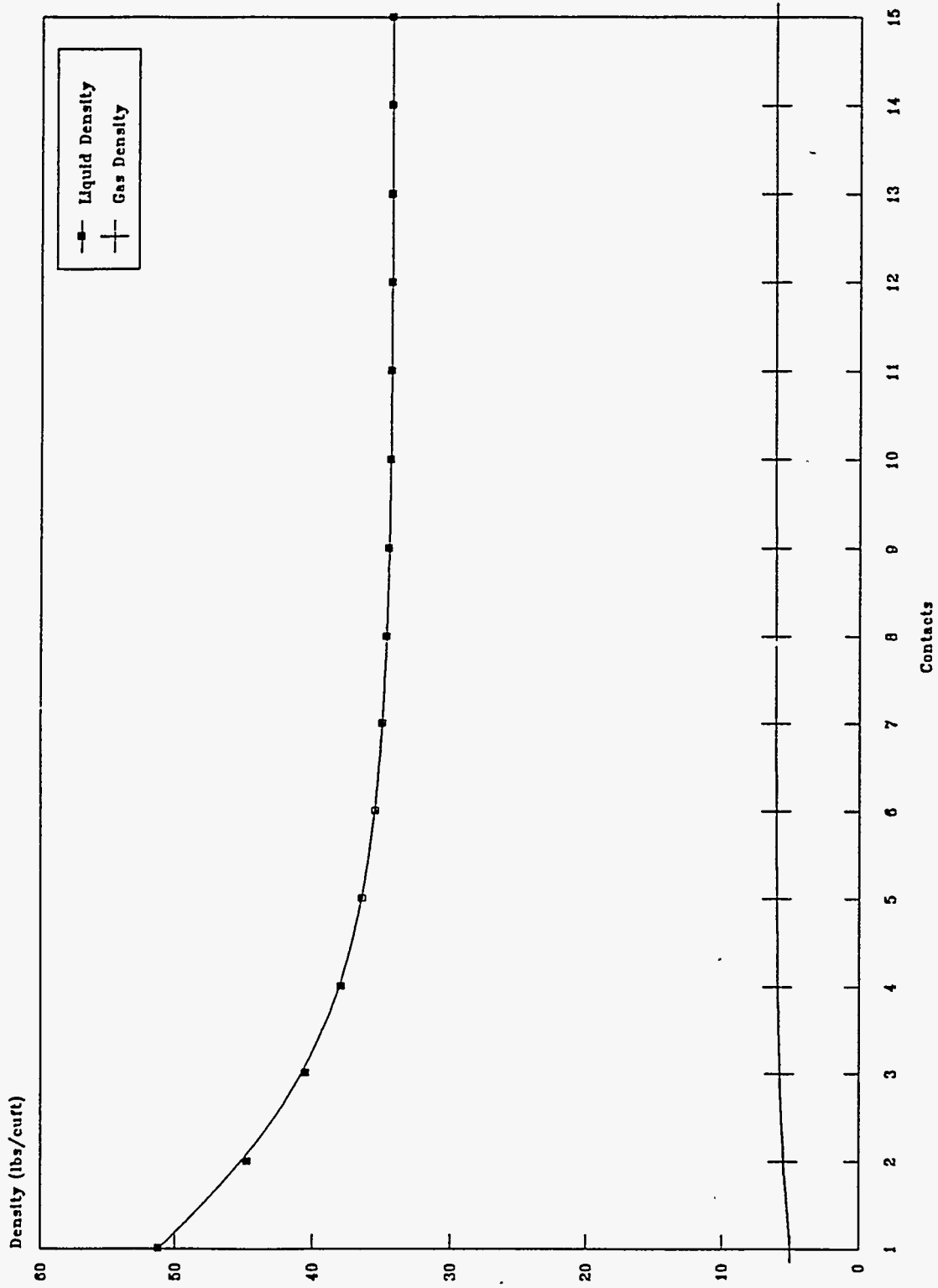


Figure 3.19 Density vs. Number of Contacts (Solvent: 40% PBG/60% NGL)

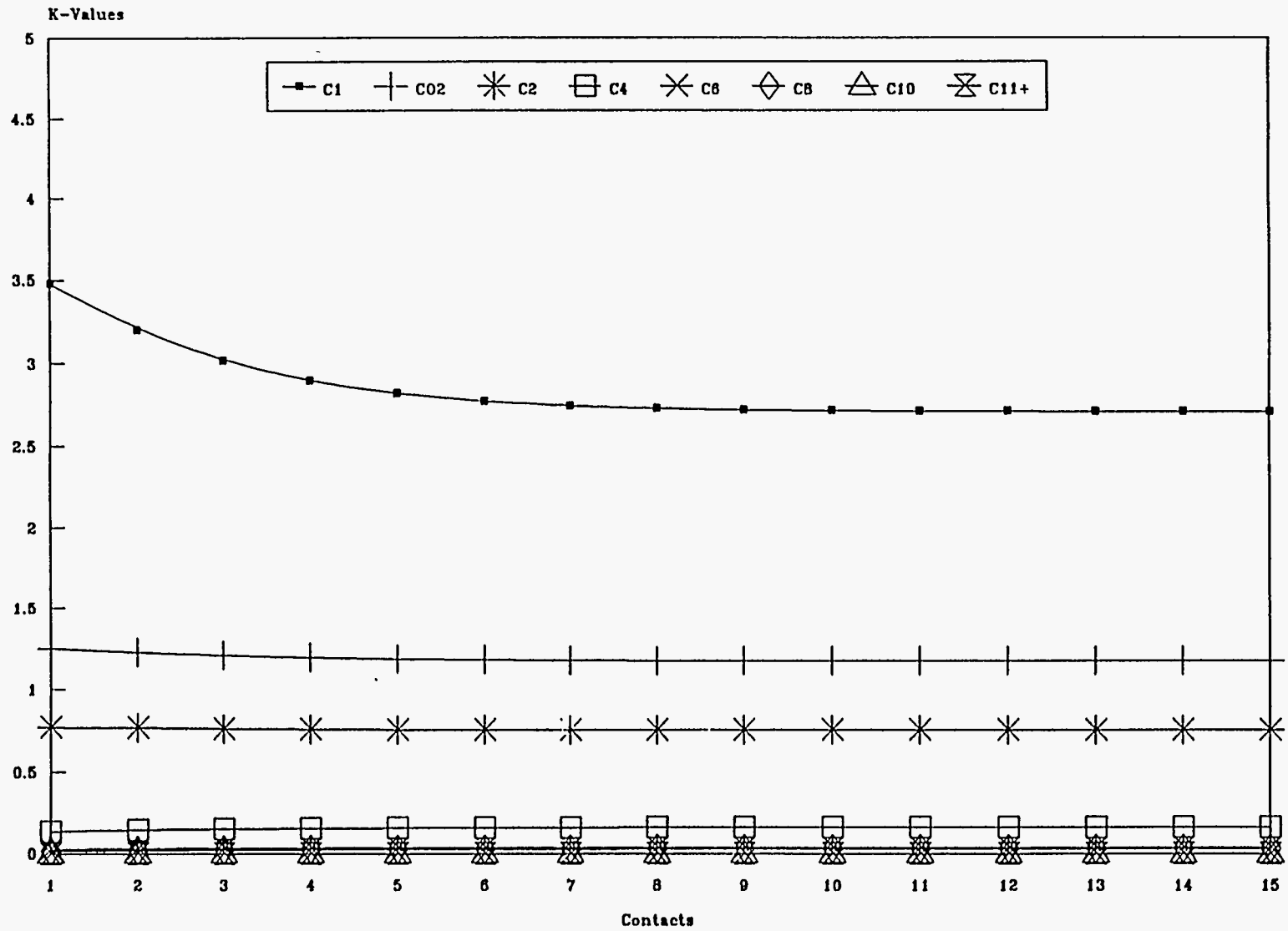


Figure 3.20 K-values vs. Number of Contacts (Solvent: 40% PBG/60% NGL)

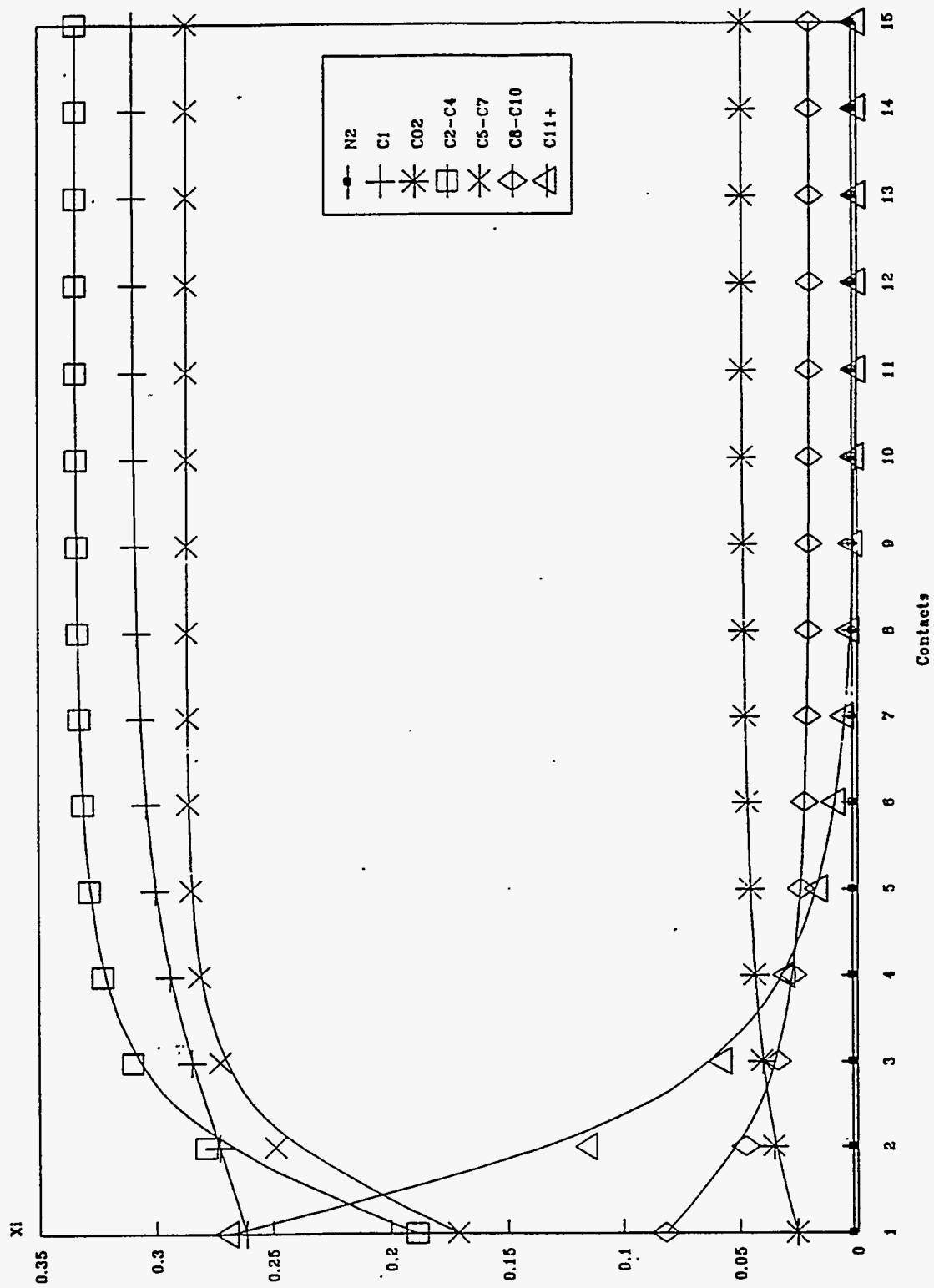


Figure 3.21 X_j vs. Number of Contacts (Solvent: 40% PBG/60% NGL)

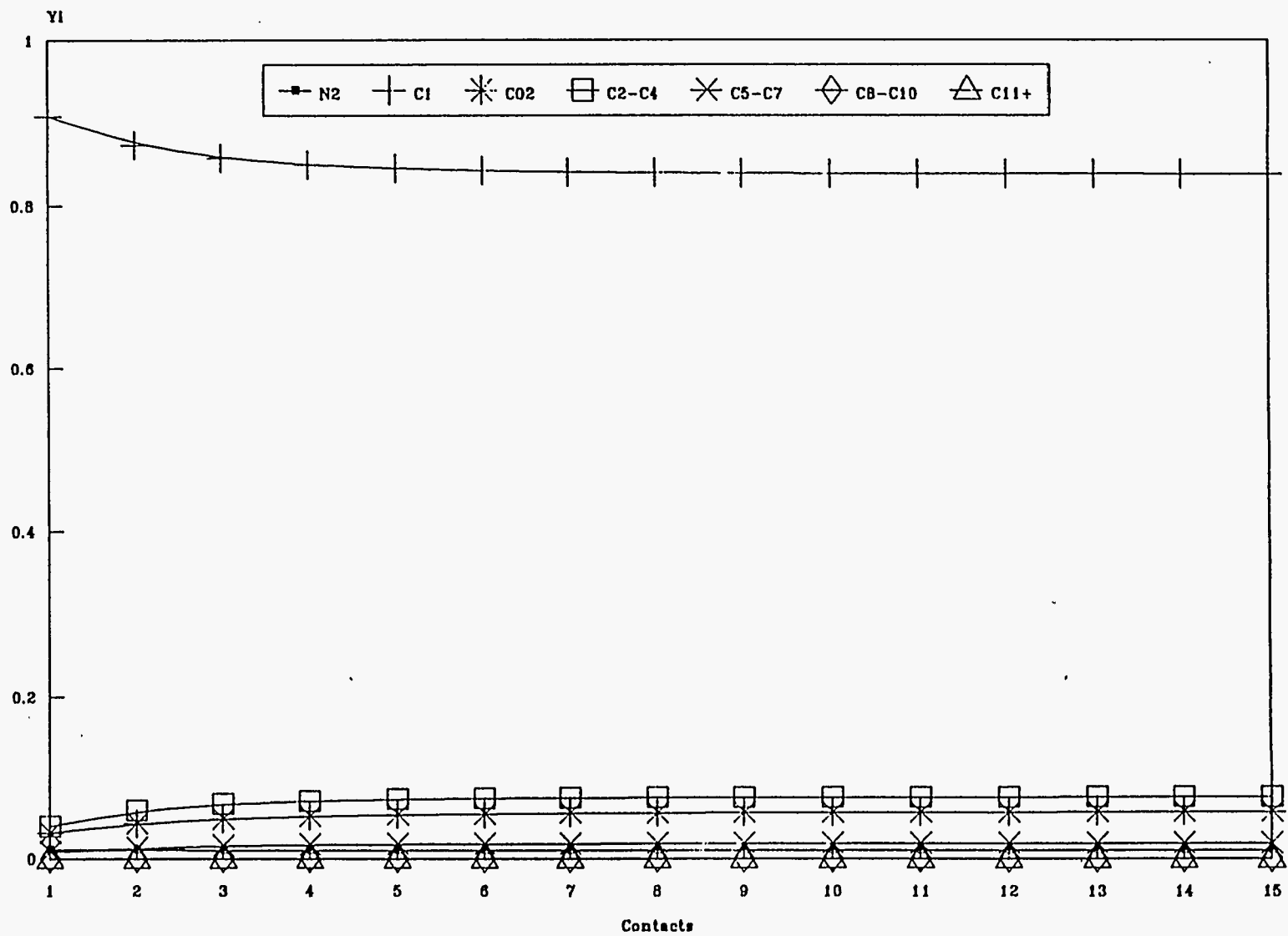


Figure 3.22 Y_i vs. Number of Contacts (Solvent: 40% PBG/60% NGL)

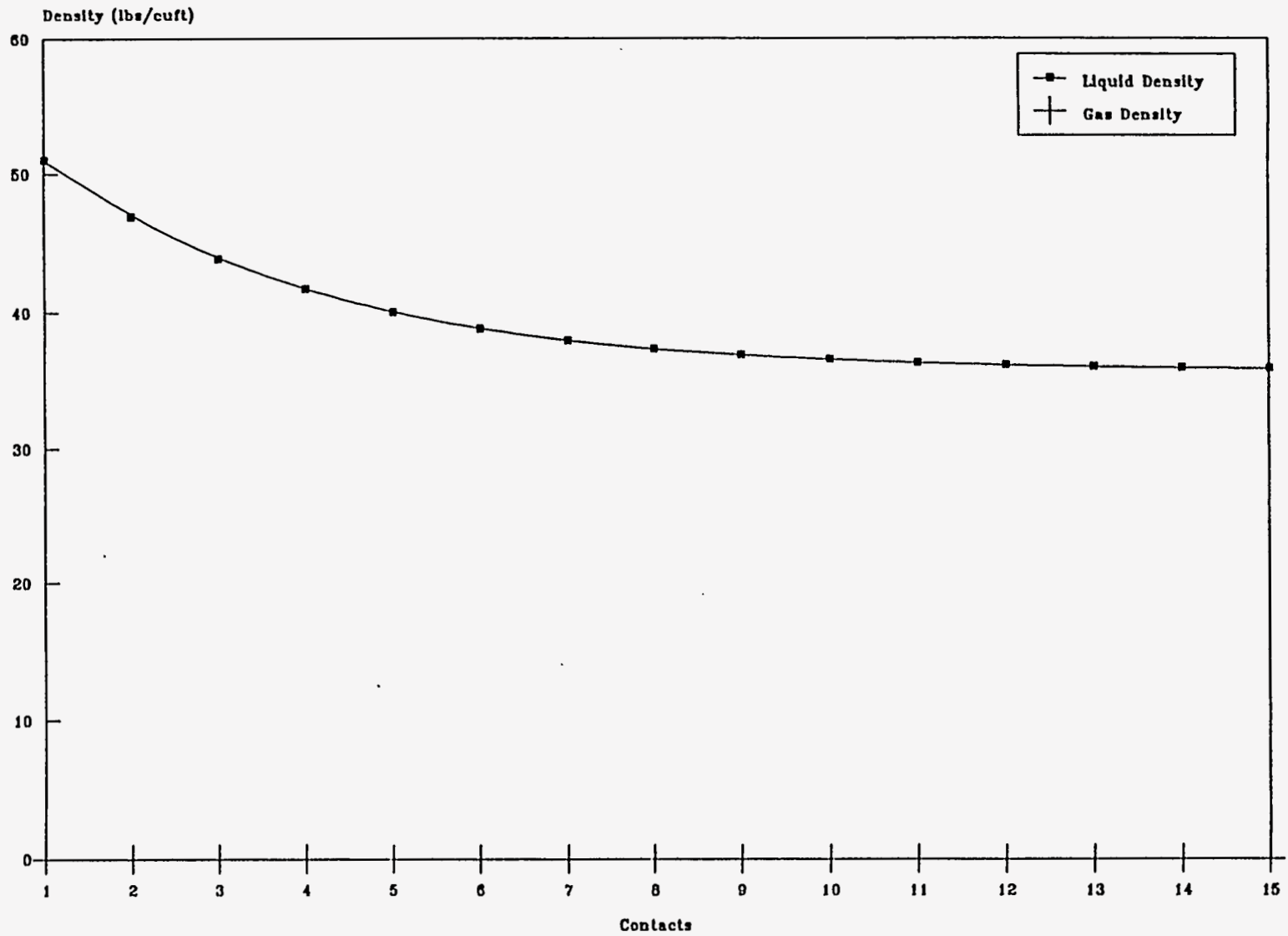


Figure 3.23 Density vs. Number of Contacts (Solvent: 36% PBG/64% NGL)

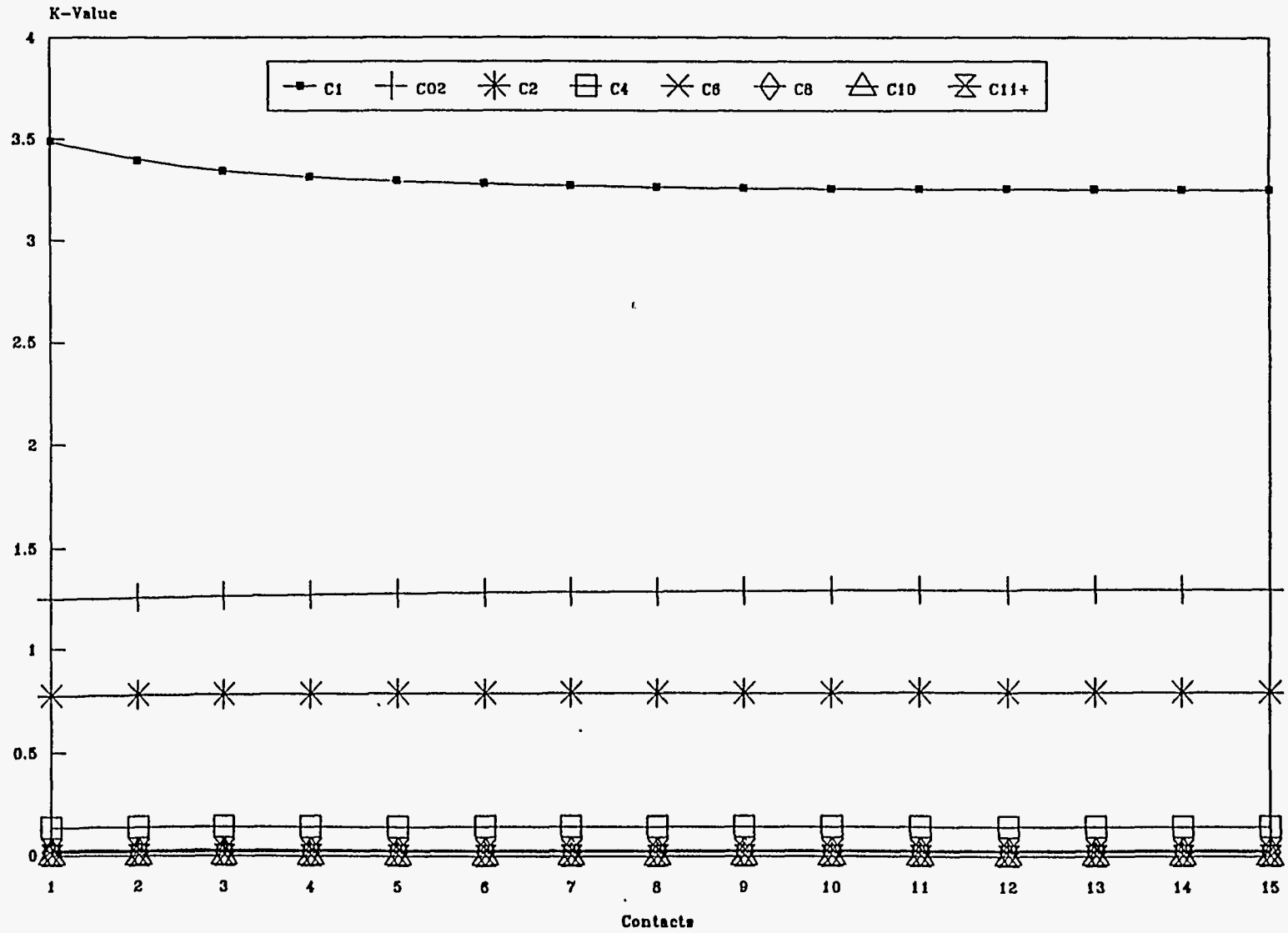


Figure 3.24 K-values vs. Number of Contacts (Solvent: 36% PBG/64% NGL)

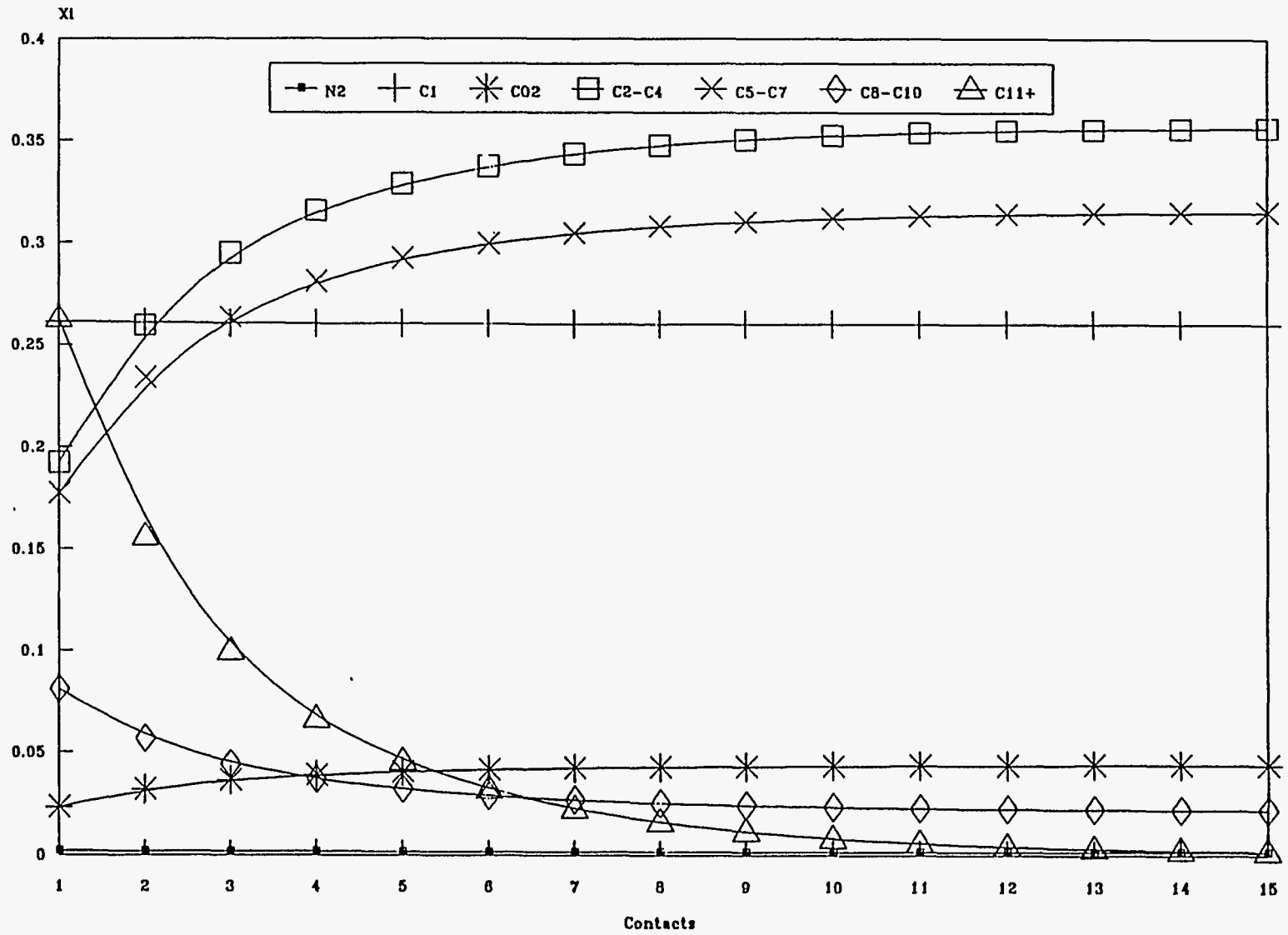


Figure 3.25 X_i vs. Number of Contacts (Solvent: 36% PBG/64% NGL)

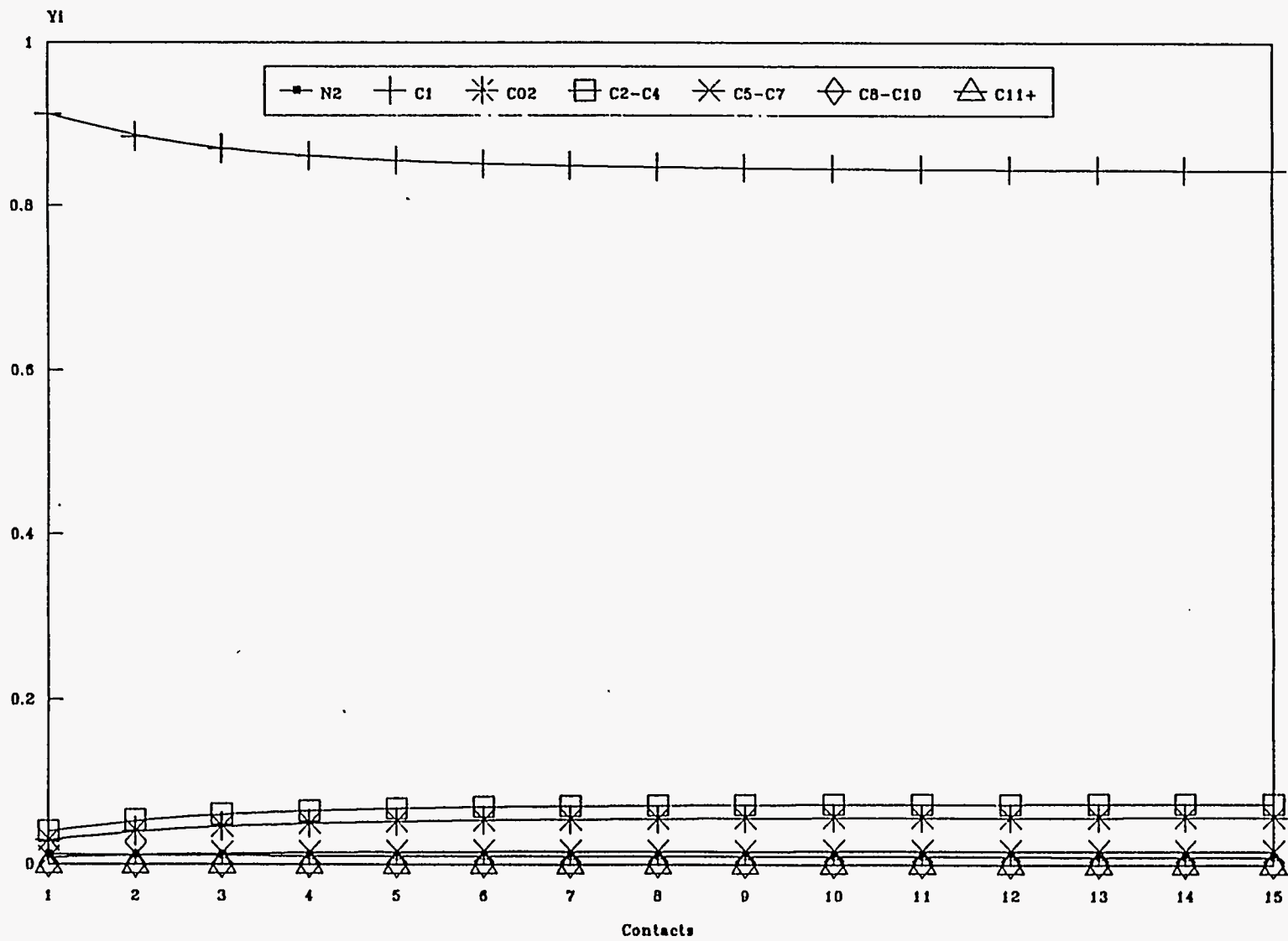


Figure 3.26 Y_i vs. Number of Contacts (Solvent: 36% PBG/64% NGL)

Component	Z ₁	MW	P _c , (Psi)	T _c , °R	ω	Ω _a	Ω _b	Ref. Density
N ₂	0.0024	28.02	493	227.6	0.04	0.457236	0.0778	0.804
C ₁	0.263	16.04	673.1	344.2	0.008	0.452477	0.08793	0.3
CO ₂	0.0022	44.01	1070	547.8	0.225	0.457236	0.0778	0.777
C ₂	0.0035	30.07	709.8	550.3	0.098	0.457236	0.0778	0.3771
C ₃	0.008	44.09	617.4	666.4	0.152	0.457236	0.0778	0.5077
C ₄	0.0159	58.12	550.7	765.6	0.193	0.457236	0.0778	0.5844
C ₅	0.0105	72.14	489.5	845.9	0.251	0.457236	0.0778	0.6101
C ₆ -C ₈	0.0667	104.71	382.8	994	0.3684	0.28	0.05945	0.7444
C ₉ -C ₁₀	0.102	128.8	318.4	1090.7	0.466	0.470967	0.04968	0.7764
C ₁₁ +	0.5229	363.0	210.8	1605.7	0.7303	0.303265	0.07023	0.9895

Table 3.1 EOS Parameters for Schrader Bluff Reservoir Fluid

Solvent	Slim Tube Simulation	Slim Tube Experiments	% Relative Deviation
100% KUPSCH Gas	41.85	37.92	9.39
100% PBG	48.46	45.01	7.12
70% PBG/30% NGL	85.56	83.63	2.6
60% PBG/40% NGL	94.55	92.57	2.09
50% PBG/50% NGL	100.0	99.0	1.0
100% CO ₂	76.45	71.63	6.31
90% CO ₂ /10% NGL	95.25	88.49	7.09
85% CO ₂ /15% NGL	100.0	98.01	1.99

* KUPSCH = Kuparuk/Schrader Bluff lean gas mixture (90:10)

Table 3.2 Recoveries From Slim Tube Experiments and Simulation

APPENDIX-A

OIL SOLVENT COMPOSITIONS

Component	Mole%
N ₂	0.24
CO ₂	0.22
C ₁	26.29
C ₂	0.35
C ₃	0.80
n-C ₄	0.57
i-C ₄	1.02
n-C ₅	0.81
i-C ₅	0.24
C ₆	0.93
C ₇	1.89
C ₈	3.85
C ₉	5.23
C ₁₀	4.97
C ₁₁₊	52.29

Table A-1 Composition of Schrader Bluff Oil at 1300 Psi and 82°F

Component	Mole%
C ₃	0.88
i-C ₄	10.09
n-C ₄	36.83
i-C ₅	12.21
n-C ₅	15.49
C ₆	13.20
Benzene	0.86
Cylohexane	1.63
C ₇	5.48
C ₈ Aromatics	0.56
C ₈₊	2.77

Table A-2 Prudhoe Bay NGL Composition

Composition	Mole%
CO ₂	0.9428
N ₂	0.60001
C ₁	89.6444
C ₂	4.29826
C ₃	2.4055
C ₄	1.2964
C ₅	0.46
C ₆	0.17091
C ₇	0.16545
C ₈	0.016364

Table A-3 Kuparuk-Schrader Bluff Lean Gas(90:10) Composition.

Component	90%CO ₂ /10%NGL	85%CO ₂ /15%NGL
CO ₂	90.0	85.0
C ₃	0.088	0.132
C ₄	4.692	7.038
C ₅	2.77	4.155
C ₆	1.569	2.3535
C ₇	0.548	0.822
C ₈	0.333	0.4995

Table A-4 CO₂/NGL Solvent Compositions.

Component	100%PBG	70%PBG 30%NGL	60%PBG 40%NGL	50%PBG 50%NGL	40%PBG 60%NGL	36%PBG 64%NGL
N ₂	0.44	0.308	0.264	0.22	0.176	0.1584
C ₁	72.24	50.568	43.344	36.12	28.896	26.0064
CO ₂	12.16	8.512	7.296	6.08	4.864	4.3776
C ₂	7.87	5.509	4.722	3.935	3.148	2.8332
C ₃	4.92	3.708	3.304	2.9	2.496	2.3344
C ₄	1.47	15.105	19.65	24.2	28.74	30.558
C ₅	0.52	8.674	11.392	14.11	16.828	17.9152
C ₆	0.24	4.875	6.42	7.965	9.51	10.128
C ₇	0.1	1.714	2.252	2.79	3.328	3.5432
C ₈	0.04	1.027	1.356	1.685	2.014	2.1456

Table A-5 PBG/NGL Solvent Compositions.

APPENDIX-B

RAW DATA FROM THE EXPERIMENTS

Table B-1 Experimental Data from 100% Kuparuk-Schrader Bluff Gas as Solvent

Time	Injection Pressure	P.V Injected (%)	Recovery (cc)	Recovery (%)	Gas Production (cc)	GOR (cc/cc)
0	1350	0	0	0	0	0
60	1397	3.70997	0	0	0	0
120	1426	7.55012	3.95447	5.1477	120.4939	30.4703
295	1452	18.7191	9.95716	12.9617	293.5241	28.8254
355	1443	22.5202	12.1427	15.8067	358.0838	29.5399
400	1450	26.6207	14.3623	18.696	426.0413	30.6171
460	1458	30.4608	16.9184	22.0234	503.6696	30.3692
535	1463	35.1992	19.2104	25.0071	570.5816	29.1935
595	1478	39.0263	20.6163	26.8372	613.9699	30.8619
655	1493	42.9576	22.3673	29.1165	687.4163	41.9463
715	1479	46.7587	23.6837	30.8301	795.3641	82.0012
775	1484	50.5728	24.6806	32.1278	958.4621	163.605
835	1485	54.3218	24.9809	32.5188	1063.796	350.707
895	1501	58.214	25.4347	33.1094	1250.418	411.318
935	1495	60.7264	25.7627	33.5364	1408.811	482.848
965	1471	62.679	25.9778	33.8165	1631.241	1033.87
1000	1465	64.8789	26.2526	34.1742	2077.409	1623.69
1030	1443	66.7144	26.4933	34.4875	2403.605	1355.17
1060	1458	68.7191	26.7596	34.8342	2760.904	1341.89
1090	1451	70.7368	27.0408	35.2002	3154.535	1399.94
1120	1455	72.5462	27.2985	35.5357	3546.859	1522.14
1150	1447	74.3556	27.4668	35.7547	3829.405	1679.03
1180	1442	76.3083	27.6393	35.9794	4120.054	1684.53
1210	1427	78.2739	27.8119	36.204	4422.726	1754.21
1240	1430	80.1484	27.9865	36.4313	4731.149	1765.74
1300	1403	83.9365	28.1442	36.6365	5016.048	1807.4
1364	1385	88.037	28.2464	36.7696	5217.306	1968.38
1420	1391	91.5777	28.3955	36.9637	5524.683	2061.43
1480	1377	95.1966	28.5787	37.2022	5920.667	2161.59
1540	1375	99.1539	28.7534	37.4296	6322.4	2299.95
1600	1361	102.994	28.8642	37.5738	6592.662	2439.92
1660	1348	106.899	28.9664	37.7069	6858.741	2602.35
1720	1351	110.817	29.0367	37.7984	7052.682	2758.98
1815	1343	116.662	29.0857	37.8621	7191.21	2827.53
1875	1328	120.581	29.1283	37.9176	7340.978	3515.47

Table B-3 Experimental Data from 90%CO₂/10%NGL Mixture as Solvent.

Time	Injection Pressure	P.V Injected (%)	Recovery (cc)	Recovery (%)	Gas Production (cc)	GOR (cc/cc)
0	1361	0	0	0	0	0
61	1375	3.90523	3.2707	4.25761	76.06013	23.255
121	1389	7.7584	4.93858	6.42877	125.7214	29.7749
181	1382	11.6376	7.78869	10.1389	209.8841	29.5297
301	1416	19.2658	13.2631	17.2652	371.9366	29.6017
361	1424	23.0539	16.207	21.0973	462.3724	30.7204
423	1431	26.9721	18.9974	24.7298	546.0124	29.9735
483	1428	30.8383	21.822	28.4066	635.1413	31.5551
543	1441	34.6264	25.1194	32.699	737.8616	31.1516
606	1432	38.6488	28.37	36.9304	836.6614	30.3946
675	1435	43.0227	31.7398	41.3171	938.0749	30.0943
735	1441	46.8368	35.2418	45.8758	1040.011	29.1086
800	1449	50.9763	38.0748	49.5637	1146.652	37.6415
861	1438	54.8685	40.8802	53.2156	1230.815	30.0005
924	1432	58.7868	43.4939	56.6179	1309.75	30.201
984	1434	62.692	45.7859	59.6015	1374.048	28.0531
1044	1421	66.4931	48.6573	63.3394	1461.348	30.4029
1105	1419	71.0362	51.386	66.8914	1543.942	30.2689
1165	1408	74.8503	54.3575	70.7596	1632.548	29.8184
1128	1412	78.8467	57.7529	75.1795	1735.269	30.2526
1315	1413	84.3921	59.8788	77.9469	1800.612	30.7375
1375	1398	88.1932	61.8982	80.5756	1864.388	31.582
1455	1377	92.0203	63.6555	82.8632	2172.81	175.504
1485	1373	93.9209	65.3149	85.0233	2503.711	199.414
1525	1359	96.4723	66.2479	86.2378	2897.865	422.46
1570	1367	99.1018	66.6057	86.7036	3305.087	1137.93
1600	1351	101.237	67.0211	87.2443	3881.68	1388.13
1630	1338	103.163	67.3641	87.6908	4382.997	1461.78
1690	1341	106.938	67.5323	87.9098	4717.819	1989.67
1776	1325	112.406	67.7134	88.1455	5101.779	2120.61
1825	1326	115.582	67.854	88.3285	5494.887	2796.16
1892	1325	119.76	67.9008	88.3895	5732.215	5064.33

Table B-4 Experimental Data from 85%CO₂/15%NGL Mixture as Solvent.

Time	Injection Pressure	P.V Injected (%)	Recovery (cc)	Recovery (%)	Gas Production (cc)	GOR (cc/cc)
0	1345	0	0	0	0	0
80	1351	5.19396	4.13979	5.38894	78.67388	19.0043
150	1358	9.51575	6.64268	8.64708	154.4726	30.2844
230	1365	14.6056	10.5792	13.7714	272.0914	29.8792
290	1359	18.4197	13.2397	17.2347	350.5039	29.4725
350	1367	22.2468	16.1345	21.003	437.2804	29.9763
410	1374	26.0479	19.236	25.0403	527.7161	29.1591
470	1380	29.888	22.1713	28.8614	615.0154	29.741
530	1375	33.7152	24.8041	32.2886	694.9961	30.3782
650	1369	41.3434	30.7152	39.9834	870.6401	29.7143
712	1363	45.2877	33.3587	43.4245	951.6664	30.6513
771	1367	49.0237	36.4879	47.4979	1046.284	30.2375
875	1359	55.6496	40.9036	53.2461	1170.699	28.1752
930	1352	59.1643	43.5322	56.6678	1249.634	30.0297
995	1359	63.2778	46.7061	60.7994	1342.683	29.3172
1055	1353	67.1049	49.8118	64.8423	1438.347	30.8022
1115	1349	70.919	52.8835	68.8407	1534.794	31.3993
1205	1344	76.6467	56.6708	73.7709	1651.367	30.7795
1265	1338	80.4738	59.8958	77.9691	1748.076	29.9871
1332	1342	84.4702	62.7928	81.7402	1834.591	29.864
1380	1334	87.7896	65.8602	85.7331	1929.993	31.1021
1440	1328	91.6168	69.8499	90.9267	2119.229	47.4307
1500	1332	95.4439	73.0132	95.0445	2445.947	103.286
1560	1334	99.258	73.5883	95.7931	2871.204	739.405
1620	1327	103.059	73.9035	96.2035	3190.866	1013.97
1681	1325	106.951	74.2209	96.6167	3595.213	1273.98
1745	1328	111.026	74.3807	96.8246	3902.329	1922.36
1850	1333	117.639	74.5639	97.0631	4362.872	2514.01
1890	1339	120.255	74.5894	97.0964	4513.685	5900.02

Table B-5 Experimental Data from 100%Prudhoe Bay Gas as Solvent.

Time	Injection Pressure	P.V Injected (%)	Recovery (cc)	Recovery (%)	Gas Production (cc)	GOR (cc/cc)
0	1372	0	0	0	0	0
120	1398	7.55012	5.37313	6.99444	143.4949	26.706
300	1433	19.0055	10.6005	13.7991	302.4109	30.401
366	1455	23.2101	12.9947	16.9158	377.1641	31.2218
426	1458	27.0112	15.2505	19.8523	446.6899	30.8208
480	1473	30.4478	16.9078	22.0096	493.7374	28.3891
540	1469	34.2619	18.8526	24.5412	562.7404	35.4807
603	1483	38.2843	20.5226	26.7152	635.4026	43.5098
660	1491	41.9162	22.1202	28.7948	738.9071	64.7877
720	1494	45.7433	23.7604	30.9299	902.0051	99.4381
780	1504	49.5314	26.0375	33.8941	1155.539	111.34
849	1510	53.8401	27.2666	35.4941	1470.234	256.041
900	1506	57.1986	28.1527	36.6476	1748.337	313.839
971	1504	61.7157	29.3051	38.1477	2118.706	321.389
1020	1497	65.6079	30.2509	39.3789	2437.322	336.883
1085	1478	68.9794	31.0156	40.3744	2757.506	418.698
1145	1484	72.8196	31.6014	41.1369	3037.439	477.876
1211	1462	77.0112	31.955	41.5972	3252.812	609.085
1260	1458	80.1093	32.2894	42.0325	3472.106	655.724
1325	1431	84.34	32.545	42.3653	3677.024	801.666
1389	1437	88.3494	32.8794	42.8006	4088.689	1230.95
1440	1418	91.5647	33.1074	43.0973	4342.223	1112.36
1502	1398	95.548	33.3545	43.419	4674.431	1344.46
1560	1377	99.1799	33.7059	43.8765	5162.418	1388.41
1623	1355	103.228	33.9616	44.2093	5523.638	1413.14
1680	1367	106.448	34.1597	44.4671	5841.731	1605.71
1728	1359	109.867	34.3301	44.689	6141.267	1757.73
1920	1348	122.13	34.5729	45.0051	6620.89	1975.1

Table B-6 Experimental Data from 70%PBG/30%NGL Mixture as Solvent.

Time	Injection Pressure	P.V Injected (%)	Recovery (cc)	Recovery (%)	Gas Production (cc)	GOR (cc/cc)
0	1355	0	0	0	0	0
60	1367	4.16558	3.209177	4.177529	95.1405	29.6464
160	1391	10.1796	5.814066	7.568427	180.6101	32.8112
310	1433	19.7084	10.3065	13.41643	327.5029	32.6978
370	1442	23.5355	13.16513	17.13763	415.5863	30.8132
430	1439	27.3627	16.07062	20.91984	505.4993	30.9459
490	1448	31.2028	18.71411	24.36099	595.1509	33.9142
550	1442	35.0039	21.10624	27.47493	665.7221	29.5014
580	1439	36.9565	23.1256	30.10362	727.4066	30.5466
610	1441	38.805	25.33454	32.97909	795.3641	30.7647
670	1447	42.6191	28.63837	37.27983	891.2888	29.0344
730	1439	46.4593	31.62267	41.16463	989.5658	32.9313
790	1432	50.2734	34.47917	44.88307	1085.49	33.5812
860	1435	54.7514	37.82773	49.24203	1193.7	32.3152
920	1424	58.6045	40.86955	53.2017	1295.113	33.3397
1010	1418	64.4103	45.01477	58.59773	1415.868	29.1312
1120	1422	71.2835	49.49443	64.42909	1556.488	31.3908
1155	1408	73.4835	50.83854	66.17878	1599.354	31.8914
1240	1396	79.5496	55.59511	72.37062	1739.189	29.3984
1320	1389	84.6394	59.30366	77.1982	1867.524	34.6052
1380	1391	88.4405	61.08019	79.51079	1928.163	34.1335
1441	1375	92.3978	63.02499	82.04242	2091.784	84.1322
1500	1359	96.0687	63.34451	82.45836	2166.537	233.956
1561	1345	99.974	63.50853	82.67187	2248.086	497.19
1651	1333	105.65	63.67894	82.8937	2357.864	644.196
1711	1335	109.438	63.86213	83.13217	2519.916	884.61
1770	1328	113.291	63.98568	83.29299	2642.763	994.326
1830	1330	117.574	64.13266	83.48432	2834.612	1305.29
1910	1325	121.518	64.24129	83.62574	2991.437	1443.58

Table B-7 Experimental Data from 60%PBG/40%NGL as Solvent.

Time	Injection Pressure	P.V Injected (%)	Recovery (cc)	Recovery (%)	Gas Production (cc)	GOR (cc/cc)
0	1360	0	0	0	0	0
65	1369	4.7774	3.24726	4.22711	105.8569	32.5988
155	1383	10.5181	6.3679	8.28938	201.5201	30.6551
268	1401	17.7037	11.7124	15.2465	358.3451	29.3433
325	1413	21.3616	14.8309	19.306	452.1788	30.0893
385	1415	25.1888	17.9771	23.4016	548.1034	30.4891
445	1423	29.0029	20.6163	26.8372	625.7318	29.4133
505	1418	32.83	24.1608	31.4512	739.1685	32.0033
565	1424	36.6701	27.3667	35.6244	837.7069	30.7372
630	1415	40.7706	29.9889	39.0378	916.6421	30.1029
747	1409	48.2166	35.6124	46.3582	1105.878	33.6506
810	1402	52.226	38.3794	49.9602	1197.098	32.9667
870	1410	56.0141	40.8269	53.1462	1272.635	30.8629
940	1403	60.466	43.1573	56.1798	1350.002	33.1996
1000	1396	64.3582	46.4782	60.5027	1453.245	31.0892
1060	1389	68.1463	49.4923	64.4263	1545.51	30.611
1130	1395	71.3226	52.8579	68.8075	1653.197	31.9962
1195	1381	76.855	55.6867	72.4899	1737.882	29.9368
1285	1377	82.4915	60.1813	78.3406	1883.207	32.3334
1345	1368	86.2666	62.7928	81.7402	1957.96	28.6243
1377	1372	88.3364	64.3712	83.7949	2005.008	29.8066
1405	1365	90.0937	65.5577	85.3394	2039.509	29.0789
1445	1361	92.7623	66.8358	87.0031	2097.534	45.4005
1475	1354	94.5457	68.231	88.8193	2150.332	37.8415
1510	1359	96.8237	69.5368	90.5191	2271.087	92.4784
1540	1352	98.6983	69.8883	90.9766	2364.451	265.636
1570	1356	100.638	70.1503	91.3177	2469.471	400.833
1605	1350	102.838	70.3633	91.595	2592.317	576.709
1635	1345	104.764	70.5763	91.8723	2720.391	601.25
1665	1339	106.626	70.5831	91.8812	2732.676	1802.22
1725	1334	110.466	70.7297	92.0719	2834.612	695.561
1790	1328	114.554	70.9214	92.3215	3003.199	879.379
1845	1336	118.094	71.0279	92.4601	3120.033	1096.97
1965	1341	125.801	71.1088	92.5655	3217.683	1206.37

Table B-8 Experimental Data from 50%PBG/50%NGL Mixture as Solvent.

Time	Injection Pressure	P.V Injected (%)	Recovery (cc)	Recovery (%)	Gas Production (cc)	GOR (cc/cc)
0	1341	0	0	0	0	0
130	1355	8.34418	5.944	7.73757	113.1754	19.0403
170	1361	10.9086	7.70349	10.028	167.5414	30.8988
320	1374	20.0338	14.1429	18.4104	353.6404	28.9002
355	1379	22.2598	15.4721	20.1407	394.6763	30.8726
485	1384	30.565	22.133	28.8115	593.0599	29.7833
545	1378	34.301	25.1535	32.7434	685.0639	30.4597
605	1381	38.1411	27.8119	36.204	762.4309	29.1029
695	1385	44.0771	32.6409	42.4901	906.9713	29.9318
770	1378	48.7503	35.819	46.6272	1010.737	32.6498
830	1371	52.4603	38.7032	50.3817	1095.161	29.2713
890	1375	56.3655	41.8281	54.4495	1197.882	32.8716
950	1369	60.2057	44.5781	58.0293	1278.385	29.2741
1020	1364	64.5275	48.0907	62.6018	1387.901	31.1783
1070	1359	67.7298	50.0312	65.1279	1451.938	32.9994
1130	1366	71.5959	53.122	69.1513	1550.215	31.7965
1195	1362	75.7355	56.3875	73.4021	1656.856	32.657
1280	1355	81.2028	61.5808	80.1624	1808.976	29.2919
1320	1349	83.6501	63.304	82.4057	1862.297	30.9414
1375	1353	87.1908	65.9326	85.8274	1945.937	31.8195
1435	1347	91.044	68.7742	89.5264	2035.327	31.4578
1500	1341	95.0534	72.0397	93.7772	2144.321	33.3774
1560	1337	98.9586	74.598	97.1075	2326.76	71.3134
1620	1342	102.721	75.2796	97.9948	2495.347	247.325
1685	1345	106.899	75.6076	98.4218	2615.841	367.315
1745	1339	110.739	75.8803	98.7768	2773.189	577.092
1805	1333	114.501	75.9612	98.8821	2878.523	1301.31
1882	1328	119.409	76	98.9326	2938.116	1537.71

CHAPTER 4

COREFLOOD EXPERIMENTS

A. INTRODUCTION

Schrader Bluff reservoir, located in the Milne Point Unit, which is part of the heavy oil field known as West Sak, is estimated to contain up to 1.5 billion barrels of (14 to 21° API) oil-in-place. The field is currently under production by primary depletion. However, the primary recovery will be much less than the expected value of 12% due to complex reservoir structure. Hence, waterflood has been implemented earlier than anticipated. The eventual implementation of enhanced oil recovery (EOR) techniques will be vital for the recovery of additional oil from this reservoir.

The availability of hydrocarbon gases (solvents) on the Alaskan North Slope make the hydrocarbon miscible solvent injection process an important consideration for the EOR project in Schrader Bluff reservoir. Since Schrader Bluff oil is heavy and viscous (41 cp. oil viscosity at reservoir conditions), a water-alternating-gas (WAG) type of process for oil recovery is appropriate as such a process tends to derive synergetic benefits from both water injection (which provides mobility control, and improvement in sweep efficiency), and miscible gas injection (which provides improved displacement efficiency). Since hydrocarbon solvents are costly, a miscible solvent slug injection process rather than continuous solvent injection is considered appropriate. The purpose of this study was to conduct coreflood experiments in order to design and develop a miscible solvent slug injection process and to evaluate the feasibility of this process for improved recovery of oil.

B. EXPERIMENTAL APPARATUS

The materials used in the experimental runs include sand, solvent gases, crude oil, and water. The crude oil sample used in all the experiments is from Schrader Bluff reservoir and collected from well G-2 in the Milne Point Unit, North Slope of Alaska. Live reservoir oil samples were prepared by recombining the Schrader Bluff crude oil with industrial grade methane gas at 1300 psi. Methane was used instead of solution gas due to the unavailability of solution gas samples from Conoco Inc., the field operator. Oklahoma No. 1 sand was used to prepare the porous medium. Appendix A shows a list of these materials and their summarized major properties, including sandpack parameters. Crude oil and solvent composition, and their properties are also listed in Appendix A.

Figure 4.1 is a schematic of the experimental setup. The apparatus can be divided into three main parts which are: (1) injection unit, (2) sandpack unit, and (3) the production unit. The injection unit provides for the injection of fluids. This part consists of pump, transfer cells containing oil and solvent, valves, and water reservoirs. The sand pack unit consists of a 4 foot long, 2 inch diameter coreholder with end plugs, a pair of pressure transducers at 1 foot length, a carrier demodulator assembly, and digital readout unit. A Ruska flash equilibrium separator, wet test flow meter, and a fractional collector along with graduated cylinders and test tubes make up the production unit, which collects, separates, and measures the produced fluids. A detailed description of the major pieces of the equipment used is given in the following sections.

Fluid Injection Pump

A dual cylinder, constant rate positive displacement dual pump (Petrophysical Services model FDS-220) was used in these experiments for injection of fluids such as water, solvents, or oil. Power drivers, controlled by microprocessors, ran the pump motors which in the constant flow rate mode could function in smooth or geared mode. In the smooth mode the pressure fluctuations at the switching of cylinders were eliminated and, in geared mode, the pump simulated a dual piston mechanical pump; i.e. the pistons moved at the same rates in opposite directions. The accuracy of the pump is 0.001 cc/min, and it is rated for 5,000 psi. The flow rate of oil or water in the experiments was maintained constant at 4 cc/min.

Sand Pack/Core Holder

The core holder is four feet long with an inside diameter of two inches. The body of the holder is made of 316 stainless steel with the end caps sealed with silver plated metal "O" rings at each end. There are three pressure tap points at one foot intervals on the holder which are connected to pressure transducers to measure the pressure drop along the core length.

Differential Pressure Transducers and Carrier Demodulators

Eight differential pressure transducers (model DP-15) and carrier demodulators (model CD-18) manufactured by Validyne Corporation were used to measure the differential pressure across the length of the core. The CD-15 carrier demodulators were built in the MCI-20 module case. The DP-15 differential pressure transducers had different pressure drop ranges. The transducers used in these experiments were of 0-20 psi, 0-80 psi, and 0-320 psi range. A pair each consisting of a low range and a high range transducer were connected between the five pressure points, in such a way that the low pressure transducer can be protected from high differential pressure by shutting it off and using the high range one. The transducers and the carrier demodulators converted pressure signals into voltage signals and sent them to a digital display. The differential pressure transducers had an overall accuracy of 1% of the full scale range.

Back Pressure Regulator

To maintain the pressure in the system above the bubble point pressure of 1300 psi of the Schrader Bluff reservoir, a dome type back pressure regulator was used. The regulator had a Teflon diaphragm, and the dome was charged with nitrogen gas at 1300 psi.

Flash Equilibrium Separator

To separate the oil and water from gas, a flash equilibrium separator manufactured by Ruska Instruments Corporation was used. The liberated gas was sent through the gas line to a wet test flow meter for measurements and the oil and water

collected into graduated cylinders or a fraction collector with 15 cc graduated test tubes.

Transfer Cells

One transfer cell of one gallon capacity was used to prepare live oil by recombining dead oil with industrial grade methane. Two other 750 cc transfer cells were used to prepare the miscible solvents and to inject gases into the sand pack during experiments.

C. EXPERIMENTAL PROCEDURE

The success of each run depended on the careful preparation of all the required equipment and materials. The following procedure was followed carefully.

Preparation of Sand Pack

The core holder was made vertical with one end plug tightened, and then packed with Oklahoma #1 sand supplied by Halliburton Services, Duncan, OK. To achieve a homogeneous packing in the core holder, air vibrators were attached to each end and carefully weighed amounts of sand were added in 200 gram increments. After addition of each batch of sand, it was poked and packed with steel rod half inch in diameter proper packing. This was continued until the core holder was fully packed. The exact weight of total sand added was noted down. The end plug was then screwed into place, making sure no sand was in contact with the sealing surface, and the core holder returned to horizontal position. The injection, production, and differential pressure transducers tubing were connected and secured tightly.

Measurement of Porosity/Pore Volume and Absolute Permeability

Water was then injected into the sand pack at a high enough rate to flush out all air within the pore spaces. The injected amount of water and produced water at the outlet end was carefully measured and monitored. The difference between the two gave the pore volume, and dividing it by volume of the core holder gave the porosity. Water was then injected into the sand pack at a constant rate and the pressure drop across the pack measured and absolute permeability calculated using the Darcy's law. The whole system was pressure tested prior to experiments for leaks at 1800 psi. At this time all equipment was checked to ensure that it was in good operating condition.

Preparation of Live Oil and Miscible Solvent

Calculated amount of dead oil was poured into a one gallon capacity transfer cell and recombined with methane gas to 1300 psi, the reservoir bubble point pressure. The cell was put on a rocking mechanism and kept rocking for 3-5 days with addition of more methane gas to maintain the pressure at 1300 psi, till the pressure stabilized at 1300 psi.

From the results of slim tube experiments (Inaganti, 1994), a 50% Prudhoe Bay Gas and 50% NGL mixture was identified as the multi-contact miscible solvent for Schrader Bluff oil. Using COATS PVT simulator to obtain the mixture density and molecular weight, calculated amount of NGL was taken in a 750 cc transfer cell and Prudhoe Bay Gas was mixed with it followed by continuous rocking. Thus a miscible solvent for studying the effect of miscible slug size was prepared.

Saturation of the Sand Pack with Live Oil

The transfer cell containing live oil was connected to the sand pack and after the entire system had been pressurized to 1300 psi, and the back pressure regulator (BPR) charged to 1300 psi, oil was injected into the sand pack. This was continued until water production became negligible at the outlet end. Oil saturation and irreducible water saturation were determined using material balance calculations.

Displacement Runs

A total of 13 displacement runs were conducted as a part of this study. These included the following with brief procedure in each set of the run given below:

- (a) Unsteady-State Waterflood (1 run): After saturating the core with live oil, water was injected into the sand pack at a constant rate of 4 cc/min. The oil, water, and gas production data and pressure drop along the length of the sand pack was monitored at every 0.1 PV injection. This was continued up to 1.8 PV injection of water.
- (b) Effect of Miscible Slug Size (4 runs): In this set of experiments, a predetermined size of miscible solvent slug (50% PBG + 50% NGL) was injected into the sand pack after saturating it with live oil, and the slug of solvent was followed by water as chase fluid. Four runs with slug sizes of 5%, 10%, 20%, and 40% of PV were conducted. Again all the production and pressure data were continuously monitored.

- (c) Effect of WAG Ratio (3 runs): After saturating the sand pack with live oil, a 5% slug of miscible solvent (50% PBG + 50% NGL) was injected followed by water slugs in WAG ratios of 11:1, 5:1, and 3:1, and the effect of WAG ratio was investigated.
- (d) Effect of Miscible Slug Size for FCM Type Process (3 runs): In these runs propane was used as a FCM solvent and the procedure was the same as described in (b) above.
- (e) Effect of Solvent Type (2 runs): In addition to study of the two solvents mentioned above, runs were conducted with Prudhoe Bay Gas (PBG) and CO₂ as solvent gases. In these runs a 5% slug of solvent gas was injected at 1300 psi into the sand pack after saturating it with oil, and the solvent was followed by continuous water injection.

Analysis of Data

The liquid samples collected in the test tubes were centrifuged to determine the exact volume of oil and water produced, while emulsion breaker was added to the samples in graduated cylinders and set aside for analysis. The volume of oil and water produced for each injected pore volume was recorded and the volume of gas produced was recorded by a wet test flow meter. The pressure drop along the length of the sand pack was plotted against the pore volume injected. The water-oil ratio, gas-oil ratio, and cumulative recovery were plotted versus pore volume injected.

Cleaning the Sand Pack

After each run, the sand pack was flushed with further 4-5 pore volumes of water. Then 3-4 pore volumes of toluene were injected under pressure to extract out any trace of oil in the sand pack. It was then followed up by 6-8 pore volumes of water injection. The separator and sampling vessels were also cleaned and made ready for the next run.

D. RESULTS AND DISCUSSIONS

Experimental Results

A total of 13 coreflood experimental runs were conducted with a 4 foot long, 2 inch diameter sand pack as part of the study to design and develop a suitable miscible solvent slug injection process for the improved recovery from Schrader Bluff heavy oil reservoir. The experiments were divided into the following five groups:

1. Unsteady-state waterflood (Run #1),
2. Effect of miscible solvent slug size (Single solvent slug followed by water injection, MCM solvent, Runs 2, 3, 4, and 5),
3. Effect of WAG ratio with MCM solvent (Multi-slug WAG, Runs 2, 6, 7, and 8),
4. Effect of miscible solvent slug size (Single solvent slug followed by water injection, FCM solvent, Runs 9, 10, and 11), and
5. Effect of solvent type (Runs 2, 9, 12, and 13).

In each of these runs, recombined Schrader Bluff oil samples were used. The following sections will describe and discuss each experimental run individually. All runs were conducted at 1300 psi pressure and room temperature conditions. The basic data collected is given in tables B1 to B13 in Appendix B.

Unsteady-State Waterflood

The first experimental run was an unsteady-state waterflood. This run was conducted to provide base case data for comparison purposes. Oil-water relative permeability data (Table B14) was also obtained from this run and is plotted in Figure 4.2. The method used in obtaining the relative permeability data is briefly discussed in Appendix C. The oil recovery at 1.2 PV injection was 61.45% (Figure 4.3). Figure 4.4 shows that water breakthrough occurred at 0.31 PV injection. The GOR behavior (Figure 4.5) was as expected in a waterflood. The plot of pressure drop versus PV injected is given in Figure 4.6 and is indicative of the propagation of the waterflood front. The oil-water relative permeability data suggests the core to be oil wet in nature.

Effect of Miscible Slug Size (MCM process)

A total of 4 runs with different slug sizes of a multi-contact miscible solvent were conducted to study the effect of solvent slug size on the displacement behavior and oil recovery. The solvent was 50 mol% PBG and 50 mol% NGL mixture and the sizes used were 0.05, 0.10, 0.20, and 0.40 PV. In each of the cases, a predetermined amount of solvent was injected into the core and was followed by water as a chase fluid in a water alternating gas (WAG) mode. Each experimental run is described below.

- (a) 0.05 PV Slug Size: This run resulted in a recovery of 72.64% at 1.2 PV injection (Figure 4.7). The water breakthrough was at 0.43 PV and the WOR (Figure 4.8) increased sharply after about 0.7 PV injection. The GOR (Figure 4.9) increased slightly at approximately 0.3 PV injection indicating possible solvent breakthrough, followed closely by water breakthrough which caused it to decrease for some time. The GOR increase again after 0.7 PV injection is due to the production of oil/solvent mixture, of which the solvent flashes into gas phase at the outlet. Figure 4.10 is a plot of pressure drop versus PV injected along the length of the core. The plot indicates a quite smooth displacement with the solvent/oil front moving in the core with a good sweep.
- (b) 0.10 PV Slug Size: In this run, a recovery of 74.16% at 1.2 PV injection was obtained (Figure 4.11) with water breakthrough at 0.46 PV injection (Figure 4.12). From the GOR plot (Figure 4.13), solvent breakthrough appears to have occurred at 0.2 PV injection. The trailing edge of the solvent slug gets produced after approximately 1.0 PV injection. The pressure drop plot (Figure 4.14) indicated the propagation of the solvent slug front in the core. There appears to be minor fingering of the solvent occurring initially until miscibility is achieved and a transition zone established.

- (c) 0.20 PV Slug Size: The oil recovery of 77.88% at 1.2 PV injection (Figure 4.15) is higher than the earlier cases because of the obvious reason of more solvent injection. The WOR plot is shown in Figure 4.16. The GOR plot (Figure 4.17) indicates solvent breakthrough at 0.15 PV injection with a steep rise in GOR. The pressure drop plot (Figure 4.18) indicates possible viscous fingering caused by the finger getting a chance to grow because of larger slug size, resulting in early breakthrough of solvent and a drop in pressure drop. There is also a possibility of the solvent channeling along the walls of the core holder, hence resulting in very early solvent breakthrough after only 0.15 PV injection. This seems likely due to the fact that no overburden pressure could be applied to the sand pack because of equipment constraints.
- (d) 0.40 PV Slug Size: The oil recovery of 78.28% at 1.2 PV injection (Figure 4.19) is the highest amongst all these four runs, but the incremental gain in recovery for additional amount of solvent injected is the least. Water breakthrough in this case is delayed until 0.78 PV (Figure 4.20) after which WOR shoots up sharply. The GOR data (Figure 4.21) indicates continuous solvent and solvent-oil mixture production after 0.2 PV onwards. The pressure drop plot (Figure 4.22) in this case also indicates severe viscous fingering resulting in sharp drop in pressure drop initially, followed by gradual rise in between (due to the sweep provided by water), and finally a slow decline as the oil is mobilized and produced from the core. Figure 4.22 also suggests a near complete mobilization of oil from the 0-1 foot length of the core by the solvent. A comparison of all the recoveries is discussed later under the discussions of results section.

Effect of Water-Alternating Gas (WAG) Ratio

A total of three runs in addition to run number 2 (with a WAG ratio of 23) were conducted to study the effect of WAG ratio. In all cases the solvent used was a mixture of 50% PBG and 50% NGL and the slug size was 0.05 pore volume, with the number of slugs varying in each run. The results for each run are given below.

- (a) WAG Ratio of 11: In this run two slugs of 0.05 PV size were injected separated by water slugs of 0.55 PV. The run resulted in recovery of 75.67% at 1.2 PV injection (Figure 4.23). From the WOR plot (Figure 4.24) and the GOR plot (Figure 4.25), the formation of oil bank in front of both the solvent slugs is evident. The second oil bank gets produced at 0.9 PV injection resulting in a sharp decrease in WOR, and a marked increase in recovery. There are two water breakthroughs as identified from the WOR plot (Figure 4.24), the first occurring at 0.36 PV injection and the second occurring at 1 PV injection. The pressure drop plot (Figure 4.26) corroborates the above behavior of multi-slug WAG process.
- (b) WAG Ratio of 5: A total of four slugs of 0.05 PV each separated by 0.25 PV slugs of water were injected alternately in this run. A recovery of 78.64% at 1.2 PV injection was obtained (Figure 4.27). The WOR, GOR, and the pressure drop plots (Figures 4.28, 4.29, and 4.30 respectively) are typical of a WAG type process. As in the earlier case (a), the formation of oil bank occurred except that the size of oil banks reduced considerably as suggested by the WOR plot (Figure 4.28). Again in this case, three water breakthrough points can be identified at 0.41, 0.90, and 1.4 PV injection.
- (c) WAG Ratio of 3: In this run, six solvent slugs, again of 0.05 PV each, were alternately injected with 0.15 PV water slugs. The highest oil recovery of 81.55% at 1.2 PV injection (Figure 4.31) resulted in this case. The WOR behavior (Figure 4.32) again reflects the nature of the WAG process. The GOR plot is shown in Figure 4.33, and the pressure drop versus PV injected plot in Figure 4.34.

Effect of Miscible Slug Size (FCM Process)

In order to study the behavior of first contact miscible displacement process, a total of three runs with varying slug sizes of 0.05 PV, 0.10 PV, and 0.20 PV were conducted. Propane was used as the FCM solvent. These three runs were conducted in gravity stable method by rearranging the sand pack in a vertical configuration and injecting the solvent slug from the top followed by water. Again in each run a predetermined amount of solvent slug was injected, which was then followed by water. The use of a first contact miscible (FCM) solvent such as propane should typically yield

the highest oil recovery compared to a multi-contact miscible (MCM) or immiscible type WAG flood. The results of these runs are given below.

- (a) 0.05 PV Slug Size: This run resulted in a recovery of 70.14% at 1.2 PV injection (Figure 4.35). This recovery is less than that obtained from the multi-contact miscible process (MCM) using a solvent mixture of 50% PBG and 50% NGL. The water breakthrough also occurs earlier at 0.41 PV injection (Figure 4.36). The GOR and pressure drop plots (Figures 4.37 and 4.38) indicate severe viscous fingering and/or channeling along the walls of the coreholder occurring in this run. The solvent propane breakthrough occurs at 0.1-0.2 PV injection and most of the solvent is produced as is evident from the GOR increase.

- (b) 0.10 PV Slug Size: In this run a recovery of 75.55% at 1.2 PV injection (Figure 4.39) was obtained. The water breakthrough occurred at 0.45 PV injection (Figure 4.40) and the WOR increased sharply thereafter. In this case too, the solvent breakthrough occurs at 0.1-0.2 PV injection as indicated by the GOR behavior (Figure 4.41). The pressure drop versus PV injected plot on Figure 4.42 clearly shows the effect of channeling and/or viscous fingering of the solvent occurring in the core during the displacement. The solvent fingers through the entire length of the core at 0.2 PV injection as suggested by a pressure drop of only 1.65 psi against the oil phase pressure drop of approximately 12.5 psi in the 3-4 feet section of the core. The fingering could be due to a highly unfavorable mobility ratio. The very early breakthrough of the solvent again suggests the likelihood of solvent channeling along the walls of the core holder. The pressure drop increases after 0.3 PV injection, indicating the better mobility control provided by the water front behind the propane slug.

- (c) 0.2 PV Slug Size: Injection of 0.2 PV slug of propane increased the recovery to 78.52% at 1.2 PV injection (Figure 4.43), which is slightly more than that obtained in the MCM process in run #4. The water breakthrough occurs at 0.51 PV injection after which the WOR rises steeply (Figure 4.44). The GOR plot (Figure 4.45) and the pressure drop plot (Figure 4.46) show similar behavior as observed and discussed in case (b) above. Again, the behavior strongly suggests the occurrence of severe viscous fingering and/or channeling during the displacement process.

Effect of Solvent Type

After studying the multi-contact miscible solvent mixture of 50 mol% PBG and 50 mol% NGL, and the first-contact miscible solvent propane, two additional runs with Prudhoe Bay Gas and Carbon Dioxide (CO₂) were conducted to study the effect of solvent type under gravity stable conditions by keeping the sand pack vertical and injecting the solvent gases at the top followed by water. Though PBG and CO₂ are not miscible with Schrader Bluff oil, their easy availability on the North Slope, and the relatively lower cost as compared to hydrocarbon miscible solvents, make their study imperative and practical. In each run, a solvent slug of 0.05 PV size was injected and followed up by water. Results of the two runs are given below.

- (a) Prudhoe Bay Gas (PBG) as Solvent: The use of PBG as solvent in a WAG type of process gave a recovery of 66.31% at 1.2 PV injection (Figure 4.47), which is about 5% higher than plain waterflood case. This indicates that a slug of PBG is effective to some extent in mobilizing additional oil. The water breakthrough occurred at 0.33 PV injection (Figure 4.48) and the WOR gradually increased until after 1.4 PV, after which it rose sharply. The plot of GOR versus PV injected is shown in Figure 4.49. The pressure drop plot (Figure 4.50) shows a favorable displacement with the flood front advancing without significant fingering, due to gravity stable displacement.

- (b) Carbon Dioxide (CO₂) as Solvent: The use of CO₂ as a solvent gave the highest recovery of 75.90% at 1.2 PV injection (Figure 4.51) as compared to other solvents. The significant mobilization of oil by CO₂ appears to be the cause of this high recovery. The water breakthrough occurs at 0.43 PV (Figure 4.52) and the solvent gas breakthrough at approximately 0.4 PV injection (Figure 4.53). The GOR increased after the breakthrough almost continuously. The pressure drop plot (Figure 4.54) indicates a favorable displacement with no significant viscous fingering of the solvent. The low pressure drops at the 1 foot and 2 foot lengths indicate almost complete mobilization and extraction of oil from the core by CO₂, thereby giving high recovery.

Discussion of Results

A summary of results of all the thirteen experimental runs is given in Table 4.1. From Table 4.1, it can be seen that the ratio of incremental oil recovery (IOR) to solvent slug injected is the highest for the CO₂ slug of 0.05 PV followed by water. A recovery versus PV injected plot comparing the recoveries for different slug sizes in the study of effect of MCM miscible slug size is shown in Figure 4.55. Incremental recovery is plotted against slug size in Figure 4.56, and so is the ratio of incremental recovery to slug size versus slug size. From these two plots it is evident that for the slug size of 0.05 PV highest IOR/PV solvent slug injected is obtained. Though from the incremental recovery versus slug size plot it appears that 0.2 PV slug size would be more appropriate, the incremental recover/slug size versus slug size plot suggests otherwise. Figure 4.55 also shows that increasing the slug size from 0.05 to 0.10 PV or from 0.2 to 0.4 PV has no significant increase in recoveries. Economic considerations need to be taken into account to conclude the economic optimum slug size.

The results of experiments to study the effect of WAG ratio are given in Figure 4.57. From this figure it appears that best WAG ratio is 3 from the recovery point of view, but the plot of incremental oil recovery/slug size versus WAG ratio (Figure 4.58) indicates a WAG ratio of 23 to be best, i.e. a solvent slug of 0.05 PV followed by 1.15 PV of water gives the best results. Another plot of IOR/PV solvent injected versus WAG ratio for single slug WAG and multi-slug WAG is shown in Figure 4.59. From this plot it can be inferred that for the same amount of solvent injected into the core, a multi-slug process gives slightly higher recovery than a single slug process. The comparison of

recoveries versus PV injected for the FCM type of miscible displacement using propane as solvent to study the effect of slug size is made on Figure 4.60. Again, from the recovery or incremental recovery point of view, a slug size of 0.2 PV gives the best results. However, the plot of incremental recovery/slug size versus slug size (Figure 4.61) indicates an optimum slug size of 0.05 PV.

Finally, a comparison of the recoveries obtained using four different solvents with the same slug size of 0.05 PV and a WAG ratio of 23 is made in Figure 4.62. From the figure, it is evident that the CO₂ gives the maximum recovery, more than even propane, or 50 mol% PBG and 50 mol% NGL mixture, which are FCM and MCM solvents respectively. This better performance of the CO₂ WAG can be attributed to the unique properties of CO₂ in mobilizing the reservoir oil in the rock pores by a combination of swelling, hydrocarbon vaporization, viscosity reduction, extraction of crude oil, and other phenomena only exhibited by CO₂ along with improved sweep efficiency.

E. CONCLUSIONS

Experimental coreflood studies were undertaken to evaluate the feasibility of miscible WAG injection process for the improved recovery of heavy oil from Schrader Bluff reservoir. Effect of solvent slug size and WAG ratio on the displacement performance were determined. These will be useful in designing appropriate solvent injection scheme for the field application.

The following conclusions are drawn from the results of the experiments discussed earlier:

1. Among the four solvents tested, CO₂, despite being immiscible, resulted in the highest incremental oil recovery for the same slug size of 0.05 PV, indicating good promise for the CO₂ WAG process in field application. The 0.05 PV CO₂ slug followed by water injection yielded 75.9% oil recovery at 1.2 PV injection, or IOR of 14.45% over waterflood.
2. The use of MCM solvent mixture of 50 mol% PBG and 50 mol% NGL to study the effect of slug size in a single-slug WAG process, indicated the highest IOR per solvent slug size for a slug size of 0.05 PV. Similar result was obtained for FCM solvent (propane).
3. The study of effect of WAG ratio on the displacement behavior for a multi-slug WAG process with a solvent slug size of 0.05 PV, and PBG-NGL mixture as MCM solvent, indicates best performance for WAG ratio of 23.
4. The multi-slug WAG process performed slightly better than the single-slug WAG, resulting in higher IOR per PV of solvent injected.
5. Finally, propane, although FCM solvent, performed poorly compared to CO₂ as well as PBG-NGL mixture due to severe fingering.

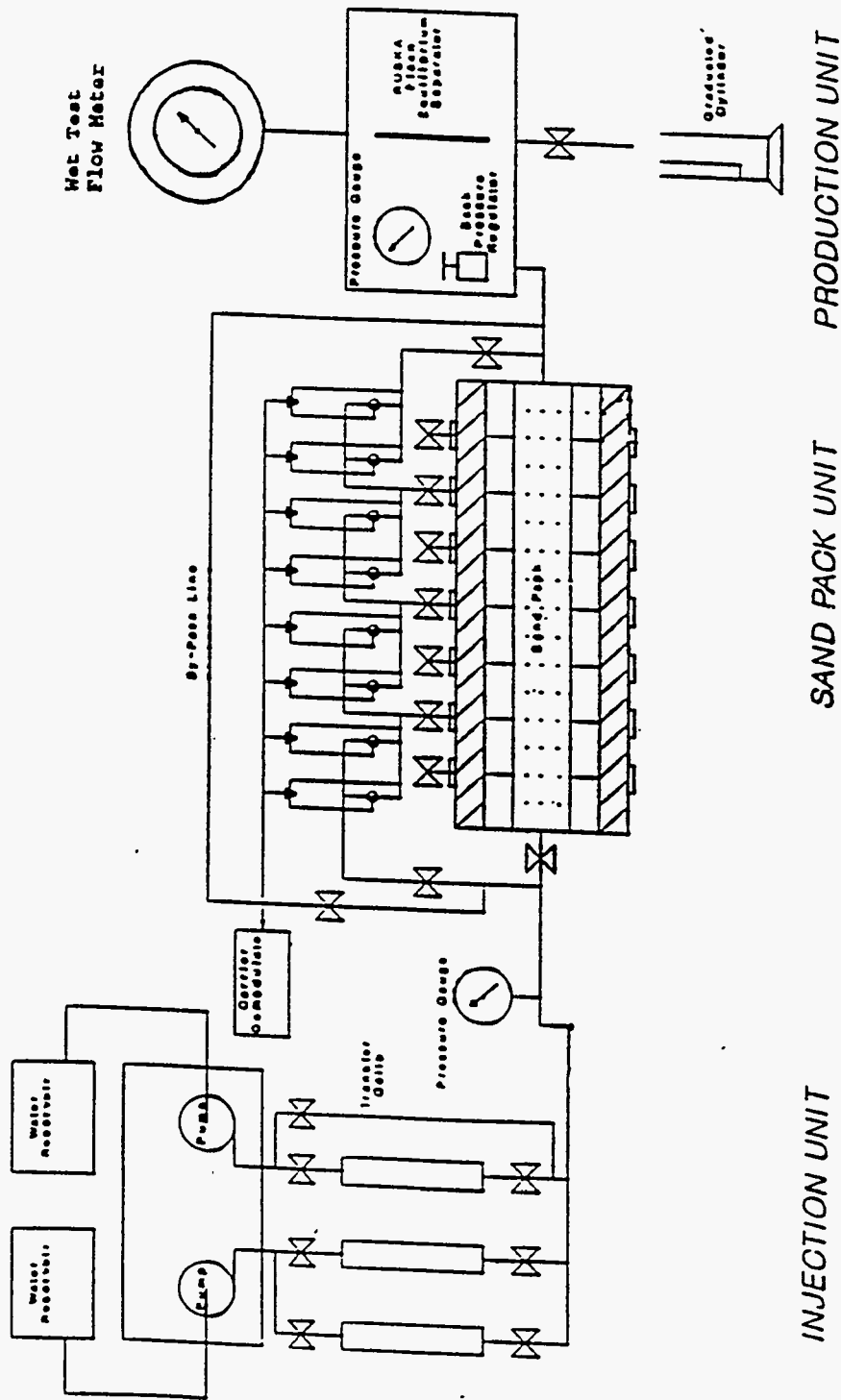


Figure 4.1 Schematic Diagram of Experimental Setup

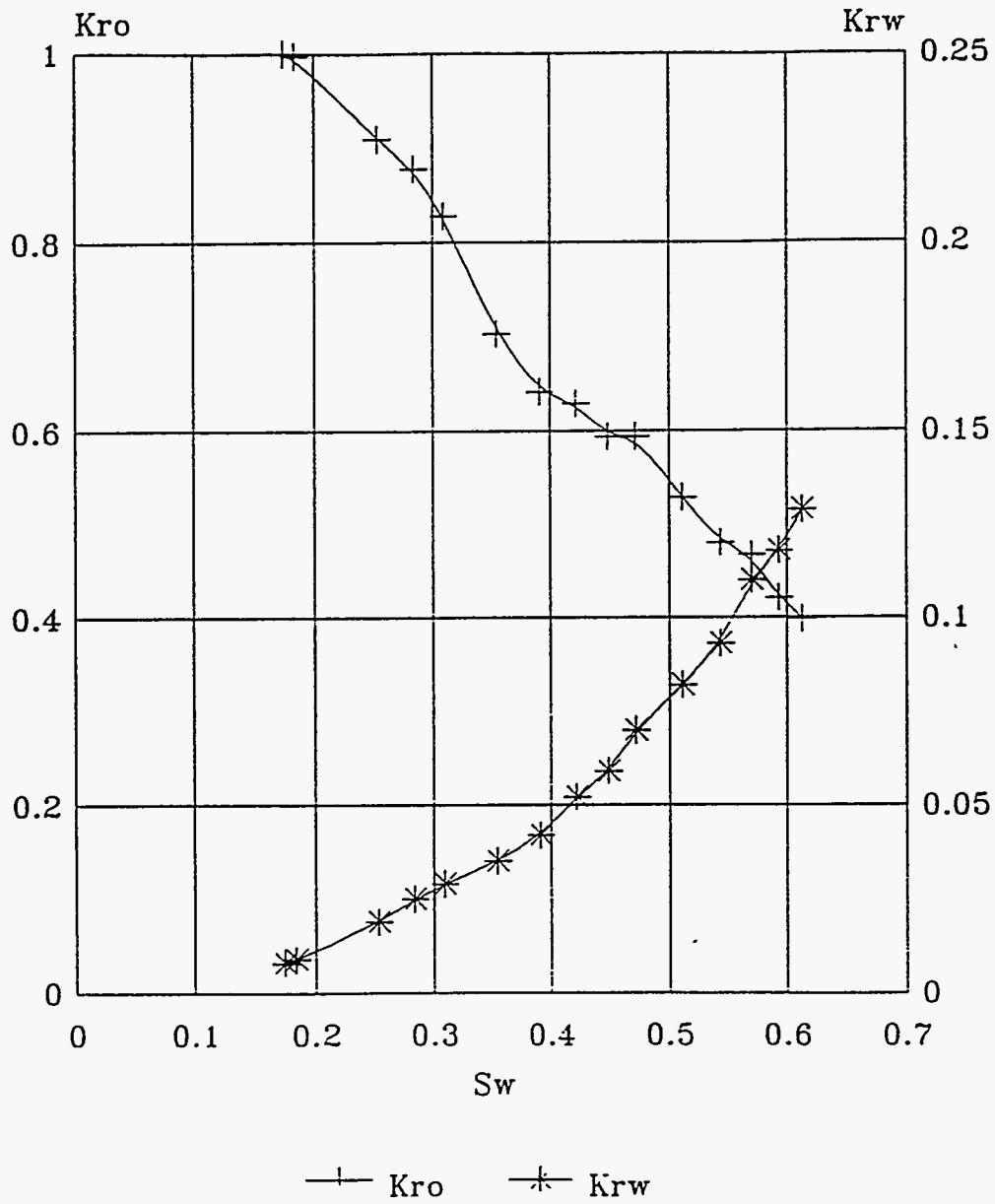


Figure 4.2 Oil-Water Relative Permeability Curves for the Sandpack

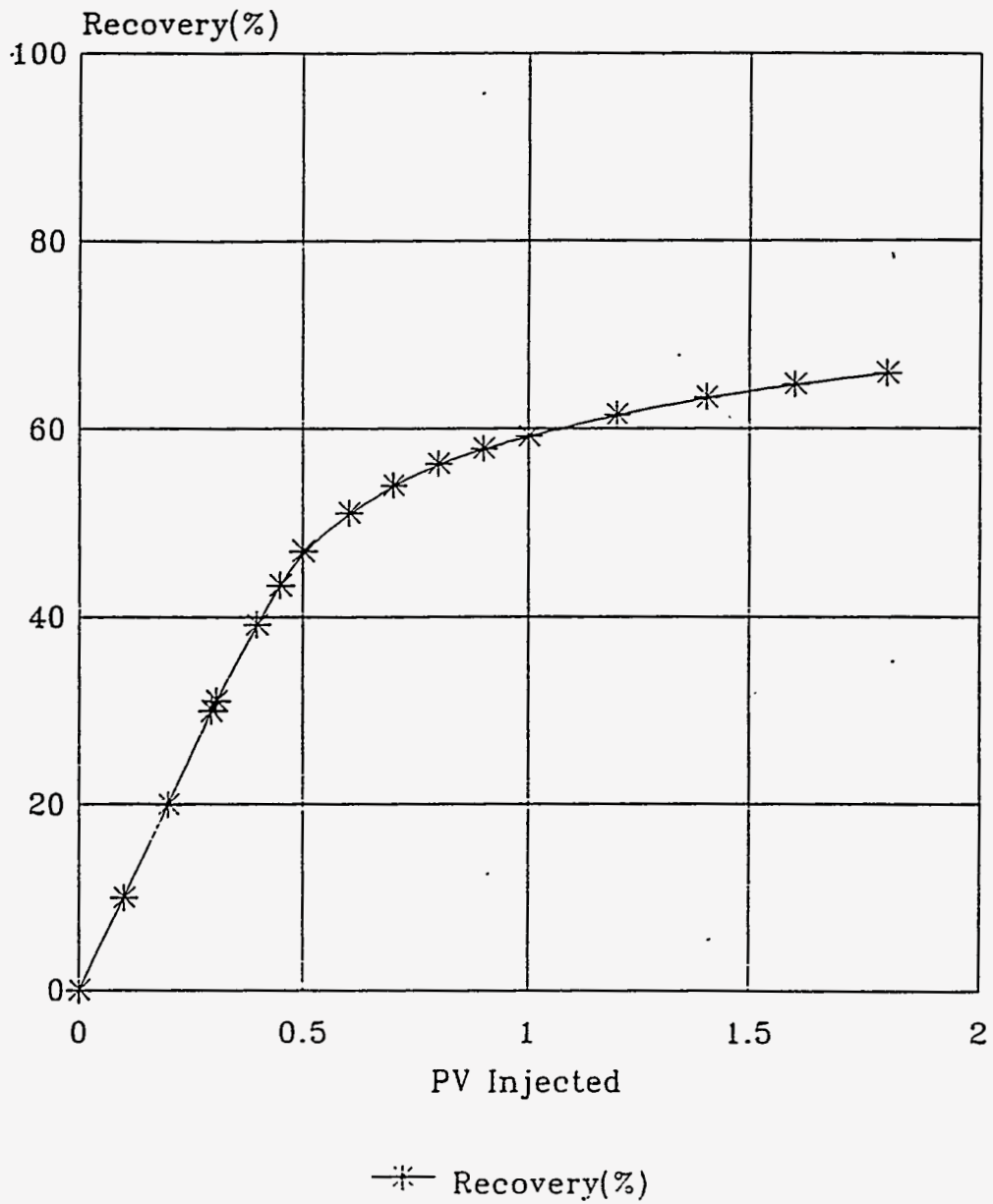


Figure 4.3 Oil Recovery vs. PV Injected (Unsteady State Waterflood)

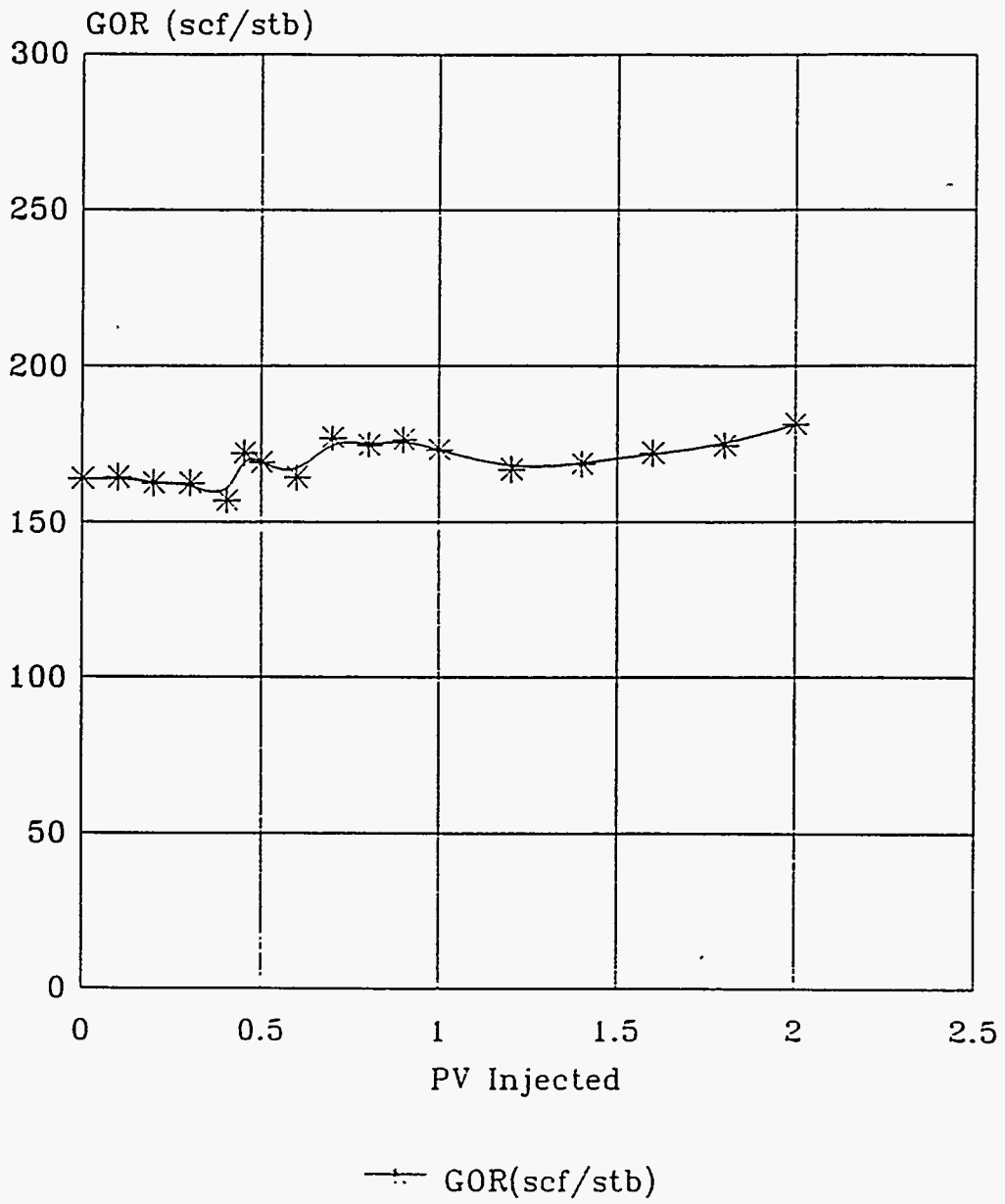


Figure 4.5 GOR vs. PV Injected (Unsteady State Waterflood)

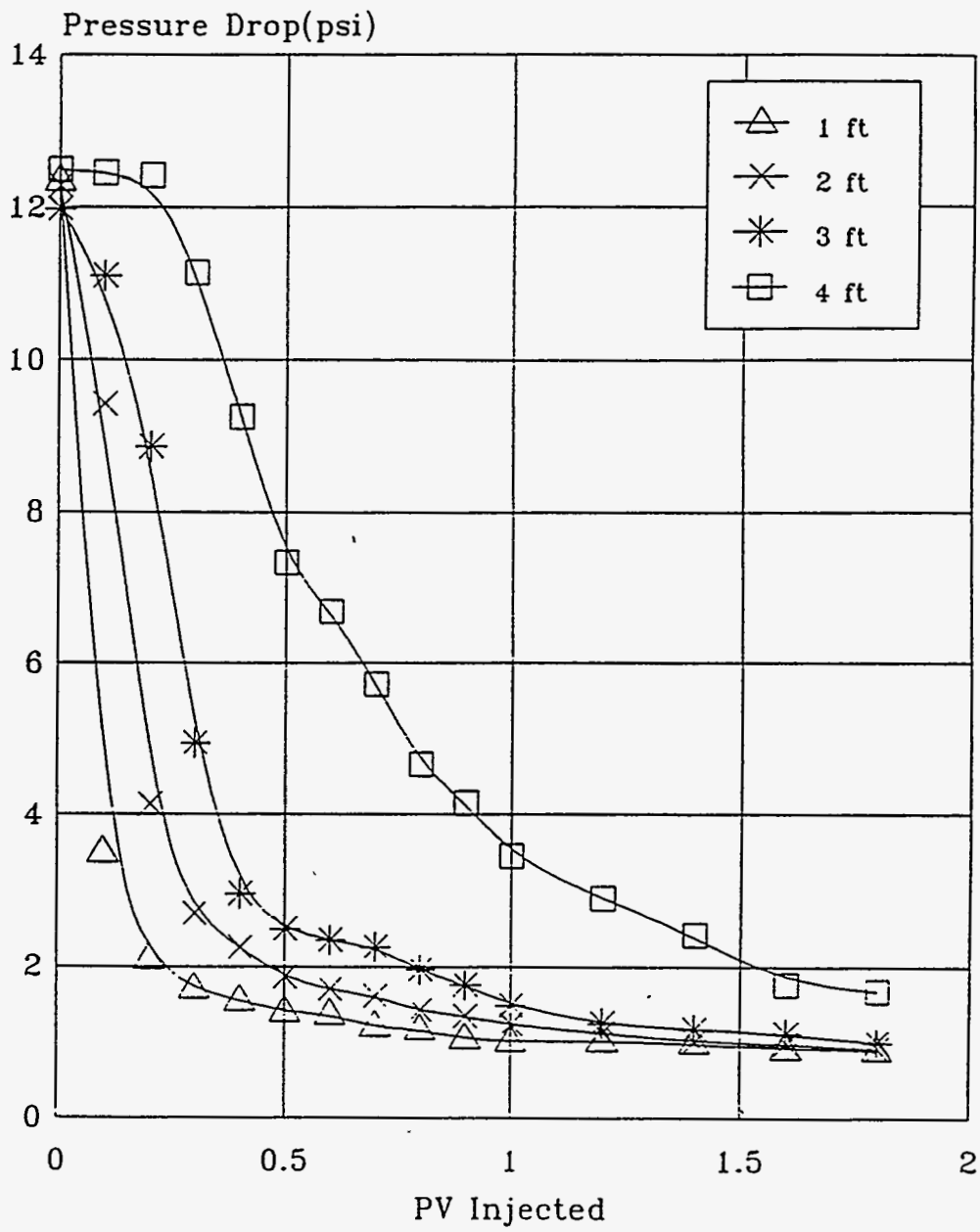
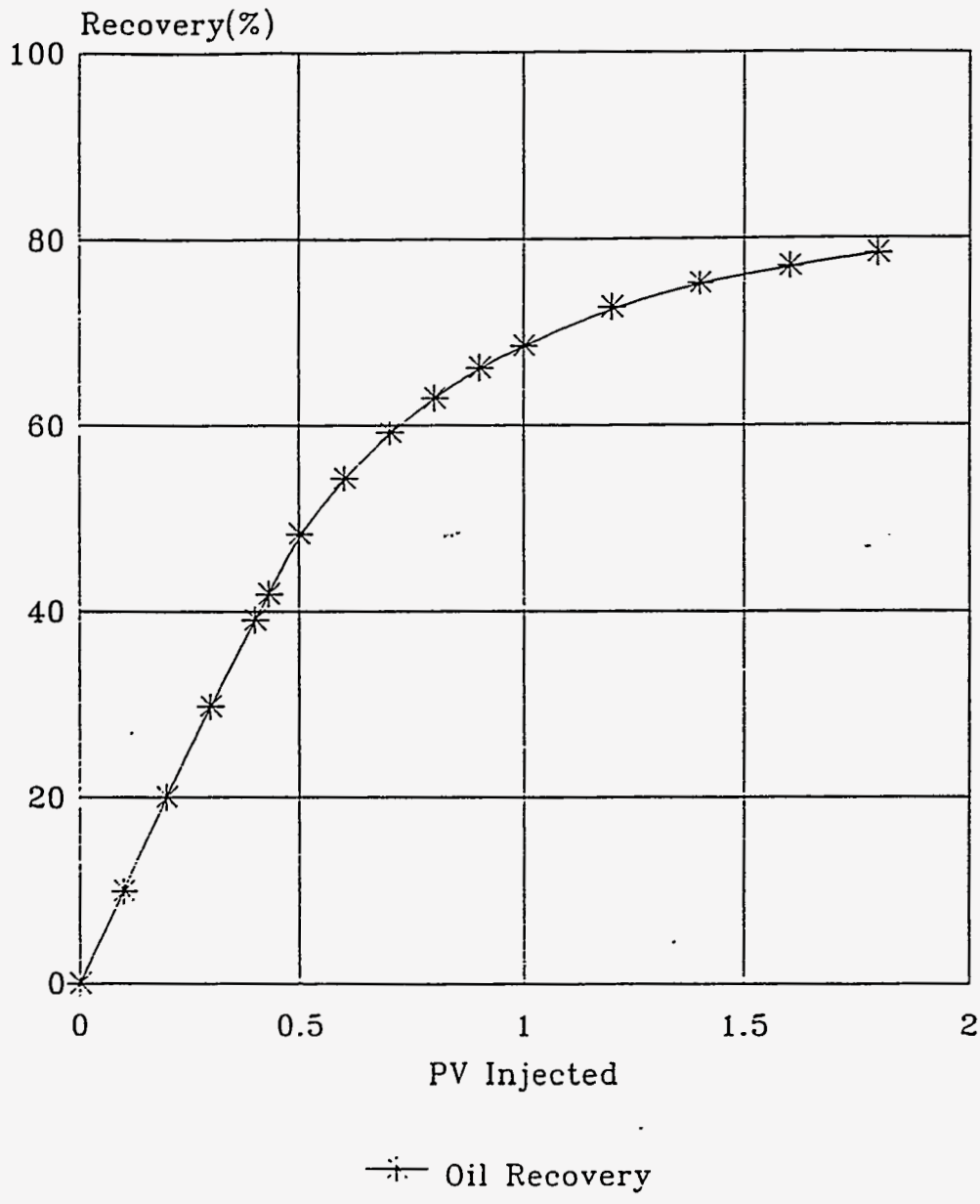


Figure 4.6 Pressure Drop vs. PV Injected (Unsteady State Waterflood)



**Figure 4.7 Oil Recovery vs. PV Injected, MCM Solvent Slug Size: 0.05 PV
(Solvent: 50% PBG/50% NGL)**

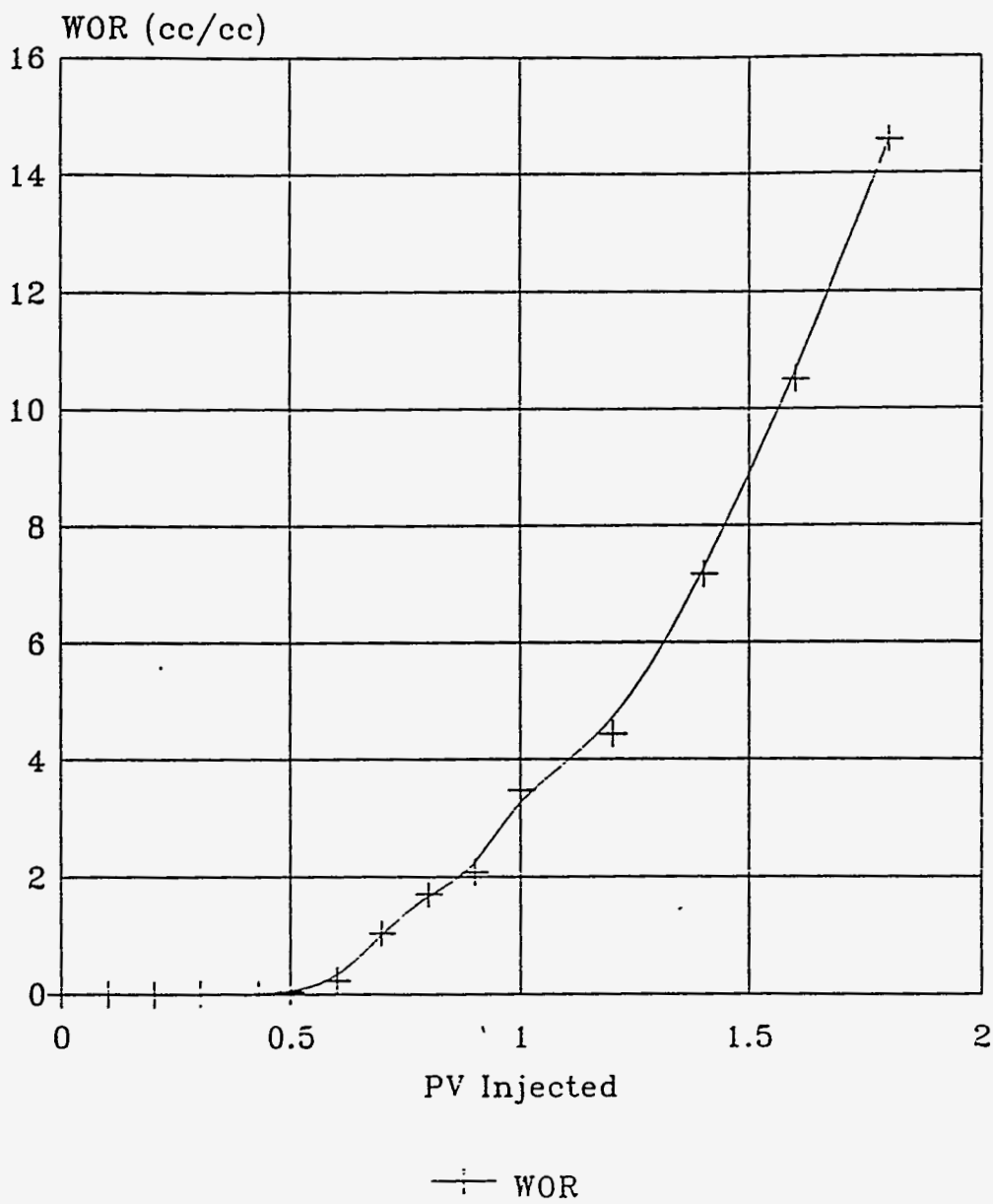


Figure 4.8 WOR vs. PV Injected, MCM Solvent Slug Size: 0.05 PV
 (Solvent: 50% PBG/50% NGL)

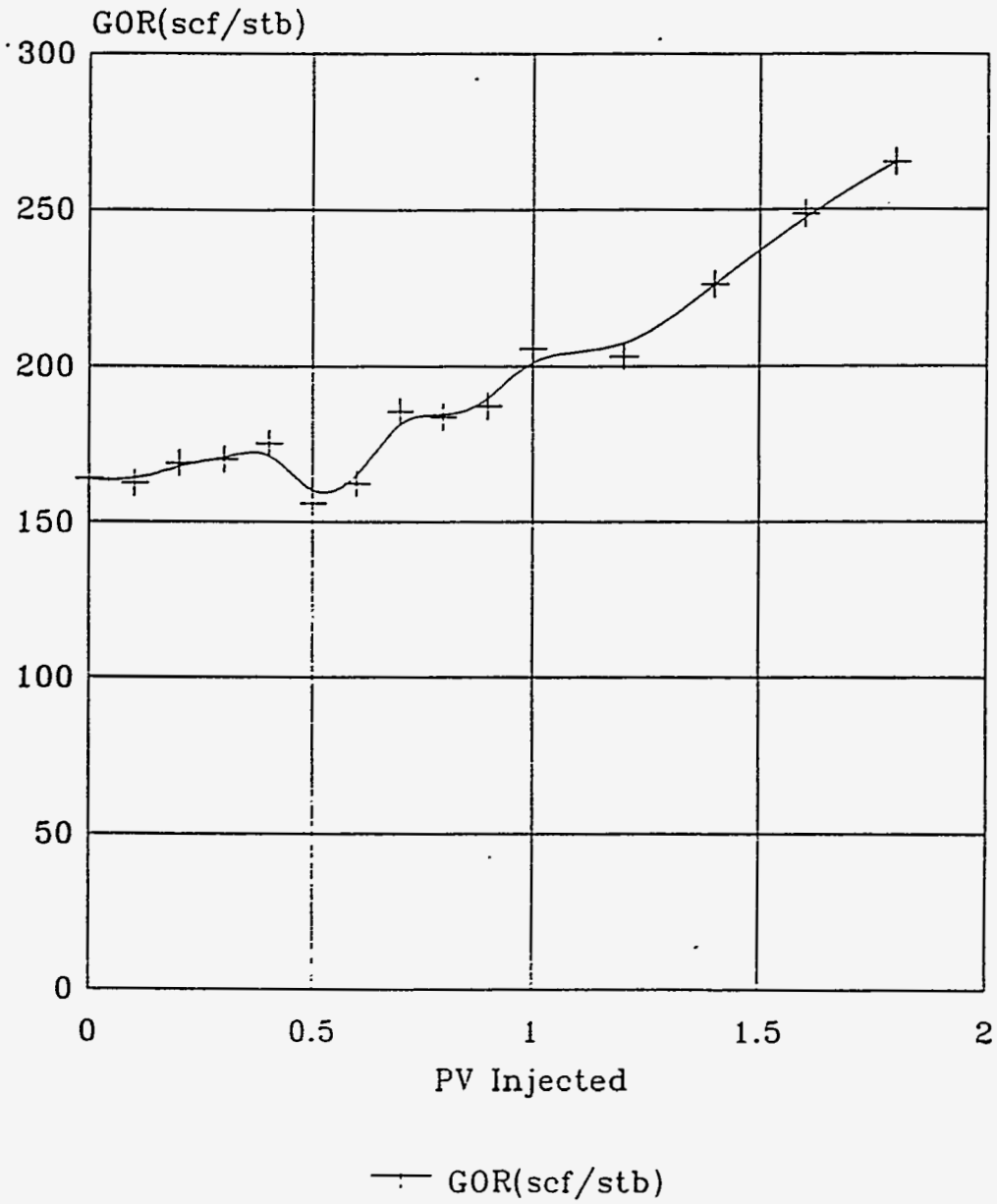


Figure 4.9 GOR vs. PV Injected, MCM Solvent Slug Size: 0.05 PV
 (Solvent: 50% PBG/50% NGL)

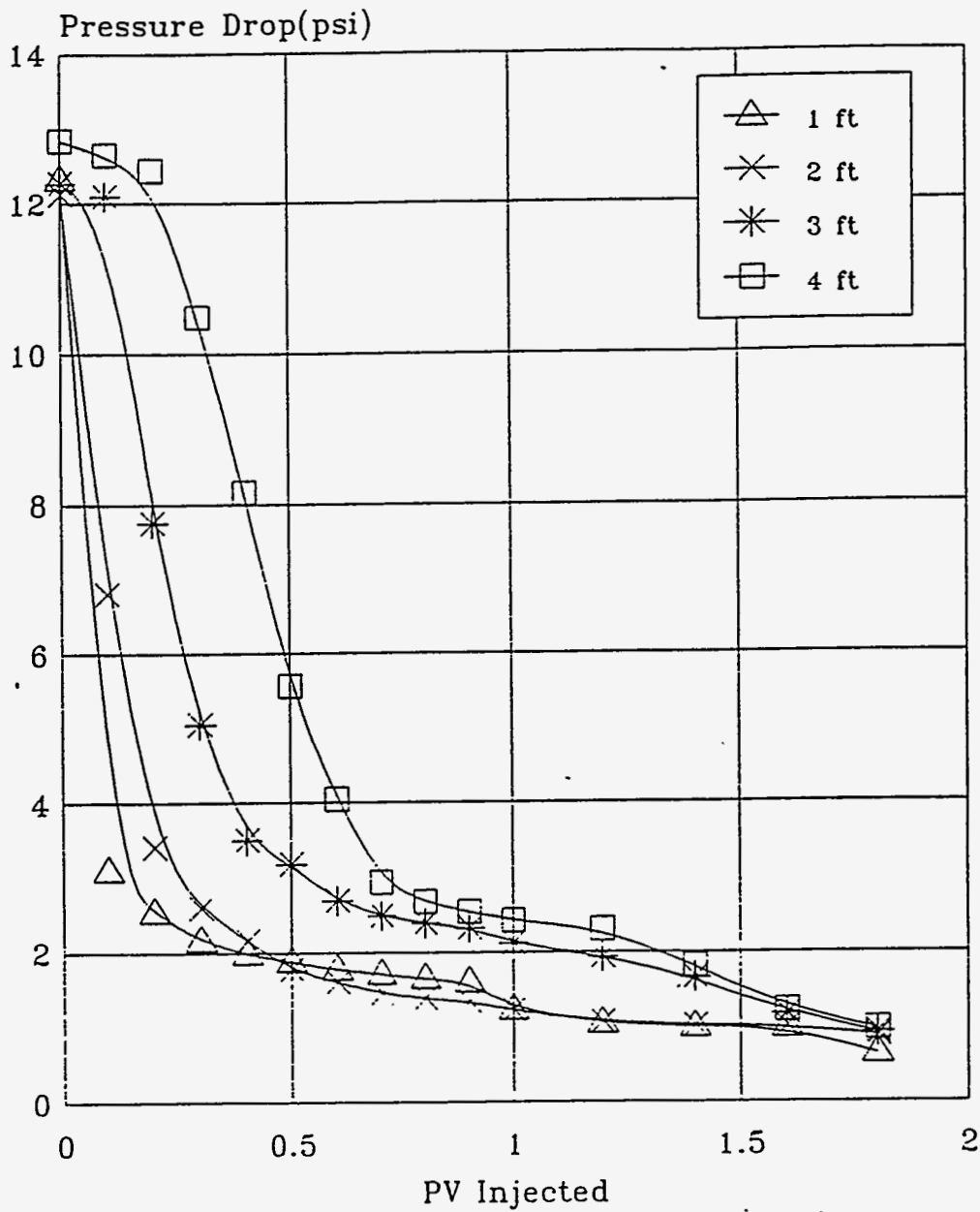
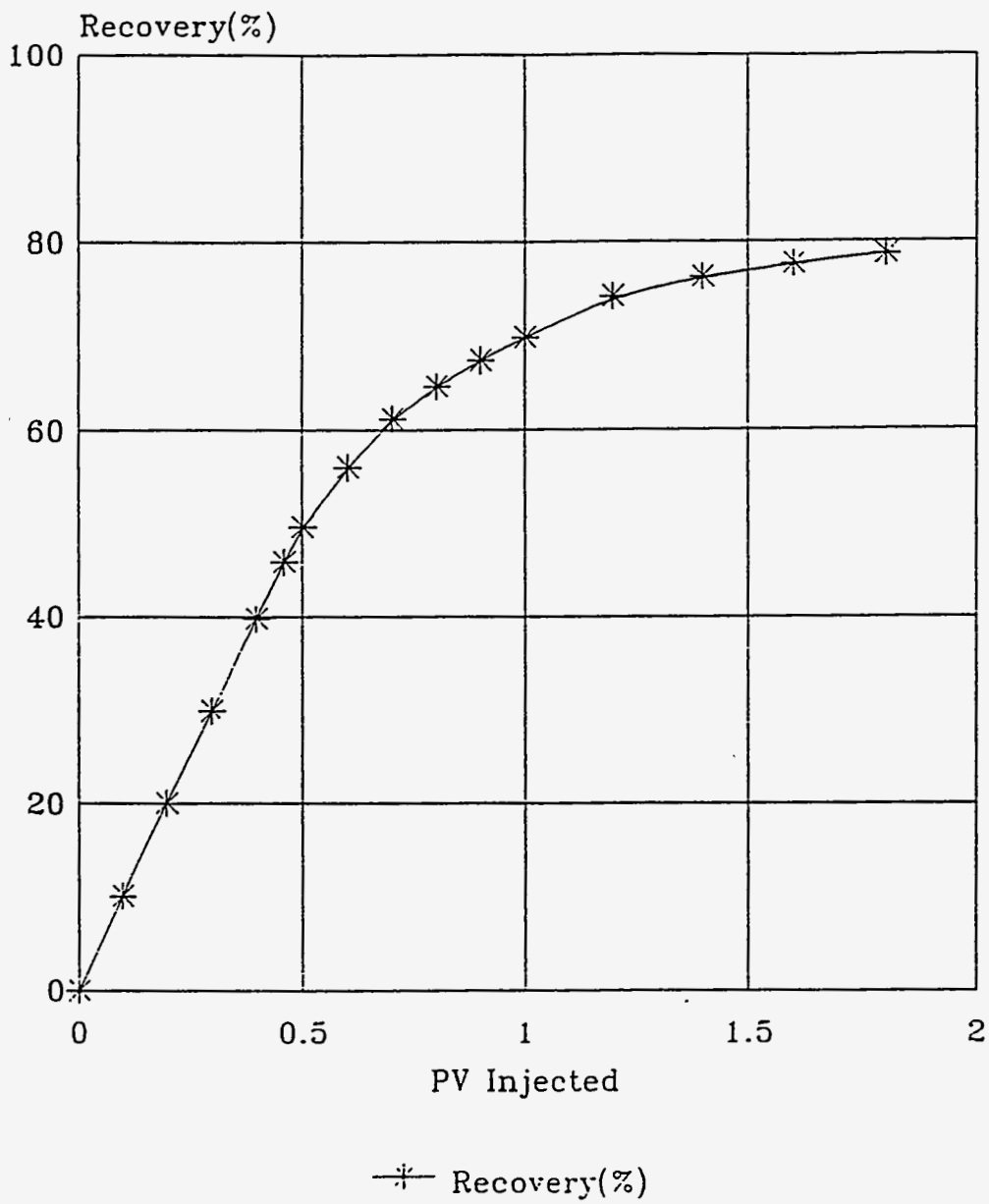


Figure 4.10 Pressure Drop vs. PV Injected, MCM Solvent Slug Size: 0.05 PV
(Solvent: 50% PBG/50% NGL)



**Figure 4.11 Oil Recovery vs. PV Injected, MCM Solvent Slug Size: 0.10 PV
(Solvent: 50% PBG/50% NGL)**

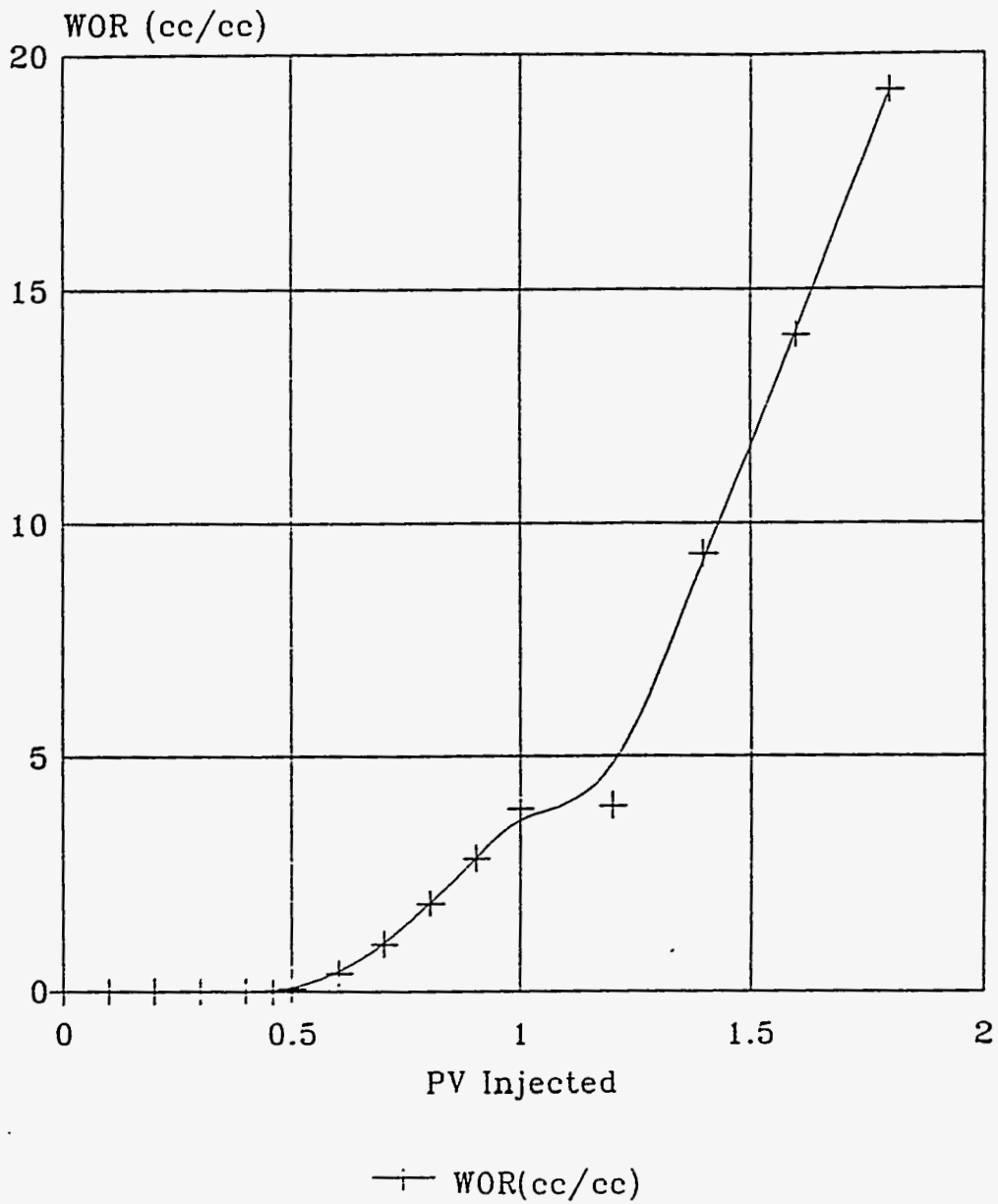


Figure 4.12 WOR vs. PV Injected, MCM Solvent Slug Size: 0.10 PV
 (Solvent: 50% PBG/50% NGL)

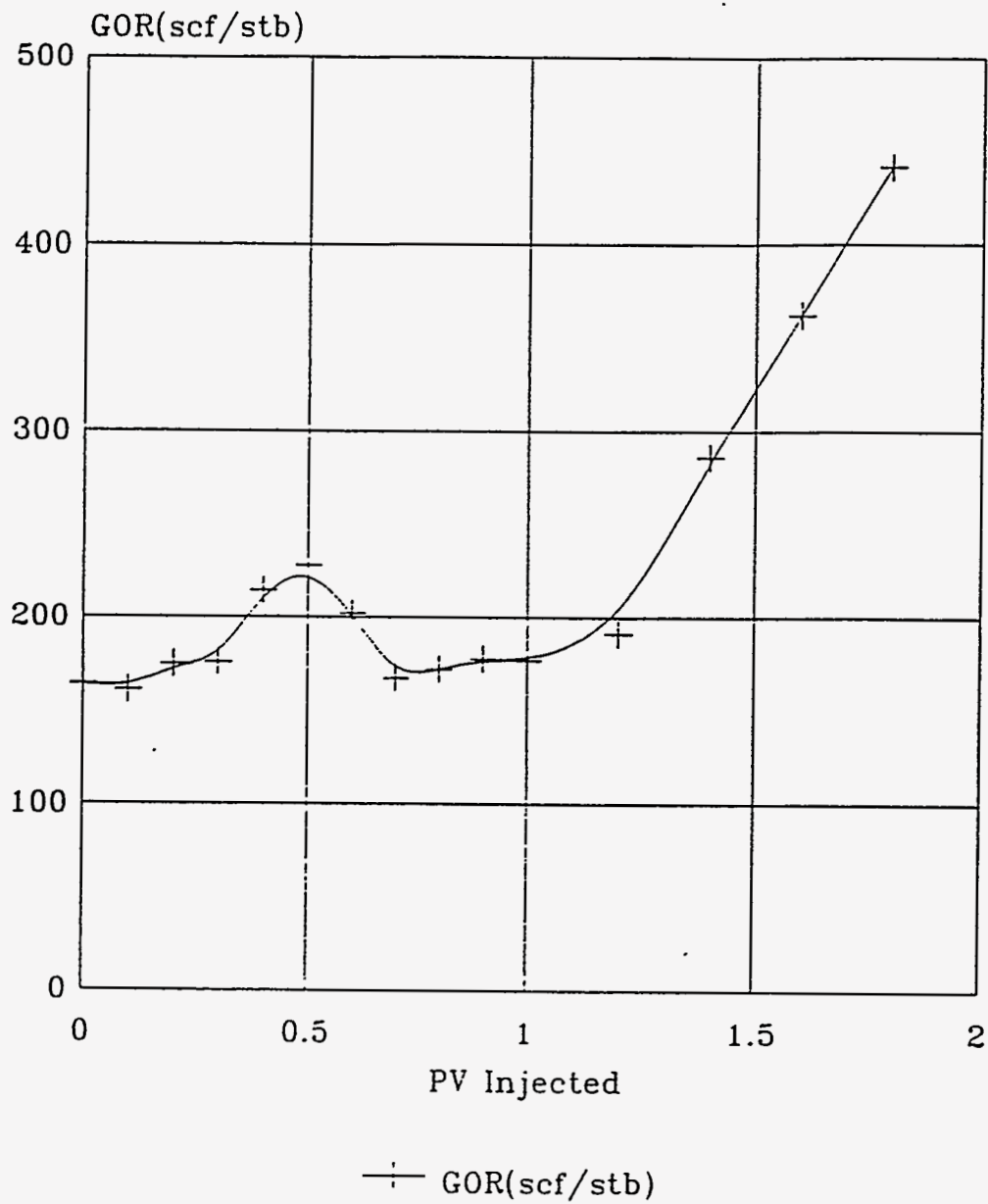


Figure 4.13 GOR vs. PV Injected, MCM Solvent Slug Size: 0.10 PV
 (Solvent: 50% PBG/50% NGL)

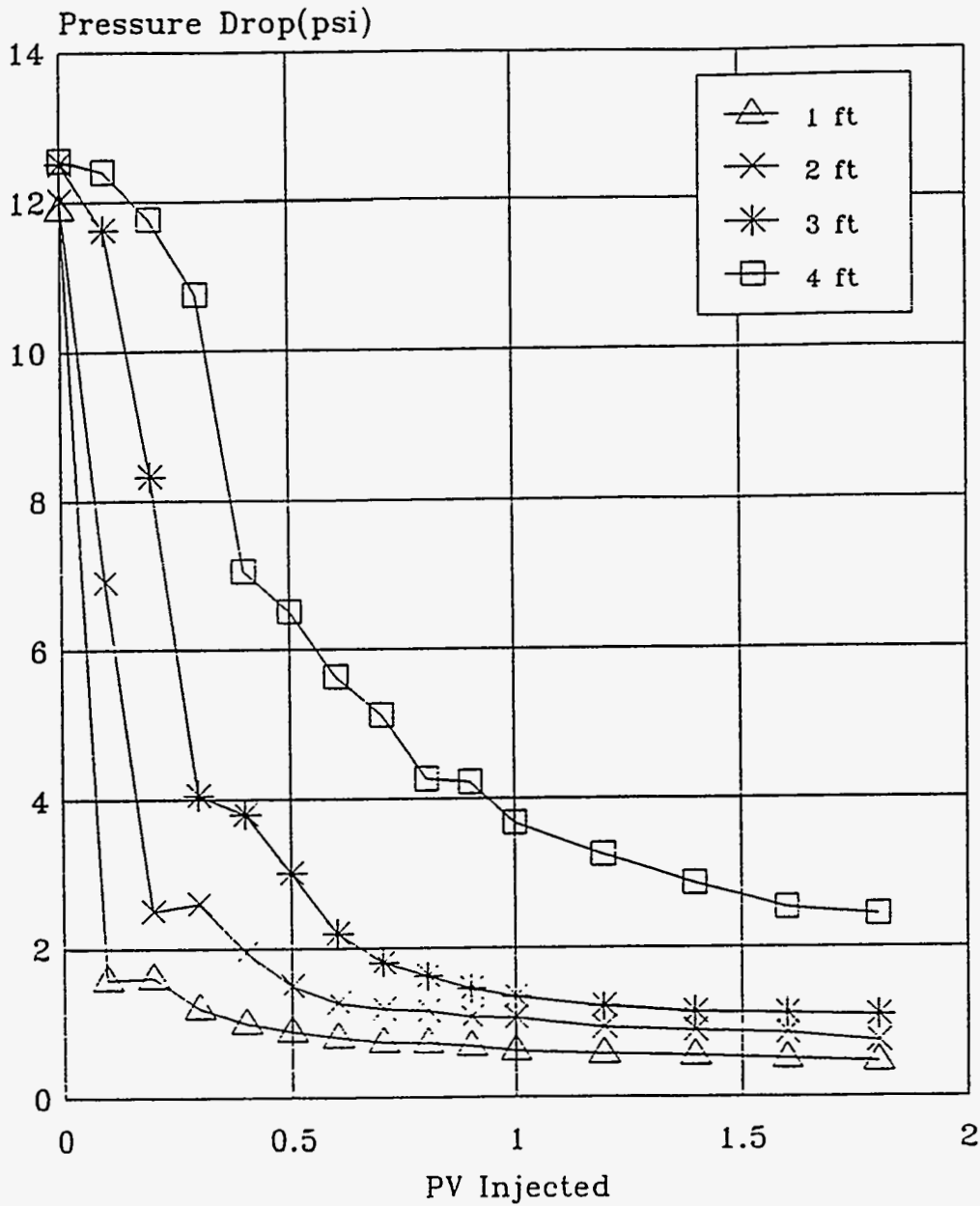
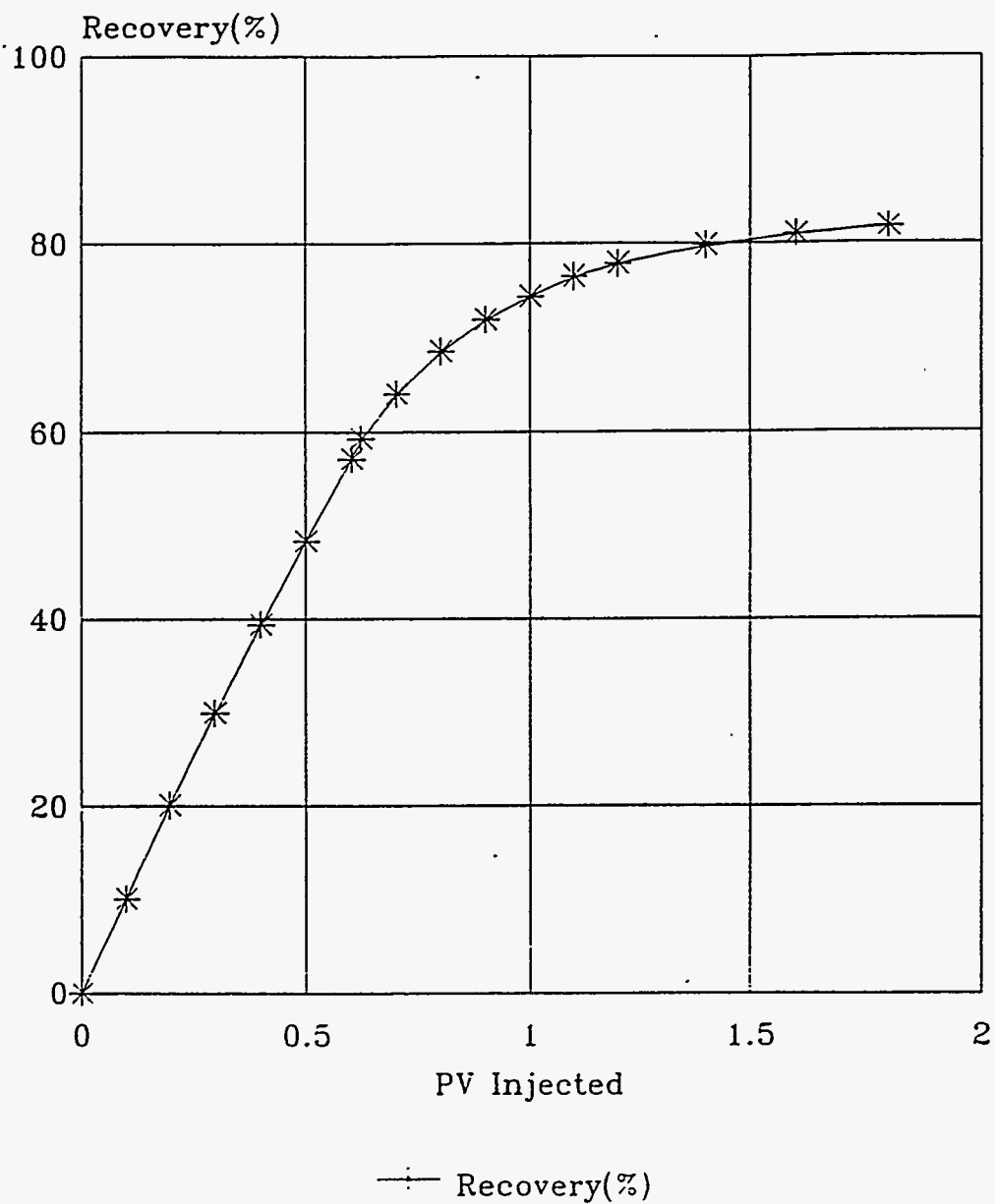
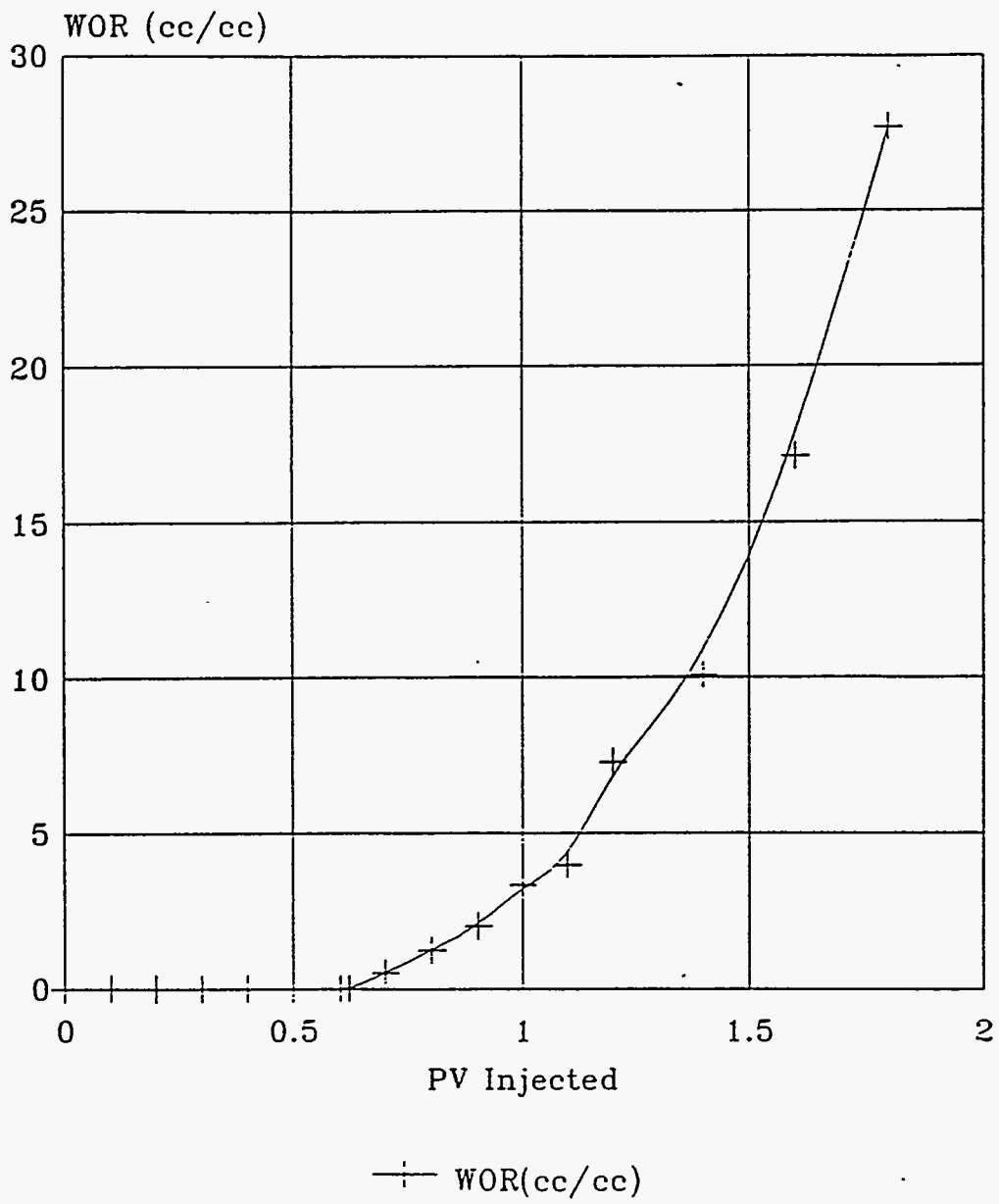


Figure 4.14 Pressure Drop vs. PV Injected, MCM Solvent Slug Size: 0.10 PV
(Solvent: 50% PBG/50% NGL)



**Figure 4.15 Oil Recovery vs. PV Injected, MCM Solvent Slug Size: 0.20 PV
(Solvent: 50% PBG/50% NGL)**



**Figure 4.16 WOR vs. PV Injected, MCM Solvent Slug Size: 0.20 PV
(Solvent: 50% PBG/50% NGL)**

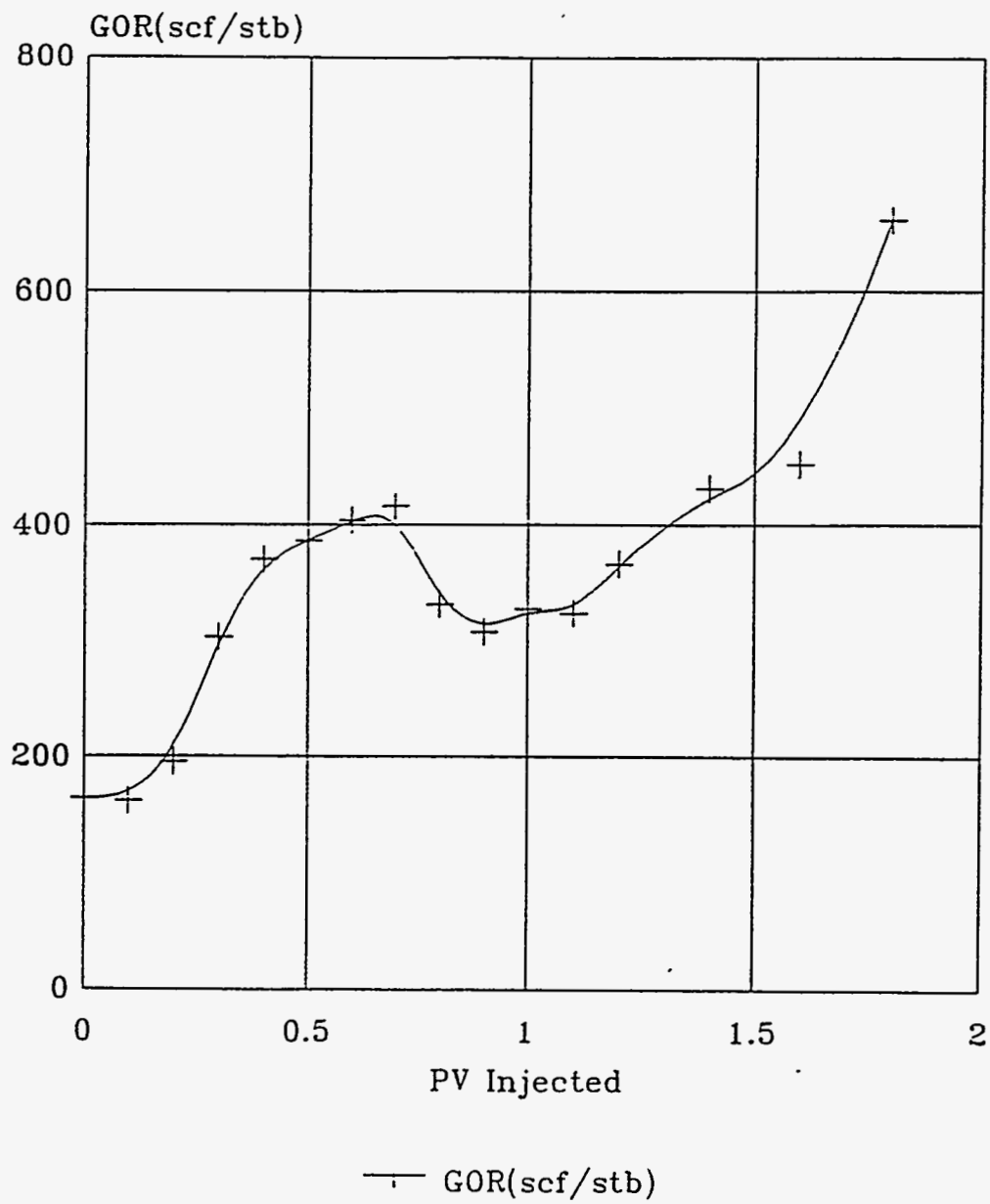


Figure 4.17 GOR vs. PV Injected, MCM Solvent Slug Size: 0.20 PV
 (Solvent: 50% PBG/50% NGL)

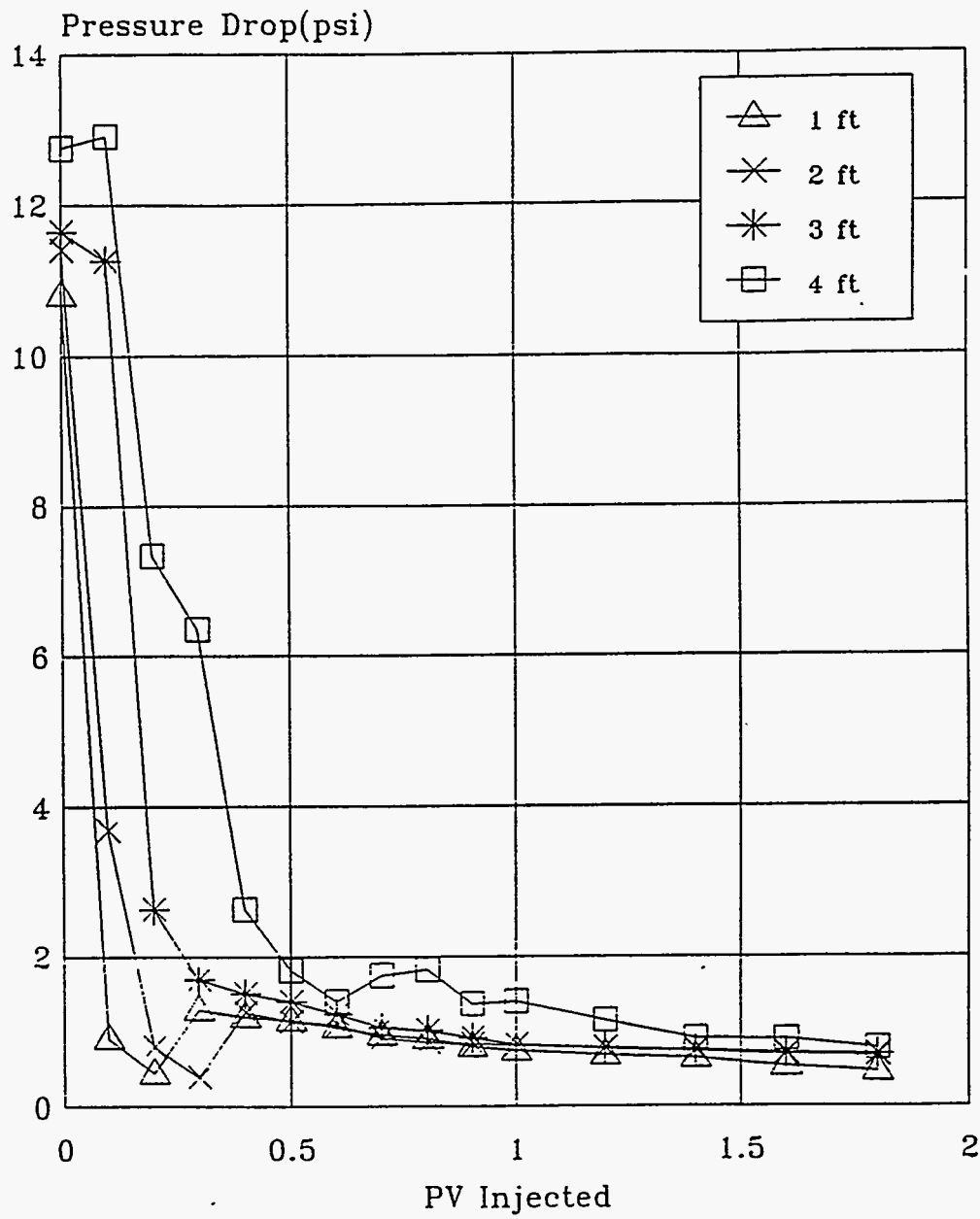


Figure 4.18 Pressure Drop vs. PV Injected, MCM Solvent Slug Size: 0.20 PV
(Solvent: 50% PBG/50% NGL)

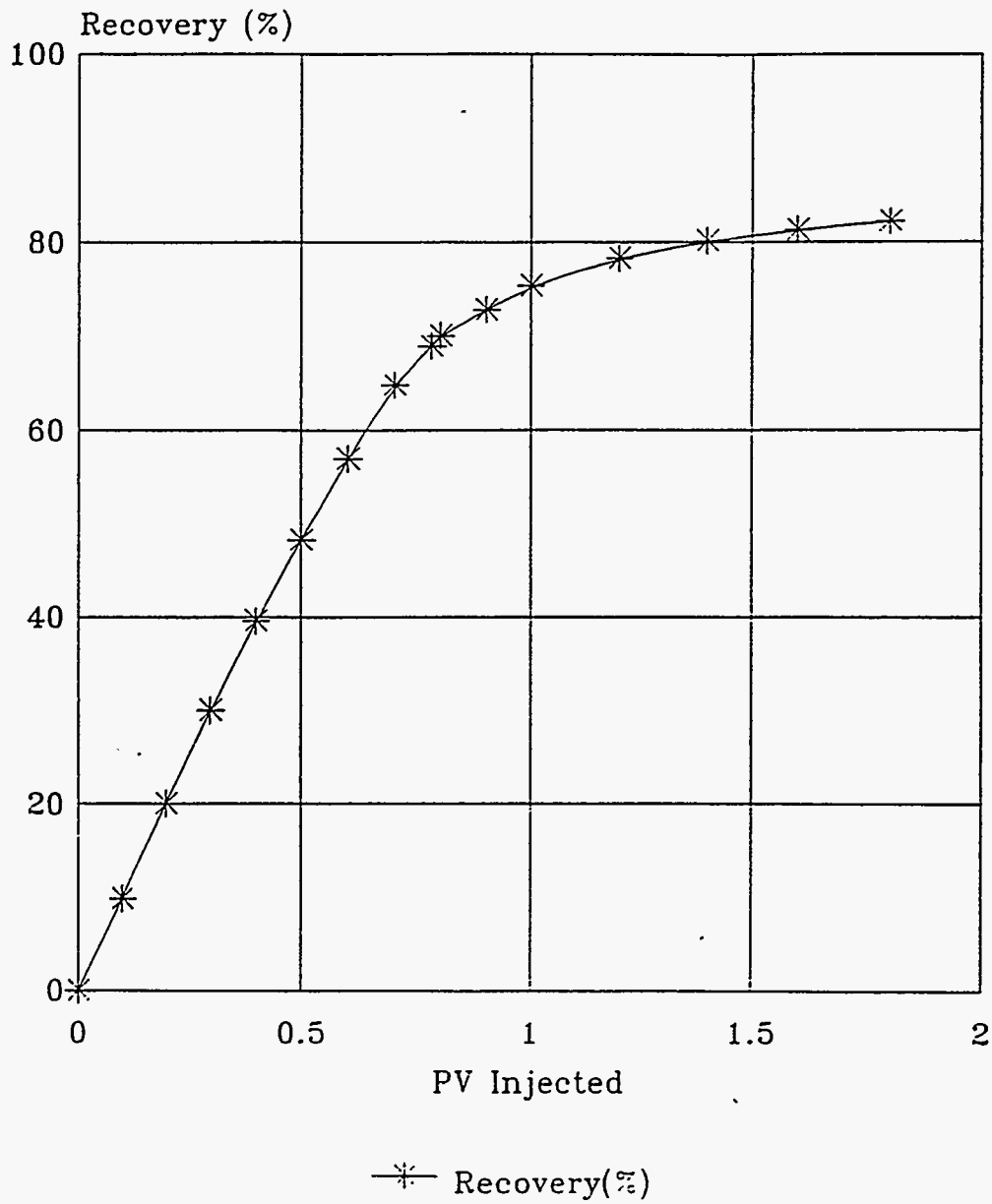
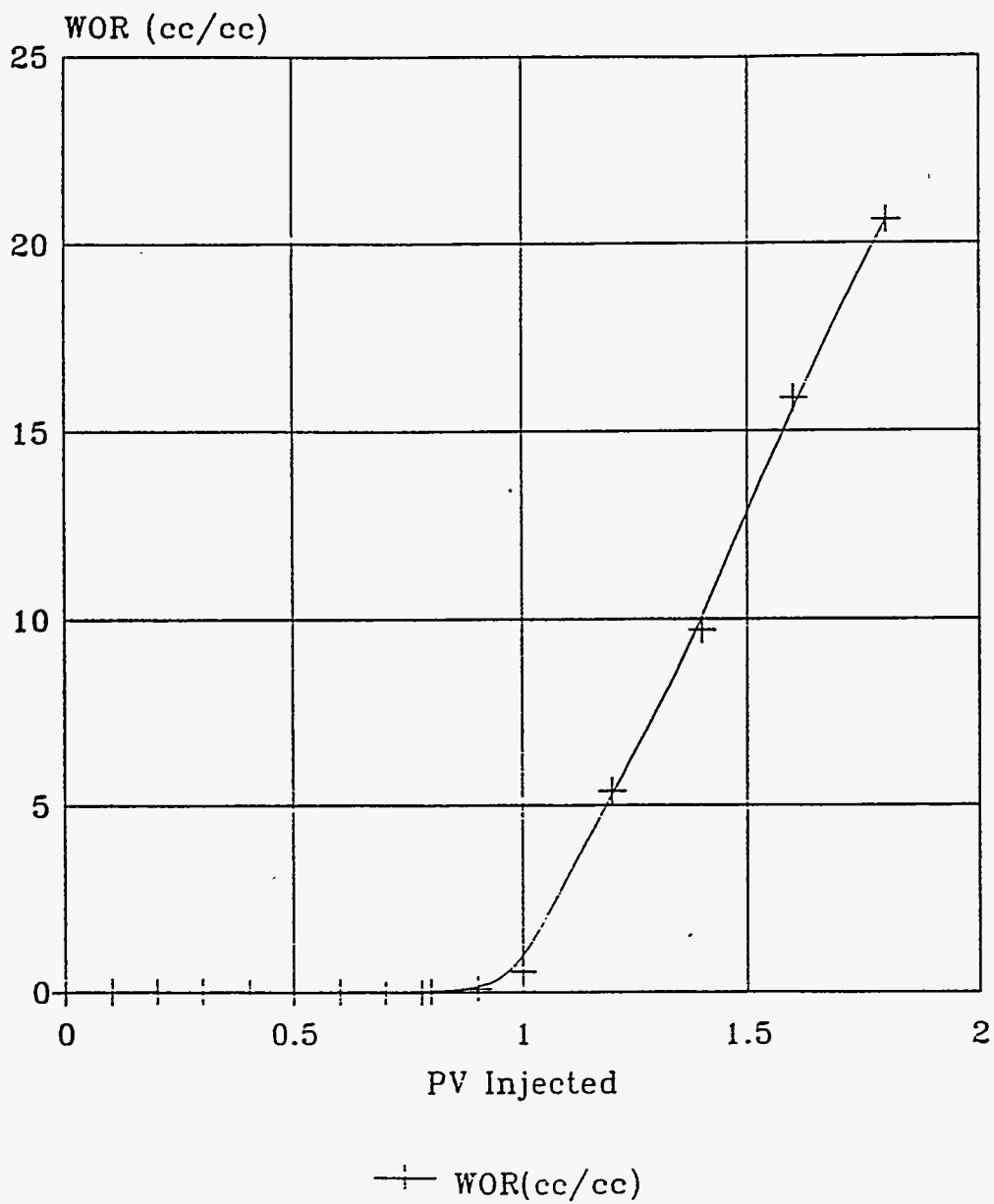


Figure 4.19 Oil Recovery vs. PV Injected, MCM Solvent Slug Size: 0.40 PV
(Solvent: 50% PBG/50% NGL)



**Figure 4.20 WOR vs. PV Injected, MCM Solvent Slug Size: 0.40 PV
(Solvent: 50% PBG/50% NGL)**

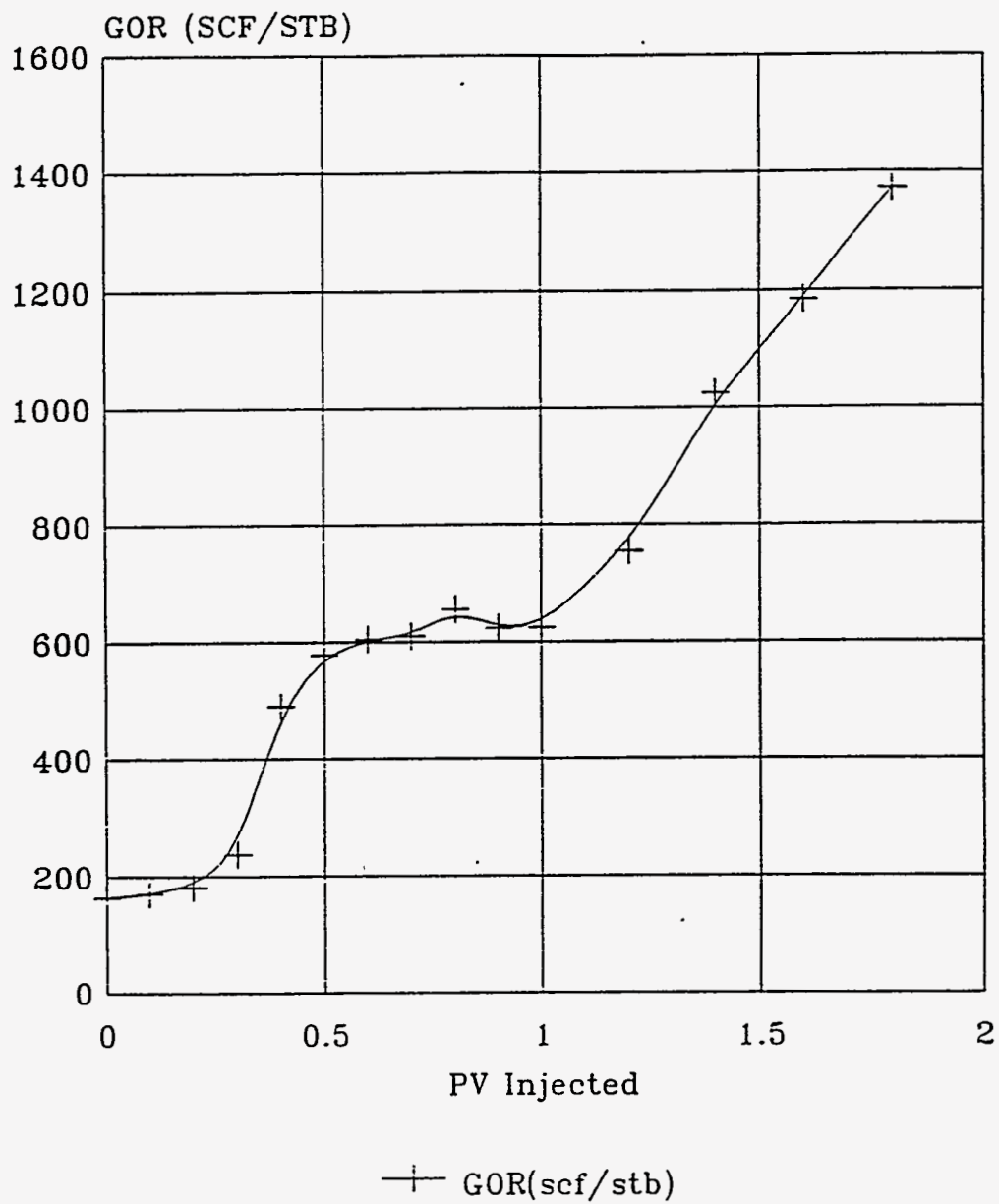


Figure 4.21 GOR vs. PV Injected, MCM Solvent Slug Size: 0.40 PV
 (Solvent: 50% PBG/50% NGL)

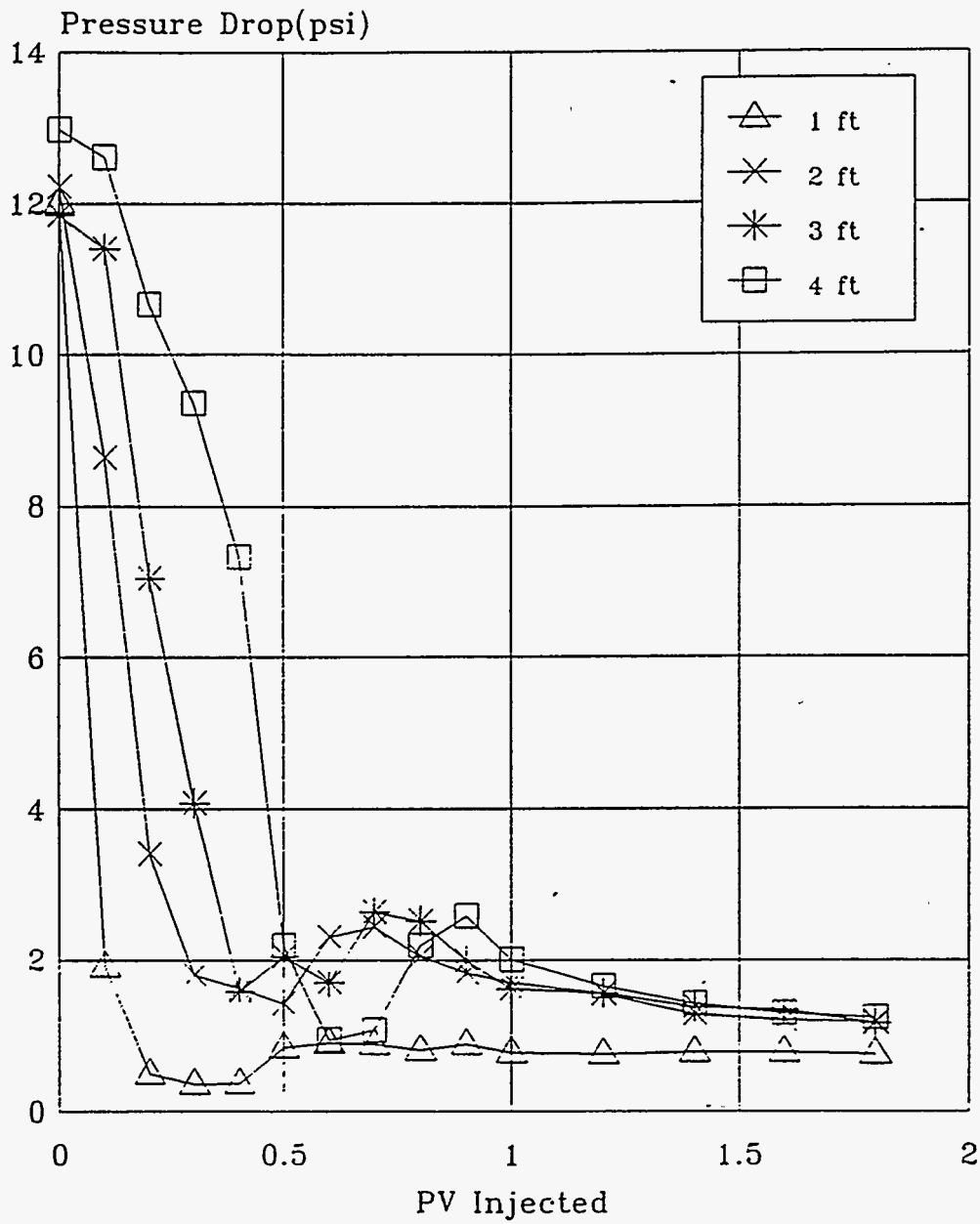
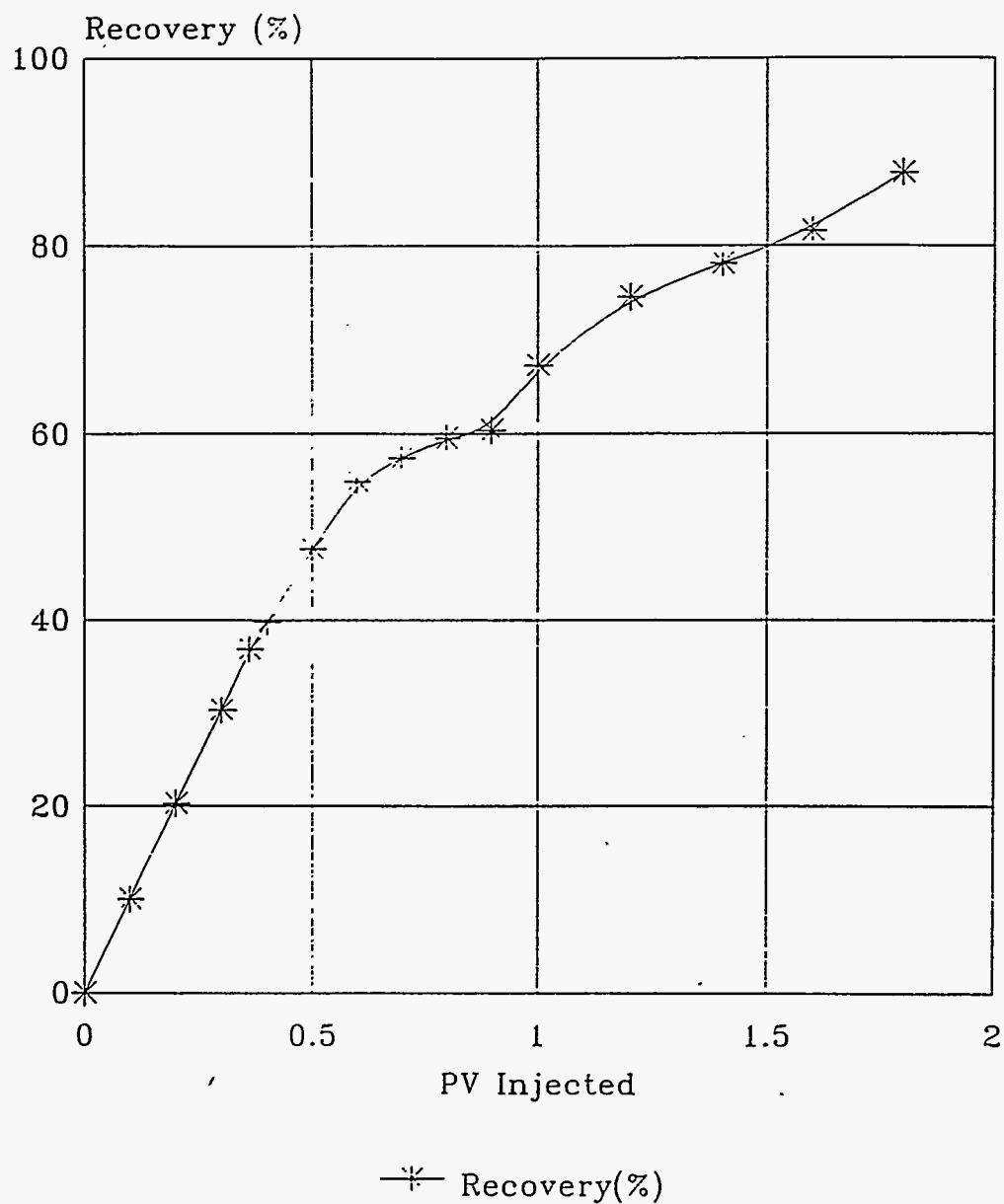


Figure 4.22 Pressure Drop vs. PV Injected, MCM Solvent Slug Size: 0.40 PV
(Solvent: 50% PBG/50% NGL)



**Figure 4.23 Oil Recovery vs. PV Injected, Multiple WAG, WAG Ratio: 11
(MCM Solvent: 50% PBG/50% NGL)**

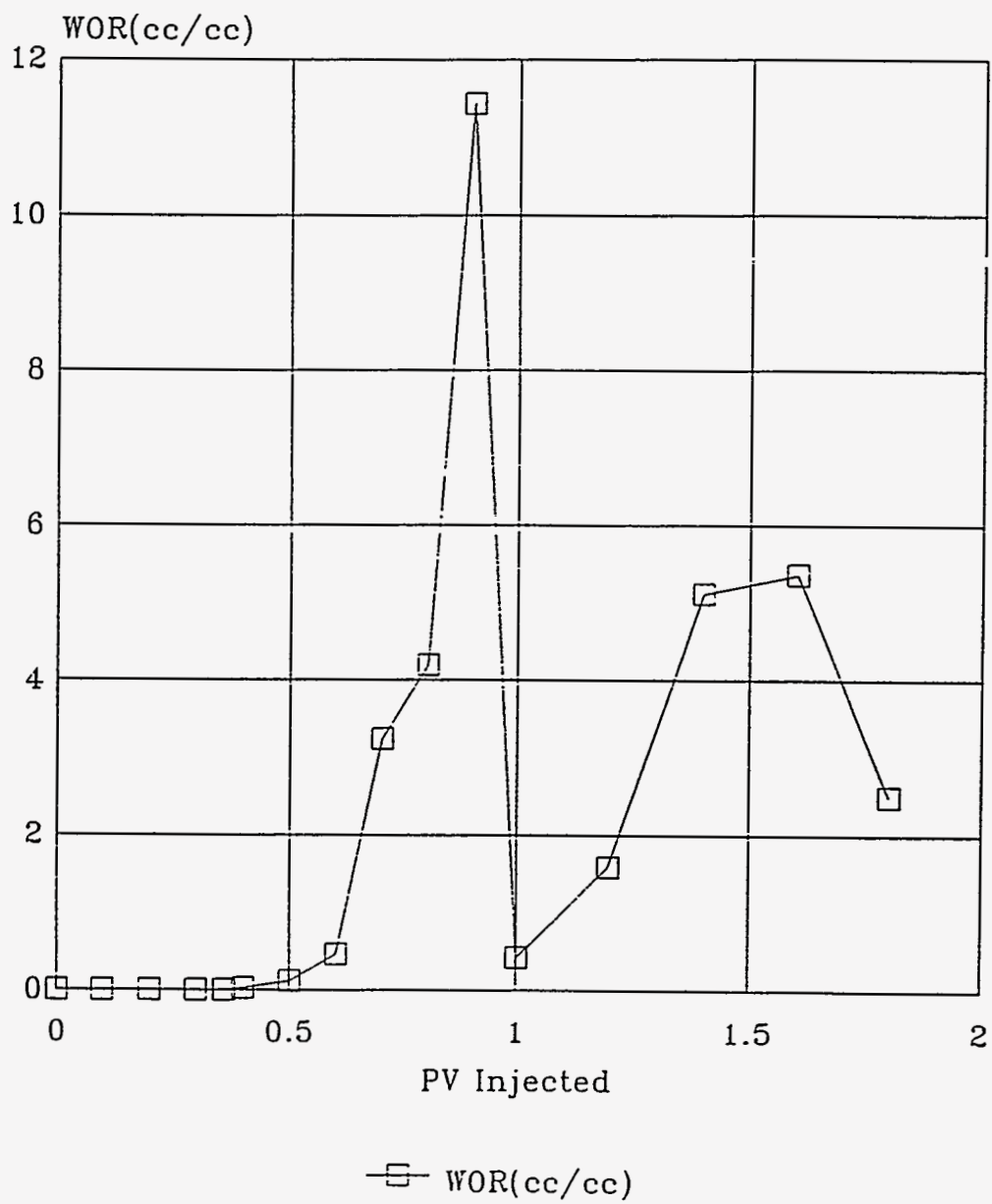
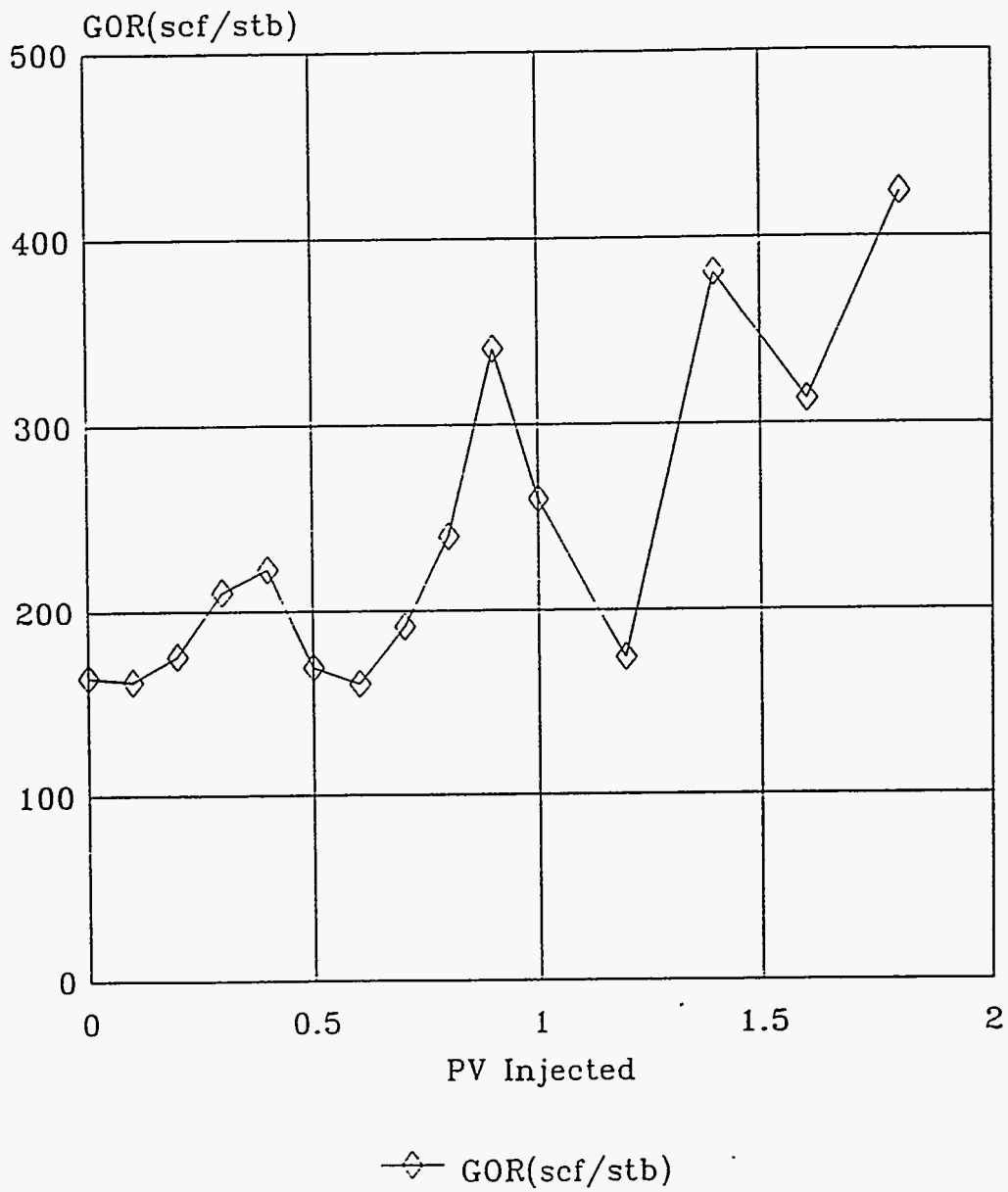


Figure 4.24 WOR vs. PV Injected, Multiple WAG, WAG Ratio: 11
(MCM Solvent: 50% PBG/50% NGL)



**Figure 4.25 GOR vs. PV Injected, Multiple WAG, WAG Ratio: 11
(MCM Solvent: 50% PBG/50% NGL)**

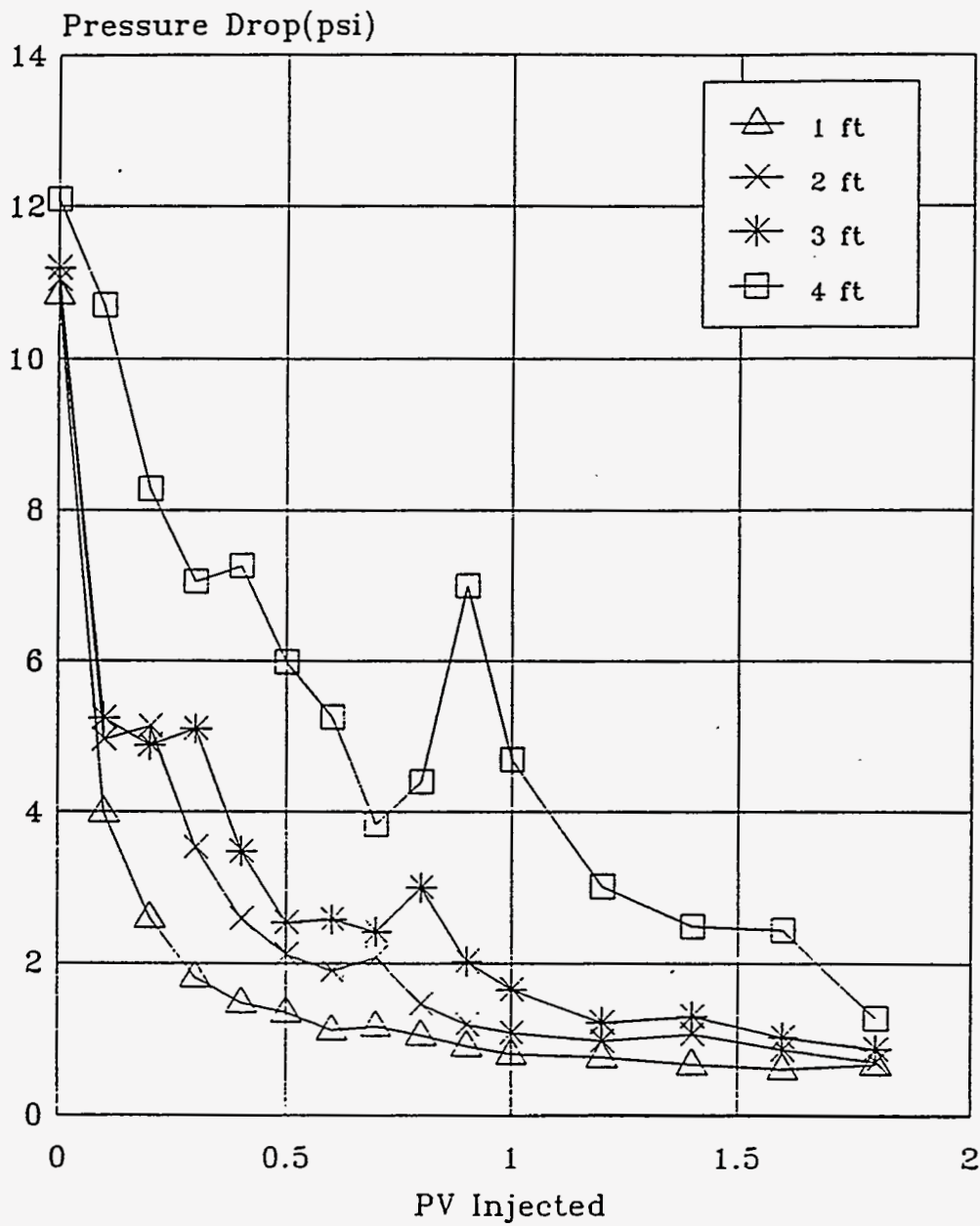
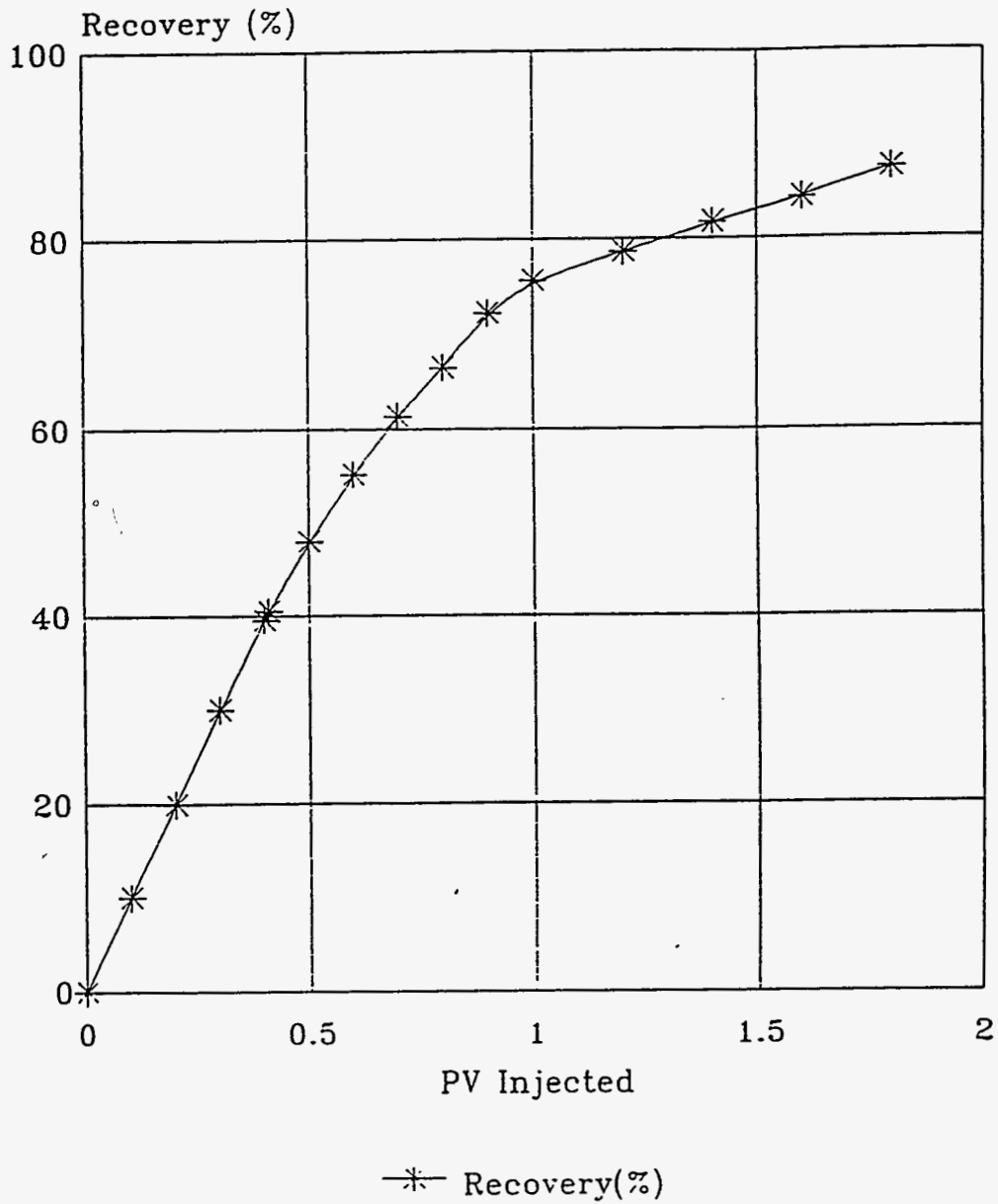


Figure 4.26 Pressure Drop vs. PV Injected, Multiple WAG, WAG Ratio: 11
 (MCM Solvent: 50% PBG/50% NGL)



**Figure 4.27 Oil Recovery vs. PV Injected, Multiple WAG, WAG Ratio: 5
(MCM Solvent: 50% PBG/50% NGL)**

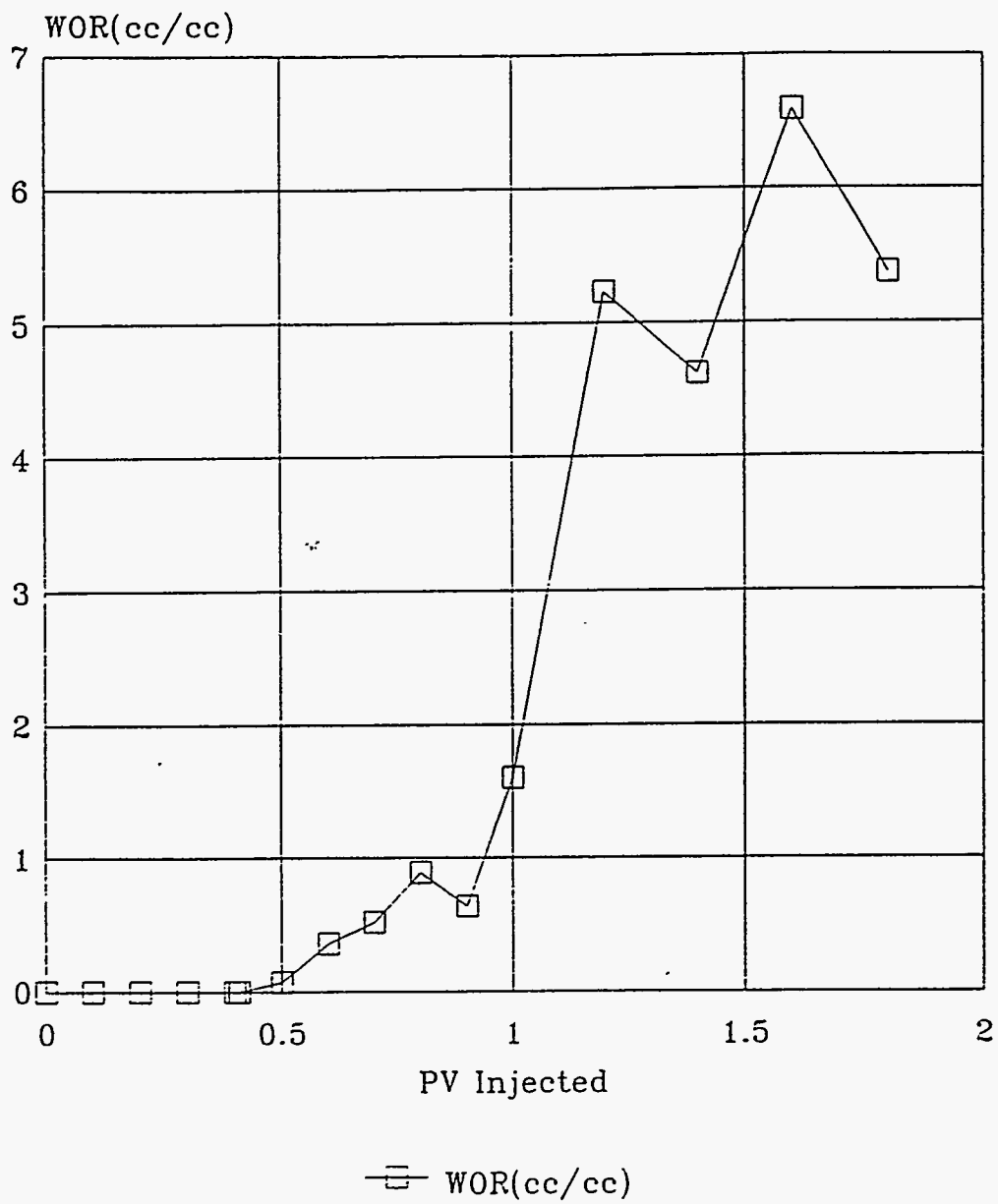


Figure 4.28 WOR vs. PV Injected, Multiple WAG, WAG Ratio: 5
 (MCM Solvent: 50% PBG/50% NGL)

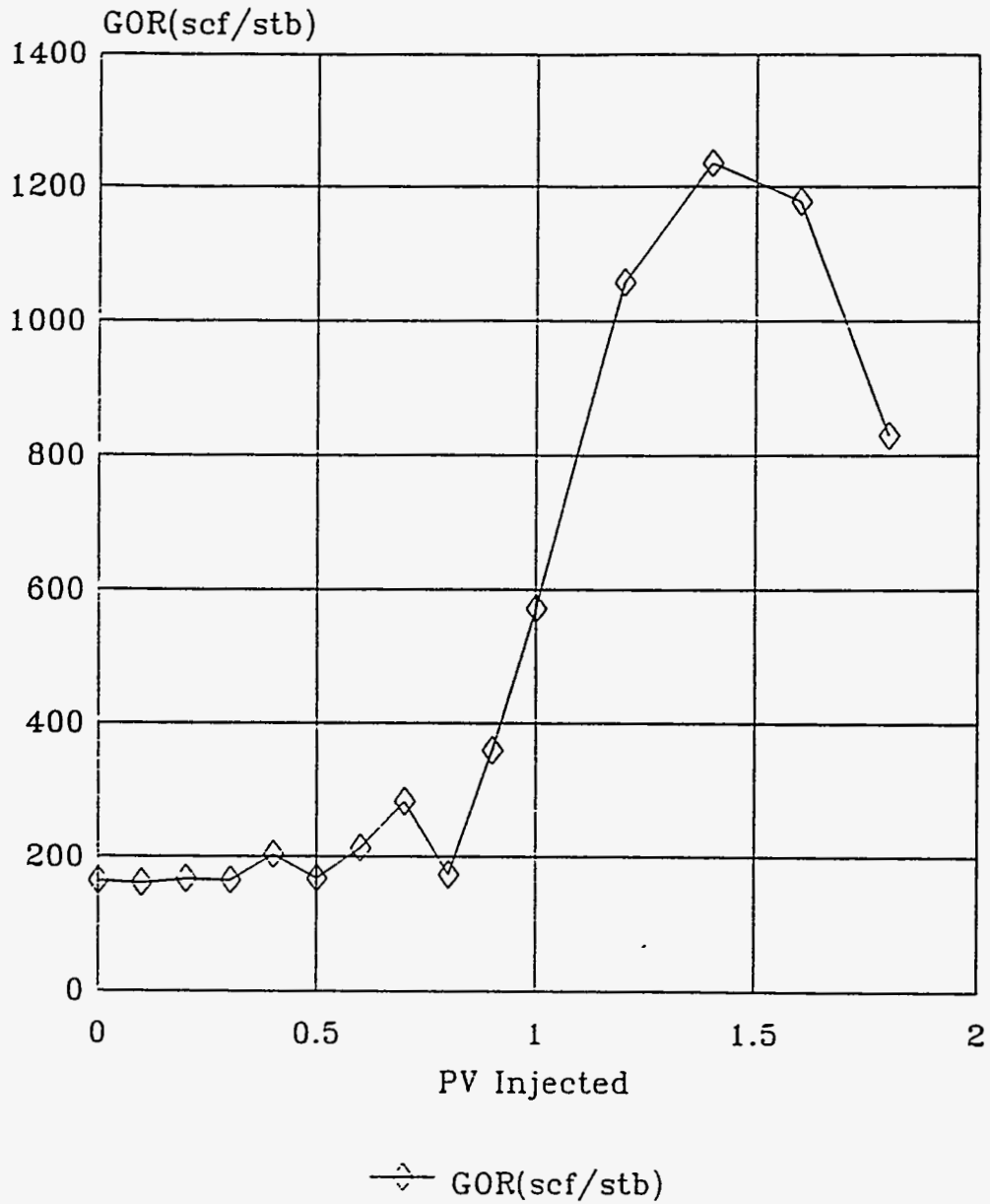
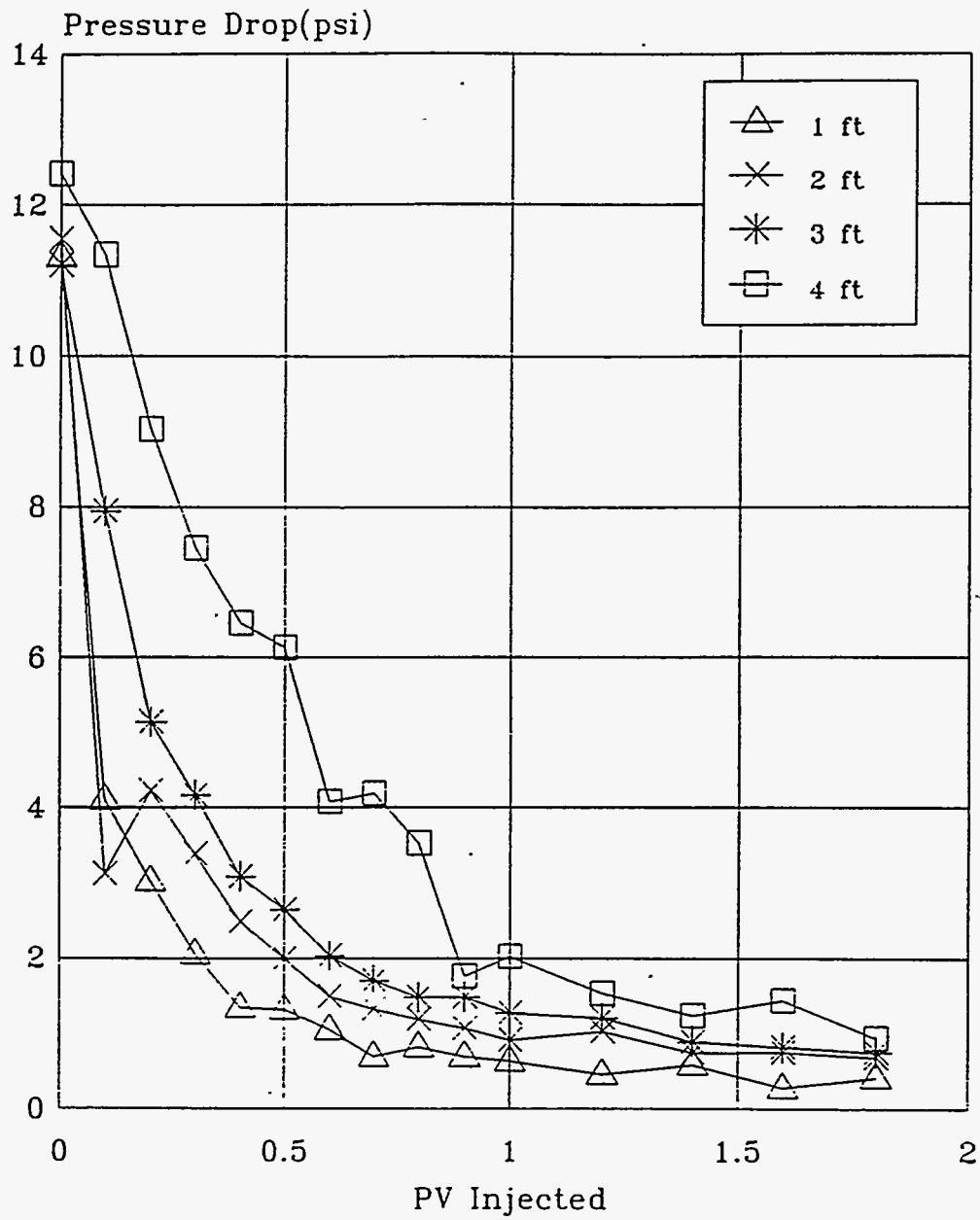
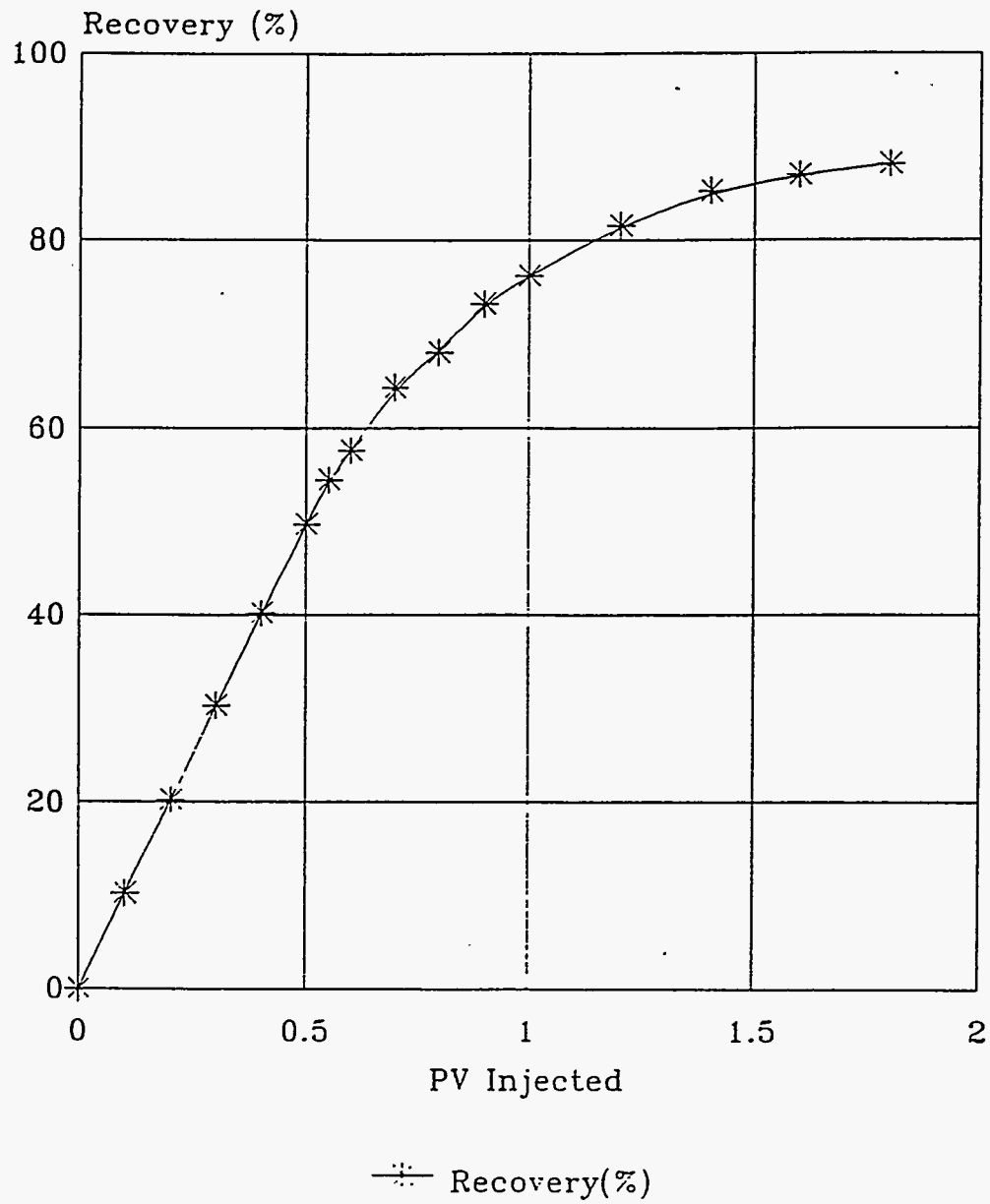


Figure 4.29 GOR vs. PV Injected, Multiple WAG, WAG Ratio: 5-
 (MCM Solvent: 50% PBG/50% NGL)



**Figure 4.30 Pressure Drop vs. PV Injected, Multiple WAG, WAG Ratio: 5
(MCM Solvent: 50% PBG/50% NGL)**



**Figure 4.31 Oil Recovery vs. PV Injected, Multiple WAG, WAG Ratio: 3
(MCM Solvent: 50% PBG/50% NGL)**

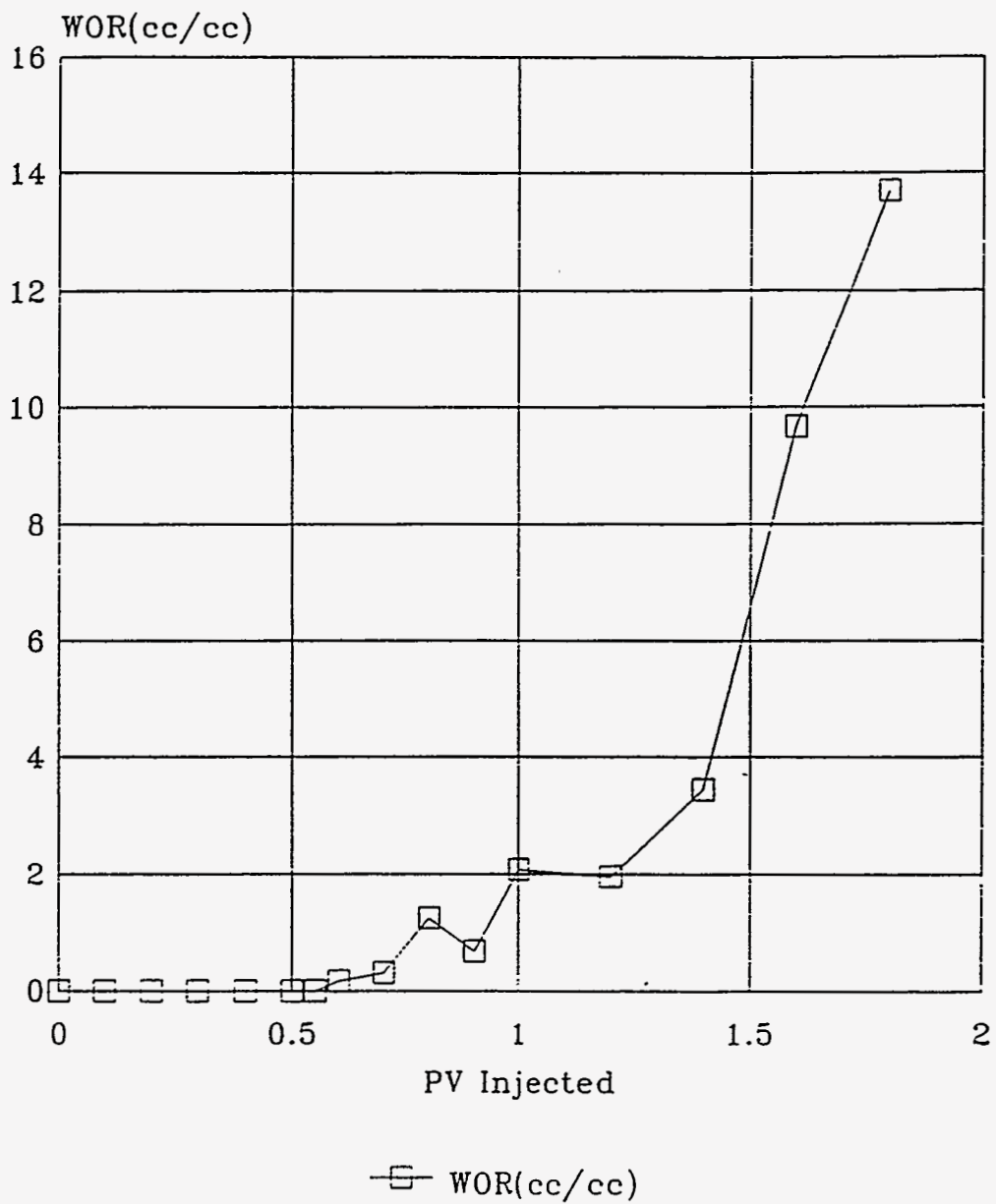
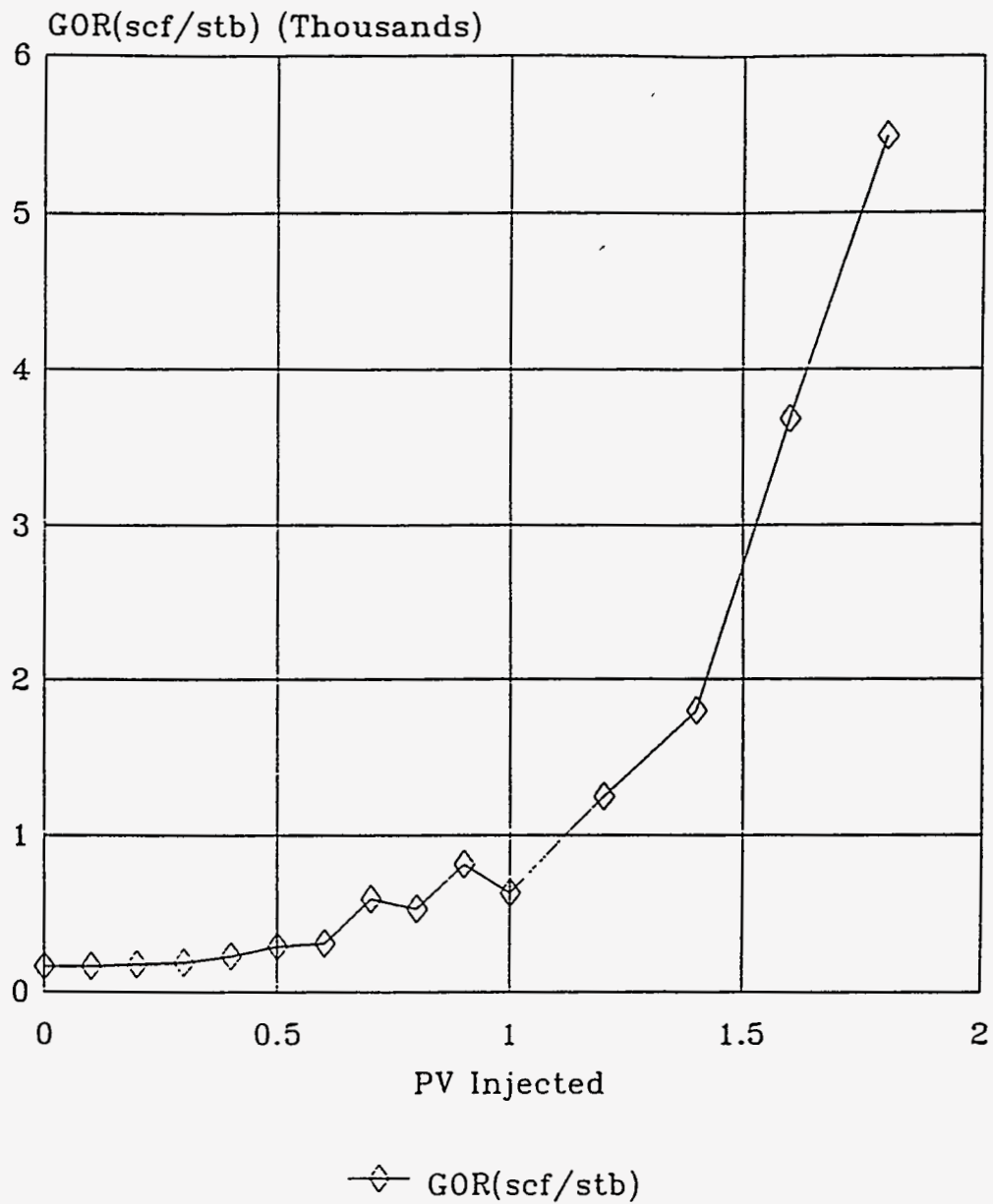


Figure 4.32 WOR vs. PV Injected, Multiple WAG, WAG Ratio: 3
(MCM Solvent: 50% PBG/50% NGL)



**Figure 4.33 GOR vs. PV Injected, Multiple WAG, WAG Ratio: 3
(MCM Solvent: 50% PBG/50% NGL)**

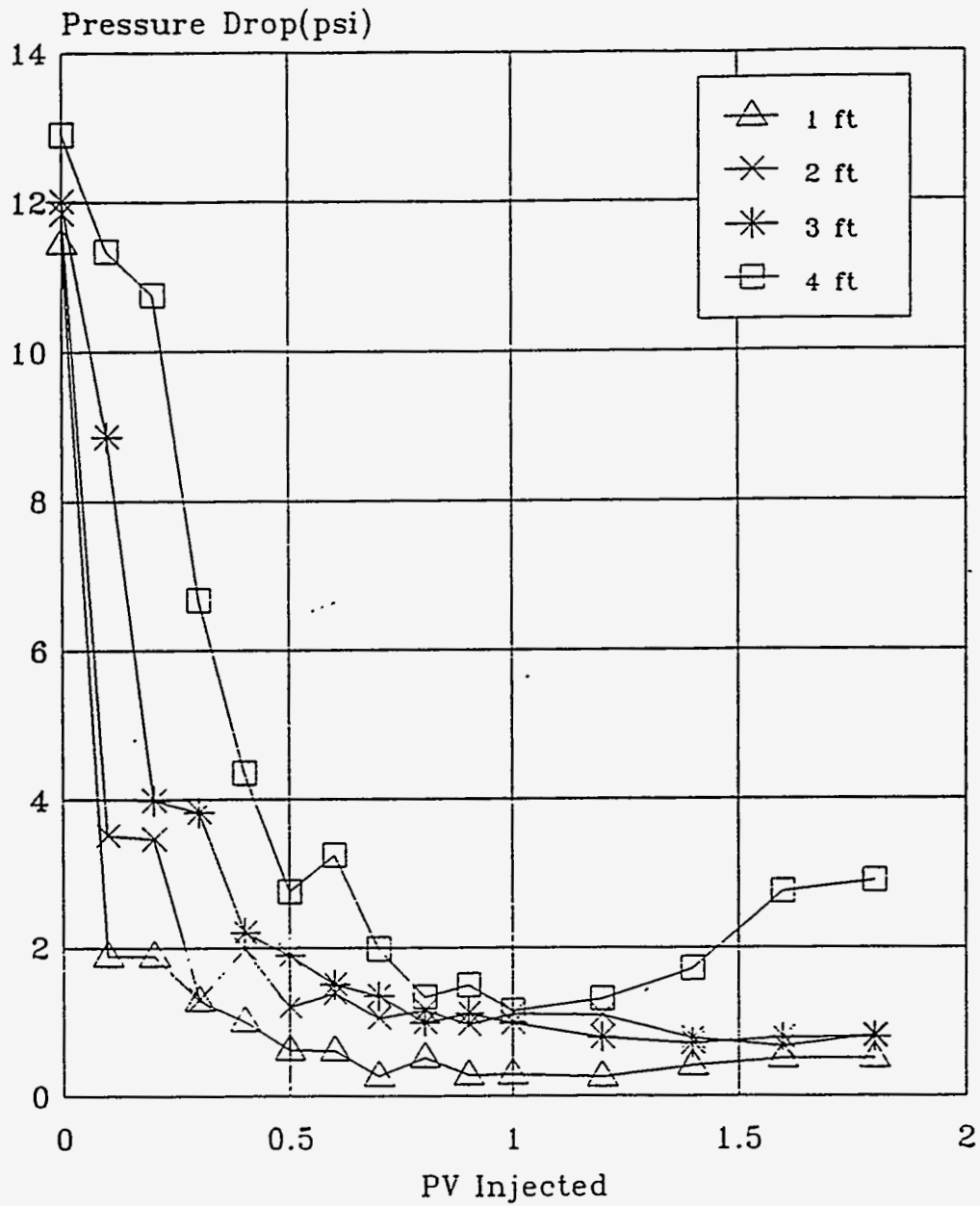
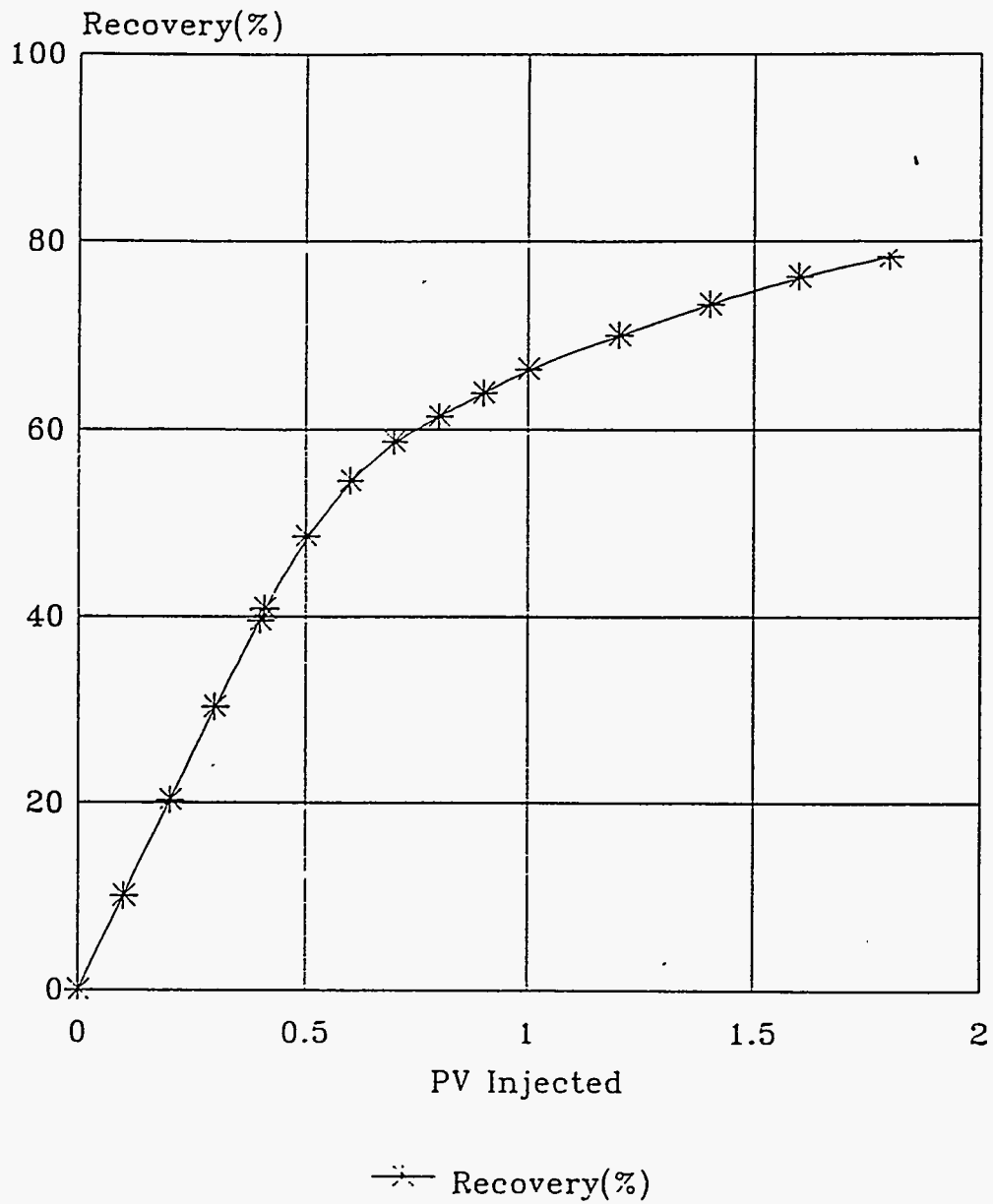


Figure 4.34 Pressure Drop vs. PV Injected, Multiple WAG, WAG Ratio: 3
(MCM Solvent: 50% PBG/50% NGL)



**Figure 4.35 Oil Recovery vs. PV Injected, FCM Solvent Slug Size: 0.05 PV
(Solvent: Propane)**

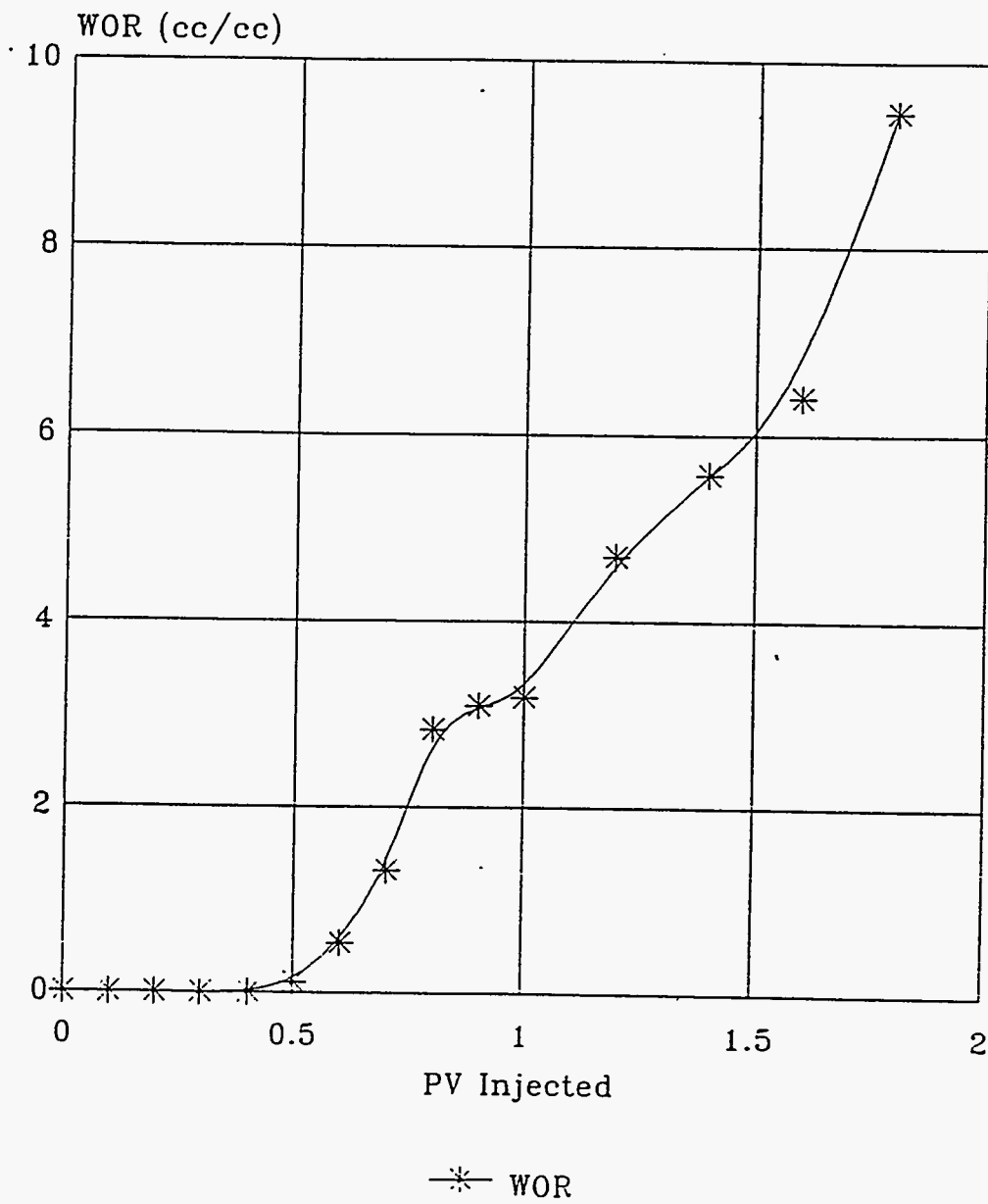


Figure 4.36 WOR vs. PV Injected, FCM Solvent Slug Size: 0.05 PV
(Solvent: Propane)

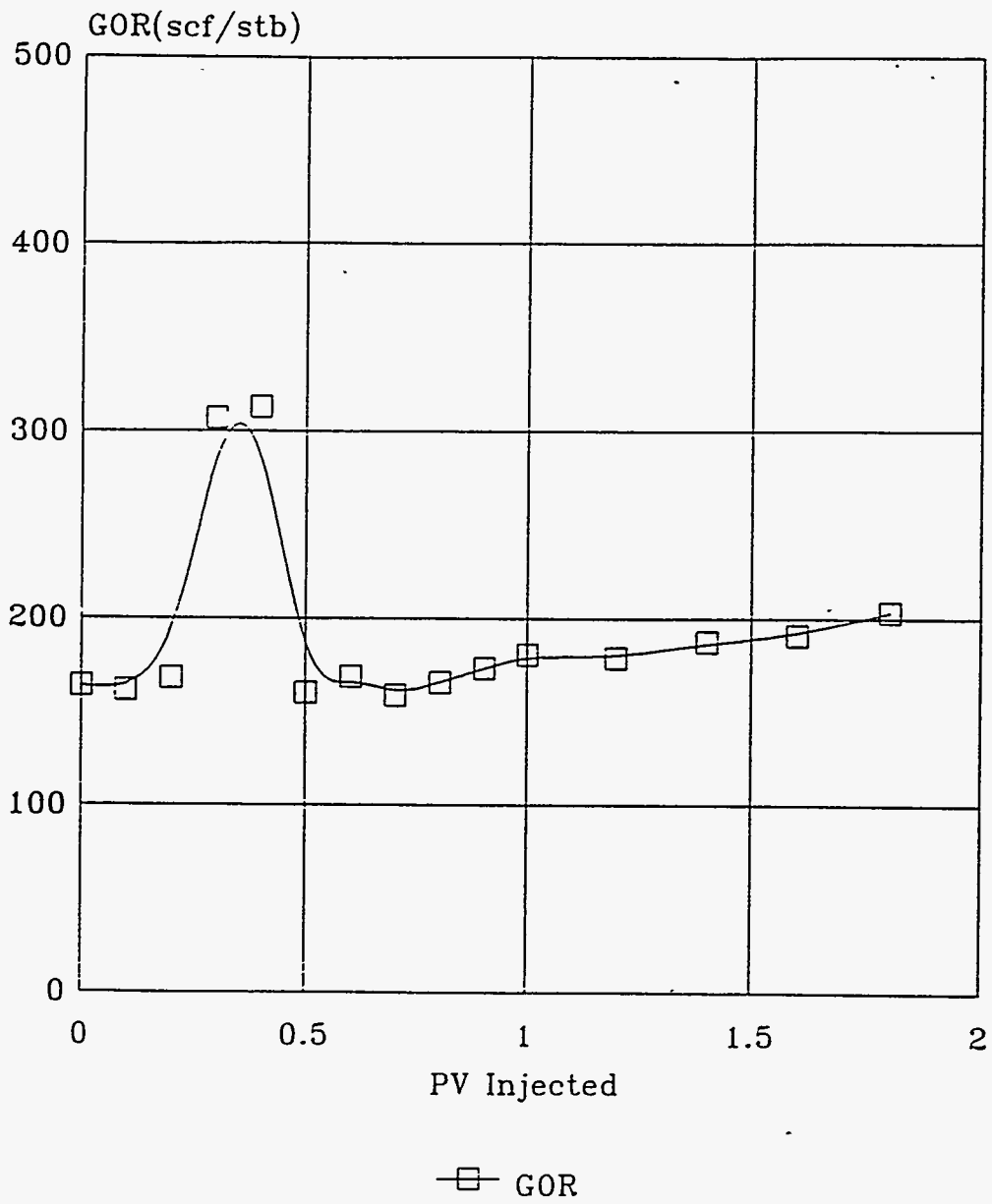


Figure 4.37 GOR vs. PV Injected, FCM Solvent Slug Size: 0.05 PV
(Solvent: Propane)

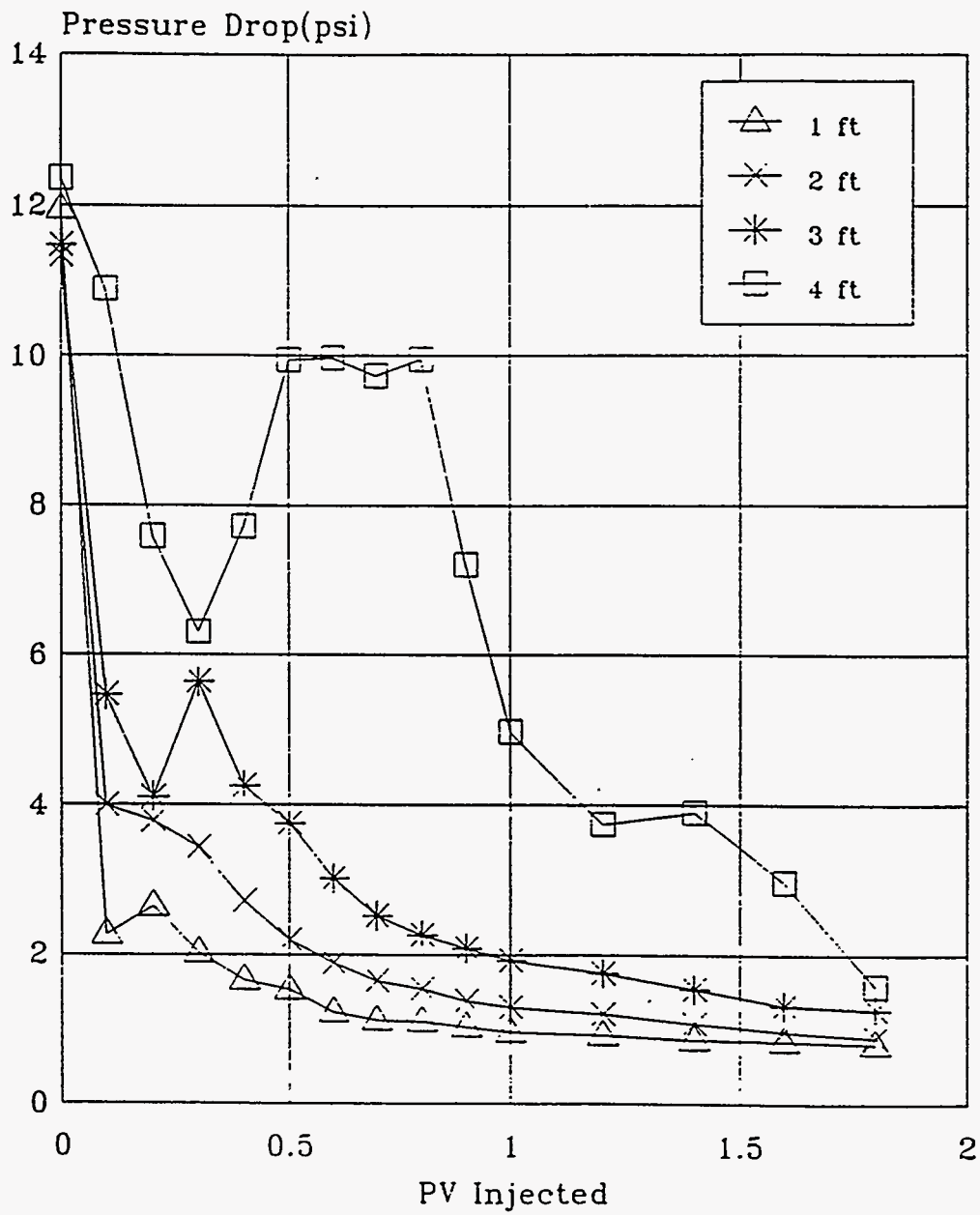
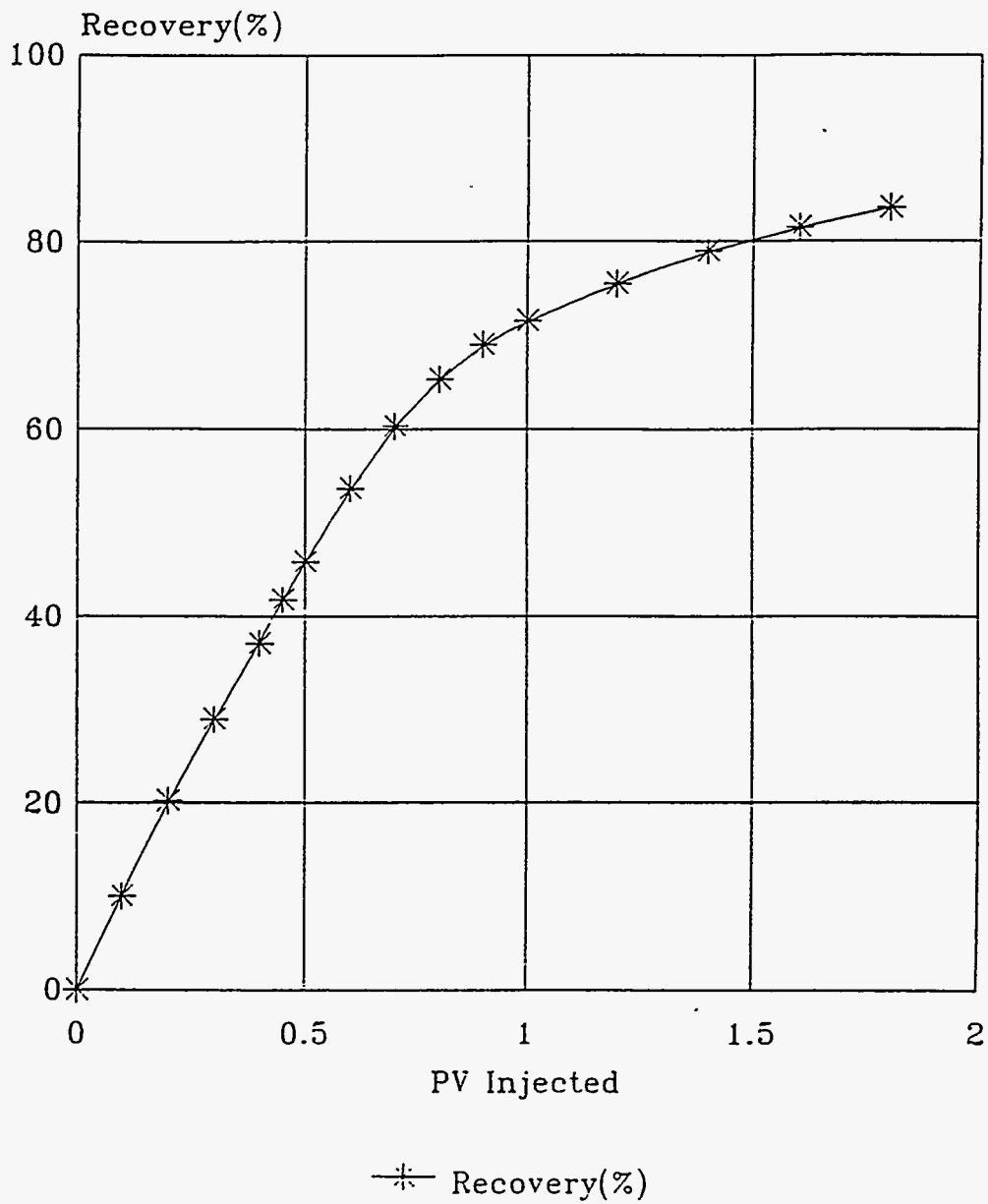


Figure 4.38 Pressure Drop vs. PV Injected, FCM Solvent Slug Size: 0.05 PV
(Solvent: Propane)



**Figure 4.39 Oil Recovery vs. PV Injected, FCM Solvent Slug Size: 0.10 PV
(Solvent: Propane)**

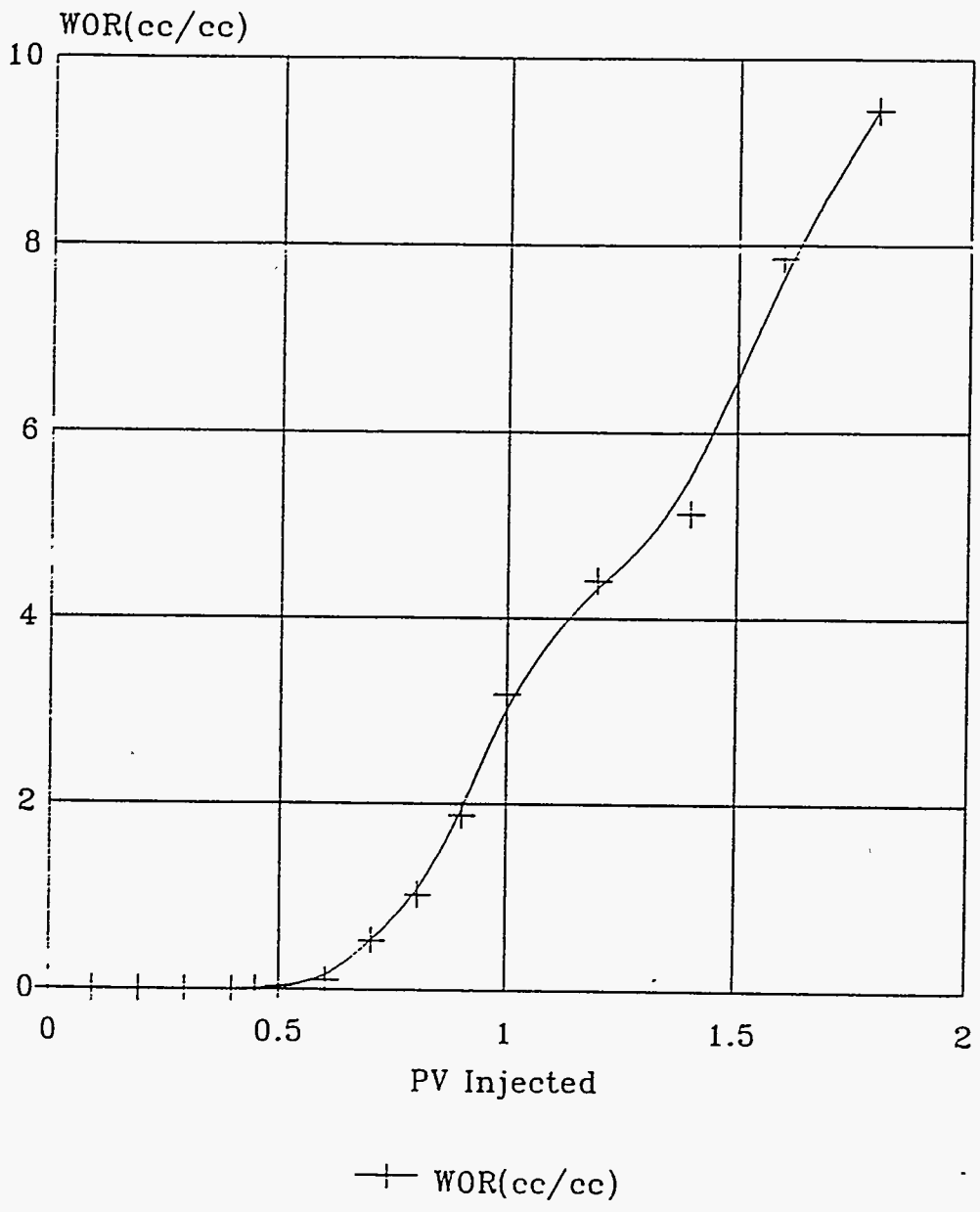


Figure 4.40 WOR vs. PV Injected, FCM Solvent Slug Size: 0.10 PV
(Solvent: Propane)

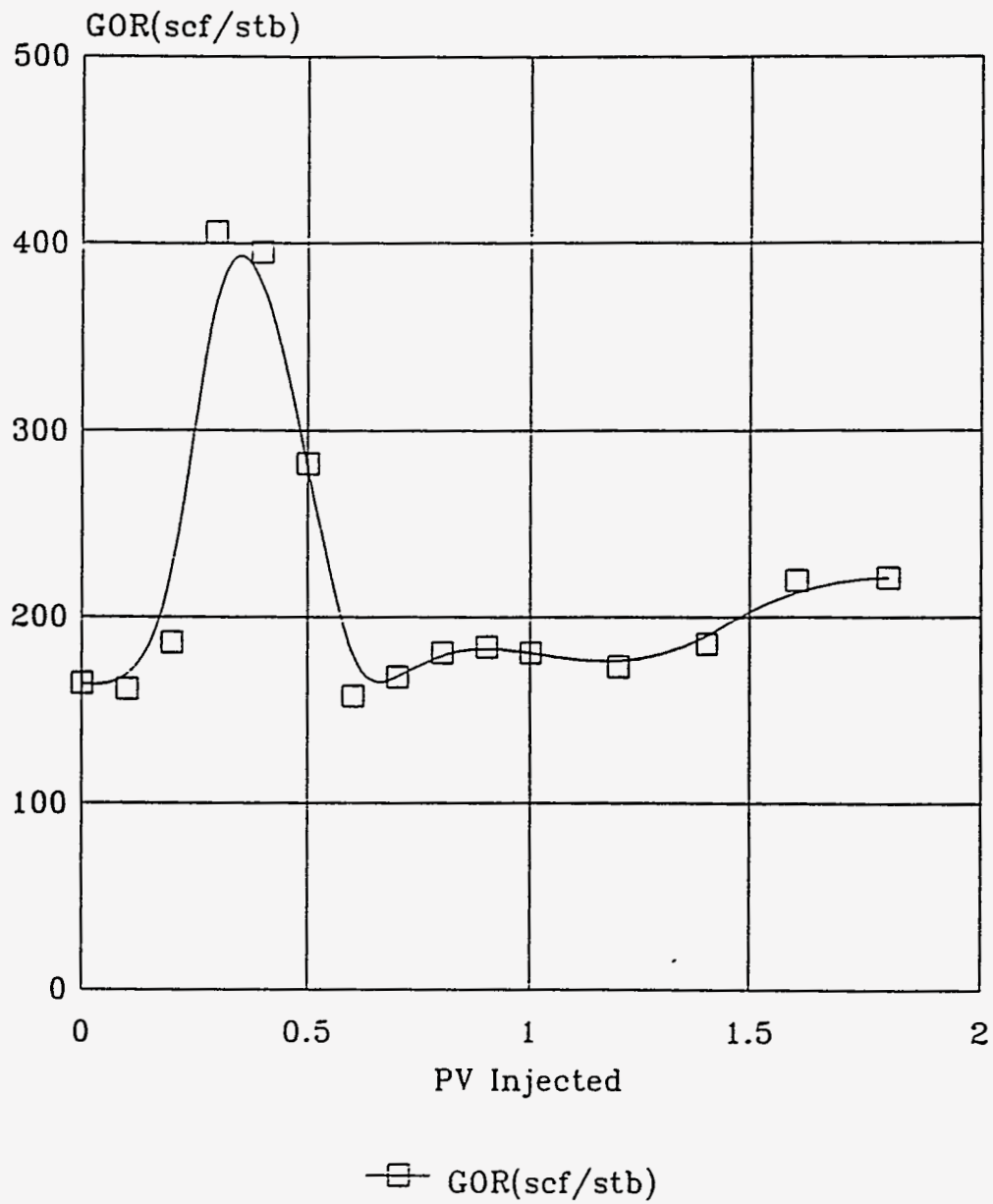


Figure 4.41 GOR vs. PV Injected, FCM Solvent Slug Size: 0.10 PV
(Solvent: Propane)

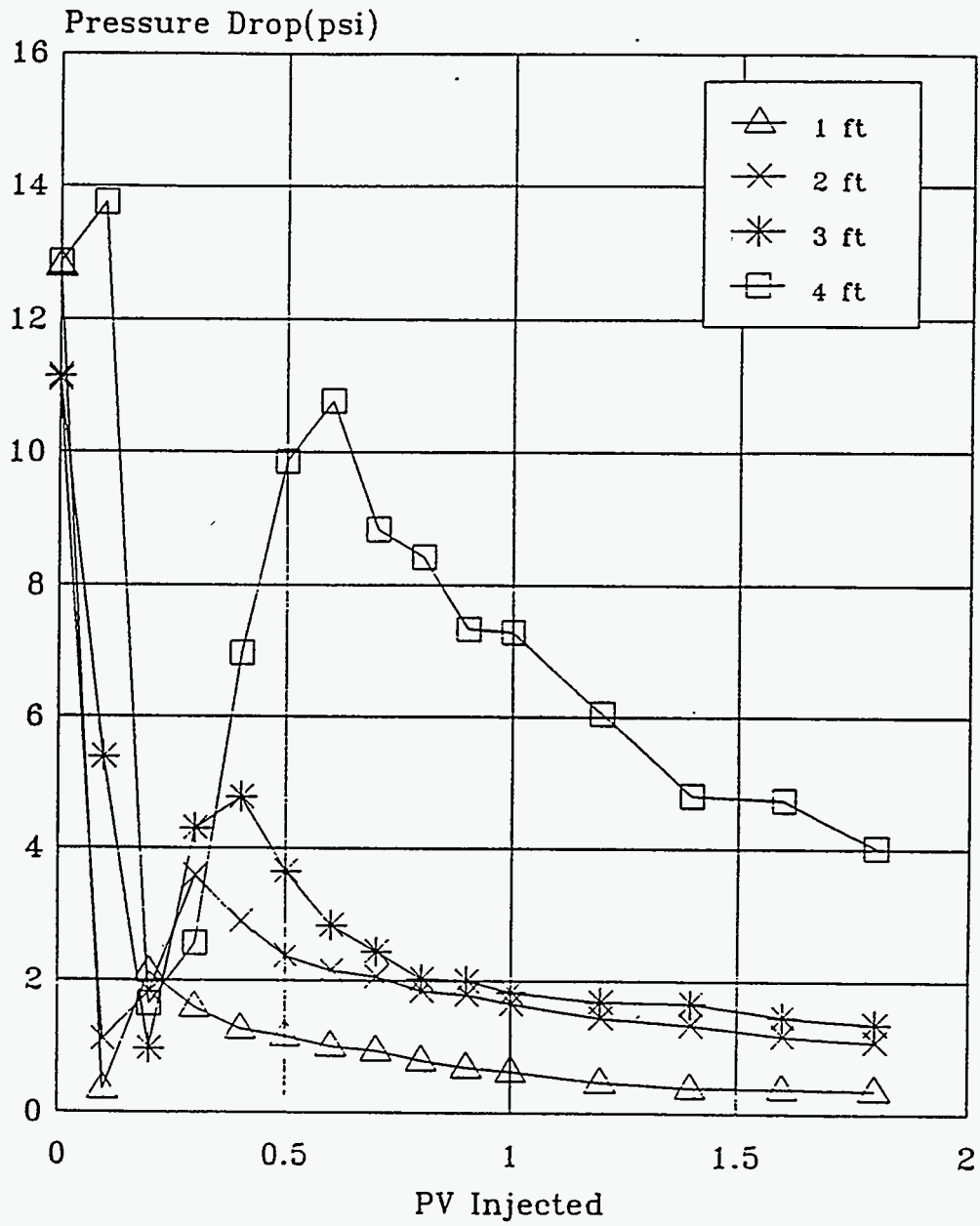
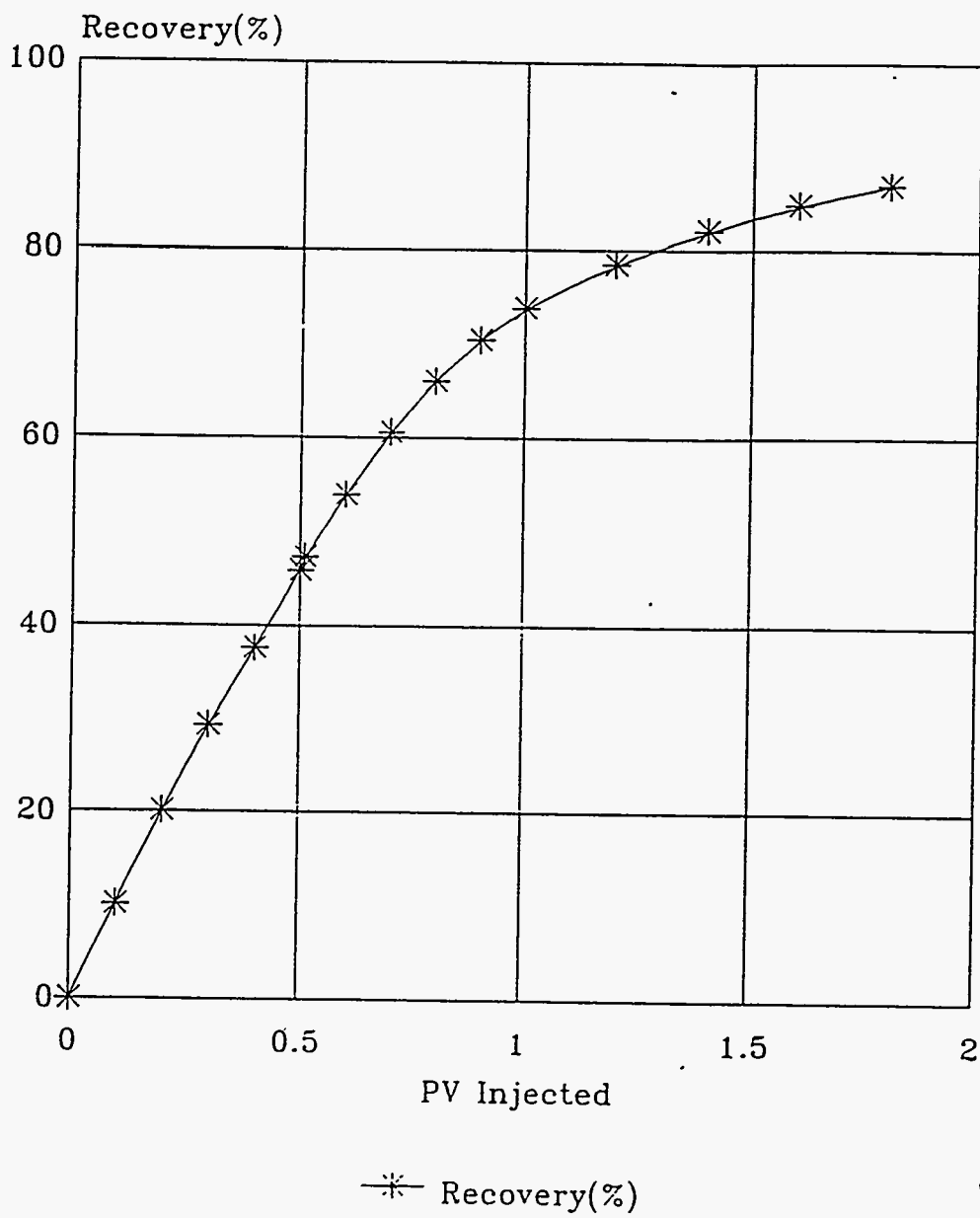
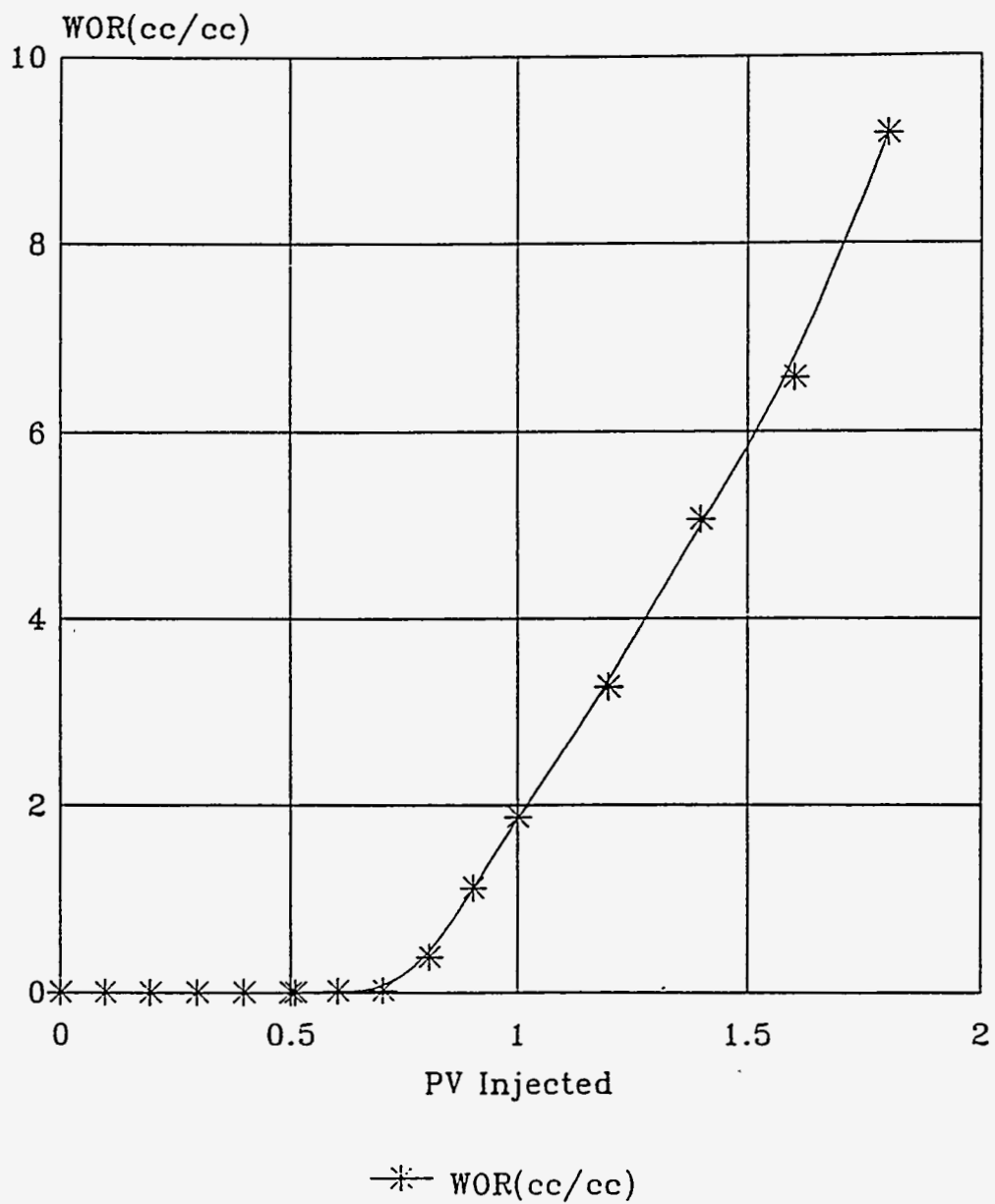


Figure 4.42 Pressure Drop vs. PV Injected, FCM Solvent Slug Size: 0.10 PV
(Solvent: Propane)



**Figure 4.43 Oil Recovery vs. PV Injected, FCM Solvent Slug Size: 0.20 PV
(Solvent: Propane)**



**Figure 4.44 WOR vs. PV Injected, FCM Solvent Slug Size: 0.20 PV
(Solvent: Propane)**

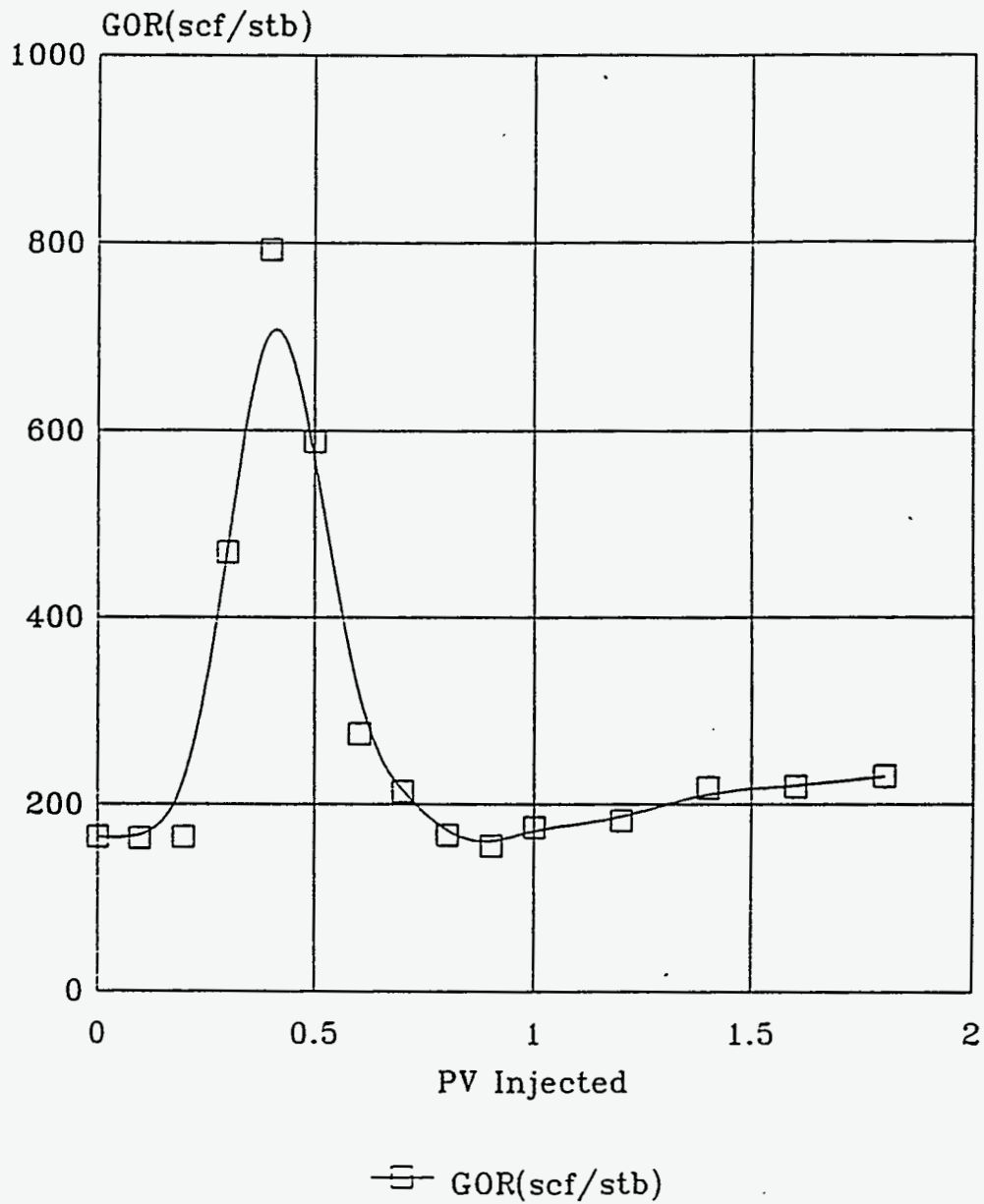


Figure 4.45 GOR vs. PV Injected, FCM Solvent Slug Size: 0.20 PV
(Solvent: Propane)

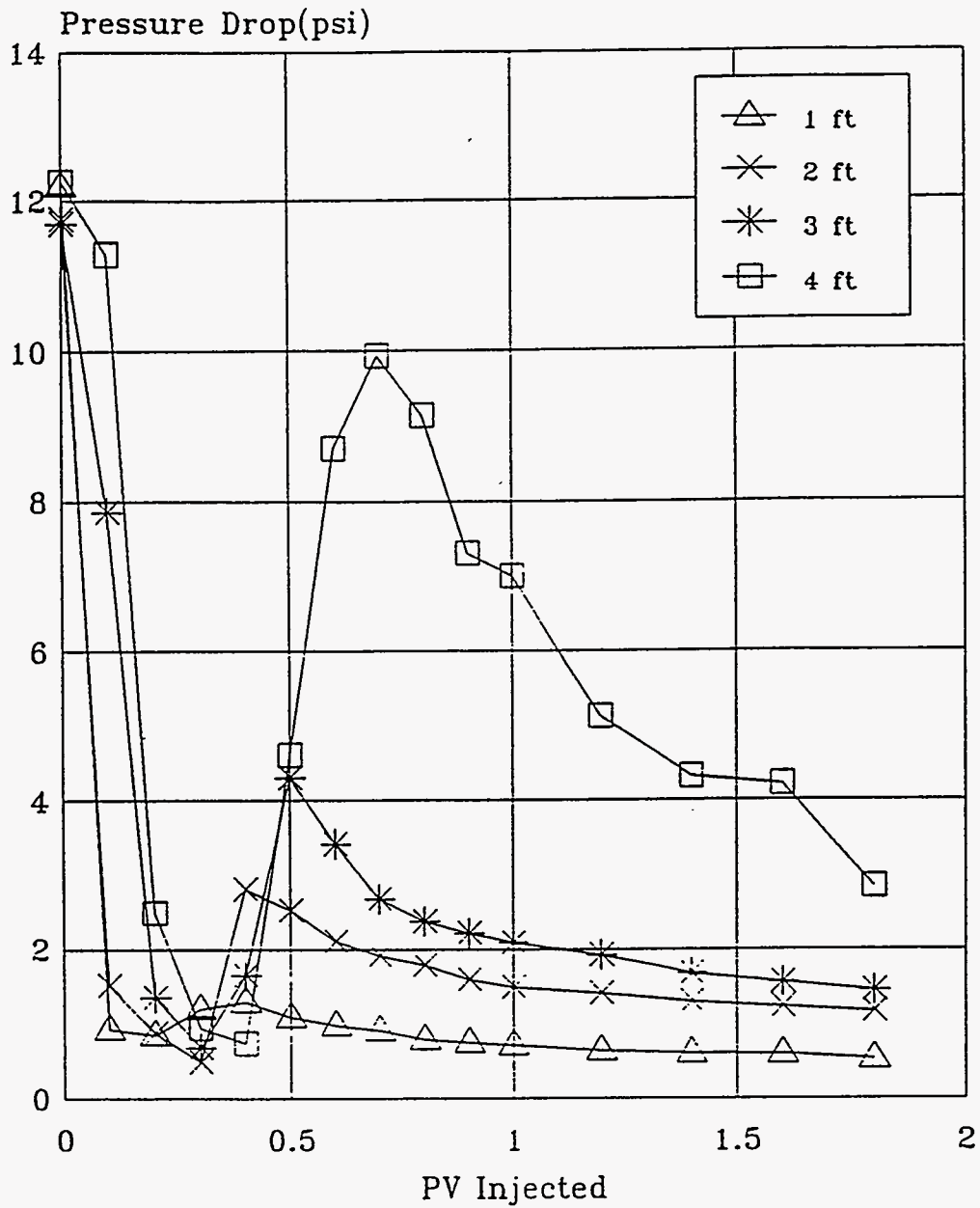


Figure 4.46 Pressure Drop vs. PV Injected, FCM Solvent Slug Size: 0.20 PV
(Solvent: Propane)

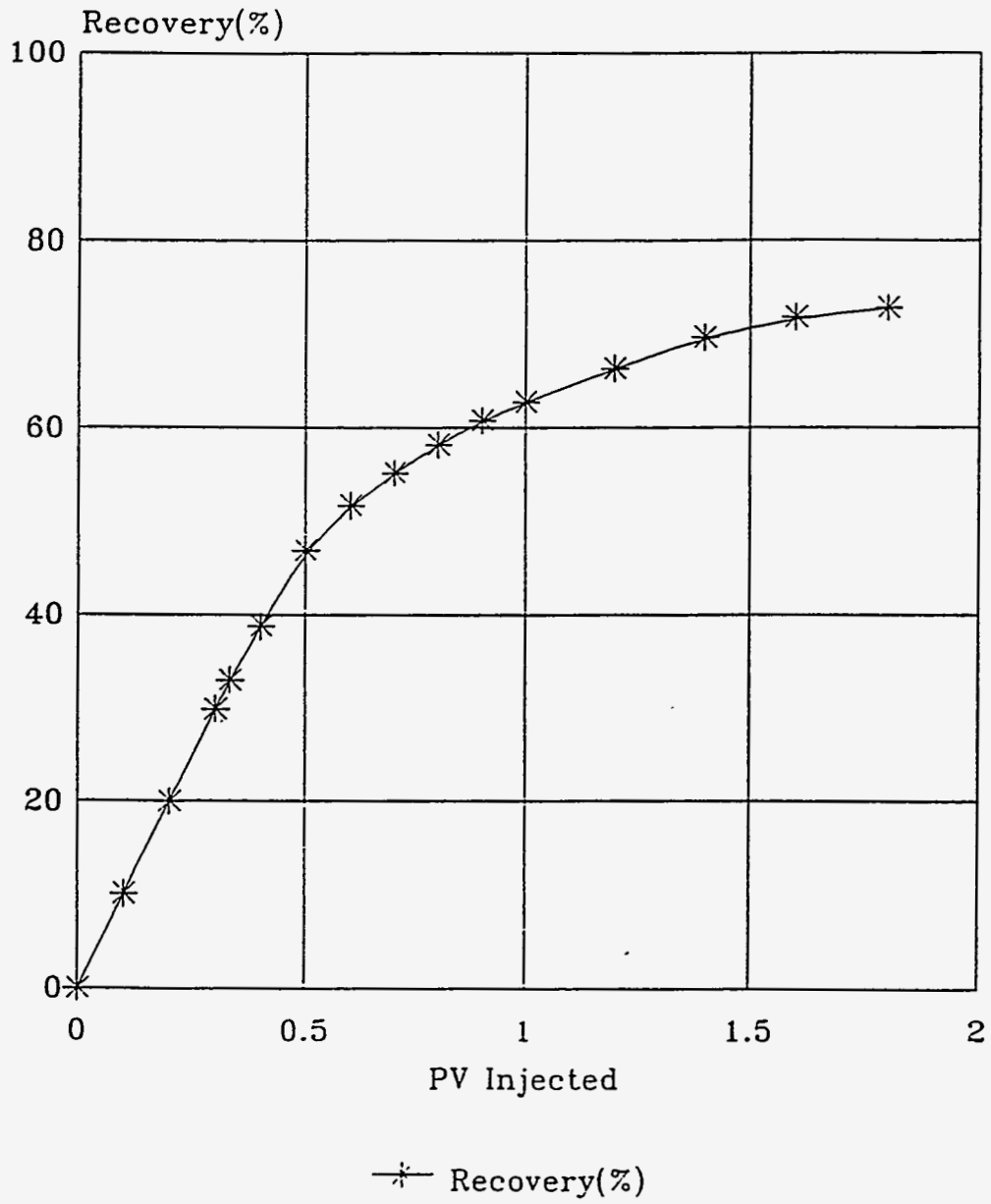


Figure 4.47 Oil Recovery vs. PV Injected (Solvent: Prudhoe Bay Gas)

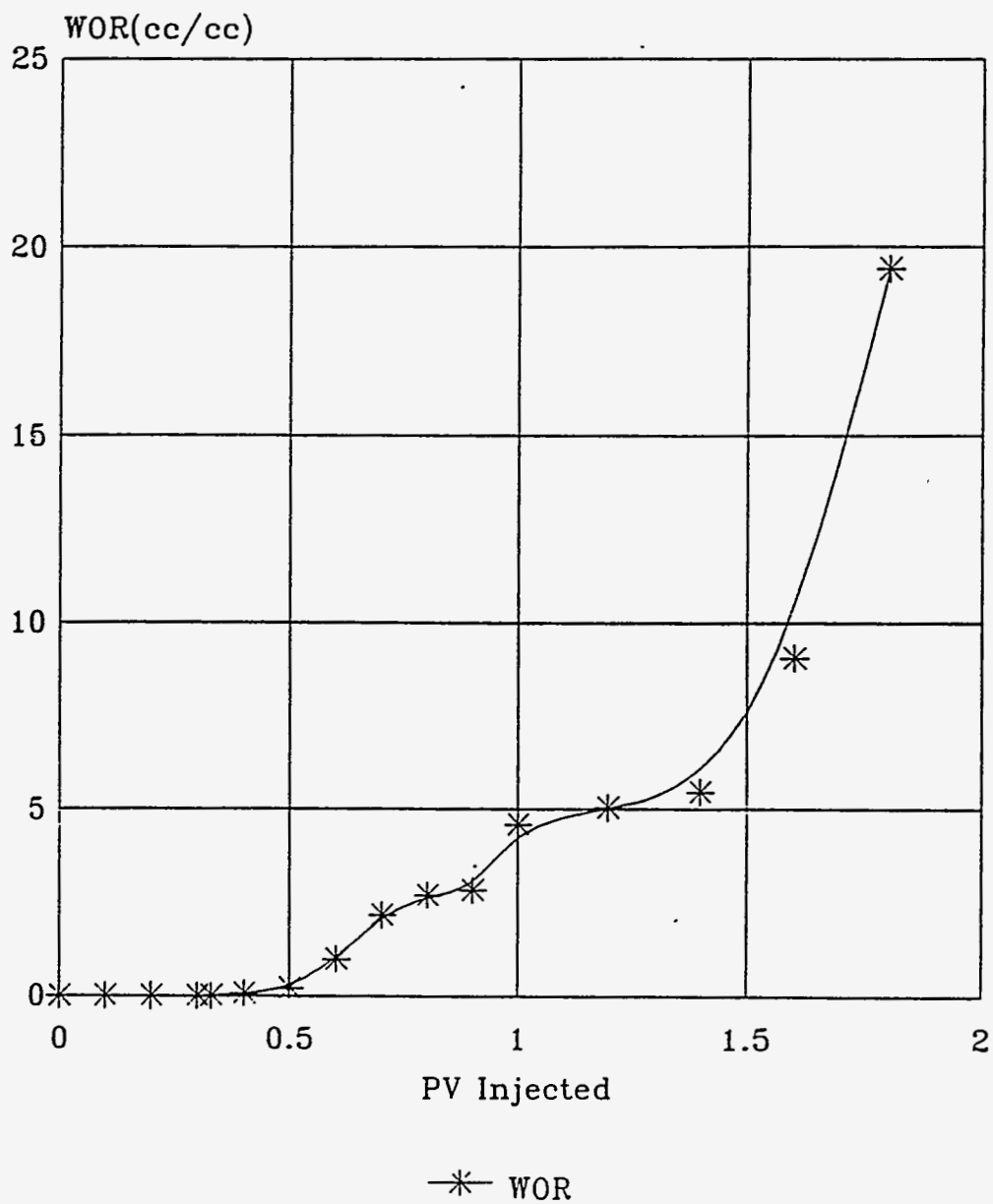


Figure 4.48 WOR vs. PV Injected (Solvent: Prudhoe Bay Gas)

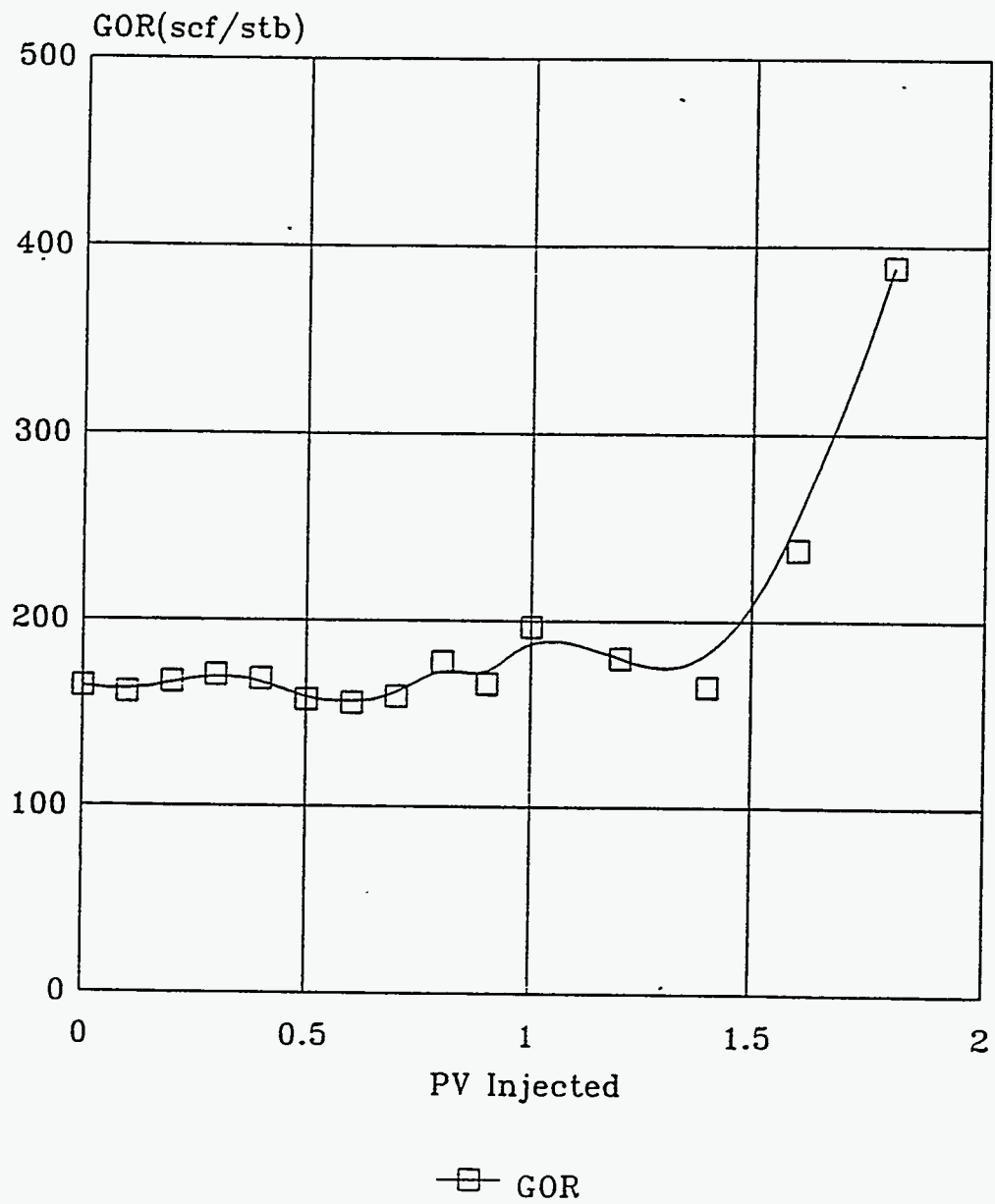


Figure 4.49 GOR vs. PV Injected (Solvent: Prudhoe Bay Gas)

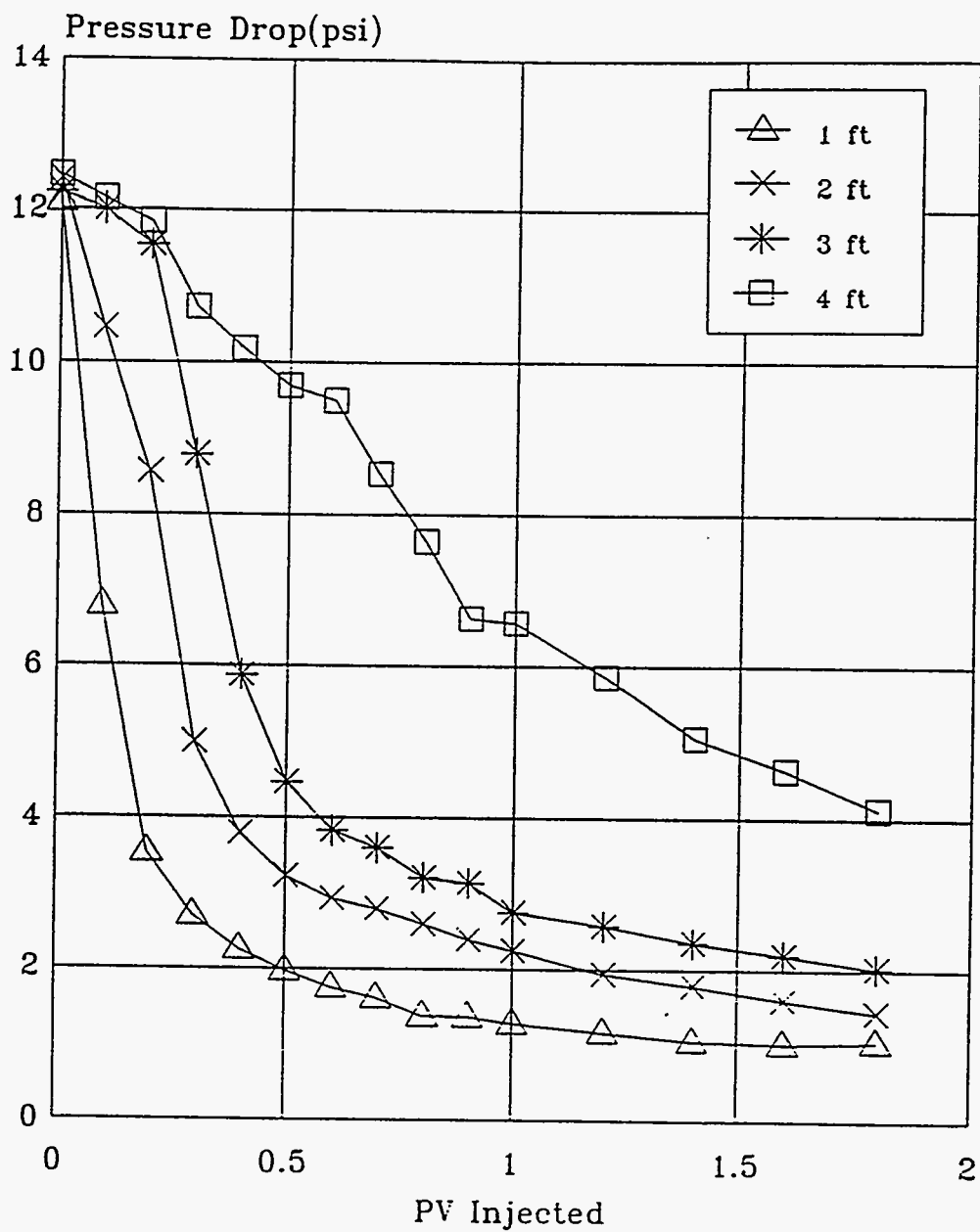


Figure 4.50 Pressure Drop vs. PV Injected (Solvent: Prudhoe Bay Gas)

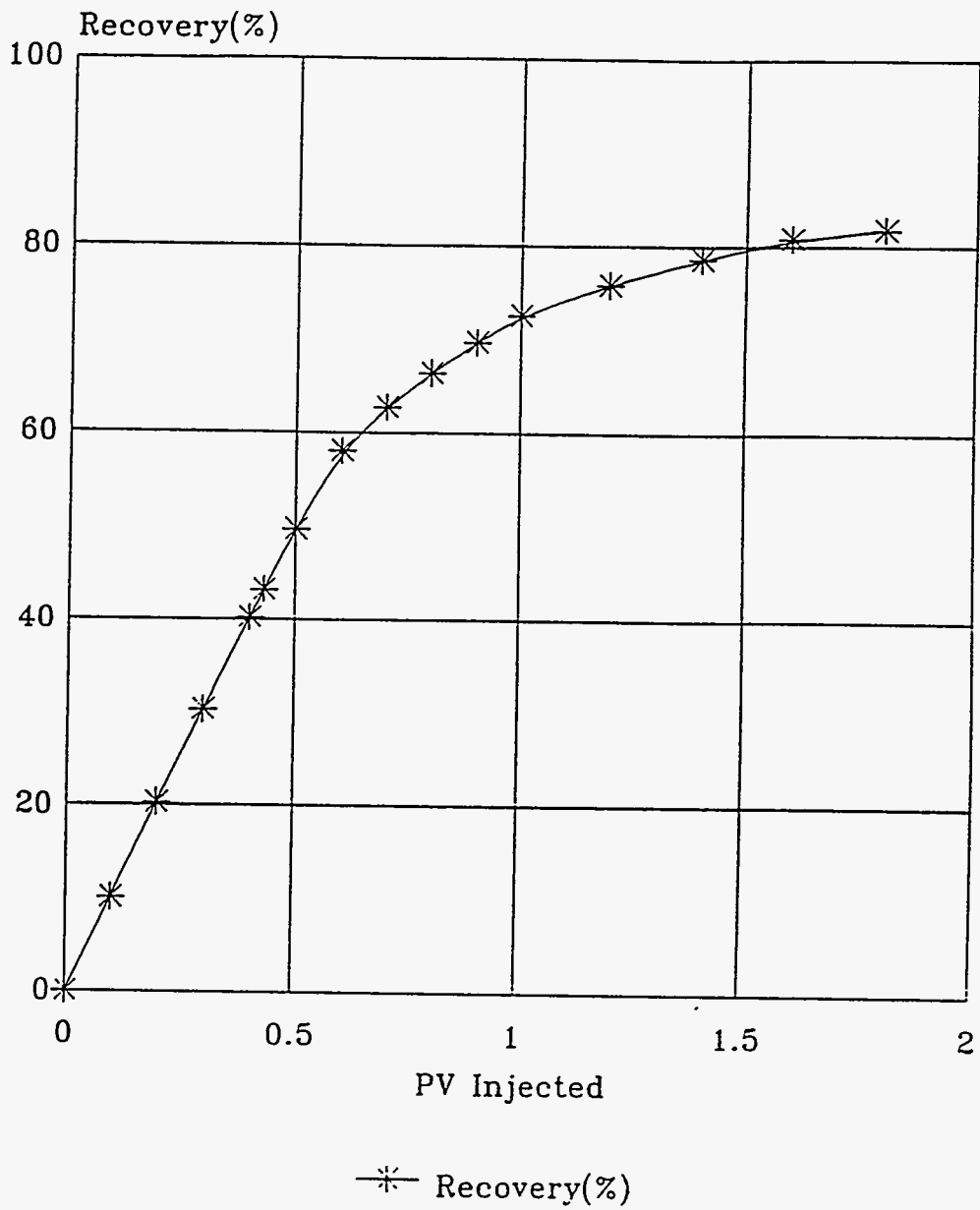


Figure 4.51 Oil Recovery vs. PV Injected (Solvent: Carbon Dioxide)

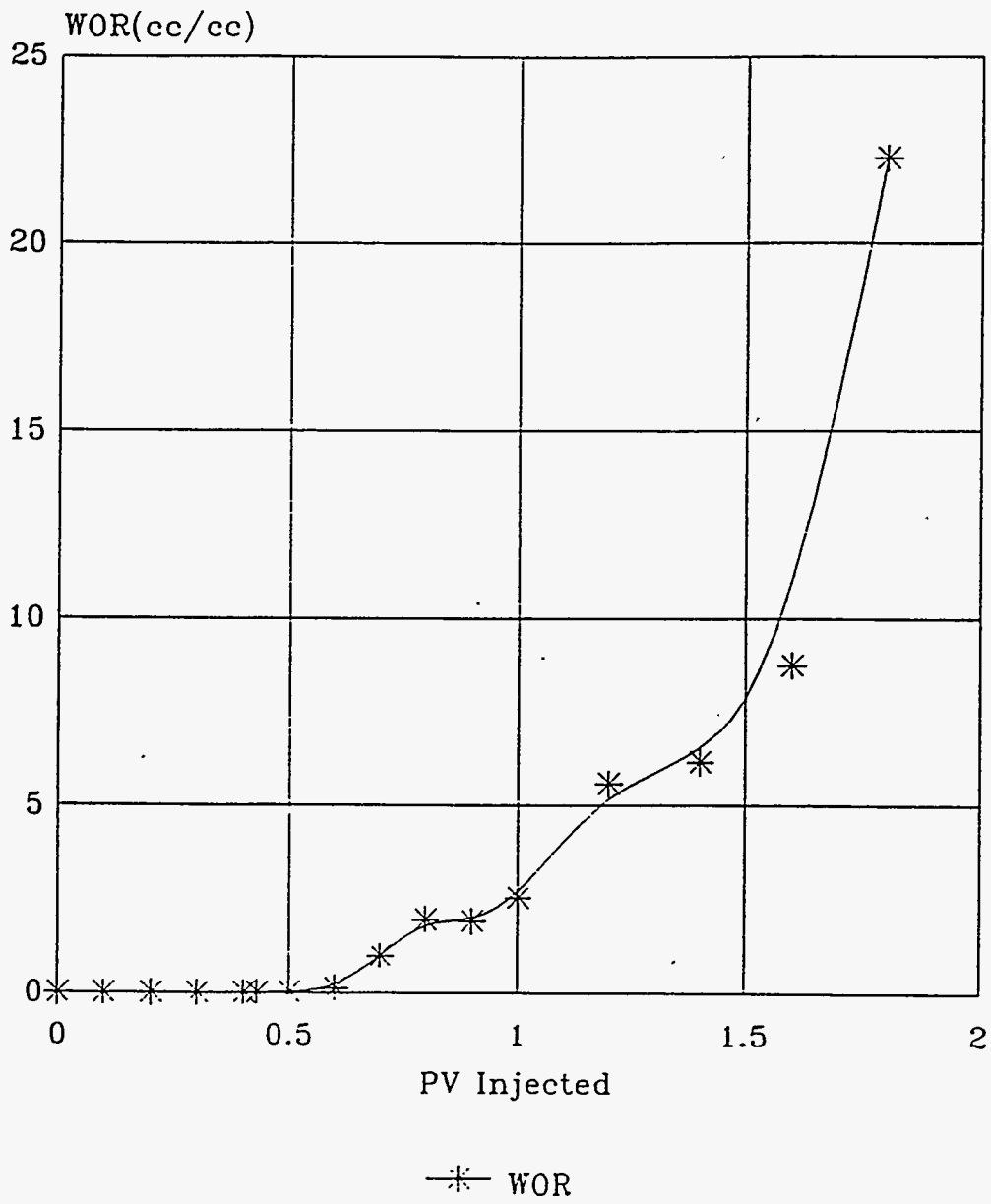


Figure 4.52 WOR vs. PV Injected (Solvent: Carbon Dioxide)

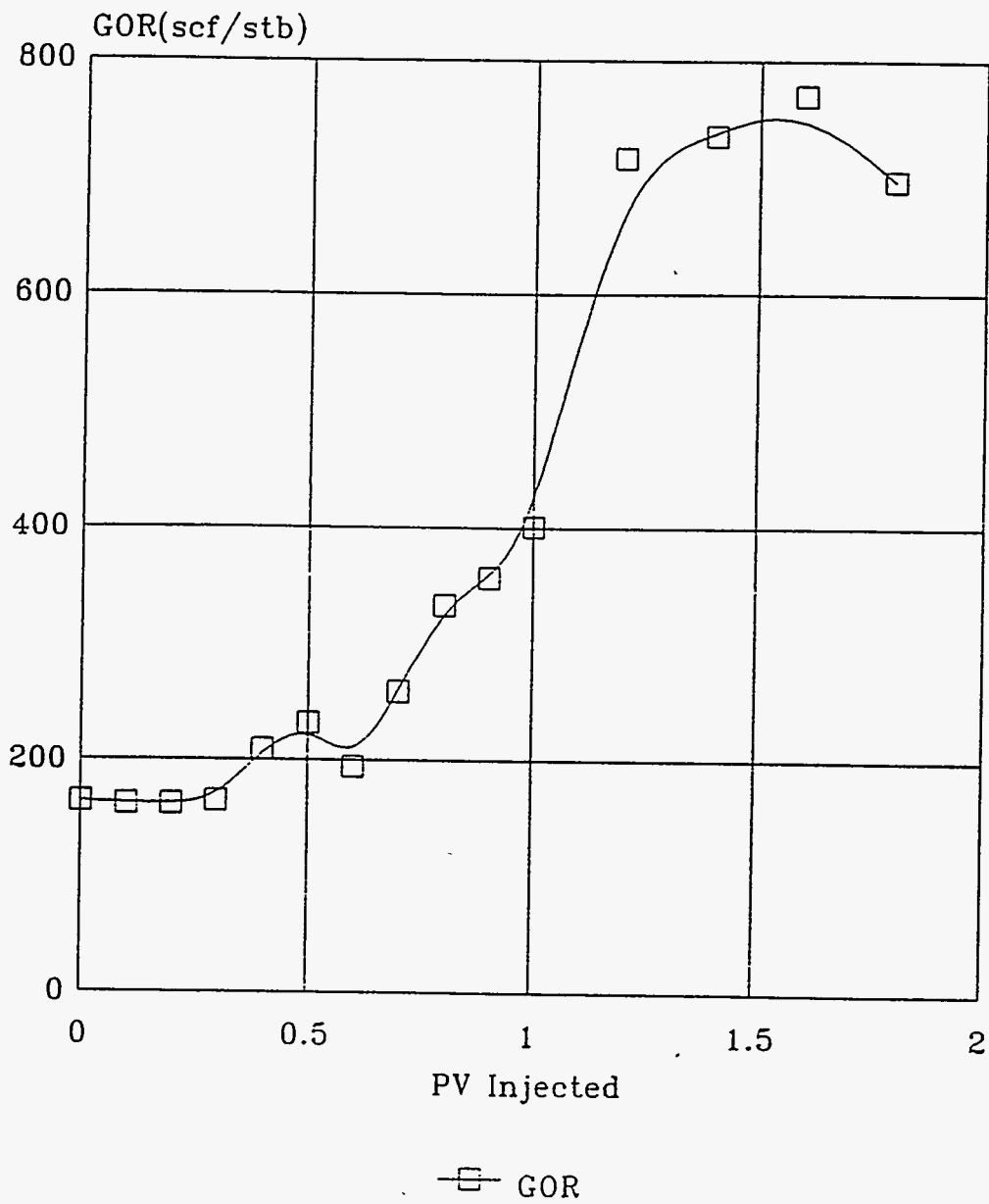


Figure 4.53 GOR vs. PV Injected (Solvent: Carbon Dioxide)

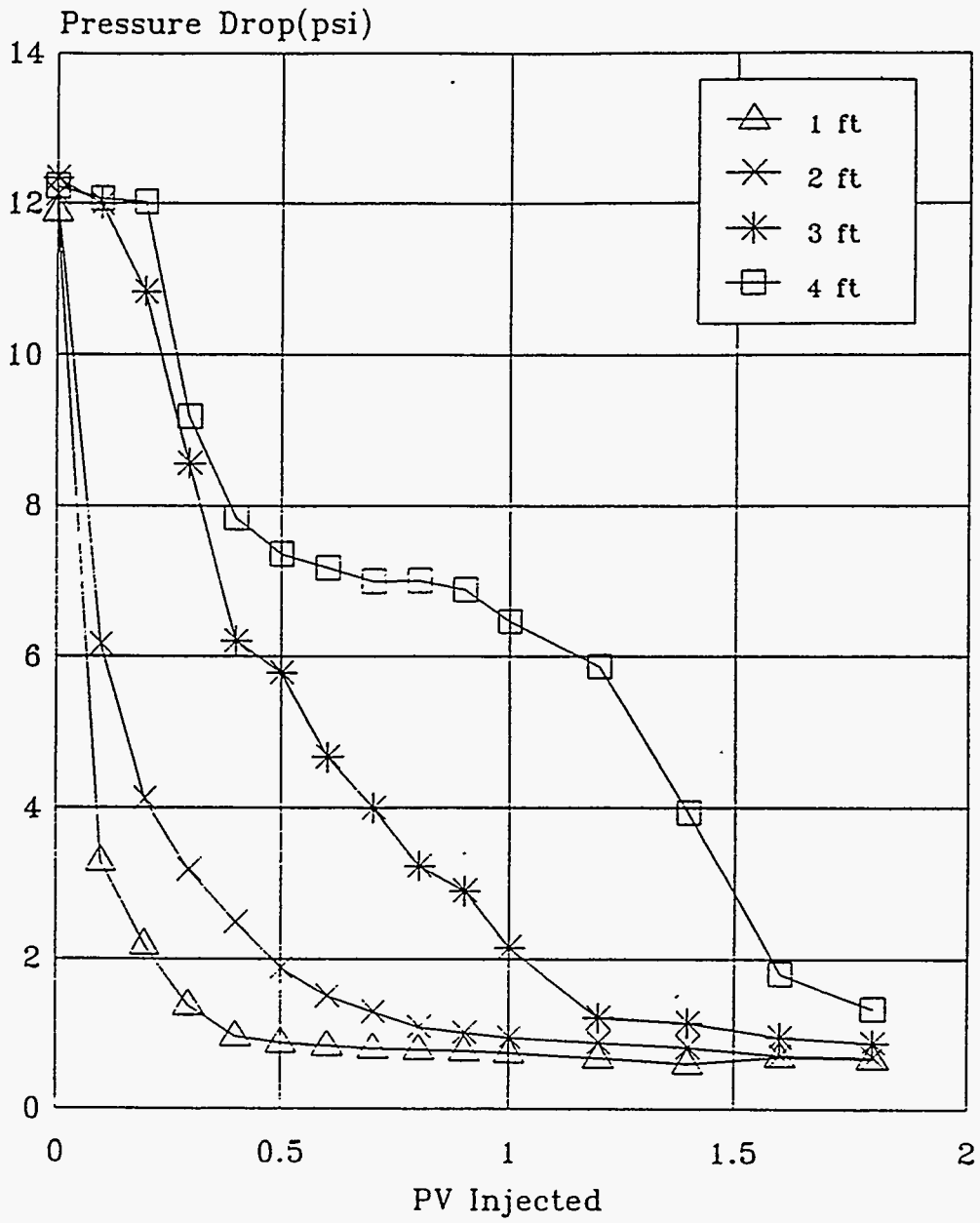


Figure 4.54 Pressure Drop vs. PV Injected (Solvent: Carbon Dioxide)

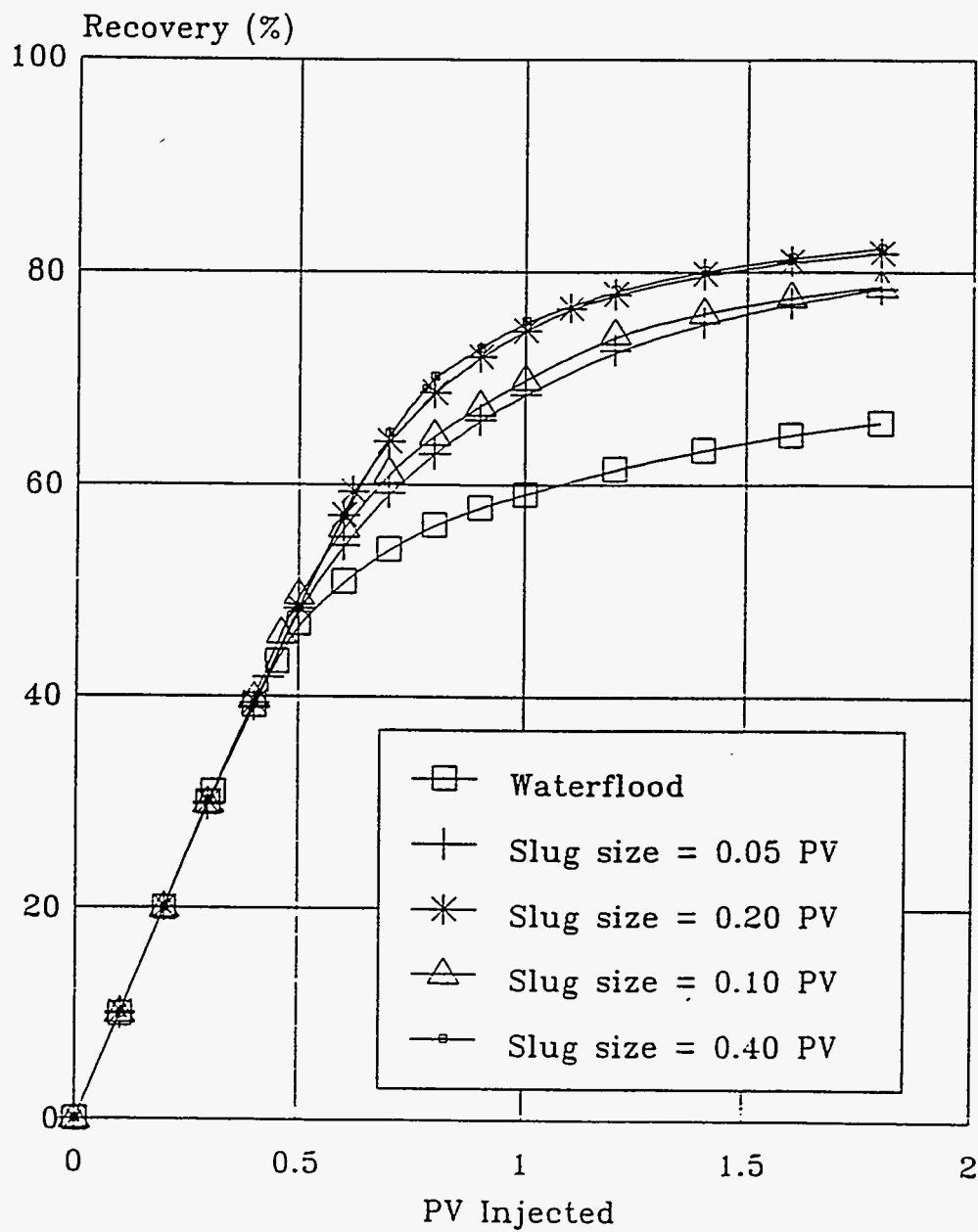


Figure 4.55 Effect of Slug Size, Oil Recovery vs. PV Injected Comparison
(MCM Solvent: 50% PBG/50% NGL)

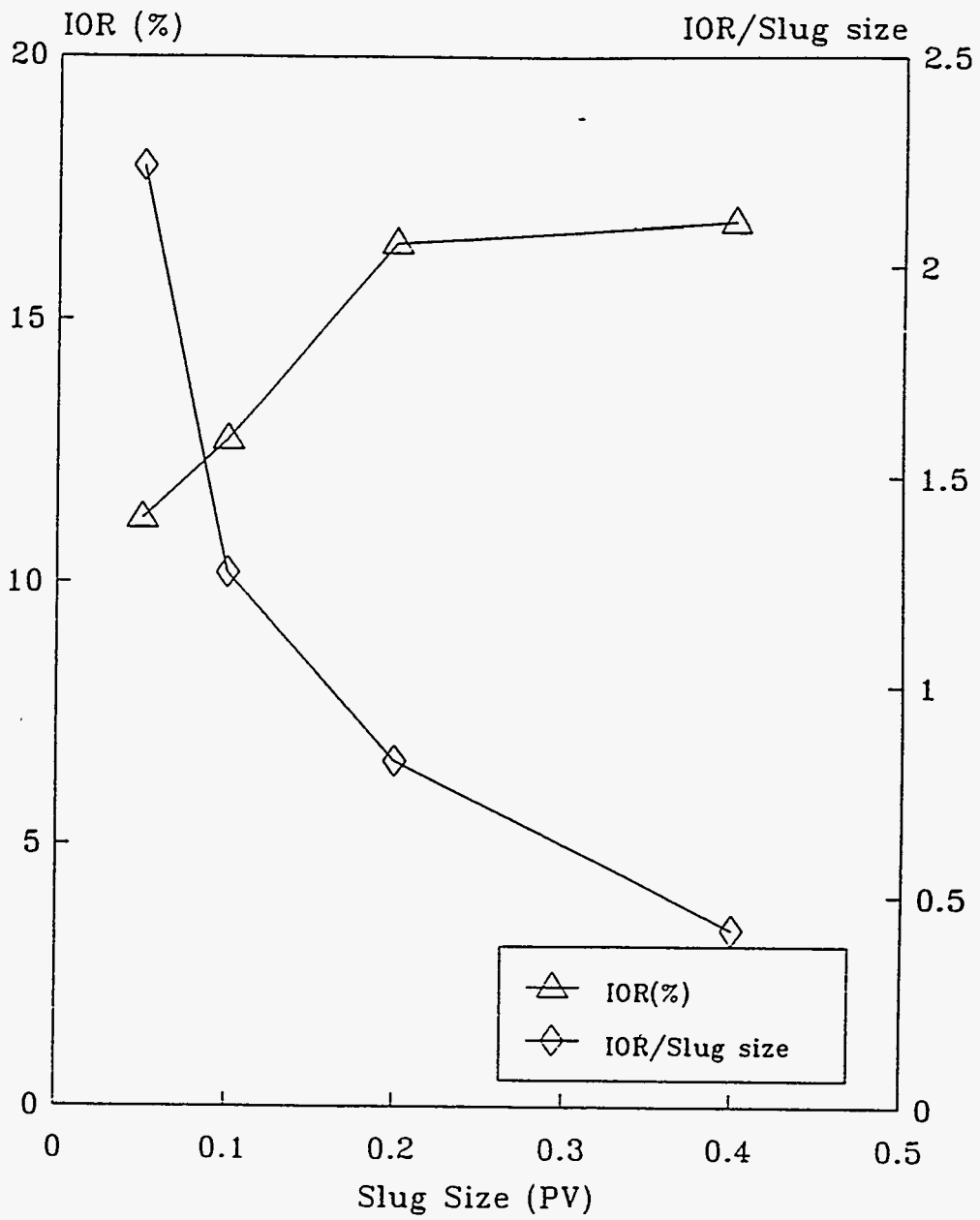


Figure 4.56 Effect of Slug Size on Incremental Oil Recovery
 (MCM Solvent: 50% PBG/50% NGL)

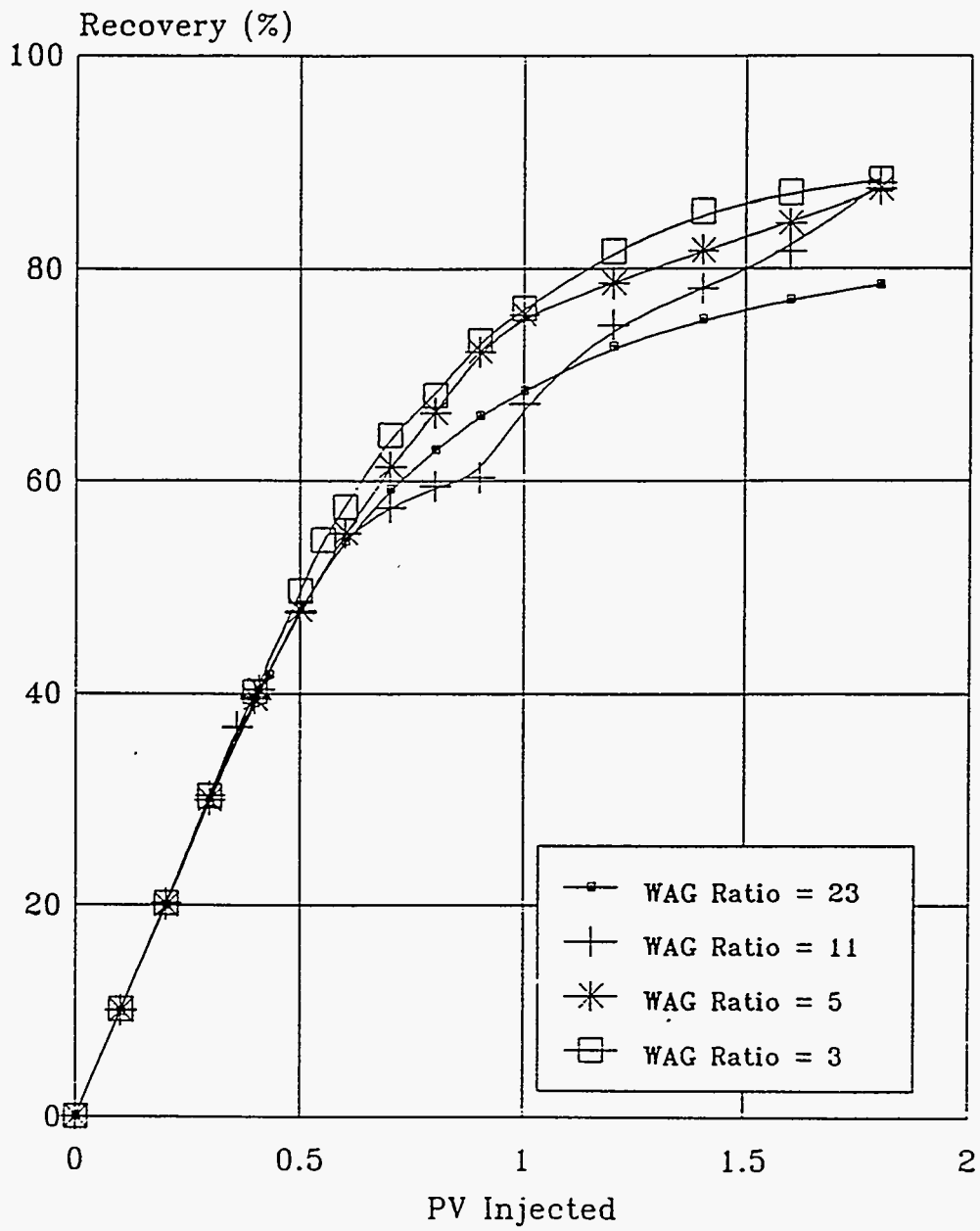


Figure 4.57 Effect of WAG Ratio, Comparison of Recovery vs. PV Injected
(MCM Solvent: 50% PBG/50% NGL)

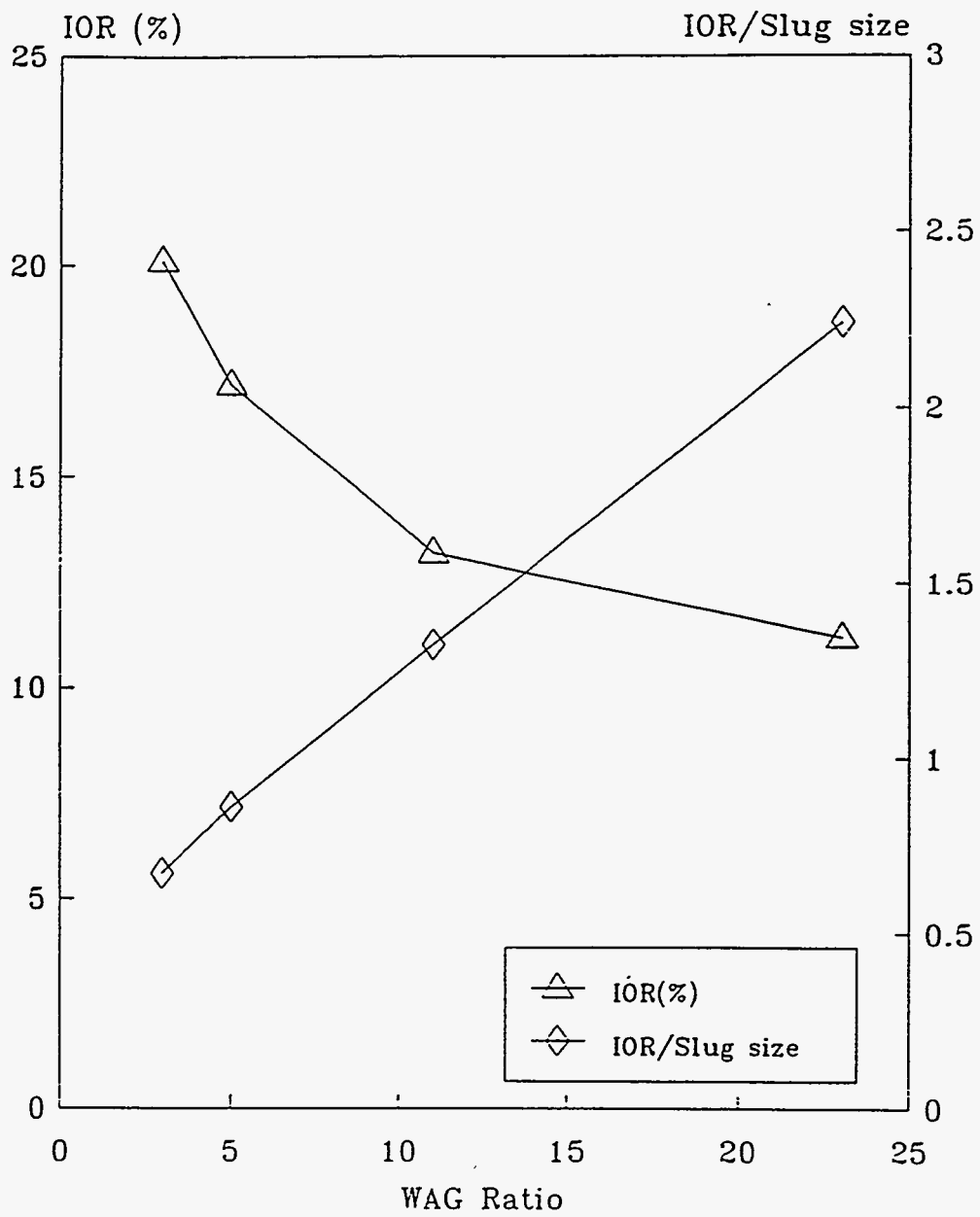


Figure 4.58 Effect of WAG Ratio on Incremental Oil Recovery
(MCM Solvent: 50% PBG/50% NGL)

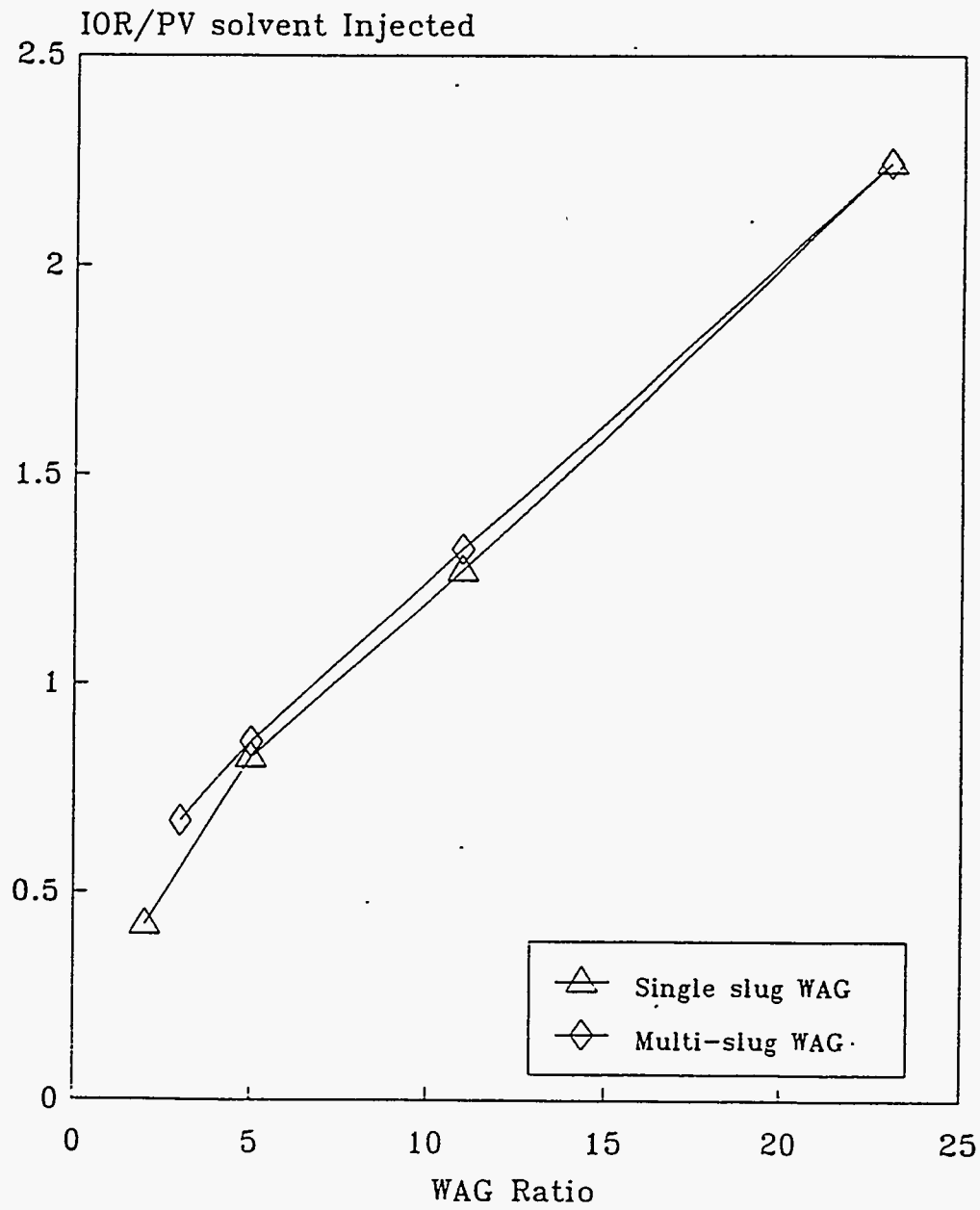


Figure 4.59 Effect of WAG Ratio on Incremental Oil Recovery, Single-slug vs. Multi-slug WAG (MCM Solvent: 50% PBG/50% NGL)

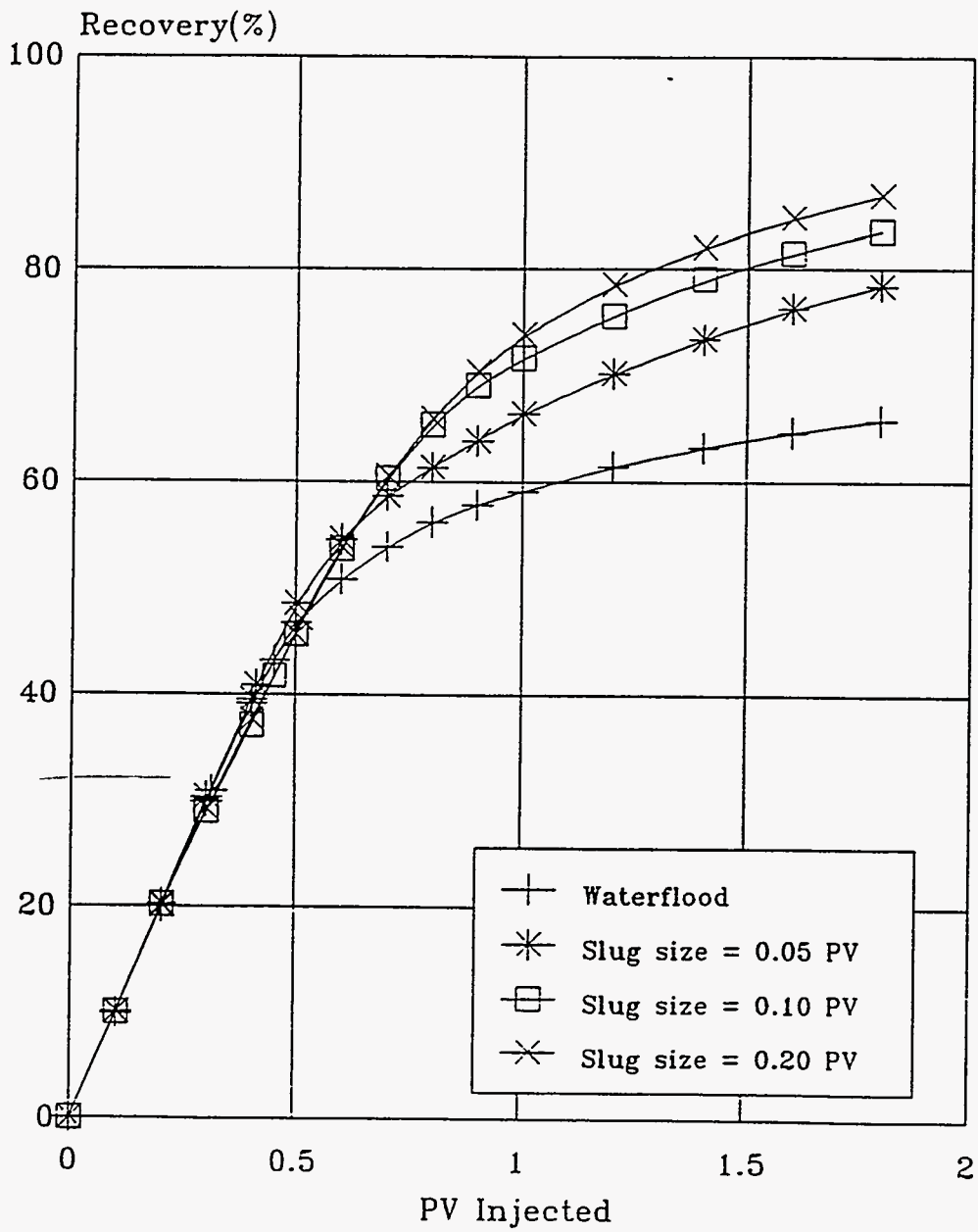


Figure 4.60 Effect of Slug Size, Recovery vs. PV Injected Comparison
(FCM Solvent: Propane)

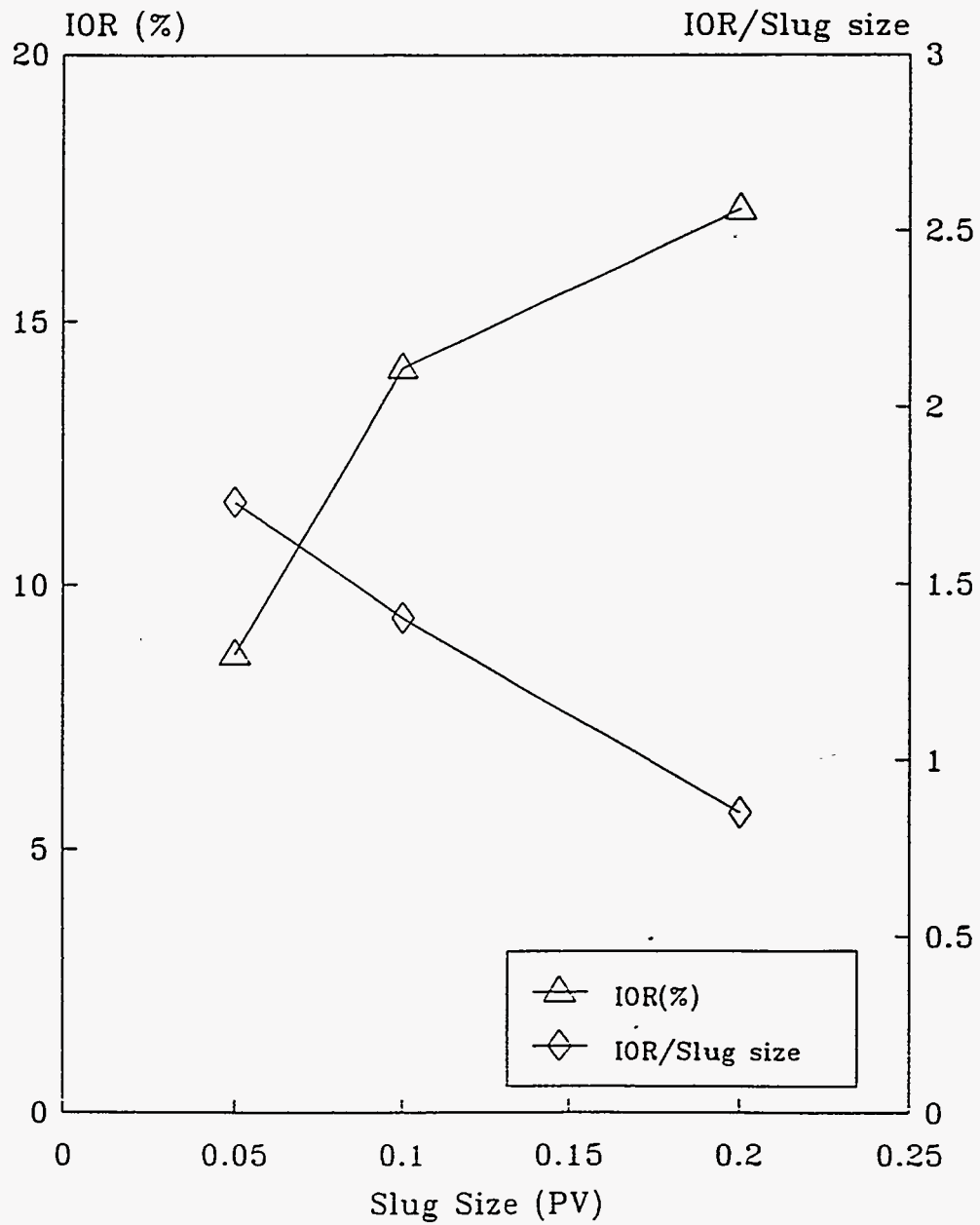


Figure 4.61 Effect of Slug Size on Incremental Oil Recovery
(FCM Solvent: Propane)

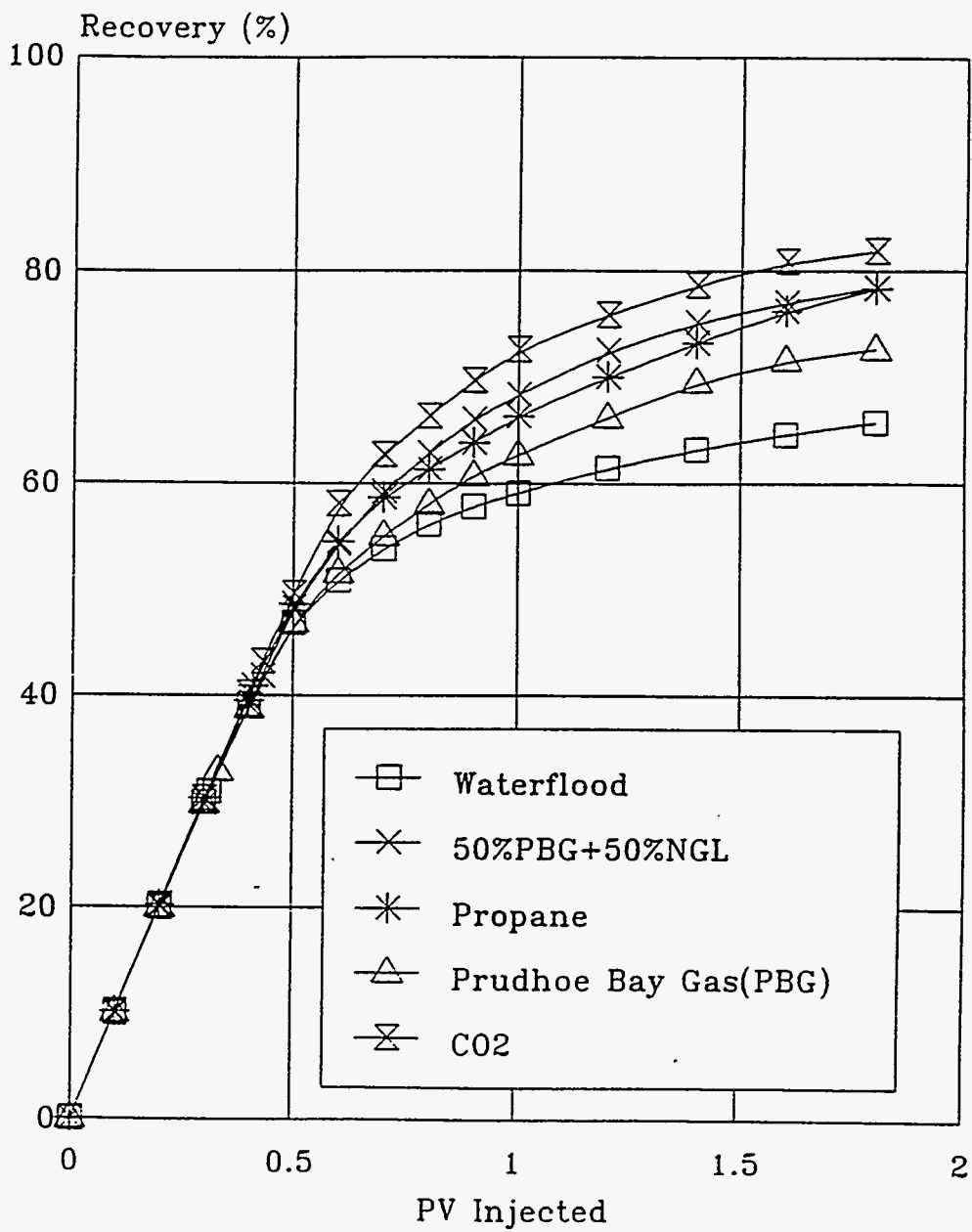


Figure 4.62 Effect of Solvent Type, Recovery vs. PV Injected Comparison

Table 4.1 Summary of Experimental Results

Run No.	Type of Flood	Solvent	WAG Ratio	Solvent Slug Size (PV)	Recovery @1.2 PV	Water BT (PV Injected)	Solvent BT (PV Injected)	IOR(%)	IOR/PV Solvent Injected
1	Waterflood	-		-	61.45	0.31	-	-	-
2	MCM WAG	50%PBG/50%NGL	23	0.05(1 slug)	72.64	0.43	0.2, 0.6	11.19	2.238
3	MCM WAG	50%PBG/50%NGL	11	0.10(1 slug)	74.16	0.46	0.3, 1.0	12.71	1.271
4	MCM WAG	50%PBG/50%NGL	5	0.20(1 slug)	77.88	0.62	0.2, 1.1	16.43	0.822
5	MCM WAG	50%PBG/50%NGL	0	0.40(1 slug)	78.29	0.78	0.2, 1.0	16.84	0.421
6	MCM WAG	50%PBG/50%NGL	11	0.05(2 slugs)	74.67	0.36, 1.0	0.1,0.6,1.2	13.22	1.322
7	MCM WAG	50%PBG/50%NGL	5	0.05(4 slugs)	78.64	0.41,0.9,1.4	0.3,0.5,0.8	17.19	0.860
8	MCM WAG	50%PBG/50%NGL	3	0.05(6 slugs)	81.55	0.55,0.9,1.2	0.3,0.6,0.8	20.10	0.670
9	FCM WAG	Propane	23	0.05(1 slug)	70.14	0.41	0.2, 1.2	8.69	1.738
10	FCM WAG	Propane	11	0.10(1 slug)	75.55	0.45	0.1, 1.1	14.10	1.410
11	FCM WAG	Propane	5	0.20(1 slug)	78.52	0.51	0.2, 0.9	17.07	0.854
12	Immiscible WAG	Prudhoe Bay Gas	23	0.05(1 slug)	66.31	0.33	0.2, 0.9	4.86	0.972
13	Immiscible WAG	Carbon Dioxide	23	0.05(1 slug)	75.90	0.43	0.3	14.45	2.890

APPENDIX A

CRUDE OIL AND SOLVENT COMPOSITIONS

TABLE A1 : Experimental Materials and Sandpack Properties

<u>Materials</u>	<u>Properties</u>
Sand	Oklahoma #1 sand
Sandpack	Porosity (\emptyset) = 33.75%
	Pore Volume (PV) = 925 cc
	Abs. Permeability (K) = 5.12 darcys
	Swi = 0.065
Water	Distilled
Methane	C.P. Grade 99.0%
CO ₂	C.P. Grade 99.8%
Toulene	Industrial Grade

Table A-2 : Composition of Schrader Bluff Live Oil
(After Inaganti, M.S., (1994))

Component	Mole %
N ₂	0.24
CO ₂	0.22
C ₁	26.29
C ₂	0.35
C ₃	0.80
i-C ₄	0.57
n-C ₄	1.02
i-C ₅	0.81
n-C ₅	0.24
C ₆	0.93
C ₇	1.89
C ₈	3.85
C ₉	5.23
C ₁₀	4.97
C ₁₁₊	52.59

Table A-3 : Prudhoe Bay NGL Composition
(After Inaganti, M.S., (1994))

Component	Mole %
C ₃	0.88
i-C ₄	10.09
n-C ₄	36.83
i-C ₅	12.21
n-C ₅	15.49
C ₆	13.20
Benzene	0.86
Cyclohexane	1.63
C ₇	5.48
C ₈ Aromatics	0.56
C ₈₊	2.77

Table A-4 : 50 mol % PBG + 50 mol % NGL Solvent Mixture Composition
(After Inaganti, M.S., (1994))

Component	Mole %
N ₂	0.22
C ₁	36.12
CO ₂	6.08
C ₂	3.935
C ₃	2.9
C ₄	24.2
C ₅	14.11
C ₆	7.96
C ₇	2.79
C ₈	1.685

APPENDIX B

RAW DATA FROM EXPERIMENTS

Table B1 : Run 1 (Unsteady State Waterflood)

PV Injected	Np (cc)	Total Pr. Drop(psi)	Pr. Drop Along The Length (psi)				Wp (cc)	Gp (scf)	WOR (cc/cc)	GOR (scf/stb)
			(1ft)	(2ft)	(3ft)	(4ft)				
0	0	49.10	12.35	12.28	11.98	12.49	0	0	0	0.00
0.10	86.0	36.45	3.50	9.40	11.10	12.45	0	0.089	0	164.55
0.20	173.0	27.50	2.10	4.13	8.85	12.42	0	0.178	0	162.66
0.30	259.0	20.49	1.71	2.70	4.94	11.14	0	0.266	0	162.70
BT 0.31	268.0									
0.40	339.0	16.00	1.55	2.25	2.96	9.24	5.7	0.345	0.08	157.01
0.45	375.0	14.20	1.45	2.03	2.66	8.06	14.8	0.384	0.25	172.25
0.50	406.0	13.10	1.41	1.86	2.50	7.33	29.2	0.417	0.46	169.26
0.60	440.8	12.10	1.37	1.70	2.35	6.68	77.7	0.453	1.39	164.48
0.70	466.8	10.80	1.21	1.61	2.26	5.72	159.7	0.482	3.15	177.35
0.80	486.8	9.20	1.17	1.42	1.96	4.65	246.7	0.504	4.35	174.90
0.90	501.2	8.30	1.05	1.35	1.76	4.14	324.7	0.520	5.42	176.67
1.00	512.2	7.20	1.02	1.24	1.49	3.45	407.0	0.532	7.48	173.45
1.20	532.2	6.30	1.02	1.13	1.25	2.90	573.0	0.553	8.30	166.95
1.40	548.2	5.60	0.99	1.01	1.18	2.42	741.0	0.570	10.50	168.94
1.60	560.2	4.78	0.92	0.98	1.12	1.76	906.0	0.583	13.75	172.25
1.80	570.2	4.50	0.90	0.92	1.00	1.68	1082.0	0.594	17.60	174.90

Table B2 : Run 2 (Effect of Slug Size)

Solvent = 50%PBG+50%NGL (Slug Size = 5% PV)

PV Injected	Np (cc)	Total Pr. Drop(psi)	Pr. Drop Along The Length (psi)				Wp (cc)	Gp (scf)	WOR (cc/cc)	GOR (scf/stb)
			(1 ft)	(2 ft)	(3 ft)	(4 ft)				
0	0	49.56	12.32	12.12	12.27	12.85	0	0	0	0.00
0.10	86.0	34.65	3.10	6.80	12.10	12.65	0	0.088	0	162.70
0.20	173.5	26.14	2.54	3.41	7.75	12.44	0	0.181	0	168.99
0.30	257.5	20.30	2.16	2.60	5.05	10.49	0	0.271	0	170.36
0.40	338.2	15.80	1.98	2.16	3.50	8.16	0	0.360	0	175.35
BT 0.43	362.2									
0.50	418.2	12.40	1.88	1.78	3.18	5.56	2.0	0.438	0.04	155.03
0.60	470.1	10.10	1.77	1.60	2.69	4.04	14.1	0.491	0.23	162.37
0.70	512.9	8.60	1.71	1.46	2.49	2.94	58.8	0.541	1.04	185.75
0.80	544.9	8.10	1.65	1.39	2.39	2.67	113.8	0.578	1.72	183.84
0.90	572.9	7.80	1.60	1.34	2.32	2.54	172.0	0.611	2.08	187.39
1.00	593.0	7.01	1.24	1.23	2.12	2.42	242.0	0.637	3.48	205.67
1.20	629.0	6.35	1.05	1.07	1.93	2.30	402.0	0.683	4.44	203.17
1.40	651.5	5.50	1.00	1.02	1.66	1.82	563.0	0.715	7.16	226.13
1.60	667.5	4.41	0.99	1.01	1.18	1.23	731.0	0.740	10.50	248.44
1.80	679.5	3.45	0.65	0.89	0.93	0.98	906.0	0.760	14.58	265.00

Table B3 : Run 3 (Effect of Slug Size)
 Solvent = 50%PBG +50%NGL (Slug Size = 10% PV)

PV Injected	Np (cc)	Total Pr. Drop(psi)	Pr. Drop Along The Length (psi)				Wp (cc)	Gp (scf)	WOR (cc/cc)	GOR (scf/stb)
			(1 ft)	(2 ft)	(3 ft)	(4 ft)				
0	0	48.95	11.90	12.01	12.50	12.54	0	0	0	0.00
0.10	87.0	32.50	1.58	6.91	11.62	12.39	0	0.088	0	160.83
0.20	173.5	24.20	1.61	2.50	8.32	11.77	0	0.183	0	174.62
0.30	258.5	18.60	1.20	2.60	4.05	10.75	0	0.277	0	175.84
0.40	344.5	13.80	1.00	1.95	3.80	7.05	0	0.393	0	214.47
BT 0.46	397.4									
0.50	429.7	11.90	0.89	1.50	3.00	6.51	1.8	0.515	0.06	227.68
0.60	484.8	9.90	0.81	1.27	2.19	5.63	22.6	0.585	0.38	202.00
0.70	529.5	8.85	0.74	1.19	1.80	5.12	67.3	0.632	1.00	167.18
0.80	560.0	7.78	0.73	1.16	1.63	4.26	124.3	0.665	1.87	172.03
0.90	584.2	7.45	0.69	1.08	1.46	4.22	192.7	0.692	2.83	177.40
1.00	604.9	6.71	0.62	1.07	1.35	3.67	273.2	0.715	3.89	176.67
1.20	642.3	5.97	0.58	0.93	1.22	3.24	420.8	0.760	3.95	191.31
1.40	660.1	5.43	0.55	0.89	1.14	2.85	587.1	0.792	9.34	285.84
1.60	672.4	5.01	0.51	0.86	1.12	2.52	759.6	0.820	14.02	361.95
1.80	681.4	4.74	0.47	0.75	1.09	2.43	932.6	0.845	19.22	441.67

Table B4 : Run 4 (Effect of Slug Size)

Solvent = 50%PBG +50%NGL (Slug Size = 20% PV)

PV Injected	Np (cc)	Total Pr. Drop(psi)	Pr. Drop Along The Length (psi)				Wp (cc)	Gp (scf)	WOR (cc/cc)	GOR (scf/stb)
			(1 ft)	(2 ft)	(3 ft)	(4 ft)				
0	0	46.60	10.80	11.40	11.65	12.75	0	0	0	0.00
0.10	87.5	28.75	0.91	3.68	11.26	12.90	0	0.089	0	161.73
0.20	173.8	11.20	0.44	0.80	2.62	7.34	0	0.195	0	195.30
0.30	258.9	9.75	1.30	0.39	1.70	6.36	0	0.357	0	302.68
0.40	340.9	6.60	1.20	1.26	1.52	2.62	0	0.548	0	370.35
0.50	419.1	5.52	1.15	1.14	1.41	1.82	0	0.738	0	386.32
0.60	494.7	4.80	1.06	1.09	1.24	1.41	0	0.930	0	403.81
BT 0.62	513.9									
0.70	554.7	4.69	0.96	0.92	1.06	1.75	20.7	1.087	0.57	416.05
0.80	594.6	4.62	0.91	0.86	1.02	1.83	70.1	1.170	1.24	330.75
0.90	624.1	3.92	0.80	0.83	0.92	1.37	129.0	1.227	2.00	307.22
1.00	645.0	3.80	0.75	0.82	0.82	1.41	198.2	1.270	3.31	327.13
1.10	663.2	3.52	0.73	0.78	0.80	1.21	270.0	1.307	3.95	323.24
1.20	674.5	3.39	0.69	0.77	0.78	1.15	352.2	1.333	7.27	365.84
1.40	691.1	3.05	0.65	0.74	0.75	0.91	519.6	1.378	10.08	431.02
1.60	701.3	2.85	0.54	0.70	0.71	0.90	694.4	1.407	17.14	452.06
1.80	707.8	2.63	0.47	0.68	0.70	0.78	874.4	1.434	27.69	660.46

Table B5 : Run 5 (Effect of Slug Size)
 Solvent = 50%PBG+50%NGL (Slug Size = 40% PV)

PV Injected	Np (cc)	Total Pr. Drop(psi)	Pr. Drop Along The Length (psi)				Wp (cc)	Gp (scf)	WOR (cc/cc)	GOR (scf/stb)
			(1 ft)	(2 ft)	(3 ft)	(4 ft)				
0	0	49.05	12.01	12.22	11.85	12.97	0	0	0	0.00
0.10	86.0	34.55	1.91	8.64	11.39	12.61	0	0.092	0	170.09
0.20	173.5	21.60	0.49	3.40	7.05	10.66	0	0.192	0	181.71
0.30	260.5	15.60	0.36	1.80	4.08	9.36	0	0.322	0	237.59
0.40	342.5	10.92	0.37	1.63	1.58	7.34	0	0.575	0	490.57
0.50	418.5	6.50	0.84	1.42	2.05	2.19	0	0.851	0	577.42
0.60	493.5	5.84	0.90	2.30	1.70	0.94	0	1.136	0	604.20
0.70	561.5	7.02	0.88	2.44	2.63	1.07	0	1.397	0	610.28
BT 0.78	597.5									
0.80	607.4	7.56	0.81	2.05	2.51	2.19	0.2	1.586	0.02	654.71
0.90	630.9	7.28	0.88	1.83	1.99	2.58	2.1	1.678	0.08	622.47
1.00	652.8	6.10	0.77	1.70	1.62	2.01	14.1	1.764	0.55	624.38
1.20	678.1	5.52	0.76	1.55	1.56	1.65	150.1	1.884	5.38	754.15
1.40	694.1	4.86	0.78	1.28	1.38	1.42	305.1	1.987	9.69	1023.71
1.60	704.3	4.62	0.78	1.20	1.34	1.30	467.1	2.063	15.88	1184.71
1.80	712.3	4.34	0.76	1.18	1.16	1.24	632.1	2.132	20.63	1371.37

Table B6 : Run 6 (Effect of WAG Ratio)

Solvent = 50%PBG+50%NGL (Slug size = 5% PV)

WAG Ratio = 11

PV Injected	Np (cc)	Total Pr. Drop(psi)	Pr. Drop Along The Length (psi)				Wp (cc)	Gp (scf)	WOR (cc/cc)	GOR (scf/stb)
			(1 ft)	(2 ft)	(3 ft)	(4 ft)				
0	0	45.20	10.85	11.05	11.20	12.10	0	0	0	0.00
0.10	87.5	24.90	3.99	4.96	5.24	10.71	0	0.089	0	161.73
0.20	175.5	20.90	2.60	5.14	4.89	8.27	0	0.186	0	175.26
0.30	262.5	17.50	1.81	3.53	5.11	7.05	0	0.301	0	210.17
BT 0.36	319.1									
0.40	344.1	14.80	1.47	2.59	3.48	7.26	0.5	0.415	0.02	222.13
0.50	412.7	12.00	1.35	2.12	2.54	5.99	8.0	0.488	0.11	169.20
0.60	476.2	10.85	1.11	1.90	2.58	5.26	36.9	0.552	0.46	160.25
0.70	497.8	9.47	1.16	2.07	2.41	3.83	106.9	0.578	3.24	191.39
0.80	515.7	9.90	1.04	1.46	3.00	4.40	181.9	0.605	4.19	239.83
0.90	522.7	11.10	0.90	1.19	2.02	6.99	261.9	0.620	11.43	340.71
1.00	582.7	8.22	0.80	1.08	1.65	4.69	286.9	0.718	0.42	259.70
1.20	646.7	5.95	0.76	0.97	1.21	3.01	387.9	0.788	1.58	173.91
1.40	676.7	5.51	0.66	1.06	1.30	2.49	541.9	0.860	5.13	381.60
1.60	706.7	4.92	0.60	0.86	1.02	2.44	702.9	0.919	5.37	312.70
1.80	760.7	3.50	0.66	0.70	0.87	1.27	837.9	1.063	2.50	424.00

Table B7 : Run 7 (Effect of WAG Ratio)

Solvent = 50%PBG+50%NGL (Slug size = 5% PV)

WAG Ratio = 5

PV Injected	Np (cc)	Total Pr. Drop(psi)	Pr. Drop Along The Length (psi)				Wp (cc)	Gp (scf)	WOR (cc/cc)	GOR (scf/stb)
			(1 ft)	(2 ft)	(3 ft)	(4 ft)				
0	0	46.50	11.32	11.55	11.21	12.42	0	0	0	0.00
0.10	87.0	26.50	4.10	3.12	7.94	11.34	0	0.088	0	160.83
0.20	173.0	21.40	3.03	4.22	5.14	9.01	0	0.178	0	166.83
0.30	259.0	17.05	2.06	3.38	4.16	7.45	0	0.267	0	164.55
0.40	342.1	13.38	1.35	2.49	3.09	6.45	0	0.371	0	202.65
BT 0.41	350.1									
0.50	414.4	12.10	1.32	2.00	2.65	6.13	4.5	0.447	0.07	167.14
0.60	477.1	8.65	1.05	1.49	2.03	4.08	26.9	0.531	0.36	213.01
0.70	531.1	7.91	0.70	1.32	1.70	4.19	54.9	0.627	0.52	282.67
0.80	575.1	7.02	0.82	1.19	1.48	3.53	93.9	0.675	0.89	173.45
0.90	625.1	5.01	0.70	1.07	1.48	1.76	125.9	0.788	0.64	359.34
1.00	655.1	4.85	0.64	0.92	1.27	2.02	173.9	0.896	1.60	572.40
1.20	681.1	4.22	0.46	1.03	1.20	1.53	309.9	1.069	5.23	1057.96
1.40	707.1	3.47	0.59	0.75	0.89	1.24	429.9	1.271	4.62	1235.31
1.60	729.1	3.30	0.28	0.76	0.82	1.44	574.9	1.434	6.59	1178.05
1.80	756.1	2.81	0.42	0.69	0.76	0.94	719.9	1.575	5.37	830.33

Table B8 : Run 8 (Effect of WAG Ratio)
 Solvent = 50%PBG +50%NGL (Slug size = 5% PV)
 WAG Ratio = 3

PV Injected	Np (cc)	Total Pr. Drop(psi)	Pr. Drop Along The Length (psi)				Wp (cc)	Gp (scf)	WOR (cc/cc)	GOR (scf/stb)
			(1ft)	(2ft)	(3ft)	(4ft)				
0	0	48.20	11.45	11.85	12.01	12.89	0	0	0	0.00
0.10	88.0	25.60	1.89	3.51	8.86	11.34	0	0.090	0	162.61
0.20	175.0	20.08	1.89	3.46	3.98	10.75	0	0.186	0	175.45
0.30	262.0	13.10	1.29	1.31	3.82	6.68	0	0.289	0	188.24
0.40	348.0	9.54	1.01	1.98	2.20	4.35	0	0.414	0	231.10
0.50	430.0	6.47	0.62	1.20	1.90	2.75	0	0.564	0	290.85
BT 0.55	471.2									
0.60	498.6	6.75	0.61	1.39	1.51	3.24	4.4	0.699	0.16	312.90
0.70	557.2	4.66	0.27	1.05	1.36	1.98	22.3	0.917	0.31	591.50
0.80	589.3	4.01	0.52	1.16	0.99	1.34	62.1	1.024	1.24	530.00
0.90	634.3	3.87	0.28	0.97	1.12	1.50	92.1	1.254	0.67	812.67
1.00	660.3	3.53	0.29	1.11	0.98	1.15	146.1	1.357	2.08	629.88
1.20	706.3	3.45	0.26	1.09	0.79	1.31	236.1	1.718	1.96	1247.80
1.40	738.3	3.62	0.41	0.78	0.71	1.72	346.1	2.080	3.44	1798.69
1.60	753.3	4.72	0.51	0.67	0.79	2.75	491.1	2.427	9.67	3678.20
1.80	763.3	5.02	0.51	0.82	0.80	2.89	628.1	2.772	13.70	5484.50

Table B9 : Run 9 (Effect of Slug Size, FCM Process)
 Solvent = Propane (Slug size = 5% PV)

PV Injected	Np (cc)	Total Pr. Drop(psi)	Pr. Drop Along The Length (psi)				Wp (cc)	Gp (scf)	WOR (cc/cc)	GOR (scf/stb)
			(1 ft)	(2 ft)	(3 ft)	(4 ft)				
0	0	47.10	11.95	11.33	11.47	12.35	0	0	0	0.00
0.10	87.5	22.60	2.27	3.99	5.46	10.88	0	0.089	0	161.73
0.20	175.5	18.10	2.64	3.78	4.10	7.58	0	0.182	0	168.03
0.30	262.5	17.40	2.02	3.43	5.64	6.31	0	0.350	0	307.03
0.40	342.3	16.34	1.66	2.71	4.25	7.72	0	0.507	0	312.82
BT 0.41	354.1									
0.50	421.7	17.41	1.53	2.19	3.75	9.94	9.0	0.587	0.13	160.20
0.60	472.5	16.10	1.23	1.89	3.01	9.97	35.9	0.641	0.53	169.02
0.70	508.5	15.01	1.12	1.65	2.51	9.73	82.9	0.677	1.31	159.00
0.80	531.5	14.85	1.10	1.54	2.26	9.95	147.9	0.701	2.83	165.91
0.90	553.5	11.70	1.03	1.38	2.08	7.21	215.9	0.725	3.09	173.45
1.00	575.5	9.15	0.96	1.30	1.92	4.97	285.9	0.750	3.08	180.68
1.20	607.5	7.61	0.92	1.20	1.75	3.74	435.9	0.786	4.69	178.88
1.40	635.5	7.38	0.86	1.08	1.54	3.90	591.9	0.819	5.57	187.39
1.60	660.5	6.09	0.84	0.97	1.32	2.96	751.9	0.849	6.40	190.80
1.80	678.5	4.52	0.80	0.88	1.26	1.58	921.9	0.872	9.44	203.17

Table B10 : Run 10 (Effect of Slug Size, FCM Process)
 Solvent = Propane (Slug size = 10% PV)

PV Injected	Np (cc)	Total Pr. Drop(psi)	Pr. Drop Along The Length (psi)				Wp (cc)	Gp (scf)	WOR (cc/cc)	GOR (scf/stb)
			(1 ft)	(2 ft)	(3 ft)	(4 ft)				
0	0	47.90	12.79	11.10	11.15	12.86	0	0	0	0.00
0.10	87.0	20.60	0.35	1.11	5.38	13.76	0	0.088	0	160.83
0.20	175.0	6.58	2.13	1.83	0.97	1.65	0	0.191	0	186.10
0.30	251.0	12.06	1.60	3.59	4.30	2.57	0	0.385	0	405.87
0.40	321.0	15.90	1.27	2.90	4.77	6.96	0	0.559	0	395.23
BT 0.45	361.9									
0.50	396.5	17.04	1.16	2.38	3.65	9.85	0.9	0.693	0.03	282.20
0.60	465.3	16.78	1.01	2.16	2.84	10.77	7.5	0.761	0.10	157.15
0.70	522.3	14.28	0.94	2.06	2.45	8.83	37.6	0.821	0.53	167.37
0.80	566.3	13.10	0.80	1.85	2.03	8.42	82.6	0.871	1.02	180.68
0.90	598.3	11.80	0.69	1.79	2.00	7.32	142.6	0.908	1.88	183.84
1.00	520.3	11.40	0.63	1.66	1.83	7.28	212.6	0.933	3.18	180.68
1.20	654.3	9.64	0.47	1.44	1.68	6.05	362.6	0.970	4.41	173.03
1.40	684.3	8.20	0.39	1.34	1.67	4.80	516.6	1.005	5.13	185.50
1.60	705.3	7.75	0.38	1.17	1.46	4.74	681.6	1.034	7.86	219.57
1.80	723.3	6.83	0.36	1.09	1.36	4.02	851.6	1.059	9.44	220.83

Table B11 : Run 11 (Effect of Slug Size, FCM Process)
 Solvent = Propane (Slug size = 20% PV)

PV Injected	Np (cc)	Total Pr. Drop(psi)	Pr. Drop Along The Length (psi)				Wp (cc)	Gp (scf)	WOR (cc/cc)	GOR (scf/stb)
			(1 ft)	(2 ft)	(3 ft)	(4 ft)				
0	0	47.92	12.20	11.76	11.70	12.26	0	0	0	0.00
0.10	87.0	21.60	0.93	1.52	7.85	11.30	0	0.089	0	162.66
0.20	174.0	5.60	0.86	0.88	1.36	2.50	0	0.179	0	164.48
0.30	253.0	3.33	1.20	0.49	0.69	0.95	0	0.412	0	468.95
0.40	326.0	6.52	1.30	2.82	1.65	0.75	0	0.776	0	792.82
0.50	396.0	12.52	1.09	2.53	4.30	4.60	0	1.055	0	587.56
BT 0.51	408.9									
0.60	466.8	15.22	0.98	2.11	3.42	8.71	0.5	1.155	0.01	274.61
0.70	524.3	15.44	0.92	1.91	2.68	9.93	1.7	1.232	0.02	212.92
0.80	571.1	14.10	0.80	1.78	2.38	9.14	19.5	1.281	0.38	166.47
0.90	609.1	11.87	0.76	1.59	2.22	7.30	61.5	1.318	1.11	154.82
1.00	639.1	11.29	0.72	1.49	2.09	6.99	117.5	1.351	1.87	174.90
1.20	680.1	9.10	0.65	1.41	1.92	5.12	251.5	1.398	3.27	182.27
1.40	710.1	7.90	0.61	1.30	1.68	4.31	403.5	1.439	5.07	217.30
1.60	734.1	7.60	0.60	1.23	1.56	4.21	561.5	1.472	6.58	218.62
1.80	752.1	6.01	0.54	1.17	1.45	2.85	726.5	1.498	9.17	229.67

Table B12 : Run 12 (Effect of Solvent Type)
 Solvent = Prudhoe Bay Gas (Slug size = 5% PV)

PV Injected	Np (cc)	Total Pr. Drop(psi)	Pr. Drop Along The Length (psi)				Wp (cc)	Gp (scf)	WOR (cc/cc)	GOR (scf/stb)
			(1 ft)	(2 ft)	(3 ft)	(4 ft)				
0	0	49.12	12.10	12.38	12.21	12.43	0	0	0	0.00
0.10	87.0	41.40	6.80	10.46	12.00	12.14	0	0.088	0	160.83
0.20	173.0	35.50	3.54	8.56	11.55	11.85	0	0.178	0	166.40
0.30	258.0	27.20	2.70	4.98	8.79	10.73	0	0.269	0	170.22
BT 0.33	284.5									
0.40	335.6	22.10	2.25	3.79	5.88	10.18	3.2	0.351	0.06	168.02
0.50	406.4	19.35	1.97	3.22	4.46	9.70	17.6	0.421	0.20	157.20
0.60	447.3	18.01	1.75	2.93	3.83	9.50	57.3	0.461	0.97	155.50
0.70	477.3	16.55	1.62	2.79	3.60	8.54	122.3	0.491	2.17	159.00
0.80	503.3	14.82	1.38	2.59	3.21	7.64	192.3	0.520	2.69	177.35
0.90	526.3	13.54	1.37	2.39	3.14	6.64	257.3	0.544	2.83	165.91
1.00	543.3	12.86	1.29	2.24	2.75	6.58	335.3	0.565	4.59	196.41
1.20	574.3	11.54	1.17	1.94	2.57	5.86	491.3	0.600	5.03	179.52
1.40	603.3	10.25	1.06	1.79	2.35	5.05	649.3	0.630	5.45	164.48
1.60	621.3	9.45	1.03	1.60	2.19	4.63	812.3	0.657	9.06	238.50
1.80	630.3	8.63	1.05	1.44	2.02	4.12	987.3	0.679	19.44	388.67

Table B13 : Run 13 (Effect of Solvent Type)
 Solvent = Carbon Dioxide (Slug size = 5% PV)

PV Injected	Np (cc)	Total Pr. Drop(psi)	Pr. Drop Along The Length (psi)				Wp (cc)	Gp (scf)	WOR (cc/cc)	GOR (scf/stb)
			(1 ft)	(2 ft)	(3 ft)	(4 ft)				
0	0	48.55	11.89	12.12	12.32	12.22	0	0	0	0.00
0.10	87.5	33.49	3.28	6.16	11.99	12.06	0	0.089	0	161.73
0.20	175.0	29.15	2.18	4.12	10.83	12.02	0	0.178	0	161.73
0.30	262.0	22.30	1.38	3.17	8.56	9.19	0	0.268	0	164.48
0.40	347.9	17.50	0.97	2.48	6.21	7.84	0	0.381	0	209.16
BT 0.43	374.1									
0.50	430.1	15.90	0.88	1.88	5.78	7.36	0.7	0.501	0.01	232.12
0.60	502.9	14.21	0.84	1.51	4.67	7.19	8.4	0.590	0.11	194.38
0.70	543.4	13.11	0.81	1.30	3.99	7.01	47.9	0.656	0.98	259.11
0.80	575.4	12.12	0.79	1.09	3.22	7.02	109.9	0.723	1.94	332.91
0.90	604.4	11.58	0.77	1.02	2.89	6.90	164.9	0.788	1.90	356.38
1.00	629.4	10.32	0.75	0.95	2.15	6.47	227.9	0.851	2.52	400.68
1.20	657.4	8.65	0.68	0.88	1.22	5.87	383.9	0.977	5.57	715.50
1.40	681.4	6.50	0.60	0.82	1.15	3.93	530.9	1.088	6.13	735.38
1.60	700.4	4.17	0.70	0.71	0.96	1.80	696.9	1.180	8.74	769.89
1.80	708.4	3.58	0.67	0.69	0.88	1.34	874.9	1.215	22.25	695.63

Table B14: Oil-Water Relative Permeability Data From Unsteady State Waterflood

WATER VISCOSITY = 1.00 OIL VISCOSITY = 41.00
 INITIAL WATER SATURATION = 0.0650 PORE VOLUME = 925.00 CC
 BASE RATE = 20.00 CC/MIN BASE DELTA P = 235.8 PSI
 EXPERIMENT FLOW RATE = 4.00 CC/MIN

REGRESSION PARAMETERS:

A1, A2, A3 = -1557.56091 453.92166 -21.58469
 B1, B2, B3 = -0.27063 0.71520 0.08654

	QI	QO	QOF	DELTA P	SW2	FO2	KRO	KRW
1	92.50	92.50	55.05	36.45	-0.155	2.794	2.412	-0.038
2	185.00	185.00	223.84	27.50	0.060	1.235	1.309	-0.006
3	277.50	277.50	312.97	20.49	0.175	0.761	1.036	0.008
4	286.75	286.75	319.87	20.00	0.184	0.731	1.017	0.009
5	370.00	362.05	371.90	16.00	0.252	0.537	0.910	0.019
6	416.25	400.50	395.00	14.20	0.283	0.465	0.878	0.025
7	462.50	433.61	415.15	13.10	0.309	0.409	0.828	0.029
8	555.00	470.77	448.89	12.10	0.354	0.326	0.703	0.035
9	647.50	498.54	476.30	10.80	0.391	0.269	0.641	0.042
10	740.00	519.90	499.22	9.20	0.422	0.228	0.629	0.052
11	832.50	535.28	518.79	8.30	0.449	0.197	0.594	0.059
12	925.00	547.03	535.79	7.20	0.472	0.172	0.594	0.070
13	1110.00	568.39	564.08	6.30	0.511	0.136	0.529	0.082
14	1295.00	585.48	586.87	5.60	0.543	0.112	0.481	0.093
15	1480.00	598.29	605.79	4.78	0.570	0.094	0.468	0.110
16	1665.00	608.97	621.84	4.50	0.593	0.080	0.421	0.118
17	1850.00	616.45	635.69	4.10	0.613	0.070	0.398	0.129

APPENDIX C

CALCULATION OF RELATIVE PERMEABILITY

To calculate relative permeabilities from an unsteady state displacement experiment, Welge developed a method for calculating the ratio of relative permeabilities as a function of saturation at the core outlet. For linear immiscible displacement of one incompressible fluid by another, Welge derived the following relationship to compute the oil-water relative permeability ratio from oil and water production data. For water displacing oil:

$$\frac{k_{rw}}{k_{ro}} = \frac{\mu_w}{\mu_o} \left[\frac{1}{f_{o2}} - 1 \right]$$

The quantity f_{o2} is given by the slope of the recovery plot, that is, the plot of Q_o against Q_i :

$$f_{o2} = \frac{dQ_o}{dQ_i}$$

Welge also showed that the saturation of the displacing phase at the core outlet can be obtained from the average saturation of the displacing phase in the core as:

$$S_{w2} = S_{wav} - f_{o2}Q_i$$

The average saturation can be easily obtained from material balance.

Welge's theory was further extended by Johnson, Bossler and Naumann (1959) to permit the calculation of individual oil and water relative permeabilities. By integrating Darcy's law for each phase along the length of the core, Johnson et. al. derived the following relationship:

$$\frac{f_{o2}}{k_{ro}} = \frac{d}{d \left[\frac{1}{Q_i} \right]} \left[\frac{1}{Q_i r} \right]$$

where

$$I_r = \frac{\left[\frac{q}{\Delta P} \right]}{\left[\frac{q}{\Delta P} \right]_{base}}$$

Relative permeability to water could then be computed from oil relative permeability using Welge's equations.

Implementation of the Welge and Johnson et al.'s technique requires the determination of two derivatives at the same value of cumulative water injection. In general, the process of differentiating experimental data by measuring slopes manually may involve significant amount of inaccuracy because of the usual scatter present in the experimental data. To overcome this problem, smooth functional relationships were fitted through the observed data by the least square method and then these functions were differentiated. This procedure was suggested by Miller and Ramey (1983). They also suggested the following functional relationships:

$$Q_0 = A_1 + A_2(\ln Q_i) + A_3(\ln Q_i)^2$$

$$\ln(Q_i I_r) = B_1 + B_2(\ln Q_i) + B_3(\ln Q_i)^2$$

These equations fitted the experimental data of this study satisfactorily.

NOMENCLATURE

f_{o2} = oil fractional flow at core outlet

I_r = injectivity ratio

k_{ro} = oil relative permeability

k_{rw} = water relative permeability

q = water injection rate

Q_i = cumulative water injection

Q_o = cumulative oil production

S_{w2} = water saturation at core outlet

μ_o = oil viscosity

μ_w = water viscosity